

INFORMATION TO USERS

This manuscript has been reproduced from the microfilm master. UMI films the text directly from the original or copy submitted. Thus, some thesis and dissertation copies are in typewriter face, while others may be from any type of computer printer.

The quality of this reproduction is dependent upon the quality of the copy submitted. Broken or indistinct print, colored or poor quality illustrations and photographs, print bleedthrough, substandard margins, and improper alignment can adversely affect reproduction.

In the unlikely event that the author did not send UMI a complete manuscript and there are missing pages, these will be noted. Also, if unauthorized copyright material had to be removed, a note will indicate the deletion.

Oversize materials (e.g., maps, drawings, charts) are reproduced by sectioning the original, beginning at the upper left-hand corner and continuing from left to right in equal sections with small overlaps. Each original is also photographed in one exposure and is included in reduced form at the back of the book.

Photographs included in the original manuscript have been reproduced xerographically in this copy. Higher quality 6" x 9" black and white photographic prints are available for any photographs or illustrations appearing in this copy for an additional charge. Contact UMI directly to order.

UMI

**A Bell & Howell Information Company
300 North Zeeb Road, Ann Arbor MI 48106-1346 USA
313/761-4700 800/521-0600**



Université d'Ottawa • University of Ottawa

Modeling of Simultaneous Removal of Easily Degradable Substrates and Chlorinated Phenols in UASB Reactors

By

 **Zuojun Ning**

**A Dissertation Submitted to the School of Graduate Studies in
Partial Fulfillment of the Requirement for the Degree of**

**Doctor of Philosophy
in Civil Engineering (Environmental)**

**The Doctor of Philosophy in Civil Engineering is a joint program between
Carleton University and the University of Ottawa, which is administrated
by the Ottawa-Carleton Institute for Civil Engineering**

**Department of Civil Engineering
University of Ottawa
Ottawa, Canada K1N 6N5
January, 1997**



**National Library
of Canada**

**Acquisitions and
Bibliographic Services**

395 Wellington Street
Ottawa ON K1A 0N4
Canada

**Bibliothèque nationale
du Canada**

**Acquisitions et
services bibliographiques**

395, rue Wellington
Ottawa ON K1A 0N4
Canada

Your file Votre référence

Our file Notre référence

The author has granted a non-exclusive licence allowing the National Library of Canada to reproduce, loan, distribute or sell copies of this thesis in microform, paper or electronic formats.

The author retains ownership of the copyright in this thesis. Neither the thesis nor substantial extracts from it may be printed or otherwise reproduced without the author's permission.

L'auteur a accordé une licence non exclusive permettant à la Bibliothèque nationale du Canada de reproduire, prêter, distribuer ou vendre des copies de cette thèse sous la forme de microfiche/film, de reproduction sur papier ou sur format électronique.

L'auteur conserve la propriété du droit d'auteur qui protège cette thèse. Ni la thèse ni des extraits substantiels de celle-ci ne doivent être imprimés ou autrement reproduits sans son autorisation.

0-612-26137-9

Canada

ABSTRACT

A dynamic model describing the simultaneous degradation of easily degradable substrates (sucrose and acetic acid (HAc)) and 2,4-dichlorophenol (2,4-DCP) in upflow anaerobic sludge blanket reactors (UASB) was developed. Two critical factors considered in the multiple substrate degradation processes were sorption and substrate interaction during degradation.

Experimental investigations on the sorption of chlorinated phenols under dynamic situations as well as the degradation kinetics of cosubstrates and 2,4-DCP considering sorption and substrate interaction were conducted first. It was found that partitioning was the dominant mechanism in sorption of chlorophenols to anaerobic granules and that metabolically mediated diffusion during sorption was negligible. Under a dynamic situation, anaerobic sorption of chlorophenols which follow sorption linearity and sorption-desorption singularity in isotherms, can be described by a dynamic model incorporating linear sorption equation. Nonequilibrium sorption caused by diffusion limitations in anaerobic reactors was found to be negligible because of the strong hydrodynamic dispersion that prevails in anaerobic reactors and the high porosity of anaerobic granules. However, minor nonideal sorption phenomena were observed for 3,4-dichlorophenol (3,4-DCP) and pentachlorophenol (PCP), both of which showed sorption-desorption isotherm hysteresis.

Substrate interaction during degradation of cosubstrates and 2,4-DCP resulted in the inhibition of acetogenesis and methanogenesis by 2,4-DCP. The effect of electron donors on 2,4-DCP degradation was found to be minimal. A modified Haldane type inhibition function was proposed to describe the degradation of 2,4-DCP. On the basis of model discrimination results, the degradation kinetics of HAc and propionic acid (HPr) were defined by the uncompetitive inhibition and Haldane type inhibition functions, respectively, with 2,4-DCP as inhibitor. Acidogenesis of sucrose to HAc or HPr followed the Monod equation since no inhibiting factor was found for this degradation process.

Knowledge obtained from the above investigations was used to develop a dynamic model for UASB reactors. Data that were obtained from experimental investigations on multiple substrate degradation in continuous UASB reactors were used to validate and verify the dynamic model. The model predicts the system responses for 2,4-DCP, 4-monochlorophenol (4-MCP), HAc, HPr and chemical oxygen demand (COD) concentration in the effluent. Based on model fitting results, it was found that the degradation rates of 2,4-DCP and cosubstrates, HAc and HPr, changed inversely as a function of the specific organic loading rate of the UASB reactors. The implication of this finding was fully discussed.

ACKNOWLEDGMENTS

I wish to express my deepest gratitude and appreciation to my supervisors, Dr. L. Fernandes and Dr. K. J. Kennedy, for their invaluable guidance, encouragement, patience and friendly help throughout the course of this research work. I am also indebted for their careful checking and correcting this manuscript.

Special thanks are given to Dr. R. Droste and Dr. R.M. Narbaitz for their suggestions and advice during my study. I would like to thank Mr. F.S. Aposaga for his help in laboratory during this research. The financial support received from my supervisors and the University of Ottawa is gratefully acknowledged.

Finally, I would like to take this opportunity to give my warmest gratitude to my family for their endless love, encouragement and support.

TABLE OF CONTENT

ABSTRACT	i
ACKNOWLEDGMENTS	iii
TABLE OF CONTENT.....	iv
LIST OF TABLES	vii
LIST OF FIGURES	ix
NOMENCLATURE	xiv
CHAPTER 1 INTRODUCTION	1
1.1 Objectives /9	
1.2 Experimental Considerations to Meet Objectives /9	
CHAPTER 2 LITERATURE REVIEW	11
2.1 Sorption /11	
2.1.1 Mechanism /12	
2.1.2 Factors Affecting Sorption /15	
2.1.3 Sorption/Desorption Equilibrium and Sorption Kinetics /19	
2.1.4 Nonideal Sorption /22	
2.1.5 Effect of Sorption on Degradation /23	
2.2 Degradation /25	
2.2.1 Anaerobic Degradation of Primary Organic Matter /25	
2.2.2 Anaerobic Degradation of Chlorinated Phenols /29	
2.2.3 Substrate Interaction in Multiple Substrates Degradation /33	
2.3 Dynamic Modeling of the Anaerobic Treatment System /39	
CHAPTER 3 EXPERIMENTAL PROGRAM, MATERIALS AND METHODS	41
3.1 Experimental Program /41	
3.2 Materials /41	
3.3 Experimental Setup and Methods /46	
3.3.1 Batch Sorption Tests /46	
3.3.2 Continuous Sorption Tests /49	
3.3.3 Batch Degradation Kinetics Tests /55	
3.3.4 Continuous UASB Reactors /57	
3.4 Analytical Methods /61	

CHAPTER 4 SORPTION	64
4.1 The Effect of Metabolic Activity on Sorption /64	
4.1.1 Sorption Isotherm /67	
4.1.2 Kinetic Sorption /71	
4.1.3 Discussion /74	
4.2 Factors Affecting Sorption /76	
4.2.1 Factor Screening /77	
4.2.2 pH /83	
4.2.3 Multicomponent Sorption /87	
4.3 Sorption Under Dynamic Situation /90	
4.3.1 Dynamic Model with Linear Sorption /90	
4.3.2 Sorption Process in CM Reactor /93	
4.3.3 Sorption Process in SC Reactor /104	
4.3.4 Discussion /108	
CHAPTER 5 SUBSTRATE INTERACTION	112
5.1 Degradation of 2,4-DCP Without Addition of Cosubstrates /113	
5.1.1 Degradation Process of 2,4-DCP /114	
5.1.2 Degradation Kinetics of 2,4-DCP /122	
5.1.3 Effect of Sorption on Degradation /125	
5.1.4 Discussion /128	
5.2 Effect of Cosubstrates on the Degradation of 2,4-DCP /129	
5.2.1 Effect of Sucrose, HPr and HAc on 2,4-DCP Degradation /130	
5.2.2 Syntrophic Relation between Dechlorination and Methanogenesis /133	
5.3 Effect of 2,4-DCP on HAc, HPr and Sucrose Degradation /135	
5.3.1 HAc /135	
5.3.2 HPr /143	
5.3.3 Sucrose /149	
5.3.4 Degradation Kinetics of HAc and HPr with Nonionized Substrates /159	
5.3.5 Discussion /163	
CHAPTER 6 EXPERIMENTAL INVESTIGATION WITH UASB REACTORS	165
6.1 Experimental Design /165	
6.2 Performance of UASB Reactors /169	
CHAPTER 7 DYNAMIC MODELING OF UASB REACTORS	175
7.1 Model Development /175	
7.1.1 Substrate Interaction Schemes in UASB Reactors /175	
7.1.2 Dynamic Model /177	
7.2 Model Validation /184	
7.2.1 Parameter Estimation Criterion /186	
7.2.2 Parameter Estimation and Model Adequacy /188	
7.3 Model Verification /191	
7.4 Discussion /200	

CHAPTER 8 CONCLUSIONS, CONTRIBUTIONS AND RECOMMENDATIONS	205
8.1 Conclusions and Contributions /205	
8.2 Recommendations for Future Studies /207	

REFERENCES	209
-------------------------	------------

APPENDIX	221
-----------------------	------------

A Composition of Feed for UASB Reactors /221	
B Composition of Dilution Solution for Batch Degradation Tests /221	
C Relation Between C_{sw} and C_s for sorption of 2,4-DCP to Anaerobic Granules /222	
D Feeding Conditions During Transient Change Periods for the 9 Experimental Runs /225	
E System Responses for UASB reactors in the 9 Experimental Runs /227	
F Estimation of the mean SRT for the UASB reactors /232	
G FORTRAN Program for Solving the Dynamic Model (Table 7-2) and Evaluating the Determinant of $Z^T Z$ /233	
H Fitting Results of the Dynamic Model to the Data for the System Responses (2,4-DCP, 4-MCP, HAc, HPr and COD)of the UASB Reactors with Adjusted Parameters /241	

LIST OF TABLES

Table 2-1 Sorption/desorption partition coefficients (K_d / K_p) for HCB and DDT	16
Table 2-2 Direct stimulating effect of cosubstrate on anaerobic CPs degradation	35
Table 3-1 Summary of the experimental program	42
Table 3-2 Physical properties of acclimated anaerobic granules	45
Table 3-3 Batch sorption tests included in experiment group E1	46
Table 3-4 Dynamic sorption experiments (E2)	52
Table 3-5 Batch degradation kinetics tests (E3 and E4)	55
Table 3-6 Operating conditions of UASB reactors	60
Table 4-1 Sorption tests conducted under specified conditions	65
Table 4-2 Equilibrium sorption of 2,4-DCP to live dormant and chemically inactivated anaerobic granules	67
Table 4-3 Sorption constant values for 2,4-DCP	68
Table 4-4 Linear model fitting results for the sorption of 2,4-DCP to NaN_3 inactivated, live (active) and live (dormant) granules	70
Table 4-5 Experimental conditions for the factorial sorption tests	78
Table 4-6 Experimental results for the factorial sorption tests	78
Table 4-7 Estimated parameters in the model for PCP	79
Table 4-8 Model comparison for PCP sorption data	80
Table 4-9 Model comparison for 2,4-DCP sorption data	82

Table 4-10	K_{d,DCP^r} estimated for CMTP granules at different pH conditions	86
Table 4-11	Dynamic sorption tests conducted in CM reactor	94
Table 5-1	Parameter estimation results for 2,4-DCP degradation kinetics	124
Table 5-2	Kinetic parameter values for anaerobic degradation of chlorophenols	129
Table 5-4	Candidate models for the kinetics of HAc degradation with 2,4-DCP	138
Table 5-5	Fitting results for the models with inhibition by HAc and 4-MCP	140
Table 5-6	Model fitting results for $f_1 \sim f_6$ with $K_{S,HAc}$ of 175.3 mg/L	142
Table 5-7	Model fitting results for $f_1 \sim f_6$ with $K_{S,HPr}$ of 281.9 mg/L	147
Table 5-8	C_{Suc} and corresponding $dC_{Suc \rightarrow HAc} / dt$ and $dC_{Suc \rightarrow HPr} / dt$	155
Table 5-9	Degradation kinetics of sucrose to HAc and HPr	158
Table 5-10	Parameter estimation results for degradation kinetics of HAc and HPr with nonionized form of substrates	162
Table 6-1	Experiments with transient feed conditions for the UASB reactors	166
Table 6-2	Feeding conditions during transient change periods for the 9 experimental runs	167
Table 6-3	The COD removal efficiencies for the UASB reactors	170
Table 7-1	Summary of the equations in the dynamic model for the UASB reactors	185
Table 7-2	Parameter values in the dynamic model estimated from batch tests	186
Table 7-3	Parameters estimated by fitting the model to data from RUN III.4	189
Table 7-4	The parameter values used in the model verification	193
Table 7-5	Comparison of the parameter values for the acetoclastic methanogenesis	203

LIST OF FIGURES

Figure 2-1	Some sorbent-sorbate interactions possibly controlling the sorption	13
Figure 2-2	Reaction scheme for the anaerobic degradation of biological polymers	26
Figure 2-3	Conceptual model for substrate interactions in reductive dehalogenation	37
Figure 3-1	Schematic diagram of CM reactor system	51
Figure 3-2	Schematic diagram of SC reactor system	51
Figure 3-3	Schematic diagram of UASB reactor system	58
Figure 3-4	Tracer test result for mixing conditions in reactor R1	61
Figure 4-1	Effect of cultivation time on degradation of 2,4-DCP by unacclimated and acclimated sludge	65
Figure 4-2	Adsorption of 2,4-DCP to serum bottle in the control	66
Figure 4-3	Comparison of biosorption of 2,4-DCP to live (active), live (dormant) and inactive anaerobic granules	69
Figure 4-4	Sorption comparison between live (dormant) and inactive granules (a) for sludge SOLR/low and (b) for sludge SOLR/high	72
Figure 4-5	Comparison of sorption results for SOLR/low sludge and SOLR/high sludge, (a) for inactive granules and (b) for dormant granules	73
Figure 4-6	Comparison of the sorption capacity of inactivated granule with that of live (dormant) and live (active) granules	74
Figure 4-7	Plot of q_e residual vs. q_e . (a) the best fitting model; (b) the model only with pH term	81
Figure 4-8	Sorption coefficients determination for phenolate and phenol form of 2,4-DCP	86

Figure 4-9 Multiple sorption of 2,4-DCP + 4-MCP. (A) 2,4-DCP sorption influenced by 4-MCP; (B) 4-MCP sorption affected by 2,4-DCP	88
Figure 4-10 Multiple sorption of 2,4-DCP and PCP. (A) 2,4-DCP sorption influenced by PCP; (B) PCP sorption influenced by 2,4-DCP	89
Figure 4-11 Test No. 1: 2,4-DCP with step input (HRT = 4.85 h)	95
Figure 4-12 Test No. 2: 2,4-DCP with step input (HRT = 0.93 h)	95
Figure 4-13 Test No. 6: 2,4-DCP with pulse input (HRT = 5.47 h)	96
Figure 4-14 Test No. 3: 2,4-DCP blank run with step input (HRT = 3.90 h)	97
Figure 4-15 Adjusted results for 2,4-DCP sorption to sludge with step input	98
Figure 4-16 Test for 3-MCP. (a) Test No. 4: step input, HRT= 5.0 h and fitted $K_d = 0.06$; (b) Test No. 5: step input, HRT= 0.93 h and fitted $K_d = 0.06$	100
Figure 4-17 Test No. 7: 3,4-DCP with step input (HRT = 5.18 h)	101
Figure 4-18 Nonideal sorption of 3,4-DCP to anaerobic granules	101
Figure 4-19 Test results for 2,4,6-TCP. (a) Test No. 8: step input, HRT = 5.18 h and fitted $K_d = 0.06$; (b) Test No. 9: pulse input, HRT= 5.31 h and fitted $K_d = 0.05$	102
Figure 4-20 Test No. 10: PCP with step input (HRT = 5.71 h)	103
Figure 4-21 (a) Test No. 11: PCP with pulse input (HRT = 5.95 h, fitted $K_d = 0.35$). (b) Test No. 12: PCP blank run with pulse input (HRT = 3.10 h)	104
Figure 4-22 Parameters estimation of D and u from the HPr transport data in SC reactor	106
Figure 4-23 Fitting result of A-D model to HPr transport data ($D/uL = 0.096$, $\varepsilon = 0.98$)	107
Figure 4-24 Model with linear sorption kinetics fitting results to 2,4-DCP data in SC reactor	108

Figure 5-1 2,4-DCP degradation without cosubstrate addition, using sludge granule R3	115
Figure 5-2 Production of 4-MCP in the degradation of 2,4-DCP without cosubstrate addition	116
Figure 5-3 Relation between 2,4-DCP degradation rate and its concentration in liquid phase	119
Figure 5-4 Effect of 4-MCP on degradation of 2,4-DCP	119
Figure 5-5 2,4-DCP degradation using sludge R4	120
Figure 5-6 2,4-DCP degradation and 4-MCP production using sludge granule R4	121
Figure 5-7 Relation between 2,4-DCP degradation rate and its concentration in liquid phase for sludge R4	122
Figure 5-8 Results of kinetic equations fitted to data from experiments	125
Figure 5-9 Stimulating effect of HAc on the 2,4-DCP degradation	131
Figure 5-10 Stimulating effect of HPr on the 2,4-DCP degradation	131
Figure 5-11 Stimulating effect of Sucrose on the 2,4-DCP degradation	131
Figure 5-12 2,4-DCP degradation with or without methanogenic inhibition	134
Figure 5-13 4-MCP production with or without methanogenic inhibition	134
Figure 5-14 Simultaneous degradation of HAc and 2,4-DCP	136
Figure 5-15 Relation of average HAc degradation rate to 2,4-DCP and HAc concentrations	137
Figure 5-16 Plot of r_{HAc} residual with r_{HAc} for model f_3 , f_3 without $K_{S,HAc}$ and f_4	144
Figure 5-17 Simultaneous degradation of HPr and 2,4-DCP	145
Figure 5-18 Relation of the HPr degradation rate to 2,4-DCP and HPr concentrations	145
Figure 5-19 Plot of r_{HPr} residual with r_{HPr} for models f_3	148
Figure 5-20 Variation of HAc concentration with time during the sucrose	

degradation with 2,4-DCP	149
Figure 5-21 Variation of HPr concentration with time during the sucrose degradation with 2,4-DCP	150
Figure 5-22 Variation of COD concentration with time during the sucrose degradation with 2,4-DCP	150
Figure 5-23 Effect of 2,4-DCP on the sucrose degradation to HAc (A) and HPr (B)	156
Figure 5-24 Possible hydrogen inhibition to sucrose degradation to HAc and HPr	157
Figure 6-1 Variation of the substrate concentrations in feed during the transient change periods for UASB reactors	168
Figure 6-2a System responses for RUN I.1	172
Figure 6-2b System responses for RUN I.3	172
Figure 6-2c System responses for RUN II.1	172
Figure 6-2d System responses for RUN II.2	173
Figure 6-2e System responses for RUN II.3	173
Figure 6-2f System responses for RUN II.4	173
Figure 6-2g System responses for RUN III.1	174
Figure 6-2h System responses for RUN III.3	174
Figure 6-2i System responses for RUN III.4	174
Figure 7-1 Schematic representation of the substrate interactions in the degradation processes in the UASB reactors for which the feed was sucrose/HAc based wastewater with 2,4-DCP	176
Figure 7-2a Model fitting results for 2,4-DCP and 4-MCP (RUN III.4)	190
Figure 7-2b Model fitting results for HAc, HPr and COD (RUN III.4)	190
Figure 7-3a Model fitting results for RUN II.4. (A) 2,4-DCP and 4-MCP	194
Figure 7-3b Model fitting results for RUN II.4. (B) HAc, HPr and COD	195

Figure 7-4a	Model fitting results for RUN III.3. (A) 2,4-DCP and 4-MCP	195
Figure 7-4b	Model fitting results for RUN III.3. (B) HAc, HPr and COD	195
Figure 7-5a	Model fitting results for RUN II.3. (A) 2,4-DCP and 4-MCP	196
Figure 7-5b	Model fitting results for RUN II.3. (B) HAc, HPr and COD	196
Figure 7-6a	Model fitting results for RUN I.3. (A) 2,4-DCP and 4-MCP	196
Figure 7-6b	Model fitting results for RUN I.3. (B) HAc, HPr and COD	197
Figure 7-7a	Model fitting results for RUN II.2. (A) 2,4-DCP and 4-MCP	197
Figure 7-7b	Model fitting results for RUN II.2. (B) HAc, HPr and COD	197
Figure 7-8a	Model fitting results for RUN III.1. (A) 2,4-DCP and 4-MCP	198
Figure 7-8b	Model fitting results for RUN III.1. (B) HAc, HPr and COD	198
Figure 7-9a	Model fitting results for RUN II.1. (A) 2,4-DCP and 4-MCP	198
Figure 7-9b	Model fitting results for RUN II.1. (B) HAc, HPr and COD	199
Figure 7-10a	Model fitting results for RUN I.1. (A) 2,4-DCP and 4-MCP	199
Figure 7-10b	Model fitting results for RUN I.1. (B) HAc, HPr and COD	199
Figure 7-11	Effect of SOLR on the values of k_{DCP^0}	201
Figure 7-12	Effect of SOLR on the values of $k_{HAc \rightarrow Meth}$	201

NOMENCLATURE

A	superficial cross-sectional area of sludge column, cm^2
C	cosubstrate or chlorophenol concentration in the effluent of reactors, mg/L
C_e	equilibrium concentration of chlorophenol in the liquid phase, mg/L
C_f	chlorophenol concentration in the influent of reactors, mg/L
C_o	initial chlorophenol concentration in reactors, mg/L ; substrate concentration of in the feed of reactors, mg/L
C_{Oct}	equilibrium concentration of the organic compound in the octanol layer, mg/L
C_{sw}	interior concentration of chlorophenol within granules, mg/L
C_w	equilibrium concentration of the organic compound in the water layer, mg/L
D	dispersion coefficient, cm^2/min
Du/L	dispersion number, dimensionless
$E(Y)$	expected system response
f	the kinetic model to be discriminated
\hat{f}	the kinetic model fitted to data
$H(\theta)$	$N \times M$ predicted response matrix
k	maximum specific substrate degradation rate, mg/g VSS/h
k_d	biomass endogenous decay rate constant, d^{-1}
K_a	dissociation constant
K_d	sorption coefficient, L/g VSS
K_i	inhibition constant, mg/L ; $(\text{mg/L})^2$ or $(\text{mg/L})^{\lambda-1}$
K_s	half-velocity constant, mg/L

l	number of sets of replicates
L	length of granular sludge column, cm
L_r	the ratio for lack of fit test
M	molar weight of substrate (g/mole); number of responses measured in the experiment
m	number of replicates
N	number of observations
n	sample size;
p	hydrogen partial pressure, bar
P	moisture constant (%)
pK_a	$-\lg K_a$, where K_a is the dissociation constant;
q	chlorophenol concentration sorbed onto sludge, mg/g VSS
q_e	equilibrium concentration of chlorophenol sorbed onto sludge, mg/g VSS
Q	influent volumetric flowrate of reactor, L/min; L/h
r	degradation rate of substrate, mg/L/h
\bar{r}	average degradation rate of substrate (mg/g VSS/h)
t	reaction time, h
\bar{t}	observed hydraulic retention time, h
t_θ	theoretical hydraulic retention time ($t_\theta = V / Q$), h
u	average pore-water velocity through the sludge column, L/min
V	effective volume of the reactor, L
X, X_e, X_0	sludge concentration in the reactor, in the effluent and in the influent, respectively, g VSS/L
Y	yield coefficient, g VSS/g substrate
Y_c	combined yield coefficient, g VSS/g sucrose
Y	$N \times M$ observed response matrix;
z	length variable along the sludge column, cm
$Z(\theta)$	residual matrix
ΔC	substrate concentration variation within a specific time interval, mg/L

GREEK LETTERS

α	fraction of molecular form of the ionizable compound
α	significance level
β_0, β_1, \dots	parameters in linear multiple regression model
ε	porosity of the sludge column
λ	positive exponent constant, dimensionless
θ	parameter matrix
ρ	correlation coefficient
ρ_{sw}	density of wet sludge granules, g/L
$\hat{\sigma}_p^2$	pooled pure error variance estimated from replicates

ABBREVIATIONS

COD	chemical oxygen demand, mg/L
$\det(\mathbf{Z}^T\mathbf{Z})$	determinant of product of transpose of the residual matrix and the residual matrix
DOC	soluble organic carbon
EPS	extracellular polymeric substances
HRT	hydraulic retention time, h
GLRT	generalized likelihood ratio test
MSL	mean squares lack of fit test
OLR	organic loading rate, g COD/L/d
SOLR	specific organic loading rate, g COD/g VSS/d
ThOD	theoretical oxygen demand, mg/L
RSS	sum of squared residuals

SUBSCRIPTS

<i>COD</i>	chemical oxygen demand
<i>DCP</i>	2,4-DCP
<i>DCP^o</i>	molecular 2,4-DCP
<i>DCP</i> → <i>MCP</i>	degradation of 2,4-DCP to 4-MCP
<i>DCP^o /HPr^o</i>	inhibition of molecular 2,4-DCP on degradation of HPr
<i>DCP^o /HAc^o</i>	inhibition of molecular 2,4-DCP on degradation of HAc
<i>HAc</i>	acetic acid
<i>HAc^o</i>	molecular HAc
<i>HAc</i> → <i>Meth</i>	degradation of acetic acid to methane gas
<i>HPr</i>	propionic acid
<i>HPr^o</i>	molecular HPr
<i>HPr</i> → <i>HAc</i>	degradation of propionic acid to acetic acid
<i>MCP</i>	4-MCP
<i>MCP^o</i>	molecular 4-MCP
<i>NCOD</i>	nonbiodegradable COD
<i>Suc</i>	sucrose
<i>Suc</i> → <i>HAc</i>	degradation of sucrose to acetic acid
<i>Suc</i> → <i>HPr</i>	degradation of sucrose to propionic acid

INTRODUCTION

Since the 1980s, the main concern in water pollution control has switched from traditional pollutants, such as BOD, TSS and heavy metals to industrial toxic organic compounds (Alexander, 1981). Chlorinated phenols are one of the major toxic organic pollutants of great public concern because of their toxic and mutagenic properties, and tendency to bioaccumulate. Four kinds of chlorinated phenols, PCP, 2,4,6-TCP, 2,4-DCP and 2-monochlorophenol (2-MCP) are listed as U.S. EPA priority pollutants because of their extensive industrial and agriculture use as either final products or precursors of wood, leather and textile preservatives, herbicides and insecticides (Silva, 1981). Chlorinated phenols are also an important class of pollutants in wastewater from the pulp and paper industry (Murray and Richardson, 1993).

The degradation of chlorinated phenols has been investigated with both aerobic and anaerobic processes (Eckenfelder and Grau, 1992; Battery and Wilson, 1989). Anaerobic reductive dehalogenation was recognized as the critical step in the biodegradation of highly chlorinated phenols that are difficult to degrade in aerobic environment (Boyd and Shelton, 1984). Under anaerobic conditions, highly chlorinated

phenols can be reductively dechlorinated to less chlorinated phenols or completely mineralized (Kennes et al., 1996; Mikesell and Boyd, 1986; Woods, 1985). The reductive dechlorination pathway for all chlorinated phenols was investigated by using anaerobic consortium acclimated to specific chlorinated phenols (Nicholson et al. 1992; Zhang and Wiegel, 1990). Effect of electron donors and electron acceptors on the extent and rate of degradation was reported in recent studies (Perkins et al., 1994; Haggblom et al., 1993a; Mohn and Kennedy, 1992).

Although degradation of chlorinated phenols has been extensively studied, utilization of this knowledge in the design of wastewater treatment systems and optimization of system operation is rarely documented. Predicting the removal of individual chlorinated phenols in biological treatment processes is still a difficult task (Grady, 1991). A significant amount of modeling work has been conducted for anaerobic processes treating biogenic or nontoxic organic matter (Andrews and Graef, 1971; Samssoon et al., 1991; Jain et al., 1992; Siegrist et al., 1993; Vavilin et al., 1994) but modeling of toxic organic compounds in anaerobic digestors has only recently been reported (Parker et al., 1994). In addition, coexistence of nontoxic organic matter and toxic organic compounds is a common situation for bioreactors treating industrial wastewaters. Degradation of both easily degradable organic matter and toxic organics would occur concurrently. However, it is not clear how the degradation processes for nontoxic organic matters and chlorinated phenols affect each other, and the way to optimize the system design and operation is not known.

In biological treatment systems that remove toxic organic compounds, the following factors have been considered as major sub-processes dominating the system performance: sorption, degradation, production and volatilization. Among them, degradation is the essential process for the removal of both nontoxic organic matter and toxic organic compounds. For soluble, easily degradable and nonvolatile organic matter, only degradation seems to be important (Andrews and Graef, 1971). However, sorption may have a strong influence on the removal of toxic organic chemicals in biological treatment systems since they have a tendency to sorb to biological solids (Woods, 1985; Tsezos and Bell, 1988; Kennedy et al., 1992). Compared to aerobic processes, volatilization is less important in anaerobic systems due to the low volatilization potential of most aromatic compounds (chlorinated phenols) as well as the weak driving force for volatilization in anaerobic reactors (Bell et al., 1993). Another often unaccounted for phenomenon is production. If the precursor of a specific chemical is involved in the degradation process, and the degradation pathway for the precursor is known, then the production of the specific chemical from the precursor can also be described by degradation (Armenante et al., 1995). To predict the simultaneous removal of both nontoxic organic matter and toxic organic compounds in an anaerobic treatment system, sorption and degradation are the most critical sub-processes and their influence in determining the effluent concentrations of individual pollutants should be fully understood.

Sorption isotherms of selected toxic organics onto microbial solids, such as activated sludge, anaerobic granules and digested sewage sludge, have been studied by

several investigators (Bell and Tsezos, 1987; Woods, 1985; Dobbs et al., 1989). A detailed investigation on sorption of 15 different chlorinated phenols onto anaerobic granules was conducted by Kennedy et al. (1992). Partitioning was considered a major sorption mechanism of toxic organic compounds to biological solids based on distinct sorption behavior between inorganic sorbent and biosolids (Wang et al., 1993; Schwarzenbach et al., 1993). However, within the context of modeling, several questions on sorption have not yet been addressed.

Although partitioning is a major mechanism in sorption, the effect of biomass metabolic activity on sorption is not clear. To better understand the role of sorption in the removal of toxic organic compounds in biological reactors, it is necessary to know how significantly sorption is affected by metabolic activity. Several investigations have been conducted on the biosorption of toxic organics to live and dead (autoclaved) microbial solids (Tsezos and Bell, 1989, Wang and Grady, 1994). However, autoclaving as a method for killing microbes not only inhibits biological activity but also causes cell lysis, which significantly changes the physical-chemical properties of the biomass and surrounding mixed liquor (Linqvist and Enfield, 1992). Therefore, results using autoclaved biomass are difficult to interpret and have limited use in improving the understanding of biosorption mechanisms (Wang et al., 1993). An alternative to autoclaving is the use of inhibitory agents that neutralize metabolic activity while minimizing cell lysis and leakage of intracellular components into the surrounding media.

Most reported investigations on sorption were conducted using sorption isotherms. Very little is known about the sorption behavior of toxic chemicals under dynamic situations in reactors. In modeling the removal of toxic organics in biological treatment processes, linear sorption equation have been used arbitrarily without the support of experimental evidence (O'Brien and Teather, 1995; Parker et al., 1994; Jacobsen et al., 1993). This leaves a degree of uncertainty in elucidating the reason for poor fitting results in model simulations. Although linear sorption equation are simple for dynamic modeling of a biological system, their validity has been challenged by sorption isotherm measurements of some toxic organics which have shown significant nonlinearity and sorption-desorption hysteresis. Moreover, sorption is a time-dependent process under dynamic situations in reactors, so that diffusion limitation and time-dependent sorption may cause nonequilibrium sorption, which can invalidate the application of linear sorption equation for bioreactors (Brusseau and Rao, 1989). For chlorinated phenols, sorption linearity was found to apply to only a portion of them and the Freundlich equation was found to be a better equation to fit the data (Kennedy et al., 1992). Hysteresis in sorption-desorption was also reported for some chlorophenols, such as 3-MCP, 3,4-DCP and PCP (Wu et al., 1993; Kennedy et al., 1992; Wood, 1985). With increasing concern over groundwater contamination, a number of studies on nonideal sorption during transport of toxic organic in sediments and soil were conducted in recent years (Brusseau and Rao, 1989; Kookana et al., 1993). It was found that sorption ideality is often not valid in modeling contaminant transport. Nonlinearity, nonequilibrium sorption and hysteresis in sorption-desorption were considered the main reasons for nonideal sorption phenomena

that were exemplified by an asymmetrical breakthrough curve (BTC) (Spurlock et al., 1995). Extensive modeling studies have been conducted to account for sorption nonideality (Dhawan et al., 1991) as well as nonequilibrium sorption and transport of chlorophenols in soil (Lee et al., 1991). However, no studies have been reported on nonideal sorption phenomena in biological reactors.

The contribution of sorption to the removal of toxic organic compounds from biological reactors was often evaluated only by sorption itself (through sludge discharge) (Fahmy et al. 1994; Yan and Allen, 1994), while the effect of sorption on degradation was not sufficiently addressed. As one of the major removal mechanisms of toxic organic compounds in bioreactors, sorption can significantly influence the toxicity and availability of toxic organics to bacteria (Duff et al., 1995; Kennedy et al., 1992). In decontamination of soil and ground water, it was demonstrated that the concentration of toxic organic compounds in the liquid phase dominated degradation, and that diffusion limitations (of sorbed chemicals) restricted the availability of toxic organics to microorganisms which also affected degradation (Scow and Hutson, 1992). However, similar information for biological wastewater treatment processes is not available (Wang and Grady, 1993). While the majority of soils and sediments tend to be inert with low organic content, biological solids are composed of 50~90% organic matter and are both sorbent and degrader. This feature may lead to a more significant sorption capacity as well as sorption-degradation correlation compared to that of soil. It is important to understand the effect of sorption on degradation in order to model the performance of bioreactors and to optimize

system operation.

Biodegradation kinetics of easily degradable organic matter under anaerobic conditions are well understood and documented (Kus and Wiesman, 1995; Pavlostathis and Giraldo-Gomez, 1991). Investigations on degradability and degradation pathways of chlorinated phenols in anaerobic processes have also been conducted. However, investigations on the anaerobic degradation kinetics of chlorinated phenols are few. The Monod and Michaelis-Menten equations have been used to interpret experimental data on the degradation of chlorinated phenols (Armenante et al., 1995; Chang and Alvarez-Cohen, 1995; Hendriksen and Ahring, 1992). The inhibiting effect of chlorophenols on their own degradation by anaerobic biomass has not been addressed. Comparatively, kinetic models describing such inhibiting effects by Haldane-type inhibition function have been reported for pure cultures (Gu and Korus, 1995; Hu et al., 1994).

When modeling the simultaneous removal of nontoxic organic matter and chlorinated phenols in an anaerobic system, degradation kinetics considering substrate interactions is rarely reported (Wrenn and Rittmann, 1995). Since the involvement of cosubstrates is important in the degradation of chlorophenols, the substrate interactions must be considered in determining the degradation kinetics of the cosubstrate and toxic organic chemical. The importance of considering substrate interaction in modeling the removal of toxic organics in biological treatment systems was addressed by Grady (1991). Features of the substrate interaction can be quite complicated (Criddle, 1992). Inhibition

may occur by one or more substrate intermediates formed during degradation of the primary substrates in a treatment system. This may, or may not be coupled to the enhancement of degradation of individual chlorophenols by cosubstrates. Typical examples are product and substrate inhibition caused by volatile fatty acids (VFAs) and hydrogen under some situations (Kus and Wiesmann, 1995; Fukuzaki et al., 1990a, 1990b). For highly chlorinated phenols, such as PCP, degradation results in several less chlorinated phenols being formed (Nicholson et al., 1992), and each of them may have a specific inhibiting effect on other degradation processes. In general, supplementation of easily degradable substrates, such as glucose and yeast extract, may significantly enhance or stimulate the dechlorinating process but enhancement of dechlorination with a specific cosubstrate varies from system to system (Mohn and Kennedy, 1992; Hendriksen et al., 1992; Kuhn et al., 1990). A few kinetic models considering substrate interaction based on cometabolism or secondary substrate mechanisms have been developed for pure cultures (Criddle, 1992). Kinetic models dealing with the effect of substrate interactions were only recently reported for chlorinated aliphatic compounds (Wrenn and Rittmann, 1995; Skeen et al., 1995). However, no inhibiting effect on substrate interaction was considered in these two models. The degradation kinetics of some important intermediate products in anaerobic processes, such as acetic acid (HAc) and propionic acid (HPr), in the presence of toxic organic chemicals, such as chlorophenols, has not been reported.

In summary, there is a lack of knowledge on sorption mechanisms and kinetics of toxic organic compounds such as chlorinated phenols to biological solids under the

dynamic conditions encountered in bioreactors. This is also true for the anaerobic degradation kinetics of both cosubstrate and chlorinated phenols considering substrate interactions. No dynamic model that describes simultaneous removal of cosubstrates and chlorinated phenols in anaerobic reactors has been reported.

1.1 Objectives

The general objective of this study is to develop a dynamic model describing the simultaneous removal of sucrose/HAc and 2,4-DCP in upflow anaerobic sludge bed (UASB) reactors. Considering the requirement of information on sorption and substrate interaction for the modeling work, the specific objectives of this study are as follows: (1) to define the effect of metabolism on sorption of chlorophenols to anaerobic sludge and other major factors affecting sorption; (2) to determine the sorption equation of chlorophenols to anaerobic biomass under dynamic situations; (3) to investigate the substrate interaction scheme of sucrose/HAc and chlorophenol degradation process; (4) to determine the degradation kinetics of individual substrates in this multiple substrate degradation environment; (5) using the knowledge gained from the above investigations, to develop, validate and verify a dynamic model for UASB reactors that simultaneously treat sucrose/HAc based wastewater and 2,4-DCP.

1.2 Experimental Considerations to Meet the Objectives

Considering the complexity of the multiple substrate degradation processes occurring in UASB reactors, this study has been simplified to investigate the removal of the most

representative organic matter, such as sucrose, HAc, and a simple chlorinated phenol, 2,4-DCP. The UASB treatment system was selected since it is a proven sustainable technology for a wide range of very different industrial effluents, including those containing toxic organic compounds (Lettinga, 1995). Sucrose and HAc were used because of their known chemical composition and the stoichiometry of their anaerobic degradation (Mosey, 1983). Selection of 2,4-DCP as the model toxic organic compound is due to the following: (1) it is used in large amounts in industry for the production of wood preservative (PCP) and herbicides (2,4-dichlorophenoxyacetic acid, 2,4,5-trichlorophenoxyacetic acid); (2) it is representative of one class of pollutants, chlorinated phenols, produced by the pulp and paper industry; (3) it is a major breakdown product of highly chlorinated phenols and other phenolic compounds in anaerobic dechlorination; and (4) it has a simple degradation pathway. The major product of 2,4-DCP degradation is 4-monochlorophenol (4-MCP) and further degradation of 4-MCP is slow and not detectable (Mohn and Kennedy, 1992). By using 2,4-DCP, substrate interaction in sorption and degradation processes can be significantly simplified. Consequently, the mass balance data analysis of individual substrates in this UASB degradation system (sucrose, HAc, HPr, 2,4-DCP and 4-MCP) can be easily conducted.

LITERATURE REVIEW

On the basis of the objectives of this study, the literature review mainly focuses on: (1) sorption of chlorinated phenols to biological solids; (2) degradation kinetics of easily degradable organic matter, such as sucrose, HAc and HPr that were used as cosubstrates in this study and are representative substrates or major intermediate products in anaerobic degradation; (3) kinetics and substrate interaction in anaerobic degradation of chlorinated phenols; and (4) dynamic modeling of simultaneous removal of easily degradable organic matters and toxic organic compounds in anaerobic treatment systems.

2.1 Sorption

In general, sorption is referred to as the process in which a chemical associated with solid phases. Sorption of pesticides by organisms has been considered an important detoxification method in aquatic environments (Wedemeyer, 1966). However, the influence of sorption on the fate of toxic organic compounds in biological treatment systems was not fully addressed until the 1980s. Sorption of toxic organic compounds, including chlorinated phenols, to biological solids has been investigated by many investigators using activated sludge (Jacobsen et al., 1993; Wang et al., 1993; Tsezos and

Bell, 1988, 1989; Bell and Tsezos, 1987; Petrasek et al., 1983), sewage sludge from digesters (Dobbs et al., 1989) and anaerobic granules (Kennedy et al., 1992; Woods, 1985) as sorbents. In these investigations, sorption isotherms were the most commonly used method in analysis of the sorption process. The sorption of chlorinated compounds to soil and sediments has also been documented in the literature (Stapleton et al., 1994; Lee et al., 1991; Boyd, 1982; Wedemeyer, 1966).

2.1.1 Mechanism

The terms, adsorption, sorption and biosorption have been used to describe the sorption of toxic organic compounds to biological solids. Partitioning has been considered the major sorption mechanism in sorption of toxic organic compounds to biological solids and bacteria (Wang et al., 1993; Kennedy et al., 1992; Dobbs et al., 1989; Bell and Tsezos, 1987). Since there is a diversity of properties for chemicals and sorbents (solid phase), the dominating mechanism for a specific sorption system can be very different from one to another. As an example Figure 2-1 shows sorption of 4-chloroaniline (4-MCA) to natural solids (Schwarzenbach et al., 1993). As shown in the figure, a 4-MCA molecule may escape the water by penetrating natural organic matter in the solid phase because of unfavorable free-energy costs of remaining in aqueous solution (partitioning). The molecule may also be associated with the mineral surface of the solids via van der Waals, dipole-dipole, and other weak intermolecular forces. Additionally, since 4-MCA is ionizable in aqueous solution the ionized sorbate will be attracted to oppositely charged surface sites. Finally, reactive moieties may bond to solid surface atoms or groups

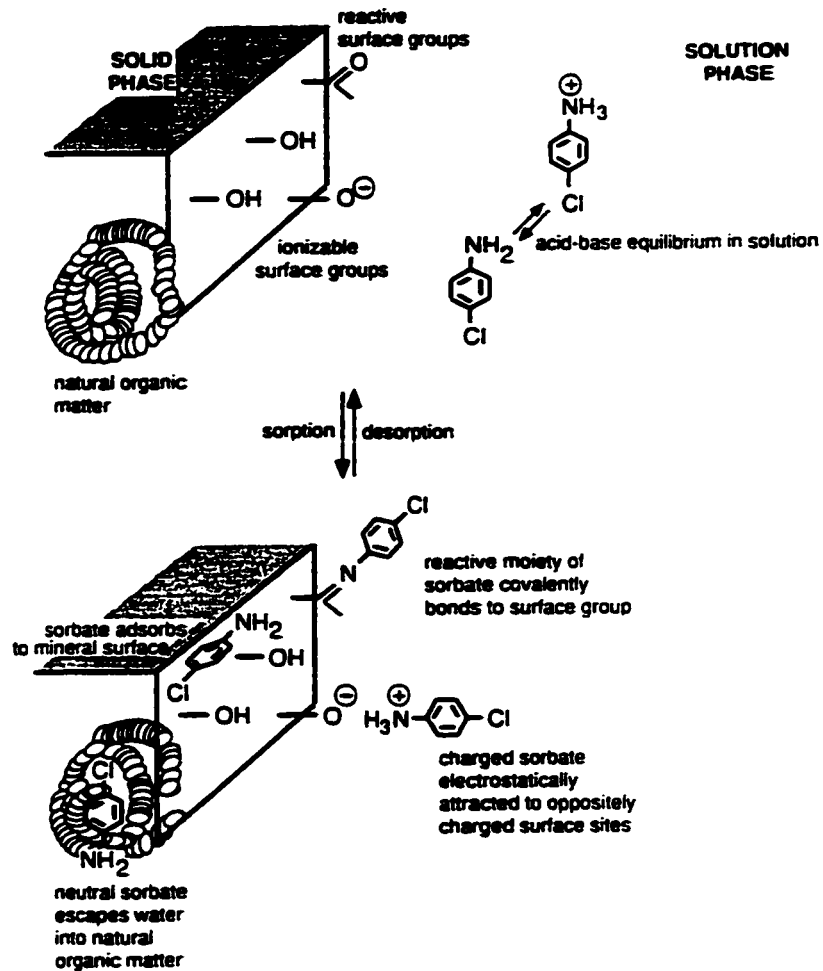


Figure 2-1 Some sorbent-sorbate interactions possibly controlling the sorption
(After Schwarzenbach et al., 1993)

(in Figure 2-1, a carbonyl group on the sorbent and an amino group on the sorbate).

As a specific kind of sorbent, biological solids contain a high portion (50~90%) of metabolically active organic matter, even though other inorganic and inert organic matter can compose a significant portion of it in some cases. Considering the hydrophobic properties of most toxic organic compounds, partitioning could be one of the dominant mechanisms in sorption of toxic organic chemicals to biological solids. This has been experimentally proved by many investigators based on the linearity of sorption isotherms (Kennedy et al., 1992; Dobbs et al., 1989; Tsezos and Bell, 1988; Sugiura et al., 1975). As direct experimental evidence showing the dominance of partitioning in sorption, Tsezos and Bell (1989) showed that 51~84% of a sorbed chemical is located in the cell interior, compared to 16~49% sorbed to the cell wall.

The importance of other physicochemical sorption mechanisms was also investigated. It was shown by Woods (1985) that, in sorption of chlorophenols to anaerobic sludge, the partition coefficient (K_d) ratio of chlorophenolate ion to chlorophenol molecules is about 0.015 ~ 0.4. In studying the mechanism of sorption on wastewater solids, Wang et al. (1993) investigated the relative importance of adsorption in sorption. It was indicated that, for organic compounds with octanol water distribution coefficient ($\lg K_{ow}$) of 2.0, the partition/sorption ratio (q_p / q) is 0.8 and with $\lg K_{ow}$ of 3.0, the ratio increases to about 0.95. Considering the values of $\lg K_{ow}$ for chlorophenols are in the range of 2.15~5.01, adsorption in sorption of chlorinated phenols

to biological solids is less important. Kennedy et al. (1992) reported on the sorption of 15 different chlorophenols to anaerobic granules and found that 8 of them followed sorption linearity very well. Comparatively, sorption of chlorophenols to activated carbon has a strong sorption nonlinearity (Streat et al., 1995).

Besides the physicochemical mechanisms involved in sorption, the effect of biomass metabolic activity on sorption is not clear in reported investigations. Tsezos and Bell (1989) observed that sorption of organic pollutants by live and dead (autoclaved) aerobic microbial cells are similarly correlated to K_{ow} , but a generalization concerning the relative magnitude of sorption by the two biomass states could not be made. Lindqvist and Enfid (1992) reported that autoclaving can make cells more hydrophobic which leads to a much higher sorption of hexachlorobenzene (HCB) to autoclaved vs live biomass (Table 2-1). Recently, using cyanide treatment of aerobic biomass, Dobbs et al. (1995) observed that sorption capacity between live and chemically killed sludge was different. However, since the chemical tested (carbon tetrachloride) was degradable in their experiment, the result obtained is not helpful in understanding whether metabolically mediated sorption was involved in the process or not.

2.1.2 Factors Affecting Sorption

Characteristics of biological solids and the related toxic organic compounds are the most significant factors affecting sorption. Since a large number of toxic organic compounds are

hydrophobic, the partitioning of them into microbial solids is highly related to organic carbon content (in particular the lipid component) of the biomass (Selvakumar and Hsieh, 1988). It has been shown that aerobic sludge has a higher sorption capacity than anaerobic sludge (Dobbs et al., 1989; Jacobsen et al., 1993; Kennedy and Pham, 1995). Sorption partitioning coefficients (K_d) from Lindqvist and Enfield (1992) for HCB and dichlorodiphenyltrichloroethane (DDT) by 5 different microbial strains are presented in Table 2-1. It was shown that the K_d values can vary over ten-fold between different live strains. Sludge source was considered as a factor influencing sorption of halogenated aromatics to anaerobic sludge. However, for biomass obtained from the same source, cell viability (granular size, collected from the reactors at different organic loading rates) has been shown to have a negligible effect on sorption (Kennedy and Pham, 1995; Yan and Allen, 1994).

Table 2-1 Sorption/desorption partition coefficients (K_d / K_p) for HCB and DDT after 20 hours of sorption/desorption to or from bacteria

Compounds	Strains ^a	$K_d \pm SE$	r^2	$K_p \pm SE$	r^2
DDT	CB1	5947 ± 192	0.989	12550 ± 637	0.972
	CB2	10395 ± 508	0.974	15720 ± 547	0.987
	TOL1	2198 ± 107	0.975	12620 ± 1470	0.870
	IS1	3212 ± 109	0.988	12560 ± 2524	0.692
	I	1271 ± 58	0.978	11980 ± 1572	0.841
	I (autoclaved)	27340 ± 937	0.987	97650 ± 3926	0.983
HCB	I	271 ± 37	0.828	975 ± 28	0.987
	I (autoclaved)	18430 ± 574	0.989	24310 ± 496	0.995

^a Strain CB1, CB2 and TOL1 were isolated from Kendaia loam soil and were identified as members of the genera *Pseudomonas*, *Bacillus*, and *Enterobacter*, respectively. Strain I was tentatively identified as a *Pseudomonas* sp., and strain IS1 was identified as an *Enterobacter* sp..

Correlation between sorption capacity and the properties of sorbates was addressed by many researchers (Dobbs et al., 1989; Woods, 1985; Karickhoff, 1981). The octanol-water distribution coefficient, K_{ow} , was commonly used to describe this correlation for neutral organic compounds, where the K_{ow} is defined as $K_{ow} = C_{Oct} / C_w$, in which C_{Oct} and C_w are the equilibrium concentration of the organic compound in the octanol layer and in the water layer, respectively. For ionizable organic compounds such as chlorophenols, the dissociation constant, K_a , was also used as a descriptor (Schwarzenbach et al., 1993; Woods, 1985) to account for the variation of sorption capacity with pH, since the sorption tendency of chlorophenol molecules to microbial solids is much higher than that of chlorophenolate ions. Solubility, functional groups (number and type) and molecule structure of target organic compounds were also used to evaluate sorption (Wang and Grady, 1994, Schwarzenbach et al., 1993; Brusseau and Rao, 1991) since all of these properties are correlated with the partitioning behavior of the target organic compounds. However, since many factors besides sorbate properties can affect the sorption results, the derived equations which associate the sorption capacity with properties of the sorbate in their studies have only limited use.

The pH effects would involve the ionization of either ionizable sorbates or charged groups on the cell membrane and cell wall if H^+ -induced damage to bacteria is not caused (Wedemeyer, 1966). Woods (1985) observed that sorption of chlorophenols to anaerobic sludge decreased as the pH value of solvents increased. This was explained by the difference in partition coefficients between chlorophenol molecules and

chlorophenolate ions. Woods (1985) showed that equilibrium sorption for a specific chlorophenol could be described by a relation between pH, pK_a and sorption coefficient, K_d . This is a consistent observation with sorption of chlorophenol to soil (Lee et al., 1991).

Although temperature is a routine parameter affecting biological treatment, few investigations on the effect of temperature on the sorption of toxic organic compounds to biological solids have been reported. Tsezos and Bell (1987) showed that the effect of temperature on biomass sorption was related to the properties of the chemicals. With activated sludge as sorbent, sorption of lindane ($C_6H_6Cl_{12}$) increased as temperature decreased; however, sorption of diazinon and malathion showed the opposite result. The van't Hoff equation ($\Delta H = -Rd \ln K / d(1/T)$) was used to describe the enthalpy or heat of sorption. In a study of sorption of halides in a lagoon, Amy et al. (1988) indicated that higher temperature seemed to favor sorption of small molecules (less than 1000 g/M) but sorption of larger molecules (larger than 1000 g/M) was more effective at low temperature. Yan and Allen (1994) also reported that the sorption of high molecular weight organochlorines was more effective at low temperature since their sorption is exothermic. No detailed study on the effect of temperature on sorption of chlorophenols to anaerobic sludge was found.

Multicomponent sorption can be a common situation in biological treatment systems but very few investigations has been conducted on this issue. Wang et al. (1993)

conducted an investigation on Multicomponent sorption. They observed that when using the same sorbent, in the presence of competing compound(s), occurrence of sorption intereffect depends on the compounds used. Based on experimental results, the authors stated that when adsorption dominated sorption, the concentration of competing species would affect the degree of competition; when partitioning dominates, the concentration of the competing species has little impact on sorption result. The multiple sorption of chlorinated aliphatics and aromatics to soil was investigated and modeled by McGinley et al. (1993). Ionic strength may vary significantly among different industrial wastewaters. Influence of ionic strength on the sorption of PCP to clay was reported by Stapleton et al. (1994). They observed an increase in sorption as a function of ionic strength when pH is higher than 8. An equation to characterize the variation of the sorption coefficient in the presence of dissolved salts was given by Schwarzenbach et al. (1993).

2.1.3 Sorption/Desorption Equilibrium and Sorption Kinetics

Sorption of toxic organic compounds to biological solids is generally considered to be a rapid process. In the sorption of lindane, PCP, diazinon and 2-chlorobiphenyl (PCB) to activated sludge, 1 and 3 d were allowed for achieving sorption equilibrium in Tsezos and Bell's experiment (1989). Kennedy et al. (1992) reported that sorption results for 16 chlorophenol congeners to anaerobic granules at 3 h were very similar to those at 24 h. Dobbs et al. (1989) used a 6 h contact time in order to achieve dynamic equilibrium in sorption. However, it was indicated that 52~95% of the sorbed chemical at sorption

equilibrium (varied with chemicals and sludge type) was sorbed to microbial solids within 30 min.

Desorption of toxic organic compounds from soil and sediments has been studied extensively (Stapleton et al., 1994; Susarla et al., 1993; Lee et al., 1991) but the investigations with microbial solids are few. The rate of desorption of toxic organic compounds from activated sludge was reported to be equal to or less than the biosorption rate (Tsezos and Bell, 1989). Sorption-desorption nonsingularity (or hysteresis) was observed in a sorption test for some chlorophenols (Kennedy et al., 1992). It was reported that sorption of 2,4,6-trichlorophenol to anaerobic granules is reversible, but a small degree of hysteresis was observed for 3,4-dichlorophenol and 3-monochlorophenol. Hysteresis in sorption/desorption of PCP with anaerobic granules was also reported (Wu et al., 1993). Lindqvist and Endfield (1992) studied sorption of DDT and HCB by five pure aerobic microbial cultures with different overall surface hydrophobicity and found that 24-68% of total mass sorbed was desorbed, and that the desorption partition coefficients for all five live strains were 1.5 to 9 times higher than the sorption coefficients.

Sorption behavior of toxic organic compounds to biological solids has been so far almost exclusively described by sorption isotherms. The Freundlich equation, $q = KC_e^{1/n}$; linear isotherm, $q = K_d C_e$; and Langmuir isotherm, $q = abC_e/(1 + bC_e)$ are the most commonly used, where, q is equilibrium concentration of sorbate in sorbent; C_e is equilibrium concentration of sorbate in liquid phase; K and n are Freundlich constants;

K_d is partition or sorption coefficient; a and b are Langmuir constants. For sorption with weak surface bonding or specific site bonding, which is related to both sorbate and sorbents, the Freundlich equation can be reduced to the linear isotherm case with $n=1$ (Schwarzenbach et al., 1993).

While the linear isotherm is applicable, for nonionizable organic compounds and a specific sorbent, the K_d is well correlated to K_{ow} . The relationship between K_d and K_{ow} for the sorption of some organic compounds to microbial solids has been reported (Dobbs et al., 1989). For ionizable organic compounds like chlorophenols, a strong correlation between K_d (based on total chlorophenol at certain pH) and K_{ow} does not exist since the different dissociation level for each chlorophenol at a certain pH and the K_d value is a lumped sorption coefficient for both chlorophenol molecules and chlorophenate ions (Kennedy et al., 1992; Woods, 1985). Using the dissociation constant, K_a , to account for the pH dependency, Woods (1985) described the relation between the lumped sorption coefficient, K_d , and the sorption coefficients for chlorophenol molecules and chlorophenate ions in the sorption of chlorophenols to anaerobic granules. The relation has the same form as that for the sorption of ionizable organic chemicals to other natural solids (Schwarzenbach et al., 1993) since the same mechanism is involved in these processes.

A distributed reactivity model (DRM) which describes the sorption of toxic organic pollutants to different reaction regions in soil and sediments by using a simple

combination of linear isotherm and the Freundlich equation was developed by Weber et al. (1992). Wang et al. (1993) proposed the adsorption-partitioning model (A-P) to account for the sorption of organic compound to microbial solids. The A-P model is a two-term equation, a linear isotherm is used for partitioning and the Langmuir isotherm for adsorption.

$$q = K_d C_e + abC_e / (1 + bC_e)$$

Using a similar form of the A-P model for sorption of chlorophenols to clay, Stapleton et al. (1994) described the sorption of chlorophenol molecules by a linear isotherm term and the sorption of chlorophenate ions by the Langmuir equation term. Wang et al. (1993) extended the A-P model to multicomponent systems by simple addition of sorption for each component. However, inter-effects among the various components in multiple sorption were not considered. An extended DRM model for sorption of multicomponents to soil and sediments with consideration of competitive effects has also been reported (McGinley et al. 1993). No kinetic model for sorption and desorption processes of toxic organic compounds to biological solids was found in the literature. However, investigations considering diffusion limitation have been reported in decontamination of soil and sediments or sorption to pure cultures (Hu et al., 1994; Stapleton et al., 1994; Susarla et al., 1993).

2.1.4 Nonideal Sorption

In modeling contaminant transport in the subsurface, the sorption process has often been

simplified as ideal sorption, which assumes instantaneous sorption equilibrium, linear isotherms and no sorption-desorption hysteresis (Brusseau and Rao, 1989). However, this simplification has been challenged by the deviations in predicting experimental data with the simplified model (Valocchi, 1985). In recent years, investigations on nonideal sorption have been conducted in order to model ground water contaminant transport (Spurlock et al., 1995; Lee et al., 1991; Brusseau and Rao, 1989). Nonideal sorption behavior has been attributed to nonequilibrium sorption, isotherm nonlinearity and sorption-desorption hysteresis.

However, since dynamic modeling of the removal of toxic organic compounds in biological treatment system is still at an initial stage, very little attention has been paid to nonideal sorption to biological solids. In the few models describing biological treatment of organic chemicals, linear sorption equation based on ideal sorption were used (O'Brien and Teather, 1995; Parker et al., 1994; Jacobsen et al., 1993).

2.1.5 Effect of Sorption on Degradation

Effect of sorption on degradation has been studied with a variety of sorbents including soil (Ogram et al., 1985), clays (Marshman and Marshall, 1981), sediments (Gordon and Millero, 1985), activated carbon, zeolite (Alvarez-Cohen et al., 1993) and pure microbial cultures (Wang and Grady, 1993). Different effects were observed when these particles were added to microbial cultures at various substrate concentrations (Gordon and Millero,

1985). Generally, it was held that sorption by inert solids or sorptive biomass incapable of degradation decreases biodegradation rates by decreasing the availability of the substrate to the microbes (Gordon and Millero, 1985) or increases the biodegradation rate by decreasing toxicity (Hu et al., 1994). Orgam (1985) investigated the effect of sorption of (2,4-dichlorophenoxy)acetic acid (2,4-D) in 4 different soils on the biological degradation rates by fitting experimental data to three assumed models. The results indicated that sorbed and solution-phase (suspended) bacteria degraded the organic compound with almost equal efficiencies but 2,4-D sorbed to soil was completely protected from biological degradation.

Very little information about the effect of sorption on degradation rates of toxic organics by microbial solids, such as activated sludge and anaerobic sludge granules, was found in the literature. In biological treatment systems, microbial solids are both sorbent and degrader. It is not clear whether sorption that causes toxic organic compounds to be concentrated onto the sorbent may enhance their microbial uptake or not. Wang and Grady (1993) used a sorptive biomass that was incapable of degrading the target chemical to investigate the effect of sorption on degradation, which is not a completely matched situation for microbial solids in bioreactor. Some investigators have considered sorption in modeling the removal of toxic organic removal in the aerobic treatment process (O'Brien and Teather, 1995; Jacobsen et al., 1993) and in municipal sludge digestion (Parker et al., 1994). In their studies, the assumption was made that only toxic organics in solution can be biodegraded by microbial solids. However, validity of the assumption was not

demonstrated.

Direct contribution of sorption to the removal of some organic compounds was evaluated based on the amount of the chemical sorbed to sludge and the amount of sludge discharged and was reported to be at about 1% or negligible in the long run (Fahmy et al., 1994; Yan and Allen, 1994). However, the indirect contribution of sorption on the removal by influencing the availability and toxicity of the toxic organic compounds to microbial solids in bioreactors was not addressed.

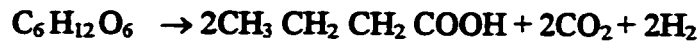
2.2 Degradation

2.2.1 Anaerobic Degradation of Primary Organic Matter

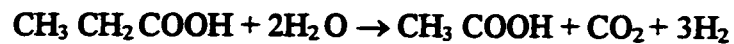
The microbial transformation mechanism and kinetics of primary organic matter such as carbohydrates, lipids and proteins under anaerobic conditions is now well understood. Figure 2-2 shows the basic anaerobic metabolic schemes and the metabolic groups involved in the degradation processes.

For simple organic compounds the stoichiometry of anaerobic degradation has been defined (Pavlostathis and Giraldo-Gomez, 1991). The stoichiometry for anaerobic degradation of glucose, HPr and HAc was summarized by Mosey (1983) as follows).

For acidogenic bacteria:



For acetogenic bacteria:



For acetoclastic and hydrogen-utilizing methanogenic bacteria:

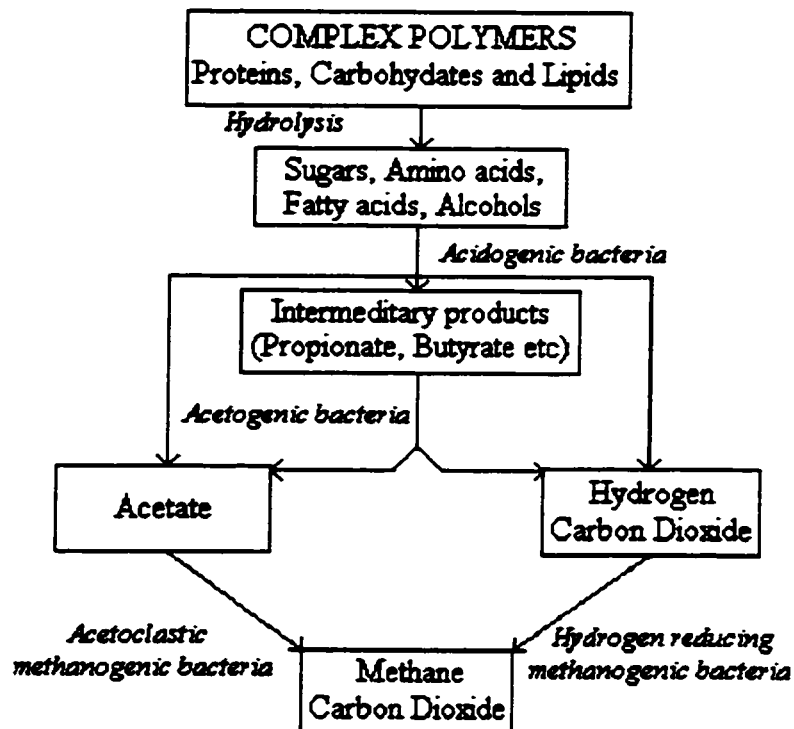
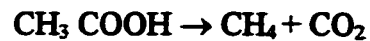


Figure 2-2 Reaction scheme for the anaerobic degradation of biological polymers (Adapted from Pavlostathis and Giraldo-Gomez, 1991)

It is known that carbon flow in the reaction scheme (Figure 2-2) for formation of each intermediary product is significantly influenced by hydrogen partial pressure since hydrogen transfer accounts for the majority of the interspecies electron transfer in anaerobic treatment systems (Schmidt and Ahring, 1995). Under low hydrogen partial pressure ($pH_2 < 10^{-6}$ bar), nearly all substrate carbon goes exclusively to acetic acid, CO_2 and hydrogen (McCarty, 1981). When the metabolic capacity of the methanogenic bacteria can not balance the increasing metabolic activity of the primary fermenters due to a higher substrate input, reduced metabolites, such as propionic acid, butyric acid and even long chain fatty acids can accumulate in the system (Schink, 1988).

Since accumulation of different intermediates can occur in anaerobic degradation systems, substrate and product inhibition have been observed. Andrew and Graef (1971) first considered substrate (unionized HAc) inhibition of methanogenesis in their kinetic study. Other substrate and product inhibitions, such as influence of HPr inhibition on degradation of itself or HAc degradation, and influence of HAc inhibition on degradation of HPr, have also been observed and modeled (Kus and Wiesmann, 1995; Mawson et al., 1991). Since propionic acid degradation is only possible at very low hydrogen partial pressure ($0 \sim 10^{-4}$ bar), hydrogen inhibition can occur in highly loaded systems or under severe transient operating conditions. Investigation of hydrogen inhibition has been reported and some efforts have been made to use hydrogen as a parameter to control anaerobic treatment systems (Strong and Cord-Ruwisch, 1995; Pauss and Guiot, 1993; Mosey and Fernandes, 1989; Archer et al., 1986). However, volatile fatty acids (VFAs)

have recently been considered to be a better indicator of operational control than hydrogen since the latter may be more related to the speed of substrate input to the treatment system (Ahring et al., 1995).

Degradation kinetics of primary organic matter, including HAc and HPr, with mixed culture in anaerobic reactors has been extensively investigated in the last 30 years. The kinetics of anaerobic treatment was reviewed by Pavlostathis and Giraldo-Gomez (1991). The Monod equation was used successfully in describing anaerobic degradation without inhibition by Lawrence and McCarty (1969). Andrews and Graef (1971) used the Haldane-type inhibition function to account for substrate inhibition of methanogenesis and considered unionized acetate instead of its total concentration as the limiting and inhibiting substrate in degradation. The results from these two investigations have been extensively cited and modified in later kinetic studies and then used in modeling different kinds of anaerobic treatment systems. Consequently, according to the consideration of limiting substrate in kinetic modeling, the investigators on anaerobic degradation kinetics of major intermediates, using HAc as an example, can be classified into two groups: one group considering the total HAc as real substrate (Ahring and Westermann, 1987; Lin et al., 1986; Heyes and Hall, 1983) and another group using unionized HAc as real substrate in their models (Kus and Wiesmann, 1995; Morvai et al., 1992; Fukuzaki et al., 1990a; Yang and Okos, 1987). Although total HAc has been used as limiting substrate by many researchers due to its simplicity, the unionized VFAs have been experimentally proven to be real limiting substrates (Kus and Wiesmann, 1995). Mosey (1983) proposed a kinetic

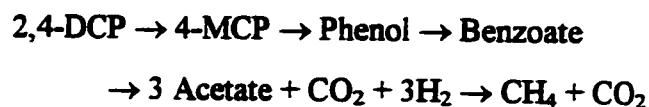
model to account for hydrogen inhibition and similar models were also developed by others (Fukuzaki et al., 1990b). However, kinetic modeling of hydrogen inhibition with experimental verification is not yet available.

2.2.2 Anaerobic Degradation of Chlorinated Phenols

Reductive dehalogenation is the initial step in biodegradation of chlorinated phenols under anaerobic conditions. Dechlorination may be followed by cleavage of the aromatic ring and ultimately mineralization to CH_4 and CO_2 (Kennes et al., 1996; Häggblom et al., 1993; Zhang and Wiegel, 1990). However, limited degradation of chlorinated phenols has been frequently documented (Mohn and Kennedy, 1992; Nicholson et al., 1992; Boyd and Shelton, 1984). Mohn and Kennedy (1992) reported that anaerobic granules, enriched in a UASB reactor with sucrose/HAc based wastewater and 2,3,6-trichlorophenol (2,3,6-TCP), 2,4,6-trichlorophenol (2,4,6-TCP) and 3,5-dichlorophenol (3,5-DCP), did not appear capable of degrading 3-MCP and 4-MCP. The reason for the variation in the extent of degradation seems related to the richness of sulfate-reducing bacteria in enriched mixed culture and available electron acceptors in degradation media (Kennes et al., 1996). However, no comprehensive study on this issue was found in the literature.

Reductive dechlorination pathways of chlorinated phenols under anaerobic conditions has been studied using different anaerobic sludges (Mikesell and Boyd, 1986; Woods, 1985; Boyd and Shelton, 1984) and the observed pathway varies with the

microbial consortia used, such as biomass unacclimated and acclimated to different chlorinated phenols (Nicholson et al., 1992). In anaerobic reactors with acclimated sludge, dechlorination usually occurs progressively in order of preference: *ortho*, *para* and *meta* but different dechlorination sequences like *ortho*, *meta* and *para* have also been observed (Nicholson et al., 1992; Woods, 1985). Zhang and Wiegel (1990) conducted a detailed investigation on the sequential anaerobic degradation of 2,4-DCP in acclimated freshwater sediments and proposed a degradation pathway for the degradation of 2,4-DCP:



The degradation pathway was not only observed by accumulation of each intermediate in 2,4-DCP degradation, but also for each identified intermediate, except for 4-MCP. The rates of degradation were not reported. However, partial degradation of 2,4-DCP has been frequently reported, where only one step of dechlorination from 2,4-DCP to 4-MCP was observed and degradation of 4-MCP was undetectable or very slow (Mohn and Kennedy, 1992; Häggblom and Young, 1990; Woods, 1985).

Only a few anaerobic dechlorinating organisms have been isolated. *Desulfomonile tiedjei* (Dolfing and Tiedje, 1987; Shelton and Tiedje, 1984), spore forming bacteria (Zhang and Wiegel, 1990) and a *Clostridium*-like bacterium (Madsen and Aamand, 1992) have been reported being involved in dechlorination. In investigating the effect of electron donor and acceptor on dechlorination, eubacteria, not methanogenic bacteria, were

suggested as dechlorinators in anaerobic treatment systems (Perkins et al., 1994; Distefano et al., 1992). Based on the sequential appearance of the degradation intermediates and different adaptation time for individual transformation steps in complete mineralization of 2,4-DCP to CH_4 and CO_2 , Zhang and Wiegel (1990) proposed that five different organisms were involved in this sequential degradation process. Two newly isolated dechlorinating anaerobes were recently reported (Christansen et al., 1995; Utkin et al., 1995). Since only a limited number of microbes capable of performing reductive dechlorination were isolated and anaerobic dechlorination often involves more than one kind of organism, the knowledge in biochemistry of reductive dechlorination is limited.

A few investigations on the effect of environmental conditions, such as temperature and pH, on anaerobic degradation of chlorinated phenols have been reported. Reductive 2,4-DCP dechlorination by anaerobic sediment slurries was observed to occur only in temperatures between 5-50°C, and degradation rates increased exponentially between 15-30°C, had a second peak at 35°C, and decreased to about 5% of the peak activity at 40°C (Kohring et al., 1989). Juteau et al. (1995) reported that dechlorination was most efficient at 37°C and that dechlorination of PCP to 3-chlorophenol (3-MCP) was still observed after biomass had been subjected to heat treatment (80°C, 60 min), suggesting that spore-forming bacteria were responsible for dechlorination. Conflicting observations on the effect of pH on dechlorination have been reported. Armenante et al. (1993) observed that reductive dechlorination of 2,4,6-TCP occurred only if the pH was within the range 8.0-8.8 and the final product was 4-MCP. Togna et al. (1995) also

reported limited dechlorination of 2,4,6-TCP to 4-MCP in an anaerobic reactor only in alkaline media (pH 8-9). However, other studies have indicated that reductive dechlorination can proceed within the normal range of pH (7.0-7.5) in anaerobic reactors (Kennes et al., 1996; Woods, 1985).

A review of the toxic organic degradation kinetics was given by Grady (1991). Compared with the extensive qualitative studies of anaerobic degradation of chlorophenols, quantitative investigations on the degradation kinetics under anaerobic conditions are quite few. Hendriksen and Ahring (1992) investigated the kinetics of PCP transformation in anaerobic granular sludge and determined a maximum degradation constant, V_m , and half-saturation constant, K_s , in describing the PCP dechlorination rate with the Mechelis-Menten equation. Kinetics of the sequential dechlorination of 2,4,6-TCP by an anaerobic mixed culture from a sewage treatment plant was studied by Armenante et al. (1995). They found that Monod equation was successful in accounting for experimental data from batch tests. In some other investigations of anaerobic degradation of chlorophenols, linear degradation kinetics were assumed in interpreting the maximum dechlorination rate (Wu et al., 1993; Mohn and Kennedy, 1992). However, effects of inhibition and sorption on the degradation rate were not considered in these studies. In investigations of PCP degradation by aerobic culture, the Haldane type inhibition function was used to describe the degradation and inhibition (Gu and Korus, 1995; Hu et al., 1994; Klecka and Maier, 1985). Degradation kinetics of 2,4-DCP by anaerobic granules has not been completely dealt with yet.

2.2.3 Substrate Interaction in Multiple Substrate Degradation

The reported substrate interactions in simultaneous degradation of chlorinated phenols and primary substrates in anaerobic treatment systems have mainly focused on the qualitative effects of primary substrates on reductive dechlorination (Juteau et al., 1995; Perkins et al., 1994; Mohn and Kennedy, 1992; Hendriksen and Ahring, 1992). Cometabolism and secondary substrate utilization have been used to account for the effect of electron donor on the dechlorination process (Alexander, 1981; Rittmann and McCarty, 1980) based on whether the degradation of toxic organics can provide energy for growth of the degraders or not. The influence of electron acceptors on reductive dechlorination has also been reported recently (Häggbloom et al., 1993a; Mohn and Kennedy, 1992). However, quantitative information on substrate interaction in simultaneous degradation of chlorophenols and primary organic substrates during anaerobic treatment is scarce. The kinetics describing the effect of monochlorophenols on the degradation of acetate and ethanol using unacclimated anaerobic sludge have been reported (Kim et al., 1994; Davies-Venn et al., 1992) but the degradation of monochlorophenols was not considered in their studies. The importance of understanding the substrate interaction in simultaneous degradation of primary substrates and toxic organic compounds in biological treatment was addressed by Grady (1991).

Enhanced dechlorination of many chlorinated organic compounds was experimentally observed and enhancement mechanisms such as cometabolism (Alexander,

1981), secondary substrate utilization (Rittmann and McCarty 1980) and enhanced flocculation (Hess et al., 1990) have been proposed. In anaerobic degradation of chlorophenols, if only reductive dechlorination occurs (no cleavage and degradation of the ring system), then cometabolism would be necessary to sustain biodegradation (Shelton and Tiejie, 1984). While chlorinated phenols can be mineralized to CH_4 and CO_2 , primary substrates are utilized as secondary substrates to support or enhance the dechlorination process. Many easily degradable organic compounds (Table 2-2) have been used as electron donors to support anaerobic dechlorination but only a few of them have been reported to have a direct enhancing or stimulating effect on dechlorination of chlorophenols. In a study of PCP transformation in anaerobic granular sludge, Hendriksen and Ahring (1992) observed that only glucose had a stimulative effect on the rate of PCP dechlorination in a comparison of various supplementary carbon compounds including acetate, butyrate, formate, hydrogen, carbon dioxide and ethanol. However, Mohn and Kennedy (1992) reported that the addition of electron donors had negligible stimulating effects on dechlorination by anaerobic granular sludge and suggested that endogenous electron donors could also support dechlorination. From Table 2-2, it seems that the stimulating effect of a specific cosubstrate varies from case to case although glucose was observed to have a positive effect on dechlorination in most references. Enhanced biodegradation of highly chlorinated phenols by the presence of less chlorinated phenols or using phenol as primary substrate was also reported (Duff et al., 1995; Lu and Chen, 1992).

Besides degradation of chlorophenols under methanogenic conditions, dechlorination using other alternative electron acceptors, such as sulfate, nitrate, manganese and ferric ions, has attracted attention in recent years. Kohring et al. (1989) observed that in the presence of sulfate, 2,4-DCP and 4-MCP were transformed stoichiometrically to 4-MCP and phenol, respectively. Häggblom et al. (1993a, 1990) observed that dechlorination and complete mineralization of 2-MCP, 4-MCP and 2,4-DCP was coupled to sulfate reduction and that assimilation of monochlorobenzoates was

Table 2-2 Direct stimulating effect of cosubstrate on anaerobic CPs degradation

Cosubstrate	CP degraded	Culture	Effect of co-substrate ^a	Reference
Yeast extract, Casamino acids, Peptone, Glucose, Galactose, Rhamnose, Arabinose, Ribose	2,4,6-TCP, 2,4-DCP	Enriched from sewage digester sludge	+, +, +, 0, 0, 0, -, -, -	Madsen and Aamand, 1992
Glucose	PCP	UASB sludge	+	Hendriksen et al., 1992
Glucose, Hydrogen, Formate, Butyrate, Ethanol, Acetate	PCP	UASB granular sludge	+, 0, 0, 0, 0, 0	Hendriksen and Ahring, 1992
Hydrogen, Formate, Acetate, Propionate, Sucrose	2,3,6-TCP	UASB granular sludge	0, 0, 0, 0, +	Mohn and Kennedy, 1992
Hydrogen, Acetate, Fructose	2,4,6-TCP	Methanogenic culture from sludge digester	0, 0, 0	Perkins et al., 1994
Glucose, Formate, Lactate, Yeast extract, Acetate	PCP	Methanogenic consortium	0, 0, 0, 0, -	Juteau et al., 1995
Ethanol, Methanol, Acetate, Glucose	2,4,6-TCP	Methanogenic culture from sludge digester	+, 0, 0, 0	Pak D., 1996

^a The symbol, '+', means: has a stimulating effect on dechlorination; '0': supports or has no negative influence on dechlorination; '-': does not support or has a negative influence on dechlorination.

coupled to denitrification. Recently, Häggblom and Young (1995) reported that a sulfidogenic consortium, enriched from an estuarine sediment that used 2-MCP, 3-MCP and 4-MCP as the only carbon sources for 5 years, can degrade 4-MCP coupled with sulfate reduction. Kennes et al. (1996) observed that addition of sulfate enhanced the initial chloride release rate and accelerated the process of mineralization of PCP. These results suggested that sulfate reducing bacteria may be an active dechlorinator under anaerobic conditions. However, it was also observed that addition of the other electron acceptors has negligible effect on dechlorination in anaerobic reactors (Juteau et al., 1995; Häggblom et al., 1993b; Mohn and Kennedy, 1992). Most recently, Wrenn and Rittmann (1995) proposed a conceptual model for substrate interactions that includes exogenous and endogenous electron donors, and multiple exogenous electron acceptors for reductive dehalogenation of chlorinated aliphatic compounds (Figure 2-3). The model suggested that, under most conditions, primary electron donor substrates stimulate reductive dehalogenation, while primary electron acceptors reduce dehalogenation. However, effect of chlorinated compounds on the degradation of primary electron donor was not considered.

Toxicity of toxic organic compounds to degradation of primary organic substrates in anaerobic process has been documented in early studies, and the basic anaerobic toxicity assay (ATA) has been described by several authors (Owen et al., 1979; Shelton and Tiedje, 1984). However, there is limited information regarding the effect of toxic organic compounds on the degradation kinetics of cosubstrates in multiple substrate degradation systems. Davies-Venn et al. (1992) investigated the impact of monochlorophenols and

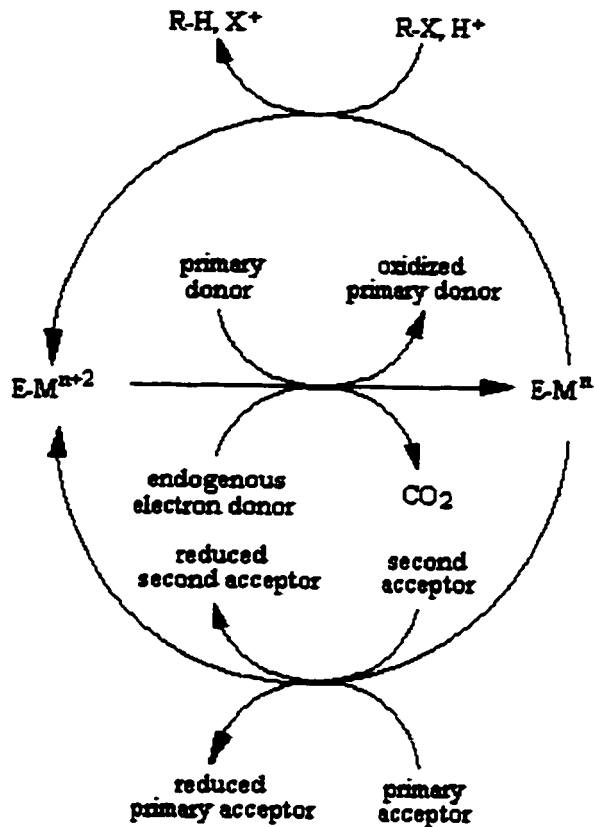


Figure 2-3 Conceptual model for substrate interactions in reductive dehalogenation. R-X and R-H represent halogenated-aliphatic substrate and dehalogenated-aliphatic substrate, respectively. E-Mⁿ is the reduced dehalogenase and E-Mⁿ⁺² is the oxidized dehalogenase (After Wrenn and Rittmann, 1995).

monochloroanilines on the kinetics of acetoclastic methanogenesis and found that both chemicals exhibited a mixed inhibition pattern with respect to acetate degradation. The same inhibition pattern was reported by Saéz and Rittmann (1993) for degradation kinetics of phenol and 4-MCP. To assess the fate and effect of toxic organic chemicals in anaerobic treatment processes, Young and Tabak (1993) proposed a multilevel protocol to determine the degradation kinetics for which all routine inhibition functions, i.e.,

competitive, noncompetitive, uncompetitive, and mixed were considered. Experimental verification of this protocol with monochlorophenols was recently reported (Kim et al., 1994). Specific investigation on the impact of highly chlorinated phenols on the degradation of important intermediates in anaerobic process, such as HAc and HPr, was not found in literature.

A number of kinetic models describing cometabolism of toxic organic compounds in the absence and presence of cosubstrate have been proposed. Most of them deal with pure cultures and aerobic conditions (Chang and Alvarez-Cohen, 1995; Chang et al., 1993; Alvarez-Cohen and McCarty, 1991; Schmidt et al., 1987, 1985). Some of these models were reviewed by Criddle (1993). In investigations on degradation kinetics for the same type of dual or multiple substrates, a modified Monod equation was often used (Machado and Grady, 1989; Klecka and Maier, 1988). Compared with traditional models that do not consider substrate interaction, the cometabolism models account for many more features, such as loss of activity in resting cells due to endogenous decay and transformation of toxic organic compounds (nongrowth substrate), increase of the rate and extent of cometabolism in the presence of cosubstrate (further classified as growth and energy substrates) and inhibiting interactions (competitive inhibition and product toxicity) (Criddle, 1993). A cometabolic kinetic model incorporating enzyme inhibition, inactivation, and recovery was also documented (Ely et al., 1995). Recently, two investigations on substrate interaction in anaerobic dechlorination were reported. In the conceptual model proposed by Wrenn and Rittmann (1995) for reductive dechlorination, a

Monod-like expression was used to account for the effects of electron donor and acceptor on reductive dehalogenation (Figure 2-3). Skeen et al. (1995) developed a kinetic model of chlorinated ethylene dechlorination under methanogenic conditions. A simple Monod equation was used to describe the simultaneous degradation of primary substrate in the degradation system. In those two models, inhibitory effects and loss of biomass activity during substrate interaction were not included.

2.3 Dynamic Modeling of Anaerobic Treatment System

Dynamic modeling of anaerobic treatment systems has been extended since the works of Lawrence and McCarty (1969) and Andrews and Graef (1971) and is mostly for the degradation of primary organic matter. Few investigations have pursued dynamic modeling of the removal of toxic organic compounds in anaerobic reactors (Parker et al., 1994).

Dynamic modeling of treatment of primary organic matter in anaerobic systems has been conducted since the 1960s. Recently, Sam-Soon et al. (1991) developed a model for UASB systems treating carbohydrate wastewaters. Their model proposes 12 essential processes incorporating 16 essential compounds that includes different physical types of COD and nitrogen. A similar but simpler model for sewage treatment was also reported by Siegrist et al. (1993). The modeling of hydrolysis controlled anaerobic digestion was presented by Jain et al. (1992). Fernandes et al. (1993) developed a dynamic model for

carbohydrate substrate degradation in sequencing batch anaerobic UASB reactors. In a universal model of anaerobic conversion of complex organic material, sulfate-reducing organisms were included and the model was used for investigating the start-up experiments for food industry wastewater (Vavilin et al. 1994).

A few efforts have also been made to predict the removal of toxic organics in anaerobic treatment systems without considering the degradation of primary organic matter. Parker et al. (1994) developed a dynamic model considering sorption and degradation to account for the fate of 10 toxic organic compounds, including 3-MCP, 4-MCP, 2,5-DCP and 2,4,5-TCP, during primary sludge digestion. A linear sorption isotherm and first-order kinetics for degradation were used in model building. No model for describing the simultaneous treatment of both primary organic matters and toxic organic compounds in anaerobic treatment system was found in the review of the literature.

EXPERIMENTAL PROGRAM, MATERIALS AND METHODS

3.1 Experimental Program

The experimental program consisted of five groups of experimental investigations (Table 3-1), which were determined based on the objectives of this study. A detailed experimental design for each group of investigations will be presented in the related part of the experimental results and analysis in the following chapters.

3.2 Materials

Chemicals. All phenolic compounds (phenol, 3-MCP, 4-MCP, 2,4-DCP, 3,4-DCP, 2,4,6-TCP, and PCP) used in the experiments were products of Aldrich Chemicals with 99% purity. Their solutions were made in 0.01 M NaOH, diluted to required concentrations with distilled/deionized Milli-Q water and adjusted to pH 7.5 using H₂SO₄. The prepared solutions were stored in the dark in a refrigerator controlled at 2~4°C before use.

Metabolic inhibitors. To exclude the effect of possible degradation on sorption and minimize cell damage, sodium azide (NaN₃) was used as the inhibitor of anaerobic granule

Table 3-1 Summary of the experimental program

Code	Main objectives (Chapter for related results)	Experimental mode	Experimental setup	Toxic organics used	Cosubstrates used	Type of sludge used
E1	Effect of metabolism on sorption and major factors affecting sorption equilibrium (Chapter 4).	Batch	Serum bottles	2,4-DCP and PCP	Not used	Unacclimated anaerobic granules enriched with sucrose/HAc (active; dormant and inactive)
E2	Evaluation of nonideal sorption under dynamic condition (Chapter 4).	Continuous	Completely-mixed anaerobic reactor; Plug-flow sludge column reactor	3-MCP, 2,4-DCP, 3,4-DCP, 2,4,6-TCP, PCP	Not used	Inactive anaerobic granules from Lake Utopia Paper Ltd; 2,4-DCP acclimated inactive anaerobic granules enriched with sucrose/HAc.
E3	Degradation kinetics of 2,4-DCP. Effect of biosorption on degradation (Chapter 5).	Batch	Serum bottles	2,4-DCP	Not used	2,4-DCP acclimated active anaerobic granules enriched with sucrose/HAc.
E4	Substrate interaction: (a) cosubstrate on 2,4-DCP degradation; (b) degradation kinetics of sucrose, HPr and HAc with 2,4-DCP (Chapter 5).	Batch	Serum bottles	2,4-DCP	Sucrose, HAc and HPr	2,4-DCP acclimated active anaerobic granules enriched with sucrose/HAc.
E5	Data for the validity and verification of a dynamic model for the UASBs (Chapter 6).	Continuous	Four UASB reactors	2,4-DCP	Sucrose, HAc and HPr	2,4-DCP acclimated active anaerobic granules enriched with sucrose/HAc.

activity in experiments E1 and E2 (Table 3-1). NaN_3 inactivates metabolic activity of all microorganisms in sludge (acidogenic, acetogenic and methanogenic) by inhibiting the electron transfer at cytochrome B. The concentration of the prepared solution for sodium azide was 1% and the final concentration used in the experiment was 0.1% (w/v). Previous tests in this experiment, based on biogas production and VFA concentrations, indicated that complete inhibition of anaerobic granular activity was achieved within 10 h after addition of the chemical inhibitor and the biomass activity could be recovered within 2 h after the inhibitor was washed out.

By inhibiting the reduction of methyl-coenzyme M (Perkins et al., 1994), Bromoethanesulfonic acid (BESA) is a specific inhibitor of methanogenic organisms. This inhibitor was used in experiment E4 to test the possible syntrophic relation between acetoclastic methanogenic bacteria and dechlorinating bacteria in the anaerobic dechlorination process. Previous tests in this investigation showed that, with degradation of HAc, acetoclastic methanogenesis was inhibited in 3 h with a BESA concentration of 0.2% (w/v) or 18 h with 0.1%. A BESA concentration of 0.2% was finally used in experiment E4. Since a much higher concentration of BESA (50 mM) is needed for inhibiting hydrogen-reducing bacteria (Zinder et al., 1984), only acetoclastic methanogenesis was inhibited with the concentration used.

Anaerobic granules. Three types of anaerobic granular sludges were used in these investigations (Table 3-1). The sludges used were: chemi-thermal mechanical pulp

(CTMP) anaerobic granules, unacclimated anaerobic granules and acclimated anaerobic granules.

(1) CTMP anaerobic granules

These anaerobic granules were obtained from Lake Utopia Paper Ltd., Canada. This sludge was used to treat CTMP wastewater from hydrogen peroxide bleaching processes and had never been acclimated or exposed to wastewater containing chlorinated phenols. The average granular size and the VSS/SS ratio of this sludge were 0.5 ± 0.3 mm and 0.908 ± 0.001 , respectively.

(2) Unacclimated anaerobic granules

Using CTMP anaerobic granules as seed biomass, the unacclimated anaerobic granules were cultivated in two lab-scale continuous UASB reactors which were operated at 35°C. During cultivation, one of the reactors was operated at a low specific organic loading rate (SOLR/low) and the other at a high specific organic loading rate (SOLR/high). Both reactors were fed with a sucrose/HAc based wastewater (Appendix A) at SOLRs of 0.27 and 0.66 kg COD/kg VSS-d, respectively, for 4 months. The VSS/SS ratios of harvested granules were 0.896 ± 0.003 for sludge from SOLR/low and 0.915 ± 0.003 from SOLR/high. The ability of the unacclimated anaerobic granules to degrade 2,4-DCP was tested. Results showed that at least five days of acclimation was needed for the sludge to begin dechlorinating 2,4-DCP.

(3) Acclimated anaerobic granules

The 2,4-DCP acclimated anaerobic granules were cultivated in four lab-scale continuous UASB reactors, using CTMP anaerobic granules as seed sludge. The feed wastewater for the reactors was similar to that for cultivating unacclimated anaerobic granules, except it contained about 10 mg/L of 2,4-DCP. Before the sludge was harvested to be used in batch experiments, the UASB reactors had been continuously operated for 9 months. The properties of anaerobic granules from the UASB reactors are summarized in Table 3-2. The acclimated sludges from reactor R1, R3 and R4 were harvested and used in experiments E3 and E4 (Table 3-1). The sludge from R1, inactivated with inhibitor NaN_3 , was used in some tests in experiment E2.

Table 3-2 Physical properties of acclimated anaerobic granules

Reactor number	Granule size (mm)	VSS/SS	Moisture content (%)	$K_{d,DCP}$ (L/gVSS)	$K_{d,MCP}^a$ (L/gVSS)
R1	1.4±0.8	0.916±0.003	90.9	0.045±0.004	0.018
R2	1.4±0.5	0.922±0.001	ND. ^b	ND	0.018
R3	2.1±0.6	0.940±0.001	88.2	0.045±0.001	0.018
R4	1.5±0.4	0.921±0.002	92.3	0.047±0.004	0.018

^a The values reported by Kennedy et al. (1992).

^b Not determined.

The appearances of CTMP anaerobic granules and the granules (acclimated and unacclimated) cultivated with sucrose/HAc based wastewater were quite different. The CTMP sludge had black color, small granule size and good granule integrity. However, the sucrose/HAc enriched sludge had much larger size granules with a layered structure:

the outer layer was a grey color and was easily broken under turbulent mixing conditions, the inner layer was a black color and showed good granule integrity. Batch degradation tests indicated that acclimated anaerobic granules could degrade 2,4-DCP immediately.

3.3 Experimental Setup and Methods

3.3.1 Batch Sorption Tests

Batch sorption tests (Table 3-1, E1) were conducted in 60 mL or 120 mL serum bottles.

The factors examined in these tests are listed in Table 3-3.

Table 3-3 Batch sorption tests included in experiment group E1

Sorption tests	Factor examined	Chemical	Anaerobic granules	Experimental design
E1-A	Metabolic activity	2,4-DCP	Unacclimated sludges from R3 and R4	Single factor
E1-B	Factors screening	2,4-DCP and PCP	CTMP sludge	Factorial
E1-C	pH	2,4-DCP	CTMP sludge	Single factor
E1-D	Multiple sorption	2,4-DCP, 4-MCP and PCP	CTMP sludge	Single factor

Experimental procedures. The same procedures were followed for all the serum bottle tests (SBT) and are described as follows.

Step 1: Preparation of samples in serum bottle

- (1) Serum bottles were sparged with nitrogen gas to flush out oxygen and

maintain anaerobic conditions;

(2) The required volumes of sludge and deionized/deoxygenated Milli-Q water were transferred anaerobically into clean serum bottles;

(3) Phosphate buffer was added to the sludge (0.04~0.06 M) for a designated working pH;

(4) Serum bottles were sealed with the butyl rubber stoppers while the head space of the bottles was sparged with nitrogen gas, and then the bottles were capped with an aluminum seal;

(5) Serum bottles were mixed on a New Brunswick orbital shaker at 200 ± 10 rpm and 35°C for 30 min;

(6) Serum bottles were left unagitated in the dark at $35\pm 1^{\circ}\text{C}$ for 24 h, prior to injection of chlorophenol solutions.

All samples were run in duplicate or triplicate. For each set of batch tests, control bottles were also prepared according to the above steps except without adding anaerobic biomass. Maintenance of anaerobic conditions in the serum bottles was examined by testing that the solution in serum bottles became colorless with the addition of resazurin solution into the bottles (final concentration in bottles 1 mg/L) before step (4) of preparation.

In sorption test E1-A, three types of unacclimated anaerobic granules: live metabolically dormant, chemically inhibited and live metabolically active biomass were

used. Metabolic activity of the three types of unacclimated biomass was controlled by the availability of suitable carbon sources or use of a chemical inhibitor, NaN_3 , as described below.

Inhibited biomass. Inhibitor NaN_3 was added after step (3) of preparation in the required concentration to be effective (final concentration of 0.1%).

Active biomass. This was granular biomass where all the anaerobic microorganisms are active. An acetic acid/sucrose solution (500 mg/L each) was added into the serum bottles about 30 min before the addition of chlorophenol solution. Activity of biomass was monitored by determining the accumulation of VFAs and production of biogas in the serum bottles.

Dormant biomass. Granular biomass was deprived of substrate for an additional 24 h. Biomass was considered dormant if the VFAs in the serum bottles were not detectable and biogas production was negligible.

The CTMP sludge was used in all other batch sorption tests (E1-B~E1-D) and the sludge was inhibited in the tests using the same concentration of NaN_3 (0.1%) as that for the inhibited unacclimated sludge.

Step 2: Sorption experiments

Kinetic sorption tests. To minimize the effect of sampling over a period of time, 120 mL serum bottles were used with a working volume of 80 mL. Initial 2,4-DCP concentration in the bottles was 12 mg/L. Samples (1 mL) were taken at 0, 0.5 min, 2, 3, and 5 h, and at 1, 3, 7 and 12 days.

Sorption isotherm tests. A 60 mL serum bottle with a working volume of 40 mL was used for this test. Sorption of chlorophenol to biomass was determined by injecting chlorophenol solution into serum bottles to form different initial concentrations ranging between 3 and 30 mg/L. Samples were taken when sorption reached equilibrium and the time for sorption equilibrium was set at 5 h based on the kinetic sorption test in this study.

Sorption isotherm tests were conducted for all groups of tests in Table 3-3. Kinetic sorption tests were only performed for E1-A. All tests were conducted with an orbital shaker at 200 ± 10 rpm and $35\pm 1^\circ\text{C}$, with an initial working pH (7.5 for E1~A, B and D; 6.8~8.1 for E1~C). Adsorption of the chlorophenol to the serum bottle surface was tested previously and found to be negligible. Leakage of cell constituents into the mixed liquor can occur as a result of cell lysis or leaky membranes. The integrity of microbial cell wall and membranes exposed to NaN_3 was evaluated. The evaluation was made by determining increase in soluble COD of mixed liquor after 72 h of exposure. No detectable difference in soluble COD was found between the mixed liquor of chemically inhibited sludge and untreated granular sludge.

3.3.2 Continuous Sorption Tests

Sorption system setup. Two kinds of reactors were used in the experimental investigation: completely-mixed anaerobic reactor (CM) and anaerobic sludge column

reactor (SC). The setups of the two sorption systems are shown in Figures 3-1 and 3-2, respectively.

The effective volume of the CM reactor, 1 L, was controlled within $\pm 5\%$ by metering pumps for influent and effluent. A built-in separator was designed to prevent sludge loss from the reactor during operation. To achieve a CM condition in the reactor, the whole setup was constructed from a glass Sovirel reactor and installed on a Junior Orbit Shaker and the mixed liquor in the reactor was mixed with a stirring bar of size 30 mm \times 8 mm. The CM condition in the reactor was examined by employing propionic acid (HPr) as a tracer under operating conditions similar to those used for chlorophenol sorption tests. It was verified by tracer test that, with a speed of 80 rpm for shaker and 200~300 rpm for stirring bar, the mixing condition within the reactor showed a typical CM mode for a sludge concentration of 10 g/L and a hydraulic retention time (HRT) of 4~5 h, or for a sludge concentration of 2.1 g/L and a HRT of about 1 h. In the experimental setup, a bellows metering pump (GRI, model 14280-003) was used for feeding and a Masterflex peristaltic pump was used for effluent withdrawal. The flowrate was controlled by the metering pump during sorption tests.

The effective volume of the SC reactor was 0.2 L, and the size of this reactor was diameter \times length of 0.033 m \times 0.235 m. Anaerobic granular sludge R1 (Table 3-2) was used as sorbent. Bulk density of the sludge in the column was 48.1 gVSS/L and the sludge column has a dispersion number (D/uL) equal to 0.096, based on HPr tracer test results.

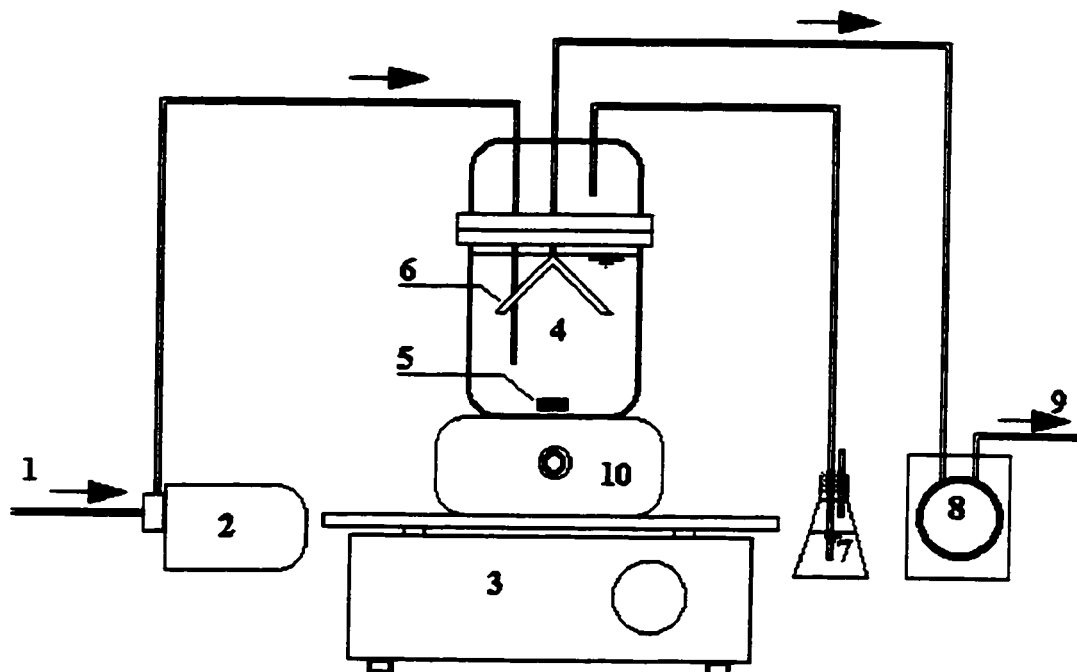


Figure 3-1 Schematic diagram of CM reactor system. 1. Feeding from solution bottle; 2. Bellows metering pump; 3. Shaker; 4. Reactor; 5. Stirring bar; 6. Solid-liquid separator; 7. Water sealing bottle; 8. Peristaltic pump; 9. Effluent; 10. Mixer unit.

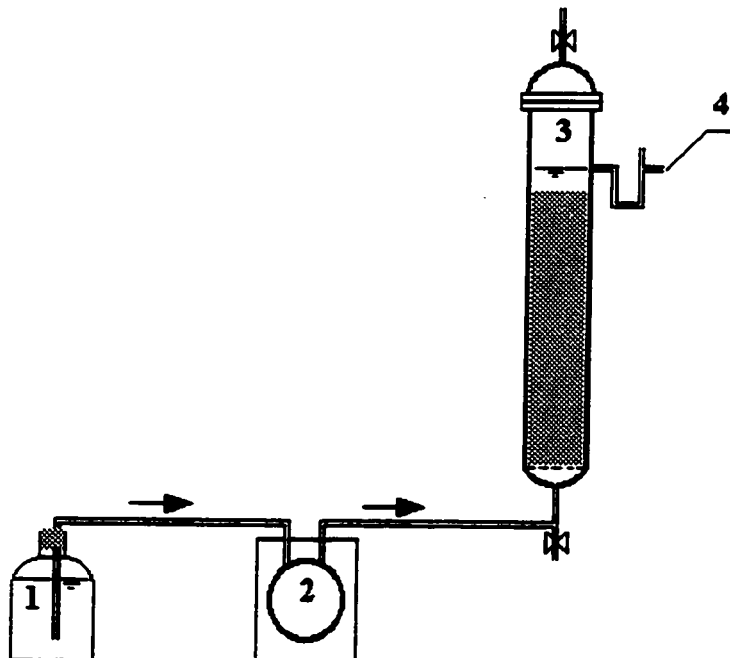


Figure 3-2 Schematic diagram of SC reactor system. 1. Feeding solution bottle; 2. Peristaltic pump; 3. Sludge column; 4. Sampling port.

A Masterflex peristaltic pump and tygon tubing were used for feeding.

Dynamic sorption experiment. Dynamic sorption experiments conducted in this study are summarized in Table 3-4. For each sorption test, only one chemical was employed. In experiment E2-A, a blank run for 2,4-DCP, without sludge addition to the reactor, was conducted in order to quantitatively justify the effect of chemical adsorbed to the system (i.e. tube, pump, glassware and reactor) on sorption results. The controlled pH of the mixed liquor in all tests in Table 3-4 was 7.5 and the experiments were conducted at $20 \pm 1^\circ\text{C}$.

Table 3-4 Dynamic sorption experiments (E2)

No.	Reactor	Chemical	Sludge Sources	Input Mode
E2-A	CM	3-MCP, 2,4-DCP, 3,4-DCP, 2,4,6-TCP, PCP	Lake Utopia Paper Limited	Step input
E2-B	CM	2,4-DCP, 2,4,6-TCP, PCP	same as above	Pulse input
E2-C	CS	2,4 -DCP	UASB reactor	Step input

Experimental procedures for the tests in CM reactor with step input were:

Sludge inactivation. 1). Add appropriate amount of sludge, deoxygenated buffer solution, sodium azide solution, sodium sulphide solution and deoxygenated distilled water into the reactor anaerobically to a total volume of 1000 mL. The final concentrations in solution were: anaerobic granules, 10.4 g VSS/L (for HRT of 4~5 h) or 2.1 g VSS/L (for HRT < 1 h); phosphate buffer, 0.04 M; sodium sulphide, 0.01%; and sodium azide, 0.1%.

The sludge concentrations used in the tests were based on the considerations of easily keeping the reactor under CM condition and using a sludge concentration that is close to those in the UASB reactors in this study; 2). bubble the solution with nitrogen gas for 5 minutes, seal the reactor and inject 10 ml of nitrogen gas into reactor to form a positive pressure inside; 3). mix the solution in the reactor at 80 rpm for shaker and 200~300 rpm for stirring bar for 1 h, then leave the solution unagitated for 18 h.

Feed solution. 1). Add chlorophenol solution as well as the same amount buffer (0.04 M) and sodium azide solution (0.1%) into a 1000 mL graduated media bottle, then dilute to 1000 mL with deoxygenated distilled water. The final concentration of chlorophenols in the feed solution was controlled within 10~30 mg/L in these tests; 2). Bubble solution for 5 minutes with nitrogen gas, cap the bottle and leave it at $20\pm 1^{\circ}\text{C}$ for temperature balance before use.

Dynamic sorption test. Before starting the sorption test, bring the solution in the reactor to CM conditions by shaking the reactor and stirring the solution. The system set-up is shown in Figure 3-1. The dynamic sorption test begins by starting the filling pump and the withdraw pump at the same time. During the sorption test, samples were taken from the effluent of the reactor every 15~60 min. The feed was sampled at both the beginning as well as the end of the test, and the average value of chlorophenol concentrations in the two samples was taken as the feed concentration. For each dynamic sorption test, the reactor was continuously run for a period at least longer than two times

the theoretical HRT based on influent flowrate. Solution pH in the reactor was measured after each test was finished. All samples were taken in duplicate.

For CM reactor with pulse input, the experimental procedures were the same as those described above, except that the concentrated chlorophenol solution was injected into the reactor at the beginning of the sorption test and no chlorophenol was added in the feed solution.

Experimental procedures for SC reactor were:

Sludge inactivation. Sludge inactivation for SC reactor was conducted in a 250 mL graduated media bottle instead of the column to ensure complete mixing. The mixed liquor in the bottle was prepared with deoxygenated distilled water under an anaerobic environment. The final concentrations in this solution were: anaerobic granules, 48.1 mg VSS/L; buffer, 0.4 M; sodium azide, 0.1%; and sodium sulfide, 0.01%.

Feed solution. Same as that for CM reactor.

Dynamic sorption test. Before the sorption test, the mixed liquor was anaerobically transferred into the column. After the system was connected as shown in Figure 3-2, the sorption test began by starting the feeding pump. The sampling schedules were similar to that for the CM reactor, except that after the test was finished, one sample of supernatant from the fully mixed solution in the reactor was taken for a mass balance assessment of chlorophenol used in the test. Other procedures were the same as those for the CM reactor.

3.3.3 Batch Degradation Kinetics Tests

Batch degradation kinetics tests covered the experiments E3 and E4 in Table 3-1. The detailed classifications of the batch degradation tests are further described in Table 3-5.

Table 3-5 Batch degradation kinetics tests (E3 and E4)

Degradation tests	Objectives	Chemical	Cosubstrates	Anaerobic granules
E3-A	Degradation kinetics of 2,4-DCP; sorption effect on degradation	2,4-DCP	Not used	Acclimated sludges from R3 and R4
E3-B	Syntrophic relation between dechlorinator and acetoclastic methanogenesis	2,4-DCP	Not used	BESA inhibited acclimated sludges from R3
E4-A	Degradation kinetics of HAc with 2,4-DCP	2,4-DCP	HAc	Acclimated sludges from R3
E4-B	Degradation kinetics of HPr with 2,4-DCP	2,4-DCP	HPr	Acclimated sludges from R3
E4-C	Degradation kinetics of sucrose with 2,4-DCP	2,4-DCP	Sucrose	Acclimated sludges from R3

Experimental procedures. Since anaerobic granules from the two UASB reactors were too large in size (Table 3-2) to be accurately transferred by pipette into serum bottles, filtered granules without supernatant were added into the serum bottles based on wet weight. Considering the exposure of granules to air, more stringent deoxygenating approaches were employed in this experiment compared with batch sorption tests.

Step 1: Preparation of samples in serum bottle

(1) Addition of filtered granular sludge into the serum bottles (5 g for 60 mL bottles and 10 g for 120 mL bottles)

(2) Serum bottles were sparged with nitrogen gas to flush out the oxygen and maintain anaerobic conditions;

(3) Addition of deoxygenated dilution water (see Appendix B for its composition) and phosphate buffer solution (final concentration 0.06 M) anaerobically into clean serum bottles to obtain a designated working pH of 7.5;

(4) The solution in serum bottles was bubbled with nitrogen gas for 1 min;

(5) Addition of sodium sulfide (only for bottles with even number of replicates, final concentration 0.01%) and resazurin solution (final concentration 1.0 mg/L) anaerobically;

(6) Serum bottles were sealed with butyl rubber stopper while the head space of the bottles was sparged with nitrogen gas, and then capped with aluminum seal;

(7) Serum bottles were agitated for 72 h at 100 rpm and $35\pm 1^\circ\text{C}$ to ensure complete oxygen depletion and reacclimation of the granules prior to injection of chlorophenol and cosubstrates solutions.

All samples were run in duplicate or triplicate for each batch of tests, control bottles were also prepared according to the above steps, except without the addition of anaerobic biomass (blank control) or without the injection of chlorophenol solution (positive control). The maintenance of anaerobic conditions in serum bottles was monitored by resazurin color change (colorless) in the bottles. It was observed during

experiments that the reduced conditions (mixed liquor colorless) could be achieved within 30 min after samples were prepared. For experiment E3-B, *BESA inhibited sludge* was used. The BESA solution was injected into serum bottles after 48 h during step (7) in sample preparation (final concentration of 0.2%). After 48 h of sludge reacclimation, HAC and HPr concentrations in serum bottles solution were zero and no gas production was detectable.

Step 2: Degradation experiments

At the initial time of the kinetic degradation experiments, deoxygenated 2,4-DCP solution (for E3 and E4) and cosubstrate solutions (only for E4) were injected into serum bottles. Then the serum bottles were agitated at 100 rpm and $35\pm 1^\circ\text{C}$. 1 mL or 2 mL samples (if COD was to be measured) were taken from serum bottles at time intervals of about 1, 3, 9, 21, and 30 h under anaerobic environment for analysis of 2,4-DCP, 4-MCP, VFAs and COD.

3.3.4 Continuous UASB reactors

System setup. Four UASB reactors were continuously operated in parallel in this study. Schematic diagram of the system is shown in Figure 3-3. The effective volume of 5.5 L was the same for all four reactors. Feeding tanks 1 and 2 (not shown in Figure 3-3) were cooled with plastic tubing wrapped around the tanks, in which tap water (2~12 °C from winter to summer) was continuously recirculated. The operating temperature of the

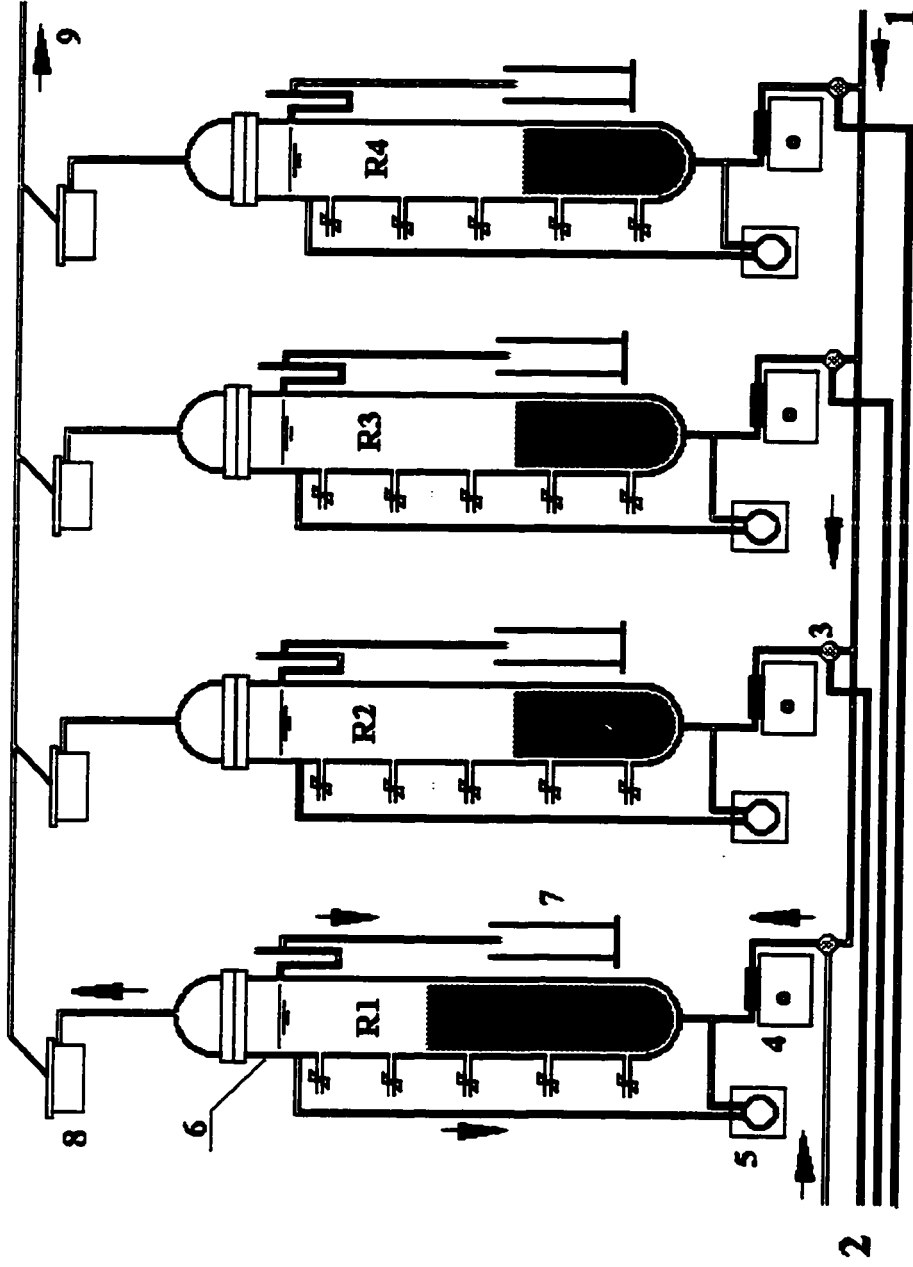


Figure 3-3 Schematic diagram of UASB reactor system. 1. Influent from the feeding tank for routine operation (same influent for all reactors); 2. Influent from the feeding tank for transient period operation (one tank for each reactor); 3. Three-way switch; 4. Harvard peristaltic pump for feeding; 5. Peristaltic pump for recirculation; 6. UASB reactor; 7. Effluent vessel; 8. Wet test gas meter; 9. Gas exhaust.

reactors was controlled at 35 ± 2 °C and maintained by the hot water tubing wrapped around the reactors (not shown in Figure 3-3). Temperature of the water in the tubing was 50 ± 1 °C. To minimize the effect of photosynthesis and heat loss, the reactors were covered with cloth during operation. A three-way switch was used to change the influent between the feed for routine operation and the feed for transient period in operation when necessary. A detailed description for application of the two feeds in operation is given in the following section.

System operation. In the first phase of operation (duration about 5 months), the system was operated to cultivate an unacclimated sludge for sorption test. During this period, the constant operating conditions were maintained to achieve steady state as shown in Table 3-6. At the end of this phase, granular sludge was harvested and used in the sorption test E1 (Table 3-1).

In the second phase of operation (about 9 months), the system was first continuously operated under routine conditions (Table 3-6) to let the system reach steady state. Then, specifically designated transient influent conditions were applied to individual reactors and the system responses (COD, HAc, HPr, 4-MCP, 2,4-DCP, pH, gas production and gas composition) during the transient influent period (1~3 days) were recorded. The experimental data obtained within this period were used to validate and verify the dynamic model for the UASB reactors. After a transient influent period, the reactor was returned to the routine operation conditions for one month. Once the reactor

reached steady state, a new designated transient influent was applied to the reactor again. During the second phase of operation, a total of 9 sets of experimental data was obtained. A detailed description of the transient feeding conditions is given in Chapter 6. At the end of this operating phase, the acclimated granular sludge was harvested and used for the batch degradation tests E3 and E4 (Table 3-1).

During the phase I and II operation periods, the supernatant recirculation flowrate in the reactor (Figure 3-3) was about 5 times the influent rate to that reactor. The mixing conditions of mixed liquor in the reactors were examined by tracer test, using fluoride

Table 3-6 Operating conditions of the UASB reactors

Operating Phase	Reactor	Influent COD (g/L)	Influent 2,4-DCP (mg/L)	SOLR (g COD/g VSS/d)	OLR (g COD/L/d)	HRT (h)
I	R1	10	0	0.27	6.5	36
	R2	10	0	0.42	9.8	24
	R3	10	0	0.66	17.4	14
	R4	10	0	0.43	9.8	24
II	R1	6	10	0.15	3.9	37
	R2	6	10	0.28	5.7	25
	R3	6	10	0.45	8.7	16
	R4	6	10	0.34	5.7	25

ion (F) as the tracer. The results from tracer test indicated typical CM conditions in all reactors with exception of reactor R1 for which a slight effect caused by dead volume was observed (Figure 3-4). Composition of the feed used in phase I and II operations is given in Appendix A.

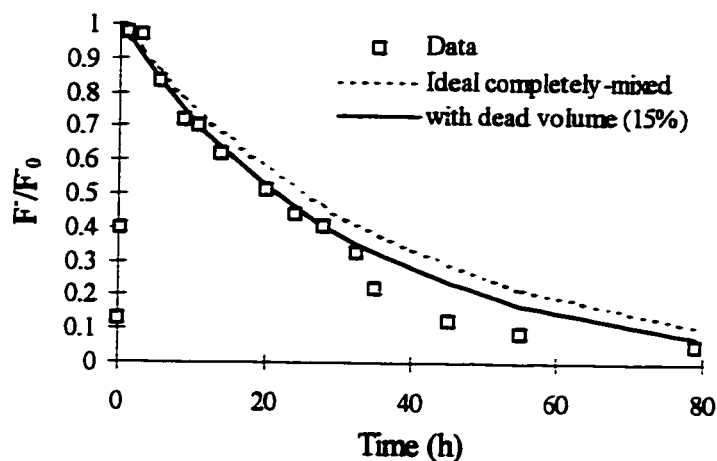


Figure 3-4 Tracer test result for mixing conditions in reactor R1

3.4 Analytical Methods

Chlorophenols. a 1.0 or 1.5 mL sample was centrifuged for 5 min in a microcentrifuge and the supernatant obtained was filtered through a Millipore 0.22 μm Millex GV 13 filter. Sample was then transferred into a 100 μL glass crimp top microvial, sealed with a Teflon/red rubber cap and stored at 4°C prior to analysis. Chlorophenol concentration was determined using a Hewlett Packard (model 1090) high performance liquid chromatograph (HPLC) with a Hypersil-ODS C18 column. The diode array detector was set at 280 nm wavelength. The column was maintained at 40°C and the flowrate of the mobile phase was set at 0.3 mL/min. For the mobile phase, a mixture of HPLC grade methanol (60%) and 0.05 M sodium acetate (40%) at pH 4.7 was applied.

VFAs. The VFAs were determined using a Hewlett-Packard 5721 gas chromatograph with a Chromosorb 101 glass column (approx. 0.635 cm × 365.8 cm) and equipped with an autosampler and integrator. The column was held at 180°C, and the temperature of the flame ionization detector was 350°C. The flowrate of the Helium carrier gas was 15 mL/min. Samples were centrifuged in a microcentrifuge for 5 min and 0.5 mL of supernatant was withdrawn and added into 0.5 mL internal standard, which contained 1000 mg/L of isobutyric acid, for analysis.

SS, VSS, pH, conductivity, granule size and COD. The SS and VSS of samples were performed according to *Standard Methods* (APHA, 1989). The pH of samples was determined with a Fisher Scientific Accumet pH meter. Conductivity was measured with a conductivity meter (Radiometer, Copenhagen) based on method 5120B in *Standard Methods*. Conductivity was used as an indirect measurement of ionic strength in this study. Size of anaerobic granules was measured using a 40 time magnifier and the average value of granules in 1 mL wet sludge was determined. COD of samples was measured according to method 5220C in *Standard Methods*.

Biogas. During batch sorption and degradation tests, biogas production was determined by acidified water displacement. In UASB reactor system, biogas production was recorded with a wet test gas meter. Biogas composition was determined by the gas chromatographic method (*Standard Methods*) using a Hewlett - Packard 5710A gas chromatograph equipped with a Porapak T column (0.635 cm × 304.8 cm), a flame

ionization detector, and an integrator. The column was maintained at 70°C and helium was used as the carrier gas (40 mL/min).

Fluoride ion. Fluoride ion was measured with DIONEX DX-100 ion chromatograph (DIONEX) equipped with an IonPac AS12A+IonPacAG12A column and a conductivity detector, and operated at room temperature. The mobile phase of the column was 2.7 mM Na₂CO₃/0.3 mM NaHCO₃ and had a flow rate of 1.5 mL/min. Samples were centrifuged in a microcentrifuge for 5 min and then the supernatant was filtered using Minisart NML syringe filters with a pore size of 0.22 μm before analytical measurement.

The experimental results and analysis on the sorption of chlorinated phenols to anaerobic sludge are presented in this chapter. The investigated topics on sorption are: the effect of metabolic activity on sorption; factors affecting sorption and sorption under dynamic situations.

4.1 The Effect of Metabolic Activity on Sorption

The basic approach used in this investigation was to compare the sorption capacities of living and inactivated anaerobic biomass for chlorophenols as well as anaerobic granules which were grown at different levels of microbial activity (SOLR). The experimental conditions under which the sorption tests were conducted are summarized in Table 4-1.

To avoid the effect of chlorophenol degradation in the sorption tests unacclimated sludge was used. Ability of the sludge to degrade 2,4-DCP was tested and the results are shown in Figure 4-1. It was observed that 4-MCP began to appear in samples after 5 d of cultivation at 35°C. As a comparison, an acclimated sludge completely degraded 2,4-DCP

Table 4-1 Sorption tests conducted under specified conditions ^a

Tests	Anaerobic granules ^b			Buffer ^c conc. (M)	Sample vol. /bottle vol. (mL/mL)	2,4-DCP/biomass concentration (mg)/(g)
	Live	Inactive	Dormant			
Isotherm (1)	SOLR/low	SOLR/low	-	0.04	40/60	(3~30)/(4.5)
Isotherm (2)	SOLR/low	SOLR/low	SOLR/low	0.06	40/60	(3~30)/(4.5)
Kinetics (1)	SOLR/low	SOLR/low	-	0.04	80/120	(12)/(4.5)
Kinetics (2)	SOLR/high	SOLR/high	-	0.04	80/120	(12)/(5.2)

^a All concentrations are final values of prepared sample in serum bottle.

^b Unacclimated sludge. SOLR/low: reactor R1 (SOLR, 0.27 kg COD/kg VSS/d); SOLR/high: reactor R3 (SOLR, 0.66 kg COD/kg VSS/d)

^c Phosphate buffer, pH 7.5.

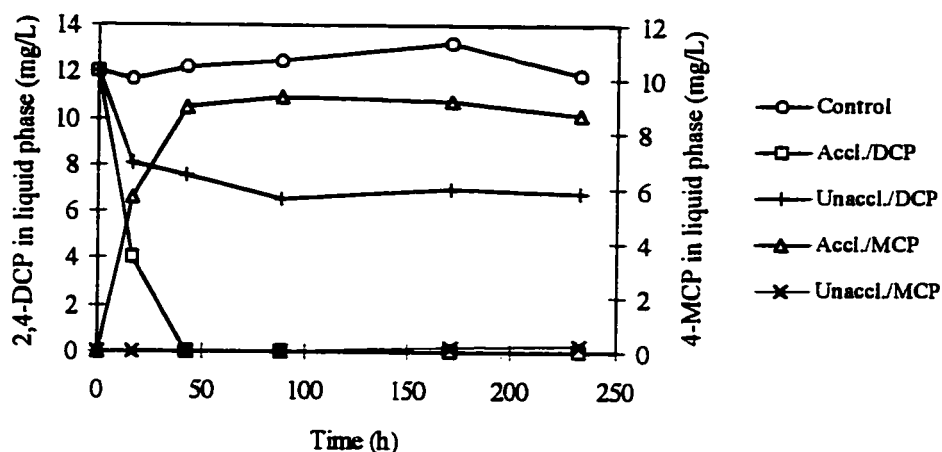


Figure 4-1 Effect of cultivation time on degradation of 2,4-DCP by unacclimated and acclimated sludge.

in about 45 h. Since an extra unidentified peak was observed in the chromatography of some samples (R3 culture) after 3 d, a control time for the sorption test within one day was considered safe to avoid the effect of 2,4-DCP degradation during sorption tests.

Based on the results from the controls used for tests described in Table 4-1, the effect of 2,4-DCP adsorption to serum bottles was evaluated. Figure 4-2 shows that 2,4-DCP adsorption to serum bottle glass or septum increases as the concentration of 2,4-DCP added increases. However, values for adsorption (the marks to the dash line in Figure 4-2) are much smaller than the standard deviation of data in replicates (error bar in the same figure). Consequently, adsorption of 2,4-DCP to the serum bottle was considered negligible and data adjustment for this type of adsorption in all other regular samples was ignored in the data analysis.

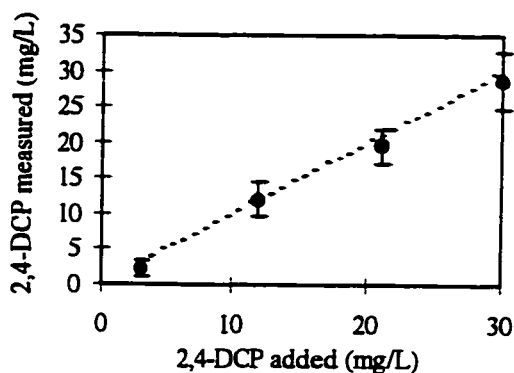


Figure 4-2 Adsorption of 2,4-DCP to serum bottle glass (control)

4.1.1 Sorption Isotherm

Sorption isotherms were first conducted for live and chemically inactivated SOLR/low granules. Averaged equilibrium data for live dormant and chemically inactivated SOLR/low anaerobic granules, at a buffer concentration of 0.04 M, are presented in Table

4-2. Since the experiments were designed based on 2,4-DCP added, a paired comparison of the means between the sorbed 2,4-DCP, q_e , on live and inactive anaerobic granules was made to test whether or not the mean difference is significant. The comparison indicates that at a significance level of 0.05, the difference between the 2,4-DCP sorbed to the two sludges is not significant.

Table 4-2 Equilibrium sorption of 2,4-DCP to live dormant and chemically inactivated anaerobic granules (SOLR/low) ^a

2,4-DCP added C_0 (mg/L)	Live sludge		Chemical inactivated sludge	
	Adsorbed, q_e (mg 2,4-DCP/gVSS)	Unadsorbed, C_e (mg 2,4-DCP/L)	Adsorbed, q_e (mg 2,4-DCP/gVSS)	Unadsorbed, C_e (mg 2,4-DCP/L)
6	0.20	5.12 ± 0.51	0.06	5.73 ± 0.29
12	0.47	9.87 ± 0.73	0.40	10.2 ± 1.47
18	0.45	16.0 ± 0.10	0.70	14.9 ± 2.45
24	0.59	21.3 ± 0.49	1.07	19.2 ± 2.89
30	1.04	25.3 ± 2.45	1.02	25.4 ± 2.28

^a 2,4-DCP adsorbed onto sludge is calculated based on the mass balance formula : $q_e = (C_0 - C_e)/X$, where X is the VSS concentration in samples.

According to Kennedy et al. (1992), when fitting the sorption data of 2,4-DCP on anaerobic granules to the Freundlich equation, the constant, $1/n$, is very close to 1.0. Therefore, for comparison with reported results, the data in Table 4-2 were fitted to the linear sorption equation, $q_e = K_d C_e$, where K_d is the sorption constant, C_e is the equilibrium concentration of the chlorophenol in solution (mg/L) and q_e is the equilibrium concentration of the chlorophenol on anaerobic biomass (mg/g VSS). Table 4-3 presents the values of the sorption constants obtained along with values reported in the literature .

Table 4-3 Sorption constant values for 2,4-DCP

Biomass	K_d ^a	95% confidence interval for K_d	R ²	Ref.
Live anaerobic granules ^b	0.035	[0.025, 0.045]	0.80	this work
Inactive anaerobic granules	0.045	[0.033, 0.057]	0.86	this work
Live anaerobic granules ^b	0.049	-	0.99	Kennedy et al. (1992)
Live aerobic sludge	0.29-0.40 ^c 0.04-0.1 ^d	-	0.97-0.99 -	Jacobsen et al. (1993)

^a For anaerobic granules, pH=7.5; unit, L/g VSS. For aerobic sludge, unit, L/g SS.

^b Live dormant anaerobic biomass. ^c Estimated from experimental data.

^d Calculated based on lg K_{ow} correlation in the pH interval 7.2-7.55.

It is shown that the values of sorption constants in this work are in the same order of magnitude as the values reported for anaerobic granules (Kennedy et al., 1992) but they are lower than those for live aerobic biomass (Jacobsen et al., 1993). More importantly, the sorption constants obtained in this study for live dormant and chemically inactivated anaerobic granules are very close. However, considering the deviation in the sample measurement results by HPLC, which is highlighted by the wide confidence intervals for K_d , the similarity of the 2,4-DCP sorption capacities between inactive and live dormant granules needs to be further justified.

It should be noted that the live anaerobic cells had been in the dark at 35°C for 24 h with no supplemental carbon source being introduced into the serum bottles prior to the injection of 2,4-DCP. Microbial activity of the granules should be endogenous in nature by this time. Analytical results of samples from live granules bottles supported this

assumption as the VFAs concentrations were negligible (undetectable by GC). Therefore, while the granular biomass was alive it in fact was *dormant* in a metabolic sense since there may be insufficient biodegradable carbon present to produce active metabolism. Based on the conditions of this test, it could be argued that a difference in sorption may exist between live metabolically active and chemically inactivated anaerobic biomass.

To clarify the possible influence of microbial activity on biosorption, isotherm tests for live (dormant), live (active with sufficient biodegradable carbon) and NaN_3 inactivated anaerobic granules were further conducted using R1 biomass. To maintain the pH of the active sludge samples around 7.5, a 0.06 M phosphate buffer was maintained for all bottles. The data from this test are shown in Figure 4-3 and linear model fitting results are presented in Table 4-4, respectively. These results indicate that the three types of SOLR/low sludges have almost identical biosorption capacities. The same results were also observed in another set of experiments that maintained a buffer concentration of 0.08 M in all serum bottles.

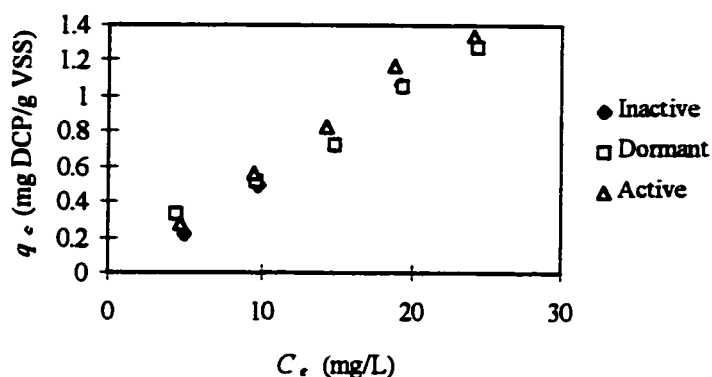


Figure 4-3 Comparison of biosorption of 2,4-DCP to live (active), live (dormant) and inactive anaerobic granules

It was observed in this test that it was difficult to maintain the initial pH value, 7.5, in the bottles containing live active anaerobic granules until sorption equilibrium was achieved (see Table 4-4). The decrease in pH was due to microbial activity of active granules that were converting sucrose first to VFAs then to methane and carbon dioxide. With the pK_a value of 7.89 for 2,4-DCP, a lower pH in serum bottles has a positive effect on sorption results since molecular 2,4-DCP has much stronger sorption tendency than its ionized form according to Woods (1985). However, with the difference in pH of about 0.1 pH unit between active granules and the other two types of granules used in the test, the positive effect on K_d as a result of lower pH value was estimated to be only about 6% (the 6% is calculated from Equation 4-8 in Section 4.2.2). A small difference exists in the values of estimated K_d between Table 4-3 and Table 4-4. This may possibly be due to the effect of ionic strength, because the only difference between these two tests was the buffer concentrations which were 0.04 and 0.06 M, respectively.

Table 4-4 Linear model fitting results for the sorption of 2,4-DCP to NaN_3 inactivated, live (active) and live (dormant) granules

Biomass	K_d	95% confidence interval for K_d	R^2	Initial pH	Final pH
Inactive	0.053	[0.046, 0.059]	0.98	7.50±0.01	7.48±0.02
Active	0.053	[0.048, 0.057]	0.98	7.50±0.01	7.37±0.01
Dormant	0.058	[0.054, 0.062]	0.99	7.50±0.01	7.46±0.03

4.1.2 Kinetic Sorption

To test whether or not the sorption of 2,4-DCP by live or inactive sludge is kinetically different, sorption was tested at different time intervals during the sorption process. Additionally, anaerobic granules, which were cultivated under different metabolic conditions SOLR/low and SOLR/high, were used to compare the sorption between live dormant and chemically inactivated anaerobic granules. It was observed that the size of granules cultivated at SOLR/high was significantly larger than that at SOLR/low. On average, R3 granules were about 2~3 mm in diameter while R1 granules were about 1~2 mm in diameter. Considering that 2,4-DCP degradation may occur after a long cultivation time, 3 to 5 d, as shown in Figure 4-1, only the data from the first day are used in the analysis.

The kinetic biosorption curves for live (dormant) and NaN_3 inactivated SOLR/low and SOLR/high granules are presented in Figure 4-4. The time intervals for the data points are 0, 0.5 min., and 2, 3, 5 and 24 h. All of the data points presented are the averages of duplicate or triplicate samples.

Figure 4-4 shows that the time for sorption equilibrium is within 2~5 h, which is consistent with the reported values in the literature (Wang et al., 1993; Kennedy et al., 1992). These results also indicate no significant difference in sorption processes between live and inactive granules. The sorption results between SOLR/low granules and

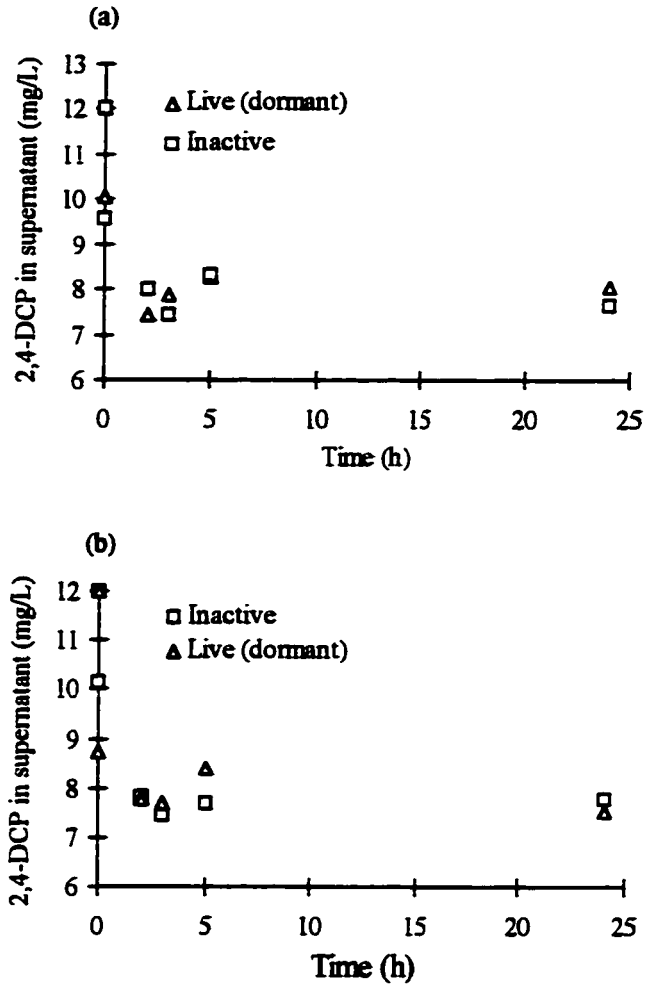


Figure 4-4 Sorption comparison between live (dormant) and inactive granules (a) for sludge SOLR/low and (b) for sludge SOLR/high.

SOLR/high granules were compared in Figure 4-5 after an adjustment of the results for the bottles with SOLR/high granules was made to eliminate the effect of slightly different sludge concentrations (see Table 4-1). Figure 4-5 indicates that differences in sorption of 2,4-DCP onto the two kinds of sludge with different metabolic activity are also not significant.

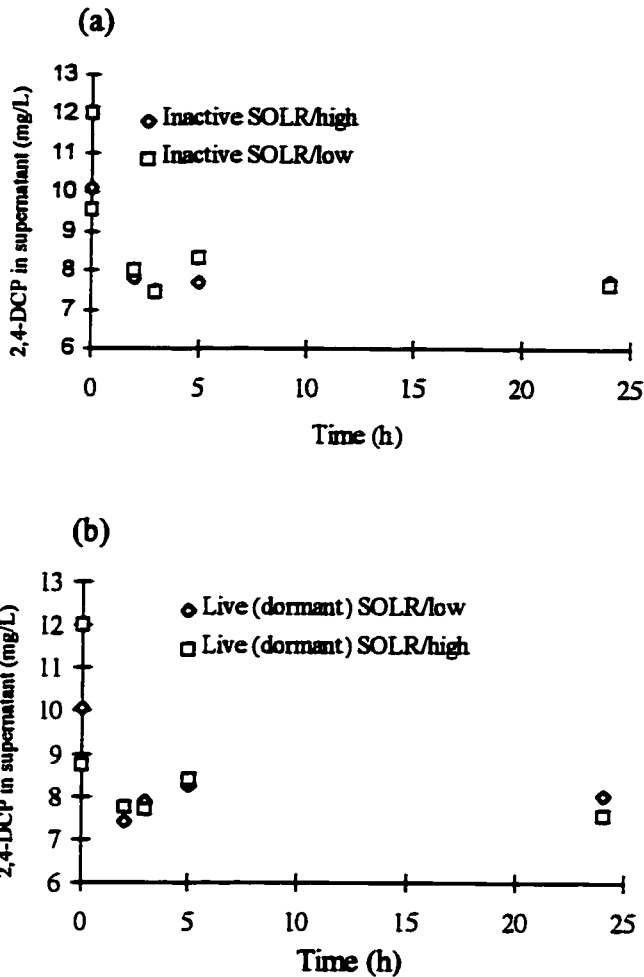


Figure 4-5 Comparison of sorption results for SOLR/low sludge and SOLR/high sludge, (a) for NaN_3 inactive granules and (b) for live dormant granules.

Additionally, data from both isotherm and kinetic sorption tests are summarized in Figure 4-6. The solid line, with slope 1.0, represents identical sorption capacities among chemically inactivated, live (dormant) and live (active) anaerobic granules. It is clear that, although there is a small deviation for some experimental data, the whole data set is fairly well distributed along the solid line.

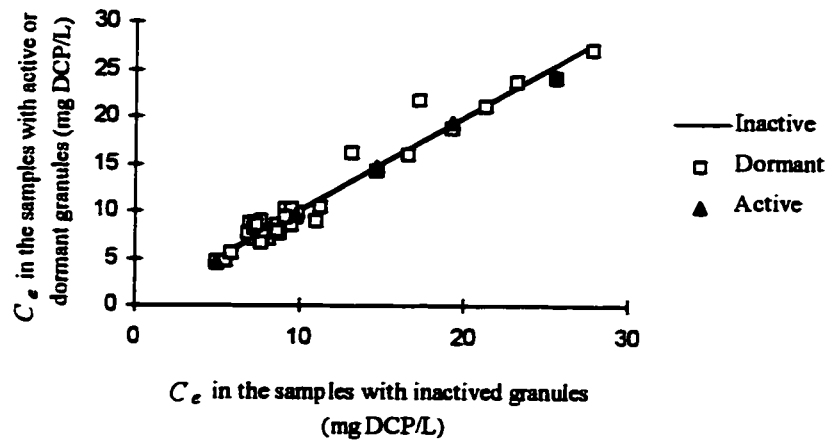


Figure 4-6 Comparison of the sorption capacity of inactivated granule with that of live (dormant) and live (active) granules

4.1.3 Discussion

It was reported that biosorption of toxic organic compounds does not significantly correlate to biological solids size variation (Kennedy and Pham, 1995) and the operating conditions of certain biological systems (Yan and Allen, 1994). The observations from this study are consistent with their conclusions. As shown in this study, although the organic content and the sizes of granules differ, the variation may not be large enough to significantly affect the sorption results, since anaerobic granules are of very high organic content and very porous (MacLeod et al., 1990). However, differences in sorption capacities can be significant depending on the source of anaerobic sludge as well as between aerobic and anaerobic solids (Kennedy and Pham, 1995).

Both sorption isotherm and kinetic sorption data from this study indicate that the differences in the sorption of 2,4-DCP to live (dormant), live (active) and chemically inactivated anaerobic granular biomass were not significant. This observation strongly suggests that anaerobic biosorption can be considered as mainly a physical-chemical process, and that metabolically mediated diffusion in the sorption process is negligible. The similarity in sorption kinetics for live and NaN_3 inactivated granules suggests that the same physical-chemical sorption mechanisms are involved in this process. As suggested by other researchers (Wang and Grady, 1994; Wang et al., 1993; Kennedy et al., 1992; Tsezos and Bell, 1989), it is reasonable to conclude that anaerobic biosorption is a combined adsorption and passive diffusion (and/or partitioning, absorption) process. However, the relative importance of these processes may significantly vary with organic compounds and physico-chemical conditions involved. The similarities between sorption kinetics of dormant and inactivated granules should be studied in more detail since no sampling was made between 0.5 min to 2 h in these sorption kinetic tests. Additionally, it should be mentioned that for sorption studies, the use of chemical inhibitors that block microbial metabolism while minimizing cell leakage and damage has significant advantages over traditional methods, such as autoclaving, used to produce dead microbes.

Most recently, Klein and Kennedy (1996) conducted a more detailed study on the effect of microbial activity on sorption of 2,4,6-TCP and 2,4-DCP. In their investigation, BESA and NaN_3 were used to inhibit methanogenic bacteria and all the anaerobes in the sludge, respectively. Their investigations also indicated that no significant difference was

observed for sorption of 2,4-DCP or 2,4,6-TCP to anaerobic sludges with different metabolic activity conditions.

The results from this study do not produce irrefutable evidence that metabolically mediated diffusion is not involved in sorption. However, there is significant evidence indicating that anaerobic biomass sorption of 2,4-DCP is mainly a physical-chemical process. Although the results from this study were limited to 2,4-DCP and specific experimental conditions, based on the results of other works with other chlorophenols using anaerobic biomass (Klein and Kennedy, 1996; Kennedy and Pham, 1995; Kennedy et al., 1992) the conclusion is expected to be true at least for anaerobic biosorption of other chlorophenols under similar sorption conditions. Further studies are required for a broader application of this conclusion, in particular for sorption systems with low sorbate concentrations where the effect of biological activity on sorption may have a greater influence.

4.2 Factors Affecting the Sorption

According to the results from the previous section and from other investigations reported (Klein and Kennedy, 1996; Kennedy and Tham, 1995; Yan and Allen, 1994), it is feasible to consider that the sorption of 2,4-DCP to anaerobic granules is mainly a physical-chemical process and it is not significantly correlated to variation of biological solids.

Consequently, more attention should be paid to the effect of physico-chemical conditions on the anaerobic sorption of chlorophenols.

4.2.1 Factor Screening

Sorption tests based on factorial design were conducted to screen out important physico-chemical factors affecting the sorption of chlorophenols to anaerobic granules. The factors selected in these tests were pH, temperature, ionic strength, and type of chlorophenol. A two level factorial design was used in the tests and Table 4-5 shows the experimental conditions controlled for those factors. Selection of 2,4-DCP and PCP was based on the fact that the two chemicals covered a broad range of values of octanol/water distribution coefficients and they are the most important chlorophenols in pulp and paper mill wastewater. 2,4-DCP is also the model chemical treated in the UASB reactor of this study. Chemically (NaN_3) inactivated CTMP anaerobic granules were used in the tests due to their small granular size, which made it convenient to transfer sludge during sample preparation. The ionic strength of solution in serum bottles was controlled by using 0.06 and 0.10 *M* of phosphate buffer in sample preparation. For easy measurement, the ionic strength was evaluated by conductivity.

The experimental results for 2,4-DCP and the PCP are shown in Table 4-6 in which the coded values 1 and -1 represent the upper and the lower limits designated for each factor. To identify the relative importance of these physico-chemical factors on

sorption, a linear regression model can be defined from the experimental data by multiple linear regression, then the significance of a specific factor on sorption can be further analyzed.

Table 4-5 Experimental conditions for the factorial sorption tests

Chemical (mg/L)	Temperature (°C)	pH	Conductivity (μmol/cm)	Sludge (gVSS/L)
18; 18 (2,4-DCP; PCP)	20; 35	6.5; 8.1	8400; 13200	5.2 (inactivated CTMP granules)

Table 4-6 Experimental results for the factorial sorption tests

No.	Temperature	pH	Ionic strength	$q_{e,PCP}$ (mg/g VSS)	$q_{e,2,4-DCP}$ (mg/g VSS)
1	1	-1	-1	2.010	1.335
2	1	-1	-1	1.849	1.365
3	1	-1	1	2.013	1.474
4	1	-1	1	1.975	1.432
5	1	1	-1	1.593	0.726
6	1	1	-1	1.707	0.914
7	1	1	1	1.659	0.793
8	1	1	1	1.798	0.762
9	-1	-1	-1	1.993	1.246
10	-1	-1	-1	1.983	1.375
11	-1	-1	1	2.155	1.341
12	-1	-1	1	2.142	1.337
13	-1	1	-1	1.508	0.662
14	-1	1	-1	1.344	0.837
15	-1	1	1	1.593	0.676
16	-1	1	1	1.659	0.792

Data analysis for PCP

Without considering chemical as a factor, the complete model for the 2³ factorial design has the form below,

$$E(Y) = \beta_0 + \beta_1 x_1 + \beta_2 x_2 + \beta_3 x_3 + \beta_{12} x_1 x_2 + \beta_{13} x_1 x_3 + \beta_{23} x_2 x_3 + \beta_{123} x_1 x_2 x_3$$

where $E(Y)$ is the system response and x_1 , x_2 and x_3 are independent variables. In this case, $E(Y)$ is the expected PCP concentration adsorbed onto granular sludge, x_1 , x_2 and x_3 represent temperature, pH and conductivity, respectively. By fitting the above model to the data, the estimated parameters are listed in Table 4-7.

Table 4-7 Estimated parameters in the model for PCP

Coefficients	Value estimated	Lower 95%	Upper 95%
β_0	1.811	1.768	1.855
β_1	0.014	-0.030	0.058
β_2	-0.204	-0.248	-0.160
β_3	0.063	0.019	0.106
β_{12}	0.067	0.024	0.111
β_{13}	-0.028	-0.071	0.016
β_{23}	0.006	-0.037	0.050
β_{123}	-0.003	-0.047	0.040

By checking the confidence interval for each parameter in the table, the parameters, β_1 , β_{13} , β_{23} and β_{123} are found to be all plausibly zero. As a result, the fitted model for the PCP data becomes:

$$\hat{q}_{e,PCP} = 1.811 - 0.204(pH) + 0.063(conductivity) + 0.067(temperature \times pH)$$

A stepwise regression approach was used to further test possible deletions of terms in

above equation and lack of fit of the reduced model. The model lack of fit was tested by comparing the values of the ratio:

$$L_r = \frac{\sum_{u=1}^n (\bar{q}_e - \hat{q}_e)^2 / \left\{ n - p - \sum_{i=1}^l (m_i - 1) \right\}}{\hat{\sigma}_p^2}$$

with the value of $F_{v1, v2}$ at desired probability level (Draper and Smith, 1966). In the equation for the ratio, L_r , $\hat{\sigma}_p^2$ is the pooled pure error variance estimated from replicates and $\hat{\sigma}_p^2 = \sum_{i=1}^l (m_i - 1) \sigma_i^2 / \sum_{i=1}^l (m_i - 1)$, m is the number of replicates, σ_i^2 is variance of replicate and l is the number of sets of replicates in the data ($l = 8$ in Table 4-6). For the value of $F_{v1, v2}$, $v1 = n - p - \sum_{i=1}^l (m_i - 1)$ and $v2 = \sum_{i=1}^l (m_i - 1)$, where n is the sample size and p is the number of parameters in the model. In the lack of fit test, if L_r is larger than $F_{v1, v2}$ at the selected level of significance, then the model displays lack of fit. The results from stepwise regression are summarized in Table 4-8.

Table 4-8 Model comparison for PCP sorption data

Model	L_r	$F_{v1, v2, 0.05}$	R^2
1.811-0.204(pH)+0.063(conductivity) +0.067(temperature×pH)	0.699	3.84	0.928
1.811-0.204(pH)+0.063(conductivity)	3.07	3.69	0.844
1.811-0.204(pH)	4.38	3.58	0.772

According to the results obtained above, the best fitting model for the PCP data is

$$\hat{q}_{e,PCP} = 1.811 - 0.204(pH) + 0.063(\text{conductivity}) \quad (4-1)$$

The plots between residual of q_e vs. q_e also show that no significant trend exists based on the best fitting model (Figure 4-7). Consequently, it is concluded that, under the conditions controlled in this experiment, the most significant physico-chemical factor affecting sorption of PCP to anaerobic granules is pH. The ionic strength also has an effect but it is much less significant than pH. Moreover, since no trend is shown in the residual plot for the best fitting model, other factors which may significantly influence the sorption can be excluded under conditions controlled in this experiment.

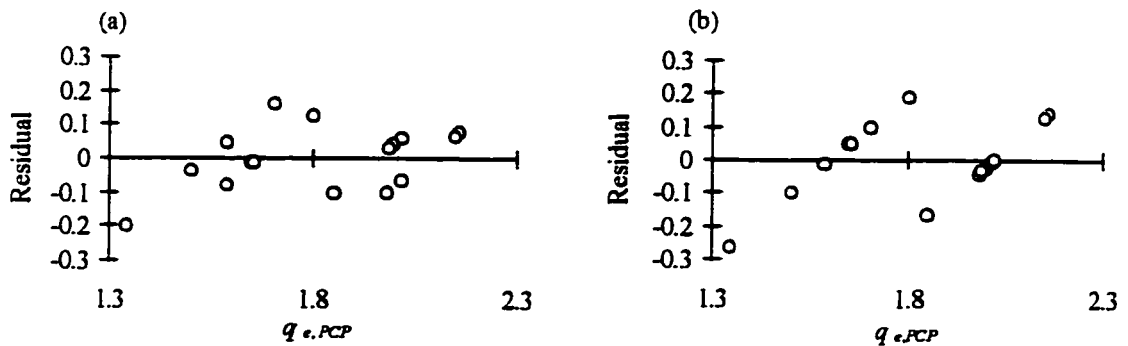


Figure 4-7 Plot of q_e residual vs. q_e . (a) the best fitting model; (b) the model only with pH term

Data analysis for 2,4-DCP

Following the same procedures, the data for 2,4-DCP are analyzed. The final results are presented in Table 4-9. The best fitting model for 2,4-DCP data is

$$\hat{q}_{e,DCP} = 1.067 - 0.297(pH) \quad (4-2)$$

Compared with the estimated coefficient of pH in the model for PCP (0.204), pH has a stronger influence on sorption of 2,4-DCP (0.297). The reason for this is that the pK_a value for 2,4-DCP ($pK_a = 7.89$) was within the pH limits in this test (6.5; 8.1) but it was not the case for PCP ($pK_a = 4.81$).

Table 4-9 Model comparison for 2,4-DCP sorption data

Model	L_r	$F_{v1, v2}$	R^2
1.067-0.297(pH)+0.033(temperature)-0.024(conductivity) +0.009(temperature×pH)-0.005 (temperature×conductivity) +0.006(pH×conductivity)	0.009	5.32	0.967
1.067-0.297(pH)	0.872	3.58	0.945

Data analysis for 2,4-DCP and PCP.

To identify the influence of sorbate properties on the sorption results, the data from both 2,4-DCP and PCP tests (Table 4-6) were jointly analyzed, assuming that the effect of blocking based on the type of chemical in these tests was negligible. In this analysis, the chemical is considered one of the factors by defining the coded value for PCP as 1 and for 2,4-DCP as -1. As a result, the whole data set is treated as a 2^4 factorial sorption test.

Using the same method discussed above, the best fitting model for the design can be expressed as

$$\hat{q}_e = 1.439 - 0.372(CP) - 0.250(pH) + 0.036(\text{conductivity}) + 0.046(CP \times pH) \quad (4-3)$$

From the derived model, it is seen that the type of chlorophenol has the strongest influence on sorption results, followed by pH and conductivity. The interaction term in this model indicates that effect of pH is correlated to the kind of chlorophenol, which is consistent with the investigations reported (Lee et al., 1991; Woods, 1985).

In summary, pH is the most important factor affecting the sorption. The effect of temperature on sorption was negligible within the temperature limits in the sorption tests. Ionic strength had an effect on PCP sorption but not on 2,4-DCP. Since no lack of fit is displayed for the best fitting models for 2,4-DCP and PCP, it is feasible to conclude that no other factors need to be considered in modeling the sorption equilibrium under the experimental conditions in the test. However, this factorial sorption test was conducted only for screening the significant factors and identifying their relative importance on the sorption of chlorophenols onto anaerobic granules. A mechanistic model for predicting sorption results still needs to be developed.

4.2.2 pH

Since pH was identified as the most important factor affecting sorption, an experiment (E1-c, Table 3-3) was designed to study the effect of pH on the sorption of 2,4-DCP to CTMP anaerobic granules in more detail. According to the objective of this study, only sorption of 2,4-DCP was examined in this experiment.

Assuming the phenolate form of 2,4-DCP does not adsorb by other major mechanisms besides partitioning (dissolving into bacteria and organic matter of anaerobic granules), then the sorption coefficient for phenolate ion and molecular 2,4-DCP can be defined individually. The sorption coefficient for phenolate ion is

$$K_{d,DCP^-} = q_{e,DCP^-} / C_{e,DCP^-} \quad (4-4)$$

where DCP^- represents phenolate form of 2,4-DCP and the other symbols have the same meaning as those in the linear sorption equation. Similar to Equation (4-4), the sorption coefficient for molecular 2,4-DCP (DCP^o) is defined as

$$K_{d,DCP^o} = q_{e,DCP^o} / C_{e,DCP^o} \quad (4-5)$$

The fraction of molecular form of the ionizable compound at any pH follows the relation,

$$\alpha = \frac{1}{1 + K_a / [H^+]} \quad (4-6)$$

On the basis of the linear sorption equation,

$$K_{d,DCP^r} = q_{e,DCP^r} / C_{e,DCP^r} \quad (4-7)$$

combining Equations (4-4), (4-5) and (4-6) into (4-7) based on mass balance, the relation between the sorption coefficient for total 2,4-DCP (K_{d,DCP^r}) to the sorption coefficients for its phenolate ion and molecular form can be deduced:

$$K_{d,DCP^r} = \frac{K_{d,DCP^o} + K_{d,DCP^-} (K_a / [H^+])}{1 + K_a / [H^+]}$$

or

$$= \alpha(K_{d,DCP^o} - K_{d,DCP^-}) + K_{d,DCP^-} \quad (4-8)$$

On the basis of Equation (4-8), the value of sorption coefficients for phenolate ion and molecular 2,4-DCP can be determined when the values of K_{d,DCP^r} under several specific pH conditions are known.

The sorption isotherm tests for 2,4-DCP were run in serum bottles at pH 6.8, 7.5 and 8.1. Under each pH condition, the tests were conducted with an anaerobic granule concentration of 5.2 g VSS/L and initial 2,4-DCP concentrations between 6~30 mg/L. The selection of 2,4-DCP concentrations was based on the 2,4-DCP concentrations expected to prevail in the UASB reactors of this study. Table 4-10 shows the sorption coefficients estimated from the tests under each pH condition. The fitting result of Equation (4-8) to the data obtained and the estimated values for K_{d,DCP^o} and K_{d,DCP^-} are shown in Figure 4-8.

From the estimated values of sorption coefficients for phenolate ion ($K_{d,DCP^-} = 0.011$) and molecular 2,4-DCP ($K_{d,DCP^o} = 0.14$), it is seen that the sorption of molecular 2,4-DCP is 12 times greater than the sorption of its phenolate ion to anaerobic granules. This observation is consistent with reported results for the effect of pH on chlorophenol sorption to anaerobic granules (Woods, 1985) and sediment (Jafvert, 1990). In the results

reported by Woods, the sorption coefficients of phenolate ion and molecular 2,4-DCP to anaerobic sludge were 0.35 and 0.17 L/g VSS, respectively, which indicates a higher sorption tendency of both forms of 2,4-DCP compared with this study. These results may be partially due to the lower concentration of the chemical used (0.03 ~ 6.0 mg/L) in the experiment, since the relative importance of other sorption mechanisms can be significant when sorbate concentration is low. Woods also observed that the ratio of sorption coefficients of molecular chlorophenol to those of chlorophenolate varies significantly from 63 for PCP to 2.5 for 2,4-DCP. However, the underlying mechanism for this variation is not clear.

Table 4-10 K_{d,DCP^r} estimated for CTMP granules at different pH conditions

pH	α	K_{d,DCP^r}	R^2
6.6	0.951	0.136±0.009	0.92
7.5	0.696	0.098±0.002	0.99
8.1	0.392	0.063±0.008	0.73

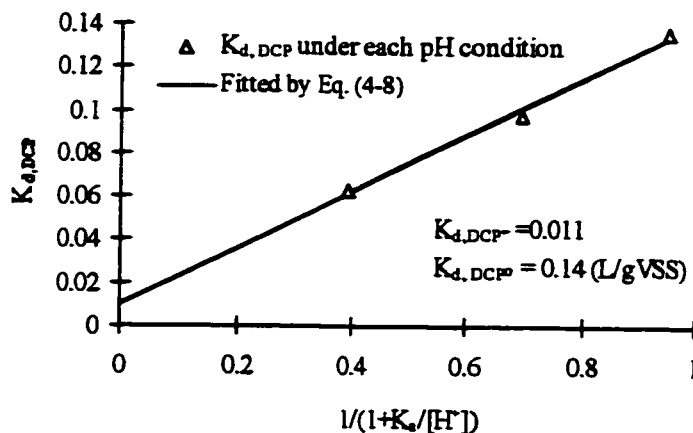


Figure 4-8 Sorption coefficients determination for phenolate and phenol form of 2,4-DCP.

4.2.3 Multicomponent sorption

Since 4-MCP could be the major product of 2,4-DCP degradation (Mohn and Kennedy, 1992), the sorption intereffect between the two chemicals in UASB reactors was of concern in this study for modeling the system. The same experimental procedures as for other sorption tests were used in the multiple sorption test. The only difference was that two chemicals were injected sequentially into serum bottles at the initial time. Besides the simultaneous sorption of 4-MCP and 2,4-DCP, simultaneous sorption of 2,4-DCP and PCP was also tested for comparison.

The experimental results for multiple sorption of 4-MCP and 2,4-DCP is presented in Figure 4-9. This figure indicates that no significant intereffect exists for co-sorption of these two chemicals. The sorption isotherms of 2,4-DCP with the initial concentrations of 4-MCP at 0, 6, 18 and 30 mg/L, respectively, are basically the same except a slight deviation of two data points for 4-MCP at 30 mg/L (Figure 4-9). Similarly, the sorption of 4-MCP was also not affected by adding 2,4-DCP (Figure 4-9).

However, unexpected results were observed for the multiple sorption of 2,4-DCP and PCP (Figure 4-10). These results show that, in the presence of PCP the sorption of 2,4-DCP significantly decreased compared with sorption of 2,4-DCP with no PCP present. This intereffect seems so strong that the effect of PCP on 2,4-DCP sorption does not change much when PCP concentration increased from 6 to 30 mg/L. Comparatively,

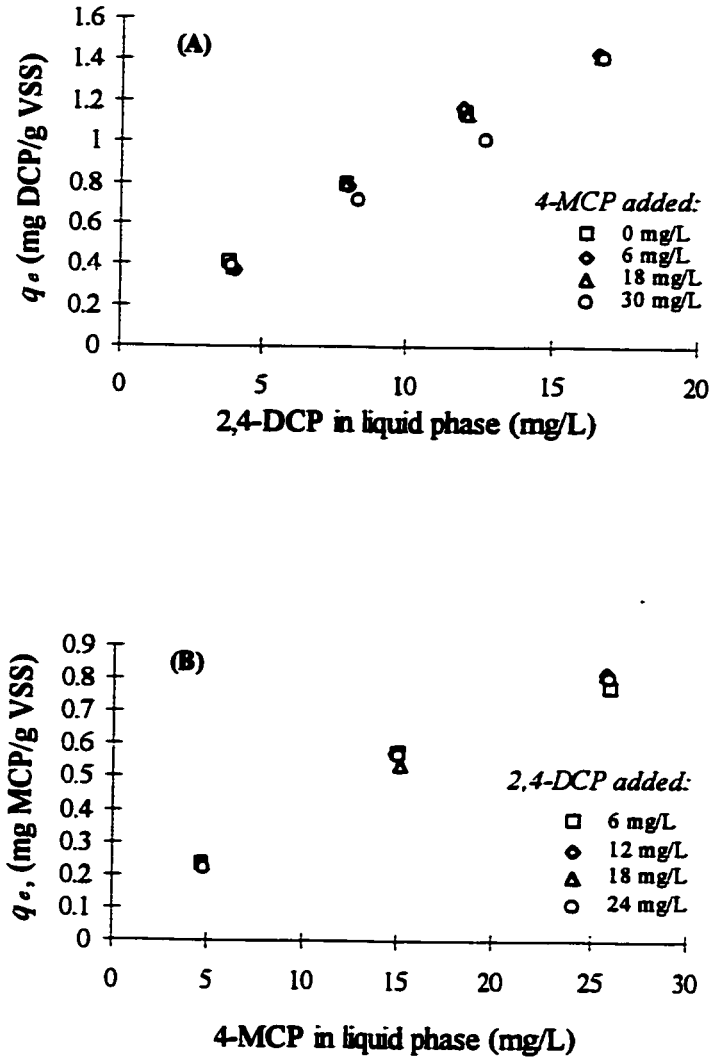


Figure 4-9 Multiple sorption of 2,4-DCP + 4-MCP. (A) 2,4-DCP sorption influenced by 4-MCP; (B) 4-MCP sorption affected by 2,4-DCP

the effect of 2,4-DCP on sorption of PCP was negligible, except for a small effect at the initial 2,4-DCP concentration of 24 mg/L. Some investigators have reported that a less chlorinated phenol could be more rapidly biodegraded when a highly chlorinated phenol such as PCP was present (Liu and Pacepavicius, 1990). The reason for the enhanced

degradation of a less chlorinated phenol was not interpreted in their investigation, it may be possibly due to the sorption intereffect observed in this study.

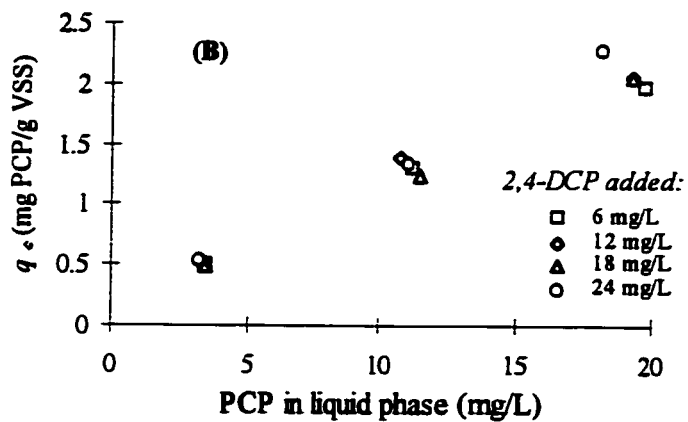
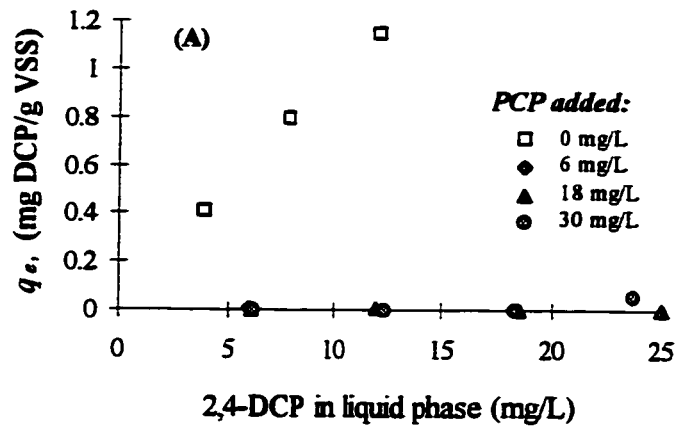


Figure 4-10 Multiple sorption of 2,4-DCP and PCP. (A) 2,4-DCP sorption influenced by PCP; (B) PCP sorption influenced by 2,4-DCP.

4.3 Sorption under Dynamic Situation

The adequacy of the application of linear sorption relation to the anaerobic sorption process under dynamic situations was tested in this section. Two types of reactors were used in the experiments for these tests: CM reactor and SC reactor. The setup of the two reactors and the experimental methods for the tests have been described in detail in Chapter 3.

To identify ideality of the sorption process under a dynamic situation, dynamic models for the two reactors need to be developed and used to fit the experimental data. The models can be developed by incorporating linear sorption relation (Equation 4-7) into the mass balance equations for the two systems. Since the mass balance equations for these systems have been well validated and documented in textbooks, nonideality of the sorption under dynamic situations can be identified if the dynamic models do not fit the experimental data. Then, kinetics describing the sorption nonideality should be pursued.

4.3.1 Dynamic Model with Linear Sorption

The following assumptions were used in the model development: (1) nonequilibrium sorption and sorption/desorption nonsingularity are absent in sorption of chlorophenols to anaerobic granules under dynamic situations; (2) chlorophenols are not degradable and are nonvolatile in the reactors; and (3) the volume occupied by biological solids in the reactors

is negligible under the experimental conditions. It can be seen that assumption (1) is to be tested in the investigation. To satisfy the second assumption, NaN_3 inactivated sludge was used in the experiments. Since the values of Henry's Law constants for chlorophenols are very low and the reactors were well sealed during the experiments, the loss of chlorophenol due to volatilization in the experiments was negligible (refer to Figure 4-2 for 2,4-DCP). Assumption (3) is valid since the granular biological solids are very porous (MacLeod et al., 1990).

For a step input of the target chemical into a CM reactor, the chemical concentration in the effluent, C , can be described by

$$\frac{C}{C_f} = 1 - \exp\left(-\frac{t}{(1 + K_d X)t_\theta}\right) \quad (4-9)$$

Equation (4-9) is obtained by incorporating Equation (4-7) into the equation for a CM reactor with step input based on the mass balance: $(dC/dt + X dq/dt)V = Q(C_f - C)$, at the initial condition of $C = 0$ at $t = 0$. In Equation (4-9), C_f is the chemical concentration in the influent [ML^{-3}]; t is time [T]; X is granular sludge concentration in the reactor [ML^{-3}]; $t_\theta = V/Q$, V is reactor volume [L^3], Q is influent flowrate [L^3T^{-1}] and subscripts, e and DCP^T , are removed to consider sorption under dynamic situation for any chlorophenols. For chemicals which are not adsorbed by anaerobic sludge, Equation (4-9) reduces to

$$C/C_f = 1 - \exp(-t/t_\theta) \quad (4-10)$$

Similarly, the mass balance equation for a CM reactor with pulse input has the form, $(dC/dt + X dq/dt)V = QC$ and the dynamic model under the same assumptions can be written as:

$$\frac{C}{C_0} = \frac{1}{1+K_d X} \exp\left(-\frac{t}{(1+K_d X)t_\theta}\right) \quad (4-11)$$

where, C_0 is the initial chlorophenol concentration in the reactor based on the input. For chemicals which are not adsorbed by sludge, Equation (4-11) becomes

$$C/C_0 = \exp(-t/t_\theta) \quad (4-12)$$

For the SC reactor, under the same assumptions as those for the CM reactor, the one dimension advective-dispersive equation (A-D) can be used to describe the transport of the sorbing chlorophenol in the reactor (Brenner, 1962),

$$\frac{\partial C}{\partial t} + X \frac{\partial q}{\partial t} = D \frac{\partial^2 C}{\partial z^2} - u \frac{\partial C}{\partial z} \quad (4-13)$$

and the boundary conditions for the SC reactor used in this experiment are:

$$\begin{aligned} uC_f &= uC - D \frac{\partial C}{\partial z}, & z = 0, t > 0 \\ \frac{\partial C}{\partial z} &= 0, & z = L \\ C(z) &= 0, & t = 0 \end{aligned} \quad (4-14)$$

where, D is the dispersion coefficient [L^2T^{-1}]; u is the average pore-water velocity [LT^{-1}] and z is a length variable along the reactor [L]. Since the anaerobic granules are very porous, the porosity of the sludge column was assumed to be equal to 1.0 (assumption 3)

and the validity of this assumption will be further verified by model fitting. Using linear sorption relation (Equation 4-7), Equation (4-13) can be rewritten as:

$$(1 + K_d X) \frac{\partial C}{\partial t} = D \frac{\partial^2 C}{\partial z^2} - u \frac{\partial C}{\partial z} \quad (4-15)$$

The boundary and initial conditions for Equation (4-15) are the same as Equation (4-14). For the non-sorbing chemical, $K_d = 0$, then Equation (4-15) becomes a conventional A-D model,

$$\frac{\partial C}{\partial t} = D \frac{\partial^2 C}{\partial z^2} - u \frac{\partial C}{\partial z} \quad (4-16)$$

Equation (4-15) is the model to describe the sorption process in the SC reactor. Equation (4-16) was used to estimate the dispersion number, D/uL , for the sludge column, where L is the length of the reactor. Equations (4-15) and (4-16) under the initial and boundary conditions described by Equation (4-14) are solved numerically in this study using the control-volume approach (Patankar, 1980).

4.3.2 Sorption Process in CM Reactor

The dynamic sorption tests conducted in the CM reactor are summarized in Table 4-11. Among the chemicals used, 2,4-DCP was studied in more detail since it was the target chemical for investigating the degradation process in the UASB reactors in this study. In

Table 4-11, the test No. shows the order in which the sorption tests were conducted.

Table 4-11 Dynamic sorption tests conducted in the CM reactor

Test No.	Chemical	Input mode	HRT (h)	Anaerobic granular concentration (g VSS/L)	Chemical concentration in influent (mg/L)	Chemical added at initial time (mg)	Final pH in reactor ^b
1	2,4-DCP	Step	4.85	10.4	23.37	NA ^a	7.40
2	2,4-DCP	Step	0.93	2.1	27.13	NA	7.45
3	2,4-DCP	Step	3.90	0.0	26.25	NA	7.52
4	3-MCP	Step	5.00	10.4	10.40	NA	7.21
5	3-MCP	Step	0.93	2.1	22.91	NA	7.28
6	2,4-DCP	Pulse	5.47	10.4	NA	27.14	7.40
7	3,4-DCP	Step	5.18	10.4	23.14	NA	7.43
8	2,4,6-TCP	Step	5.18	10.4	13.07	NA	7.41
9	2,4,6-TCP	Pulse	5.31	10.4	NA	27.17	7.43
10	PCP	Step	5.71	10.4	16.30	NA	7.36
11	PCP	Pulse	5.95	10.4	NA	27.17	7.40
12	PCP	Pulse	3.10	0.0	NA	27.17	7.49

^a Not applicable. ^b Initial pH of feed and solution in reactors was controlled at 7.5 (see Chapter 3).

2,4 -DCP. Previous studies have indicated that the sorption isotherm of 2,4-DCP to anaerobic sludge can be well described by linear sorption isotherm and no hysteresis was observed in its sorption-desorption isotherm. Therefore, only nonequilibrium sorption could affect the validity of application of linear sorption equation to the sorption process. The tests for 2,4-DCP were first conducted at an HRT of 4.85 h, since this value is close to the lower limit for practical HRTs used in the operation of UASB reactors. Data from sorption test No.1 are shown in Figure 4-11. Equation (4-9) was used to fit to the data by adjusting the value of K_d based on the least squares principle. The results indicate that the data are well described by the model with linear sorption equation. For further

confirmation, a test at $HRT < 1$ h and a test with pulse input of 2,4-DCP were also conducted. In Figure 4-12, the results from the test at HRT of 0.93 h indicate the same conclusion as that at HRT of 4.85 h. For the test with pulse input, deviation between the experimental data and the model (Equation 4-11) was observed for the initial 20 min but the model follows the data quite well afterwards (Figure 4-13). The deviation may be caused by diffusion limitation in the reactor when the concentration gradient of 2,4-DCP in reactor was high at the initial time.

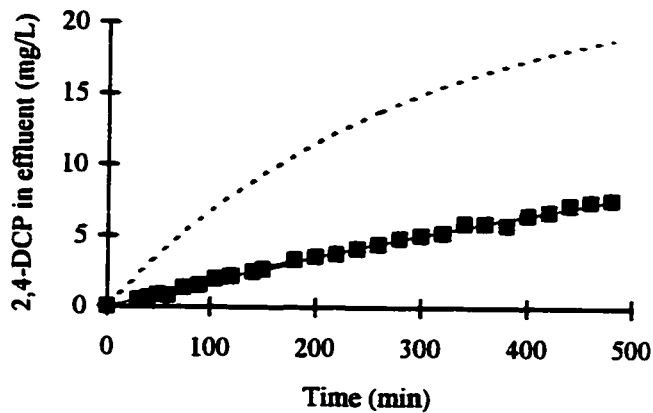


Figure 4-11 Test No. 1: 2,4-DCP with step input ($HRT = 4.85$ h). The curve, \cdots , represents the model without sorption; — , the model with sorption (fitted $K_d = 0.31$) and \blacksquare , experimental data.

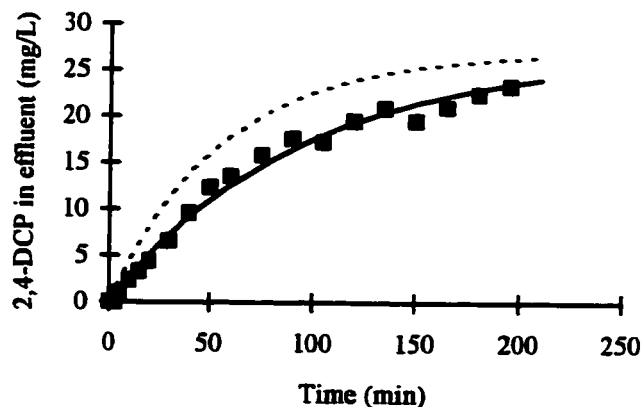


Figure 4-12 Test No. 2: 2,4-DCP with step input ($HRT = 0.93$ h). The curve, \cdots , represents the model without sorption; — , the model with sorption (fitted $K_d = 0.35$) and \blacksquare , experimental data.

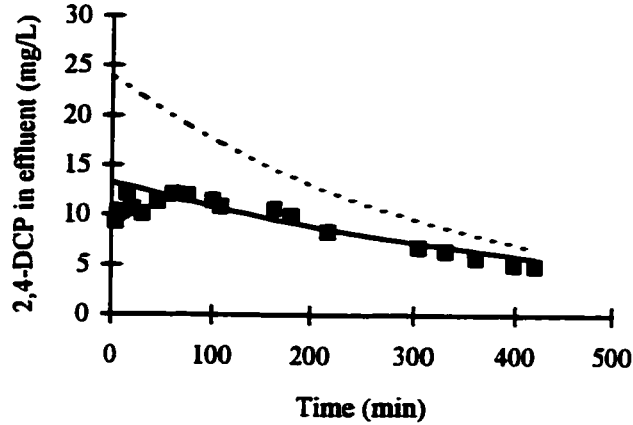


Figure 4-13 Test No. 6: 2,4-DCP with pulse input (HRT = 5.47 h). The curve, ----, represents the model without sorption; —, the model with sorption (fitted $K_d = 0.049$) and \square , experimental data.

A test without anaerobic granules in the reactor (Test No. 4) was also carried out for correcting the effect of 2,4-DCP sorption to the system (tygon tubing, feeding pump, separator and inner surface of the reactor). The need for this correction was highlighted by the best fitting K_d values obtained for the results shown in Figures 4-11~4-13. Although the data were well fitted by the model with linear sorption equation, the fitted sorption coefficient values, K_d , vary significantly. From previous serum bottle sorption isotherm experiments in this study, the average K_d value for the same anaerobic granules was 0.054 but only the fitted K_d in Figure 4-13 is close to this value. The results for the blank run (Test No. 3) are presented in Figure 4-14 in which the difference shown between the curve without sorption and the data indicate a significant adsorption of 2,4-DCP to the system. However, it should be noted that, since previous experiments (Figure 4-2) had proved that the adsorption to inner surface of reactor (glassware) is negligible, adsorption to the feed pump, tygon tubing and solid-liquor separator must have occurred. This explains why the

test with pulse input had a closer sorption coefficient value to that of the sorption isotherm. In analyzing the results from Figure 4-14, 2,4-DCP adsorption to the system follows the model with linear sorption equation. To account for the adsorption by the model (Equation 4-9), it is assumed that the same amount of anaerobic granules exist in the reactor as that in Test No. 1.

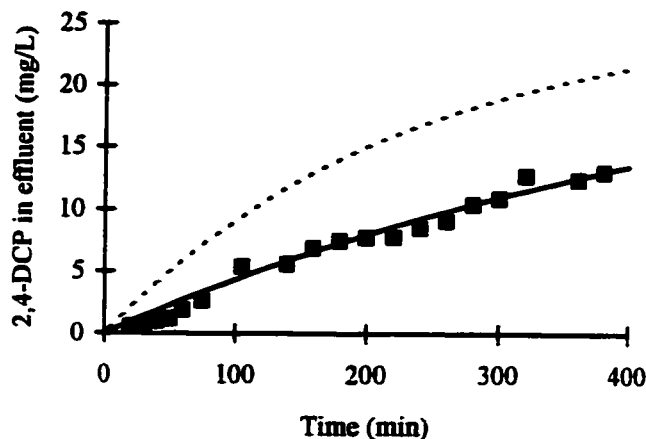


Figure 4-14 Test No. 3: 2,4-DCP blank run with step input (HRT = 3.90 h). The curve, —, represents the model without sorption; —, the model with sorption (fitted $K_d = 0.14$) and the marker, ■, experimental data.

Nevertheless, the results from the blank test (Figure 4-14) cannot be directly used in the adjustment of the data from the sorption test with sludge. Even if the operating conditions can be controlled under exactly the same conditions between the two sorption tests, the sorption process occurring in the blank reactor was different from sorption with sludge. At a specific time, 2,4-DCP available for adsorption by the system is much higher in the blank than it is in the reactor with sludge. To solve this problem, a simple method was employed in the data analysis. The method is based on the following assumption: the adsorption of 2,4-DCP to the system is only determined by the 2,4-DCP concentration in

solution. This assumption is reasonable since it is consistent with the underlying concepts of linear sorption equation. The procedures for data adjustment are illustrated as follows. From Figure 4-13, the difference, ΔC , between the model without sorption (Equation 4-10) and the model (Equation 4-9) fitted data can be expressed as the difference between the two models,

$$\Delta C = C_f \{ \exp[-t/(t_\theta(1 + K_d X))] - \exp(-t/t_\theta) \} \quad (4-17)$$

Since the concentration of 2,4-DCP under the condition with sorption, C , is the value that should be adjusted, the term, $\exp(-t/t_\theta)$, in the equation above is replaced with a function of C based on Equation (4-9). Thus the equation used in data adjustment for the adsorption of 2,4-DCP to system components is obtained:

$$\Delta C = C_f \left[\left(1 - C/C_f\right) - \left(1 - C/C_f\right)^{(1+K_d X)} \right] \quad (4-18)$$

Applying Equation (4-18) to adjust the data shown in Figure 4-11, the adjusted results are presented in Figure 4-15 below.

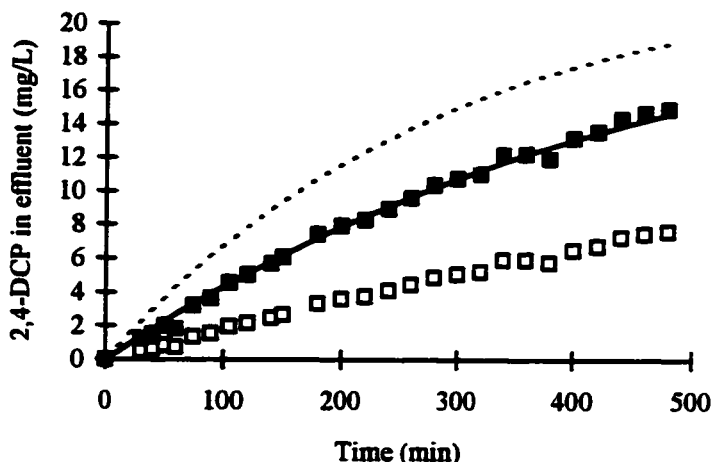
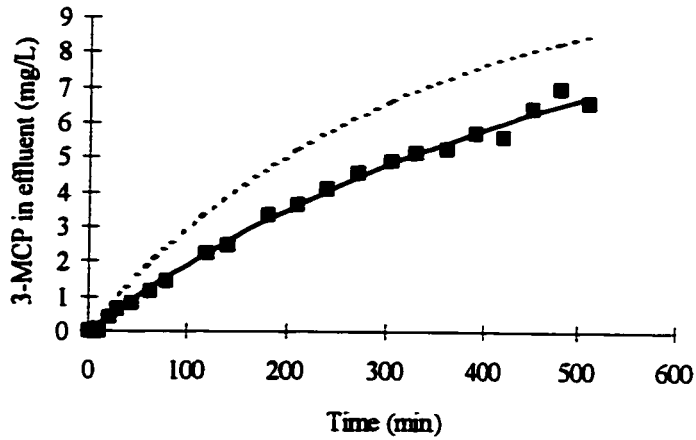


Figure 4-15 Adjusted results for 2,4-DCP sorption to sludge with step input (Test No. 1) The curve, —, represents the model without sorption; —, the model fitted to adjusted data (fitted $K_d = 0.065$); and the marks, \blacksquare and \square , represent the adjusted and unadjusted experimental data, respectively.

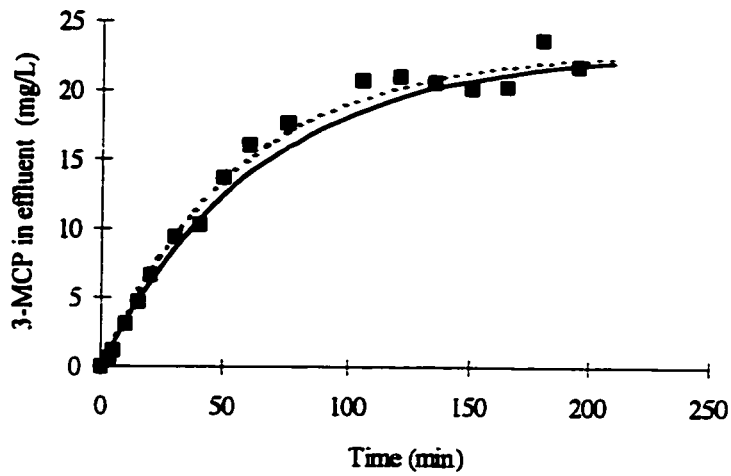
As indicated in Figure 4-15, for the model fitted to adjusted data the K_d value is equal to 0.065, which is of the same magnitude as the value, 0.054, obtained from the serum bottle sorption isotherm of 2,4-DCP.

3-MCP and 3,4-DCP. It was reported by Kennedy et al. (1992) and Woods (1985) that the sorption of 3-MCP and 3,4-DCP to anaerobic granules follows sorption isotherm linearity but both showed hysteresis in sorption-desorption. Dynamic sorption tests were conducted in this study to identify the effect of hysteresis on the sorption process. Figures 4-16 (a) and (b) show the results for 3-MCP with step input at HRT of 5.0 and 0.93 h, respectively. Very good fitting results between the model with linear sorption equation and the experimental data were observed in the figure. Comparing the K_d value, 0.01, reported (Kennedy et al., 1992) for sorption isotherm of 3-MCP, the best fitted K_d value in both Figure 4-16 (a) and (b) is 0.06. Due to the effect of 3-MCP sorption to the system, the fitted sorption coefficient value has increased, which is a consistent observation with that for 2,4-DCP.

The sorption results for 3,4-DCP are presented in Figure 4-17 and the figure shows that the sorption process seems to follow the model with linear sorption equation well. However, using an expanded scale as in Figure 4-18, lack of fit of the model to the data becomes apparent. This lack of fit can be more clear in the residual plot (not shown) for the fitted results. In Figure 4-18, the use of two other K_d values to fit the data clearly



(a)



(b)

Figure 4-16 Test for 3-MCP. (a) Test No. 4: step input, HRT= 5.0 h and fitted $K_d = 0.06$; (b) Test No. 5: step input, HRT=0.93 h and fitted $K_d = 0.06$. The curve, ---, represents the model without sorption; —, the model with sorption and the marker, ■, represents experimental data.

indicates the inadequacy of the model with linear sorption equation. However, a more detailed investigation is needed to confirm this nonideal sorption phenomena. Comparatively, nonideal sorption of 3-MCP was not observed in the tests (Figure 4-16)

although 3-MCP also displayed hysteresis in its sorption-desorption similar to 3,4-DCP. This is possibly because of the weak sorption tendency of 3-MCP to anaerobic granules compared with that for 3,4-DCP ($K_d = 0.096$ from Kennedy et al., 1992) and nonideal sorption of 3-MCP may be masked by adsorption of 3-MCP to system components.

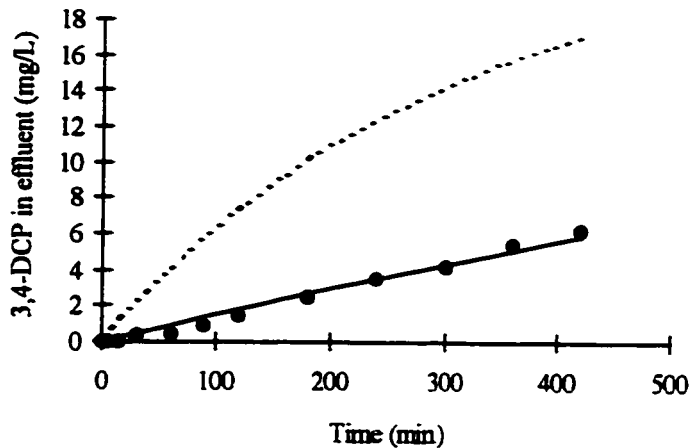


Figure 4-17 Test No. 7: 3,4-DCP with step input (HRT = 5.18 h). The curve, ----, represents the model without sorption; —, the model with sorption (fitted $K_d = 0.35$) and the marker, •, experimental data.

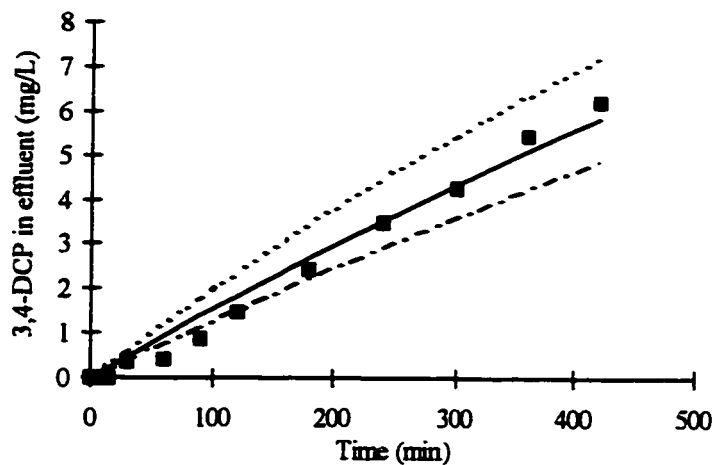


Figure 4-18 Nonideal sorption of 3,4-DCP to anaerobic granules. The curve, ----, represents the model with fitted $K_d = 0.25$; —, the model with fitted $K_d = 0.35$; ---, the model with fitted $K_d = 0.45$ and the marker, ■, experimental data (Test No. 7).

2,4,6-TCP and PCP. For 2,4,6-TCP sorption to anaerobic sludge, there is no hysteresis in its sorption-desorption isotherm but the sorption does not follow isotherm linearity. However, similar to 2,4-DCP, the experimental data for 2,4,6-TCP sorption fit the model with linear sorption equation quite well in this dynamic sorption process (Figure 4-19).

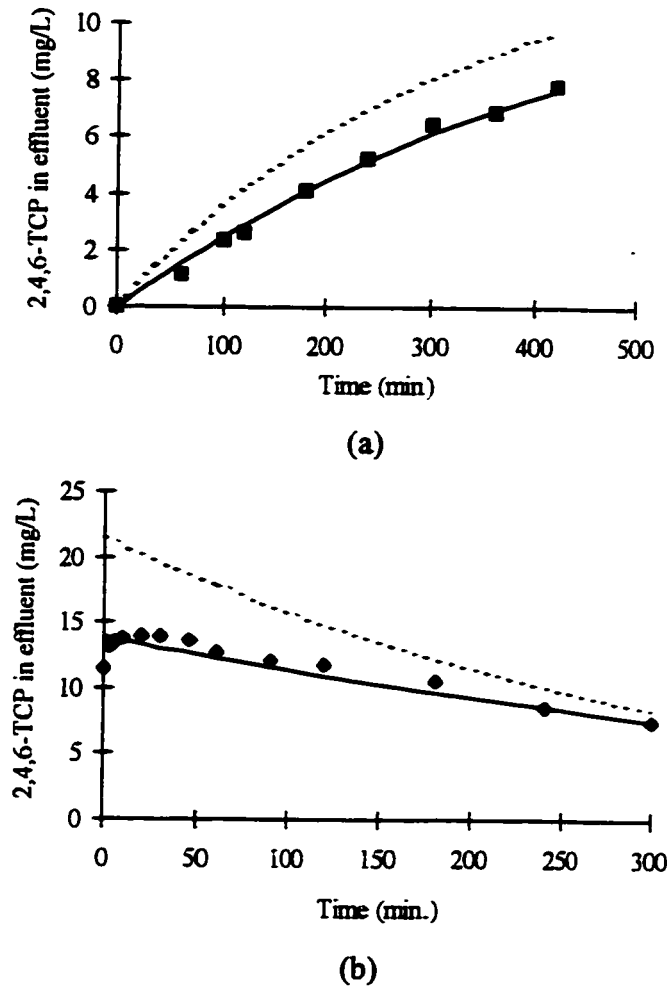


Figure 4-19 Test results for 2,4,6-TCP. (a) Test No. 8: step input, HRT= 5.18 h and fitted $K_d = 0.06$; (b) Test No. 9: pulse input, HRT= 5.31 h and fitted $K_d = 0.05$. The curve, ----, represents the model without sorption; —, the model with sorption; the marker, •, represents data.

Biosorption of PCP to biological solids has been extensively studied and inconsistent conclusions were reported in the literature about sorption linearity and

sorption-desorption singularity (Woods, 1985; Kennedy et al., 1992; Wu et al., 1993). Since PCP has a low pK_a , 4.8, the chemical will be highly ionized under the pH values controlled in this experiment compared to other chlorinated phenols. Furthermore, PCP has a low solubility and high sorption tendency in its molecular form, thus ionization will significantly affect the solubility and sorption characteristics of PCP. The experimental data and model fitting results for PCP with step input are shown in Figure 4-20.

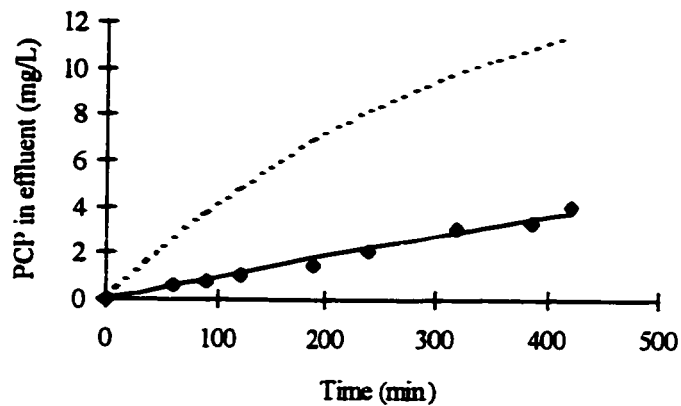


Figure 4-20 Test No. 10: PCP with step input (HRT = 5.71 h). The curve, ---, represents the model without sorption; —, the model with sorption (fitted $K_d = 0.35$) and the marker, ♦, experimental data.

Figure 4-20 shows that dynamic sorption of PCP to anaerobic granules with step input can be described well by model with the linear sorption equation under the experimental conditions employed in this study. However, the sorption of PCP with pulse input shows a different picture, in which the experimental data do not follow the model with linear sorption equation [Figure 4-21(a)]. To further confirm the nonideal sorption phenomena, a blank run with pulse input of PCP was conducted and the results are presented in Figure

4-21(b) for comparison. Although nonideal sorption of PCP was observed, the mechanism for this phenomenon is not clear.

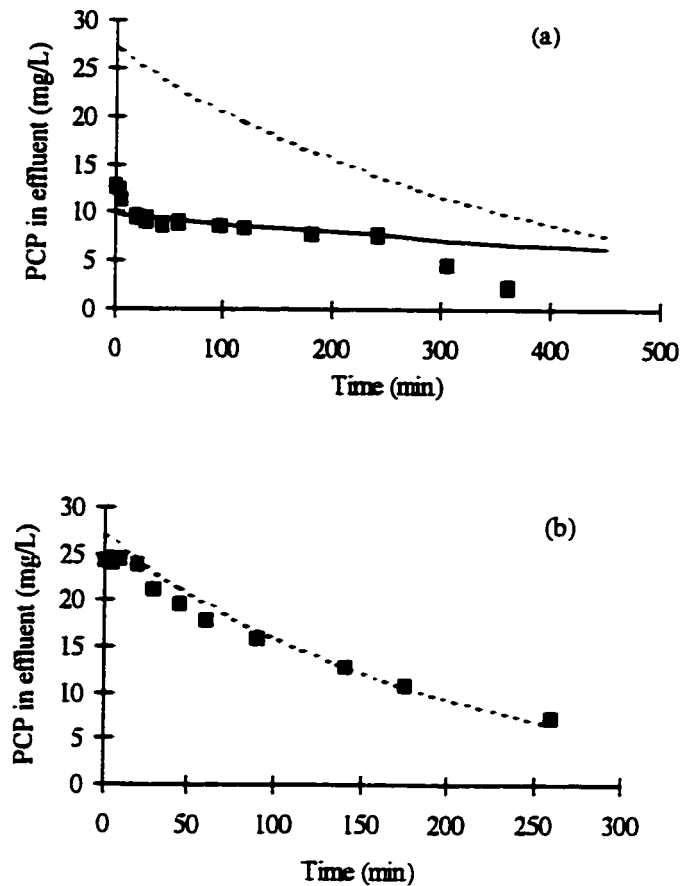


Figure 4-21 (a) Test No. 11: PCP with pulse input (HRT = 5.95 h, fitted $K_d = 0.35$). (b) Test No. 12: PCP blank run with pulse input (HRT = 3.10 h). The curve, —, represents the model without sorption; —, the model with sorption. The markers, ■, are for data.

4.3.3 Sorption Process in SC Reactor

The results from the CM reactor have indicated that the sorption processes of chlorophenols to anaerobic granules can be basically described by the dynamic model with

linear sorption equation, suggesting that the effect of diffusion limitations of chlorinated phenols within anaerobic granules in the dynamic sorption processes is minimal. However, nonequilibrium sorption could be related to the mixing condition in the sorption system (Brusseau and Rao, 1989). Although the prevailing mixing condition in the laboratory anaerobic reactor is completely mixed, nonideal mixing conditions caused by dead volume and short circulating are commonly observed in practice for anaerobic reactors. To examine the correlation of the sorption process with mixing condition, the sorption of 2,4-DCP was conducted under plug flow condition with longitudinal dispersion in a SC reactor.

At a bulk anaerobic granule concentration of 48.1 g VSS/L, the SC reactor was first run using propionic acid (HPr) as the tracer to determine the dispersion characteristics of the reactor. Then, the same sludge column was run under the same operating conditions using 2,4-DCP to identify possible nonequilibrium sorption phenomena. Based on the experimental setup, the transport of tracer, HPr, can be described by a commonly used model shown in Equation (4-16) under boundary conditions of Equation (4-14). The model parameters, D/uL , and porosity of sludge column, ε , were estimated by nonlinear regression based on the least squares principle. Since no quantitative information on sludge column porosity is available in the literature, both parameters were determined by curve fitting. The average retention time, \bar{t} , calculated from HPr output data was found to be almost the same as the theoretical HRT, t_0 , for the SC reactor. Hence, there was no dead volume within the reactor. The

parameters estimated were $D/uL=0.096$ and $\varepsilon=0.98$ for SC reactor by minimizing the sum of squared residuals (RSS) between the predicted and the observed HPr concentration in effluent, as indicated in Figure 4-22. Using these two parameter values, the result of model fitting to HPr data is very good (Figure 4-23). Although a high concentration of sludge filled the reactor, it is of interest to observe that the estimated porosity of the sludge column is very close to 1.0. This is an indirect evidence of anaerobic sludge porosity (MacLeod, et. al., 1990), and it indicates a significant difference in the internal particle structure between biological solids and soil.

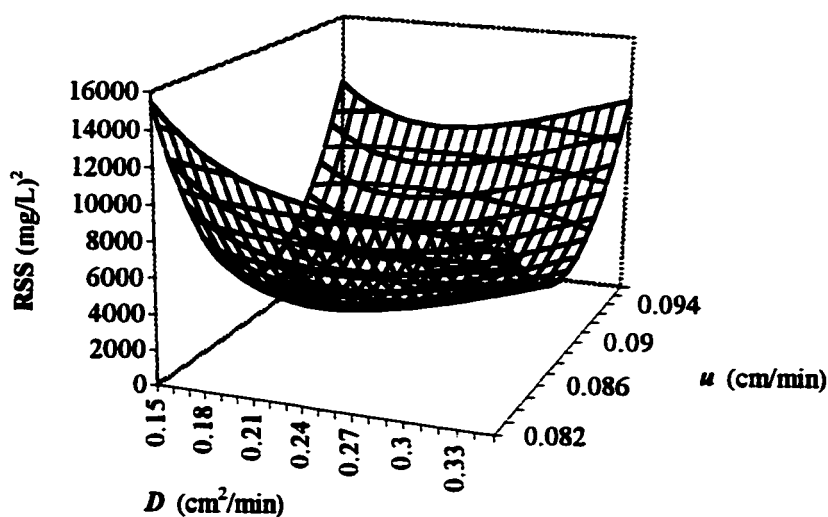


Figure 4-22 Parameters estimation of D and u from the HPr transport data in SC reactor. At the best fit, $D = 0.20$; $u = 0.089$ and $\varepsilon = 0.98$. $D/uL = 0.096$ ($L = 23.5$ cm)

The experimental data from the 2,4-DCP sorption test in the SC reactor were analyzed using Equation (4-15) under the same boundary conditions as those for HPr data analysis. The sorption coefficient value, K_d , in Equation (4-15) was determined by data fitting.

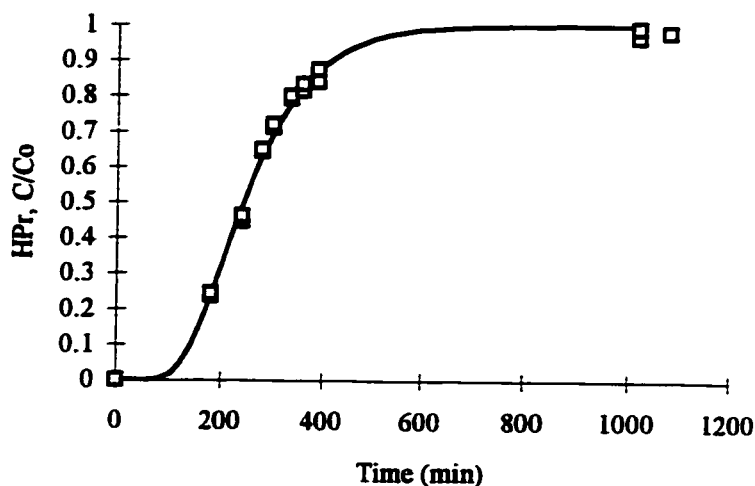


Figure 4-23 Fitting result of A-D model to HPr transport data ($D/uL=0.096$, $\varepsilon = 0.98$)

The same D/uL and ε values estimated from the HPr test were used in the analysis because the operating conditions involved in both tests were the same. In Figure 4-24, the experimental data for 2,4-DCP and the model simulation results using different sorption coefficient values are presented. For comparison, the data and model fitted results for HPr are also included.

It can be seen that the experimental data for 2,4-DCP fit the model very well at $K_d = 0.098$, suggesting that the linearity of 2,4-DCP sorption to granules is independent of mixing condition in the reactor. The simulation results in Figure 4-24 also show a significant influence of sorption on the retention time of 2,4-DCP in the reactor. As indicated by the HPr data, the average HRT is 4.5 h for the condition without sorption, however, with sorption the HRT for 2,4-DCP increased to 23.5 h. This is clear evidence that the degradation of toxic organics can be affected by sorption in a biological reactor.

Although the direct removal of chlorinated phenols by sorption in a reactor may be negligible in the long run, the sorption process can significantly increase retention time of the chemical in the reactor, thus making degradation possible for these less easily degradable organics.

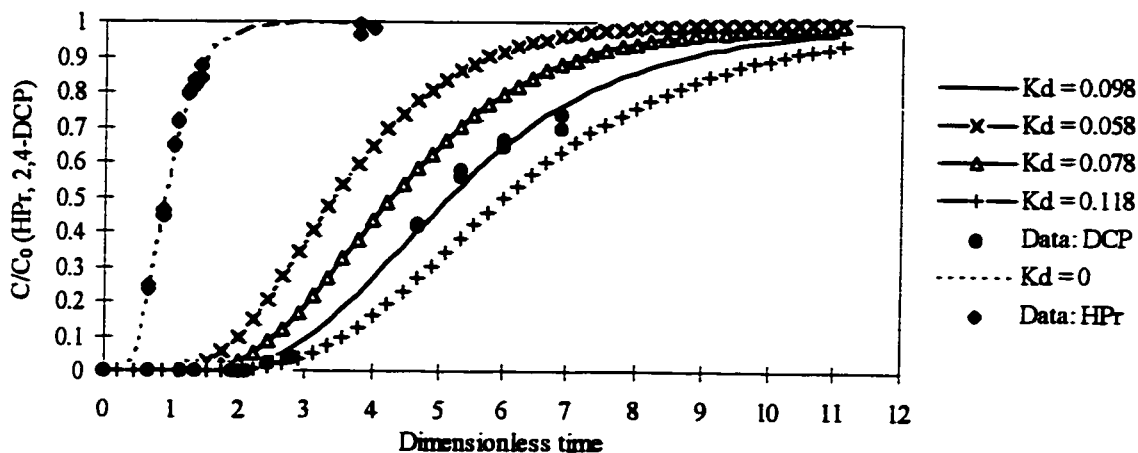


Figure 4-24 Model with linear sorption kinetics fitting results to 2,4-DCP data in SC reactor

4.3.4 Discussion

Considering that very strong hydrodynamic dispersion occurs in a bioreactor, a conventional approach using an asymmetrical breakthrough curve was not used to identify nonideal sorption in this study. Alternatively, these experiments were run mostly in a CM reactor, which is a more realistic representation of a real treatment system. However, the principle used to identify nonideal sorption is the same as that for chemical transport in

soil, which is that, if a dynamic model with linear sorption equation cannot fit the experimental data properly, then the sorption process suffers from nonideal sorption (Brusseau and Rao, 1989).

As indicated by model fitting results for all five chemicals, the nonequilibrium sorption caused by diffusion limitation is negligible in anaerobic reactors due to the strong hydrodynamic dispersion and high porosity of anaerobic granules. However, for 3,4-DCP and PCP that showed the sorption-desorption hysteresis in sorption isotherm (Kennedy et al., 1992), minor nonideal sorption was observed in this study. For the chlorophenols with nonlinear sorption isotherm (2,4,6-TCP and PCP), the 2,4,6-TCP sorption follows the model with linear sorption equation well, but the test for PCP provided a result that needs to be further clarified. With pulse input the data did not follow the model with linear sorption equation, but with step input opposite results were observed. The possible reason for this is that, with step input the concentration of PCP in the system was limited within a narrow range in which the linear sorption equation would be valid. However, with pulse input, PCP concentration varied dramatically during the sorption process. Since the step input mode prevails in field scale bioreactors, the possible nonideal sorption under dynamic situation in reactors caused by sorption isotherm nonlinearity could become insignificant. However, the reason for the deviation between data and the model fitting result after $t > 4$ h for pulse input of PCP (Figure 4-21a) is not clear.

The effect of sorption on degradation is highlighted by the results from this study.

As indicated in Figure 4-24, the higher K_d value of a toxic chemical, higher sludge concentration in the reactor, and smaller D/uL in the reactor, the longer the retention time of the chemical within the reactor. Note that, although this observation is not surprising, it may be a useful guide in the design and operation of treatment systems since an extended retention time is beneficial to degradation of toxic organics in reactors. Without considering the effect of sorption on degradation, the contribution of biosorption was often underestimated because direct removal of toxic organics by sorption is negligible in biological treatment systems (Jacobsen, et. al., 1993; Yan and Allen, 1994).

Dynamic sorption tests showed that sorption to the system is significant. Sorption to the system may also be significant for field scale reactors. The combined action of sorption to system components and sludge may be an important factor in equalizing the toxic organic concentration in a biological treatment system. This is a reasonable interpretation of the phenomena observed in practice, where it is found that the concentration of toxic organics in the effluent is often much more stable compared to their concentration in the influent. Quantitatively precise estimation of sorption coefficients for the system is difficult to obtain. The results for 2,4-DCP indicated that, when excluding the effect of sorption to system components, the sorption coefficient based on fitted data is very close to the coefficient value obtained from serum bottle sorption isotherm tests, which suggests that the coefficient estimated from sorption isotherms can be a good approximation for the dynamic system.

Sound experimental evidence for evaluating adequacy of linear sorption equation under dynamic conditions has been provided in this study. As observed in this investigation, sorption in the continuous system was limited to a narrow concentration range of sorbate due to dilution, which minimized the effect of nonideal sorption and permitted the application of linear sorption equation to the system. Most continuous full-scale treatment systems have similar situations. In addition, the concentrations of toxic organic compounds in most wastewaters are often very low and intensive hydrodynamic dispersion prevails in the system. Under these conditions, linear sorption equation could be a reasonable simplification for modeling the sorption process in the treatment system (O'Brien and Teather, 1995). However, care is highly suggested for situations under which transient input of chemicals with strong sorption-desorption hysteresis to the system is involved. Since the results in this study were limited to a few chlorinated phenols which generally obey close-to-linear sorption isotherm in their sorption behavior (Kennedy et al., 1992), more detailed study should be made for a more general conclusion, especially for some chemicals with strong sorption-desorption hysteresis and time-dependent sorption.

SUBSTRATE INTERACTION

For modeling the multiple substrate degradation process in UASB reactors, it is essential to consider substrate degradation interactions and degradation kinetics of each substrate as well as sorption. However, only a few investigations have been reported on substrate interaction during anaerobic degradation of chlorinated aliphatic compounds (Kim et al., 1994; Wrenn and Rittmann, 1995). Information in the literature on either substrate interaction and/or degradation kinetics for simultaneous removal of easily degradable substrates and chlorinated phenols in UASB reactors is rare.

According to the objectives of this study, the degradation kinetics of 2,4-DCP and easily degradable cosubstrates (HAc, HPr and sucrose) were investigated with consideration of substrate interaction. Considering the interaction among the degradation processes of each substrate (sucrose, HPr, HAc and 2,4-DCP) in UASB reactors, the degradation kinetics for each substrate were determined by analyzing the experimental data from a series of specially designed batch degradation tests. Adequacy of these degradation kinetics was examined by model fitting results to data and model discrimination. Results presented in this chapter include: degradation kinetics of 2,4-DCP

with or without cosubstrate; syntrophic relation between chlorophenol dechlorinator and acetoclastic methanogenic bacteria; and degradation kinetics of HAC, HPr and sucrose in the presence of 2,4-DCP. The major features of substrate interaction for the simultaneous anaerobic degradation of the easily degradable substrates and 2,4-DCP were analyzed.

5.1 Degradation of 2,4-DCP without Addition of Cosubstrates

While anaerobic treatment of 2,4-DCP follows the same general reductive dehalogenation mechanism as highly chlorinated phenols like PCP, its overall process is much simpler. Except for some specially enriched microbial cultures, 4-MCP is the major end product of anaerobic degradation of 2,4-DCP. Further degradation of 4-MCP is either very slow or not detectable (Mohn and Kennedy, 1992).

Similar to other chlorophenols, degradation kinetics of 2,4-DCP is affected by many factors such as degradation pathway, sorption-degradation interaction, cosubstrate interaction and toxicity to mention a few. The effect of cosubstrate interaction on 2,4-DCP degradation could be minimized by not adding cosubstrate into the system. Another difficulty in studying 2,4-DCP degradation by anaerobic granules is the effect of sorption on degradation. Since 2,4-DCP removal by anaerobic sludge granules is a sorption-degradation coupled process, studies that do not differentiate between sorption and degradation effects may limit the understanding of true degradation kinetics. It was indicated in Chapter 4 that partitioning is the dominating mechanism of 2,4-DCP sorption

to anaerobic granules, and the sorption process under dynamic situations can be described by linear sorption equation. With this knowledge, it is possible to investigate the degradation kinetics of 2,4-DCP in detail.

5.1.1 Degradation Process of 2,4-DCP

Batch experiments for 2,4-DCP degradation were conducted by means of SBT and the procedures were described in Section 3.3.3. Anaerobic granules used were obtained from reactor R3 and R4, respectively. The physical properties of sludge R3 and R4 were given in Table 3-2.

Figure 5-1 shows the variation of 2,4-DCP concentration in the liquid phase as a function of reaction time for different initial 2,4-DCP dosage, using R3 anaerobic granules. It was observed that within first 3 h, sorption dominated the 2,4-DCP removal from the liquid phase, since only trace concentrations of 4-MCP byproduct were detected. After sorption equilibrium was achieved, production of 4-MCP was observed to be proportional to the removal of 2,4-DCP in the mixed liquor. This result would also tend to suggest that 2,4-DCP can be utilized as a sole carbon source by this acclimated enrichment or that sufficient endogenous degradation was occurring to support degradation of 2,4-DCP. The slight difference observed in the slopes of the process curves after 3 h, which is related to different initial 2,4-DCP dosages, highlights possible inhibition of degradation in some cases.

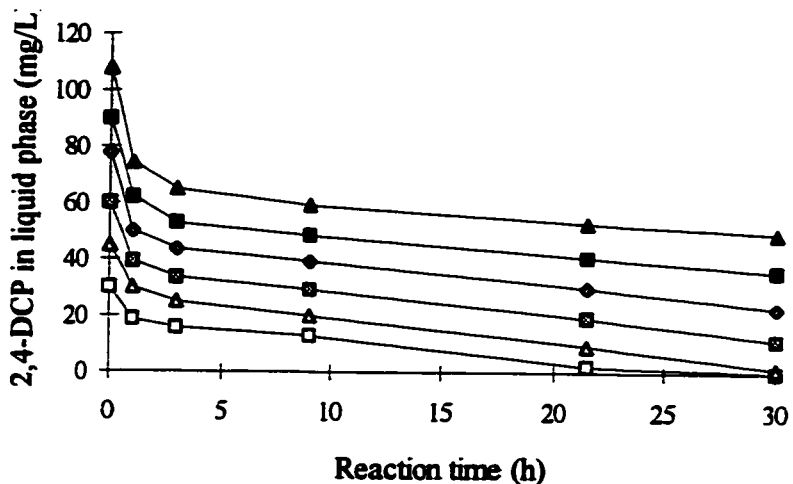


Figure 5-1 2,4-DCP degradation without cosubstrate addition, using R3 sludge granules. For the curves from top to bottom, the initial 2,4-DCP concentrations were 108, 90, 78, 60, 45, and 30 mg/L.

Production of 4-MCP during the same experiment is shown in Figure 5-2. HPLC analysis also revealed three minor peaks indicating production of phenol, 2-MCP and 4-chlorobenzonate. These peaks, although minor, do indicate the possibility of another degradation pathway or further degradation of 4-MCP. However, a detailed mass balance analysis proved that 2,4-DCP to 4-MCP was the major degradation pathway of the process.

By assuming no other degradation pathway for 2,4-DCP and assuming that 4-MCP is not further degradable, then 2,4-DCP lost in a time interval should be equal to 4-MCP produced. Considering the sorption of 2,4-DCP and 4-MCP to anaerobic granular sludge, a relation between the two chemicals can be quantitatively expressed as:

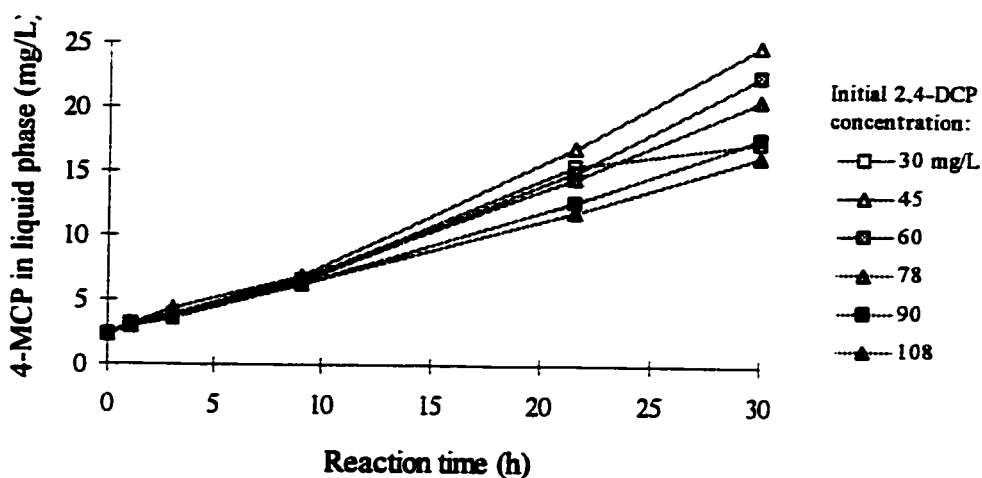


Figure 5-2 Production of 4-MCP in the degradation of 2,4-DCP without cosubstrate addition

$$\Delta C_{DCP} (1 + K_{d,DCP} X) = \Delta C_{MCP} (1 + K_{d,MCP} X) (M_{DCP} / M_{MCP}) \quad (5-1)$$

where, ΔC_{DCP} and ΔC_{MCP} are 2,4-DCP and 4-MCP concentration variations in a specific time interval; $K_{d,DCP}$ and $K_{d,MCP}$ are the sorption coefficients for 2,4-DCP and 4-MCP (L/gVSS), respectively; M_{DCP} and M_{MCP} are molar weights for the two chemicals; and X is the anaerobic granular sludge concentration (g VSS/L). Using sorption coefficients of 0.045 and 0.018 for 2,4-DCP and 4-MCP, respectively (Table 3-2), the theoretical ratio of $\Delta C_{DCP} / \Delta C_{MCP}$ was 0.97 based on the anaerobic sludge concentration of 14.7 g VSS/L in this experiment. The ratio calculated from the experimental data obtained within 9.0~30.0 h was 1.12, suggesting that about 13% of 2,4-DCP removal was the result of another

degradation pathway or further degradation of 4-MCP. Analysis of experimental data also indicated that 2,4-DCP removal by sorption was dominant in the first 3 h of sampling time, since the ratio of $\Delta C_{DCP}/\Delta C_{MCP}$ (1.63 ~ 2.12), for initial 2,4-DCP concentration greater than 45 mg/L at 3 h, was much higher than 1.12 obtained when sorption reached equilibrium. The existence of the other degradation pathway for 2,4-DCP and further degradation of 4-MCP would have no or negligible effect on the analysis of degradation kinetics of 2,4-DCP since only the data for 2,4-DCP were used in this analysis.

The effect of toxicity on 2,4-DCP degradation is seen more clearly by observing 4-MCP production rates (Figure 5-2). For an initial 2,4-DCP concentration of 45 mg/L the 4-MCP production rate was higher than at an initial 2,4-DCP concentration of 30 mg/L. However, the 4-MCP production rate decreased when the initial concentration of 2,4-DCP was greater than 60 mg/L, indicating the toxic effect of 2,4-DCP on the degradation process above that concentration. It was also shown that the production rates of 4-MCP were almost the same for all initial conditions within 3.0~9.0 h of sampling time and the sensitivity of anaerobic bacteria to 2,4-DCP increased significantly after 9 h. Because of this lag phenomenon, only data at sampling times 9.0, 21.5 and 30.0 h were used to analyze the degradation kinetics.

On the basis of experimental results shown in Figures 5-1 and 5-2, the relationship between the average degradation rate of 2,4-DCP at each time interval (9.0~30.0 h only) and 2,4-DCP concentration in liquid phase is presented in Figure 5-3. In the determination

of the degradation rate, the effect of sorption was also considered as shown in Equation (5-2). Since 2,4-DCP degradation rate did not change dramatically within the experimental time interval, the differential method in determining \bar{r}_{DCP} should not cause significant error.

$$\bar{r}_{DCP} = \frac{(C_{DCP,1} - C_{DCP,2})(1 + K_{d,DCP}X)}{(t_2 - t_1)X} \quad (5-2)$$

where, \bar{r}_{DCP} is the average degradation rate (mg/g VSS/h); C_{DCP} is the measured 2,4-DCP concentration in the liquid phase that includes both ionized and unionized forms of 2,4-DCP (mg/L); and t = reaction time (h).

As shown in Figure 5-3, the 2,4-DCP degradation rate decreased when its liquid phase concentration was higher than 15~20 mg/L, which is an indication of inhibition of 2,4-DCP degradation above that concentration (Figure 5-3). To examine the toxic effect of 4-MCP produced in the process on 2,4-DCP degradation, correlation between the 4-MCP concentration in the liquid phase and the 2,4-DCP degradation rate as well as 4-MCP production rate was evaluated (Figure 5-4). It was seen that 4-MCP exerted no toxicity on the 2,4-DCP degradation process. The consistency in the variation between 2,4-DCP degradation rate and 4-MCP production rate confirmed that 4-MCP was the dominant degradation product.

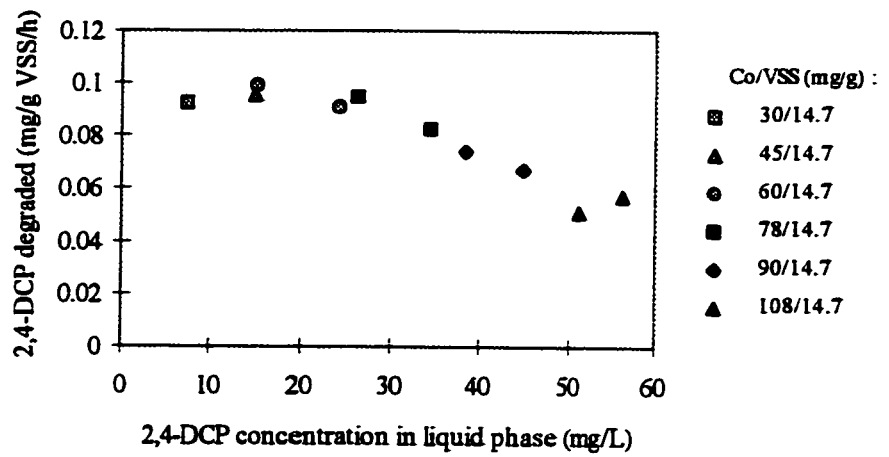


Figure 5-3 Relation between 2,4-DCP degradation rate and its concentration in liquid phase.

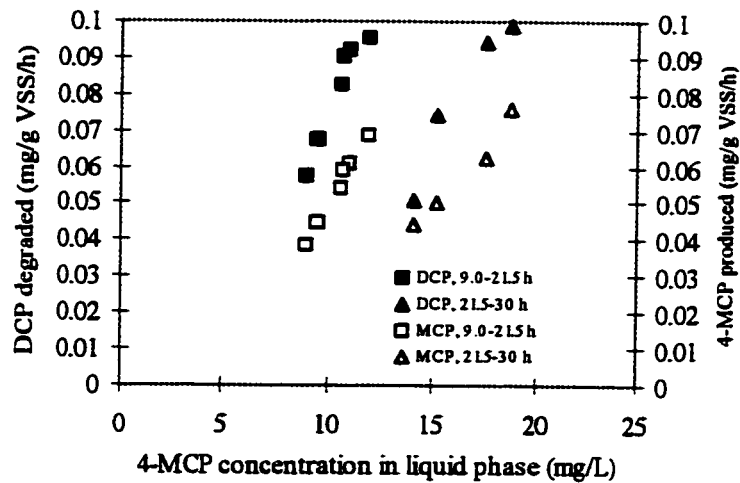


Figure 5-4 Effect of 4-MCP on degradation of 2,4-DCP

Degradation of 2,4-DCP was further investigated using R4 anaerobic granules with a wider range of the initial concentrations of sludge and 2,4-DCP. Besides the experiments conducted at higher initial dosage of 2,4-DCP (30~90 mg/L) and at a sludge concentration of 9.56 g VSS/L, other experiments were run at low initial dosage of 2,4-DCP (6~24

mg/L) and with different concentration of granules (3.71~7.43 g VSS/L). The variation of 2,4-DCP and 4-MCP concentrations in the liquid phase under the condition of lower initial 2,4-DCP dosage is presented in Figure 5-5. The results in this figure show that

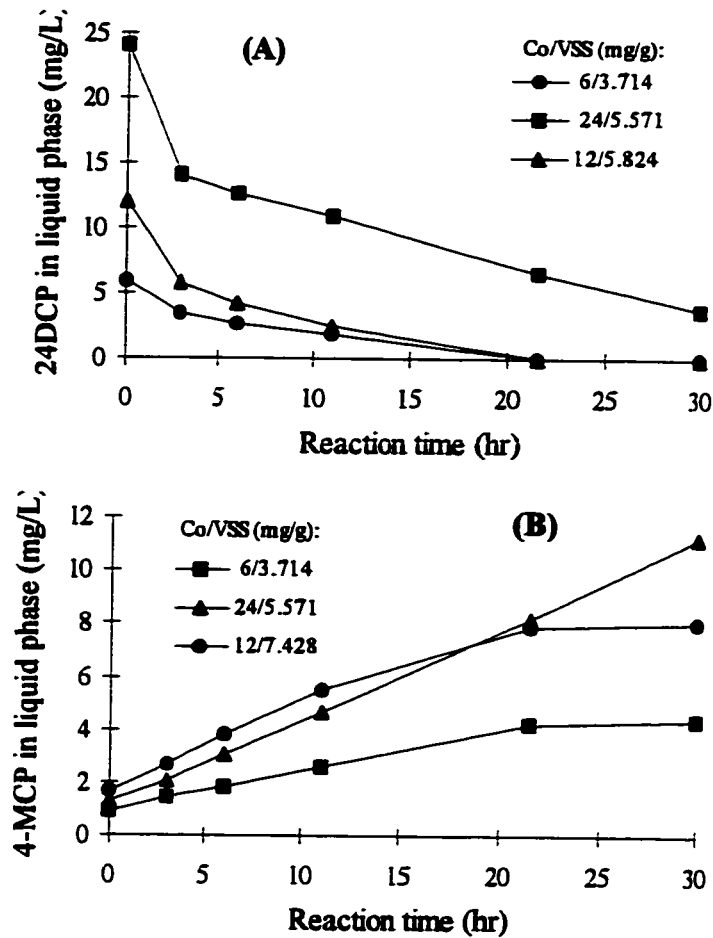


Figure 5-5 2,4-DCP degradation using sludge R4. (A) 2,4-DCP degradation; (B) 4-MCP production.

sorption and degradation processes were both affected by sludge concentration. Higher sludge concentration leads to greater removal of 2,4-DCP by sorption and faster removal

of 2,4-DCP by degradation. When 2,4-DCP concentration in the liquid phase was as low as about 6 mg/L, it began to influence the degradation rate of 2,4-DCP or the production rate of 4-MCP significantly. The degradation process curves for high 2,4-DCP dosage with sludge concentration of 9.56 g VSS/L (Figure 5-6) were similar to those in Figure 5-1. Similar to the results obtained with R3 granules, 4-MCP was the major product of 2,4-DCP degradation when using R4 sludge, and 2,4-DCP removed at different C_0/VSS was directly proportional to 4-MCP produced (Figure 5-6).

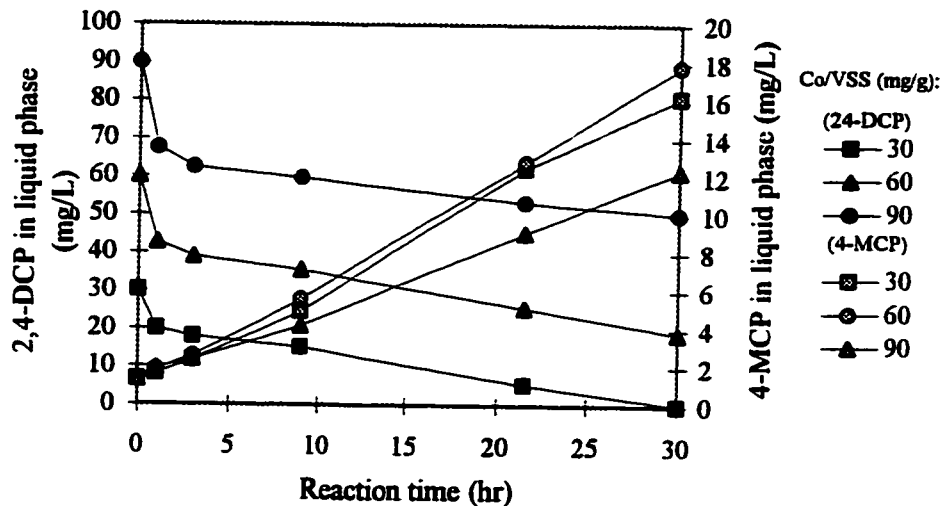


Figure 5-6 2,4-DCP degradation and 4-MCP production using sludge granule R4, sludge concentration: 9.56 g VSS/L.

To identify the effect of 2,4-DCP concentration in the liquid phase on specific degradation rate and toxicity, the averaged degradation rate at each time interval was calculated (Equation 5-2). The relationship between the average degradation rate and 2,4-DCP concentration in the liquid phase is shown in Figure 5-7. As discussed previously,

only the data at time intervals of 6~30 h and 9~30 h for the initial 2,4-DCP concentration 6~24 mg/L and 30~90 mg/L, respectively, were used in this analysis. Figure 5-7 presents a more complete picture of the influence of concentration of 2,4-DCP in the liquid phase on its degradation rate. Within the concentration range of about 0~15 mg/L, the degradation rate of 2,4-DCP increased significantly as the concentration increased; beyond 30 mg/L, degradation was inhibited significantly as the concentration increased.

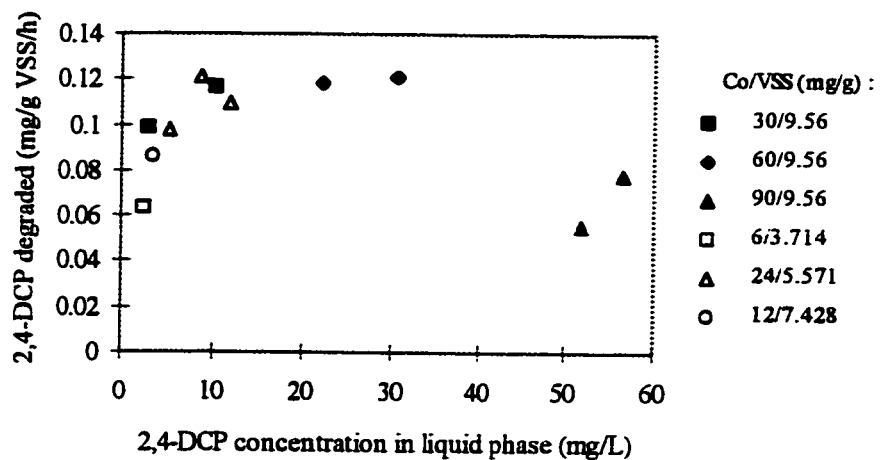


Figure 5-7 Relation between 2,4-DCP degradation rate and its concentration in the liquid phase for R4 sludge

5.1.2 Degradation Kinetics of 2,4-DCP

In describing the degradation of organic compounds with inhibition, the Haldane inhibition equation (HIE) was commonly used (Grady, 1991). Considering that only unionized DCP can be degraded, the HIE equation for 2,4-DCP degradation has the form given below,

$$r_{DCP} = -\frac{1}{X} \frac{dC_{DCP}}{dt} = \frac{k_{DCP^0} C_{DCP^0}}{K_{s,DCP^0} + C_{DCP^0} + C_{DCP^0}^2 / K_{i,DCP^0}} \quad (5-3)$$

in which, C_{DCP^0} is unionized 2,4-DCP and $C_{DCP^0} = C_{DCP} / (1 + 10^{pH - pK_a})$, k_{DCP^0} is the maximum unionized 2,4-DCP degradation rate, K_{s,DCP^0} and K_{i,DCP^0} are half-velocity constant and inhibition constant for unionized 2,4-DCP, respectively.

If degradation was not associated with sorption, then 2,4-DCP removal curves can be used to estimate the parameters in the equation by nonlinear regression. In this case, sorption was dominant in the 2,4-DCP removal from the liquid phase within the first 3 h, which makes it impossible to estimate the parameters without considering diffusion limitation and sorption kinetics. Since there is a lack of information on the ultrastructure of anaerobic sludge granules, analysis of sorption with diffusion limitation in the initial time period of the 2,4-DCP removal process curve may obscure model discrimination for the degradation process. To avoid this problem, the averaged specific degradation rates presented in Figure 5-3 and 5-7 were used. Parameter estimation was conducted by nonlinear regression software using *SAS*. The results for the HIE are given in Table 5-1.

The estimation result in Table 5-1 for the HIE was not satisfactory. Except for the maximum specific degradation rate, k , the precision of estimated values of K_s and K_i was poor, suggesting the equation does not describe the data well. The correlation matrix

Table 5-1 Parameter estimation results for 2,4-DCP degradation kinetics

Model	Sludge	k_{DCP^0} (mg/g/h)		K_{S,DCP^0} (mg/L)		K_{i,DCP^0} (mg/L)		Sum of squared residual
		Value	95% confidence interval	Value	95% confidence interval	Value	95% confidence interval	
Haldane equation	R3	0.29	[-0.01, 0.59]	9.04	[-6.01, 24.1]	10.3	[-3.58, 24.2]	0.000199
	R4	0.20	[0.08, 0.33]	2.87	[-0.65, 6.39]	24.3	[-6.04, 54.4]	0.00163
Modified equation	R3	0.14	[0.12, 0.16]	2.07	[0.36, 3.78]	65.1	[54.8, 75.4]	0.000132
	R4	0.17	[0.13, 0.21]	2.06	[0.53, 3.59]	67.5	[45.5, 89.6]	0.00129

for the estimated parameters showed a high correlation among parameters (not shown). By comparing the simulated results and experimental data, it was seen that although the HIE described the data well when 2,4-DCP concentration in liquid phase was less than 20 mg/L, it failed to predict the downward trend shown in the data when inhibition becomes significant (Figure 5-8). To rectify this shortcoming of the HIE, a modified form of the HIE was proposed to describe the data. The form of the modified equation is

$$r_{DCP} = -\frac{1}{X} \frac{dC_{DCP}}{dt} = \frac{k_{DCP^0} C_{DCP^0}}{K_{S,DCP^0} + C_{DCP^0} + \frac{C_{DCP^0}^2}{(K_{i,DCP^0} - C_{DCP^0})}} \quad (5-4)$$

In Equation 5-4, the inhibition constant K_{i,DCP^0} was modified to $(K_{i,DCP^0} - C_{DCP^0})$. Although the modification was simple, this change allowed the downward trends in data to be reflected. As indicated in Table 5-1, by employing the modified HIE, the precision of estimated parameters was significantly improved. The predicted results using either of the two equations with their estimated parameters are presented in Figure 5-8. It is seen that the modified HIE fits the data better than the HIE.

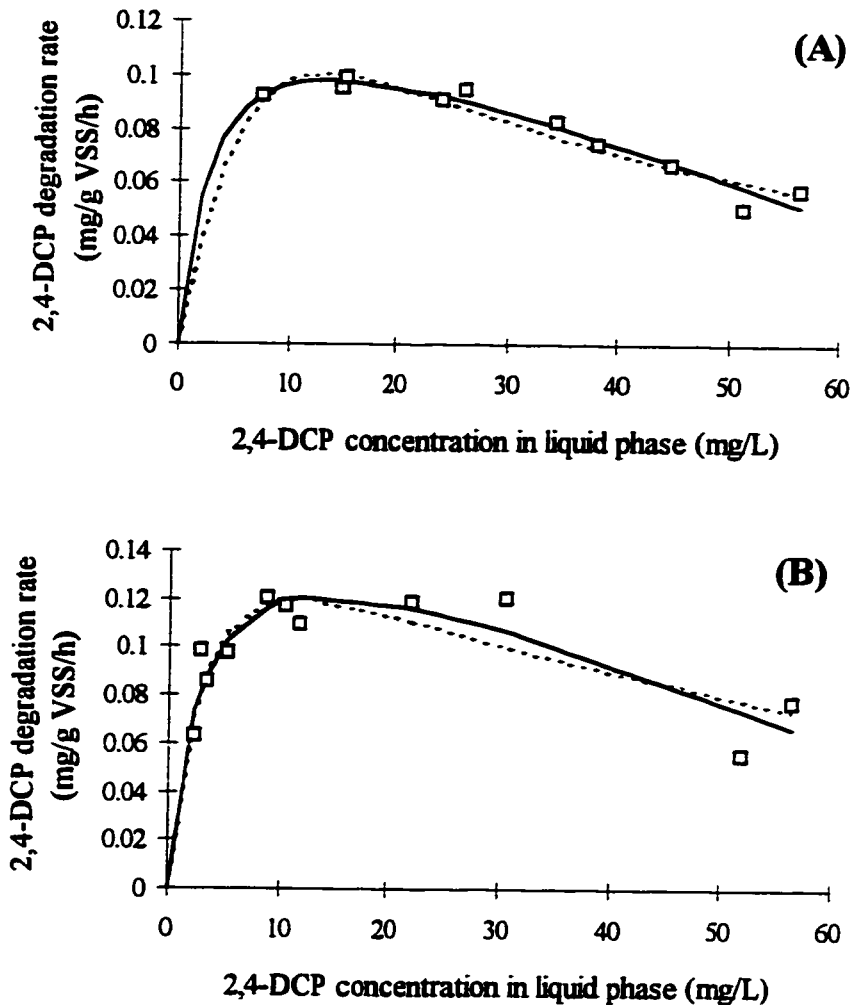


Figure 5-8 Results of kinetic equations fitted to data from experiments (A) using R3 anaerobic sludge granule. (B) using R4 anaerobic sludge granule. The mark represents data; ----, HIE and — , modified HIE equation.

5.1.3 Effect of Sorption on Degradation

In the analysis of 2,4-DCP degradation kinetics, it was assumed that no interaction between the sorption of 2,4-DCP and sorption of 4-MCP occurred in the SBT test, and this assumption was confirmed by Figure 4-9. Another assumption was that the 2,4-DCP

concentration in the liquid phase dominated the degradation process. This assumption was demonstrated to be correct in decontamination of soil and sediment where sorption of toxic organic chemicals to soil and sediment decreased the availability of these chemicals to microorganisms in the liquid phase (Hu et al. 1994; Gordon and Millero, 1985). However, direct experimental evidence for this assumption was not available for biological solids (Wang and Grady, 1992). In anaerobic treatment systems, granular sludge works as both sorbent and degrader, which leads to a high correlation between sorption and degradation.

A qualitative conclusion for this question can be drawn from the inhibiting effect of 2,4-DCP on its degradation by sludge granules R3 and R4. From Figure 5-8, the specific 2,4-DCP degradation rate has the highest value at approximately the same 2,4-DCP concentration in the liquid phase (10 ~15 mg/L) for both R3 and R4 granules. Since the inhibition effect of 2,4-DCP to sludges R3 and R4 was the same, as indicated by the values of $K_{i,DCP}$ for both sludges (Table 5-1), it could be stated that 2,4-DCP concentration in the liquid phase determined the toxicity effect as well as degradation rate.

Further confirmation of the above statement needs information on the 2,4-DCP concentration in the solid phase (sludge granules). However, the solid phase of anaerobic granules is heterogeneous. The sorbed 2,4-DCP is virtually distributed in different domains, such as intragranular pore solution, microbial cell, inert organic compounds and extracellular polymeric substances (EPS), unevenly within granules (Fukuzaki et al.,

1995). Conventional analysis methods used at the present time can only measure the average concentration of sorbed 2,4-DCP using extraction procedures (Kennedy et al., 1992). For simplicity, an average concentration of 2,4-DCP within granules (including intra-granule pore and solid phases), labeled as the interior concentration of 2,4-DCP, is used in the analysis.

Considering the interior concentration concept and the assumption of linear sorption equilibrium, a relationship between the interior concentration, C_{sw} , and the 2,4-DCP concentration in the liquid phase, C_e , can be derived (see Appendix C),

$$\frac{C_{sw}}{C_e} = K_d \rho_{sw} (1 - P) \quad (5-5)$$

Since the values of parameters in the right side of the equation are all measurable, C_{sw} / C_e can be evaluated. The effect of other factors, except for P and ρ_{sw} , on C_{sw} / C_e has been lumped into K_d . Since variation of ρ_{sw} is very small for different sludges [for anaerobic granules, $\rho_{sw} = 1.028 \sim 1.082$ kg/L (Hendriksen and Ahring, 1996); for aerobic floc, $\rho_{sw} = 1.015 \sim 1.034$ kg/L (Andreadakis, 1993)], ρ_{sw} is not sensitive to C_{sw} / C_e evaluation. Assuming a ρ_{sw} value of 1.060 kg/L for sludge granules R3 and R4, and using the information on the properties of granular sludge provided in Table 3-2, the calculated C_{sw} / C_e values for R3 and R4 granules are 5.63 and 3.84, respectively. As a result, the interior concentration of 2,4-DCP for R3 and R4 granules are 84.5 and 57.6 mg/L, respectively, for a corresponding 2,4-DCP concentration in the liquid phase of 15 mg/L. Apparently, the difference in the interior concentration of 2,4-DCP cannot match the

similarity of the inhibiting effect of 2,4-DCP to the two anaerobic granules. This fact confirms that the 2,4-DCP concentration in the liquid phase determined the 2,4-DCP degradation rate and its toxicity effect.

5.1.4 Discussion

Using the modified HIE, the estimated parameters K_{S,DCP^0} and K_{i,DCP^0} for the two anaerobic sludges R3 and R4 are very similar to each other (Table 5-1). This observation is reasonable since the sludge characteristics were expected to be the same due to the similarities in their enrichment procedure. The difference in k values can be explained by unequal enrichment of the species responsible for the degradation of 2,4-DCP, which may be a result of the different specific organic loading rates used in the enrichment procedure. Table 5-2 lists some kinetic parameter values available in the literature for anaerobic degradation of 2,4-DCP and other chlorophenols. Comparing the parameter values in Table 5-2 with those in Table 5-1, the values obtained in this study were in the same range as the values reported in the literature (for 2,4-DCP, $k_{DCP^0} = k$ and $K_{S,DCP^0} = 0.71K_S$ at pH of 7.5).

The modified HIE gave a more accurate description of 2,4-DCP degradation by considering 2,4-DCP inhibition. Additionally, the modified HIE can also be used to describe complete inhibition of the degradation process. Han and Levenspiel (1988) proposed a model to account for complete biomass inhibition but their equation was more

complex and required more parameters to be estimated.

Table 5-2 Kinetic parameter values for anaerobic degradation of chlorophenols

Chemical	Biomass	Model	k (mg/gVSS/h)	K_s mg/L	K_i mg/L	Reference
2,4-DCP	WTP digester sludge	Michaelis-Menten	0.147 ^a	0.47	-	Armenante et al. 1992, 1995
2,4-DCP	WTP digester sludge	Linear	0.248 ^b	-	-	Chang et al. 1995
<i>Other chlorophenols</i>						
PCP	Anaerobic granules	Linear	0.61	-	-	Wu et al., 1992
PCP	Anaerobic granules	Michaelis-Menten	0.461	0.58	-	Hendriksen and Ahring, 1992
2,3,6-TCP	Anaerobic granules	Linear	0.27	-	-	Mohn and Kennedy, 1992
2,4,6-TCP	WTP digester sludge	Michaelis-Menten	0.372 ^a	0.27	-	Armenante et al. 1993, 1995
3,5-DCP	Anaerobic granules	Michaelis-Menten	0.425	-	-	Hendriksen and Ahring, 1992
4-MCP	WTP digester sludge	Michaelis-Menten	0.089 ^a	173.5	-	Armenante et al. 1993, 1995

^a The reported values were equal to kX (mg/hr), where X is biomass concentration (not reported).

^b Dimension for reported k value: mg/L/d.

5.2 Effect of Cosubstrates on the Degradation of 2,4-DCP

In biological treatment systems, degradation of toxic organic compounds is often coupled with the degradation of primary organic matter. For the degradation of chlorinated phenols in anaerobic treatment systems, easily degradable organic matter works as the electron donor to support the growth of dechlorinator. Some of them may directly stimulate the degradation of chlorinated phenols (Hendriksen and Ahring, 1992). In this

investigation, the cosubstrates selected were sucrose, HAc and HPr. These easily degradable organic substances were also the primary substrates for the UASB reactor part of this study.

5.2.1 Effect of Sucrose, HPr and HAc on 2,4-DCP degradation

The effect of sucrose, HPr and HAc on 2,4-DCP degradation was investigated by means of SBT. The experimental procedures were the same as those for 2,4-DCP degradation kinetics study, except for the addition of the cosubstrate at the starting time of the tests.

No stimulating effect was observed for all three cosubstrates used in these experiments. As indicated in Figures 5-9 and 5-10, a slightly negative influence on 2,4-DCP degradation was observed with HAc and HPr. The negative effect of sucrose on the overall 2,4-DCP degradation rate was less significant (Figure 5-11). Additionally, it is seen from the removal process curves in each of the figures that sorption of 2,4-DCP to sludge with cosubstrates was a little faster than without cosubstrates, according to the relative position of each curve at reaction time 1.5 ~ 3.0 h. Since the same sludge concentration was used in these tests, the difference in sorption between the process curves with and without cosubstrate suggests a possible interaction of a small portion of 2,4-DCP with the cosubstrates in sorption. This interaction may be a reason for the slight negative influence due to addition of cosubstrate. Another possible reason is the competition between 2,4-DCP degradation and cosubstrate consumption to support the dechlorinator growth .

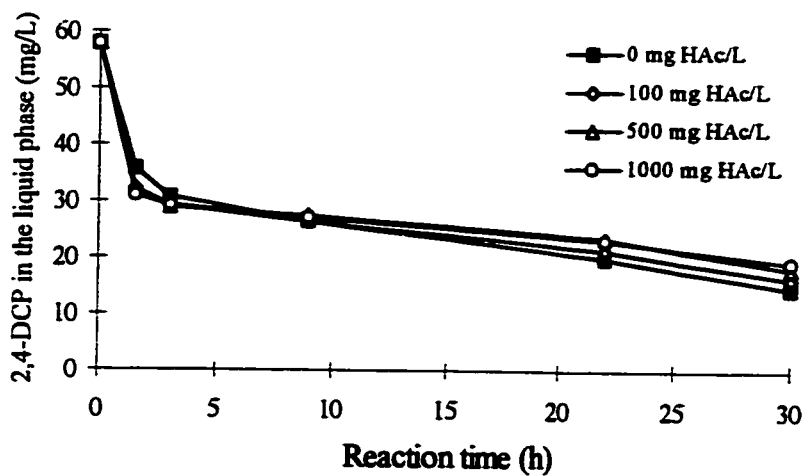


Figure 5-9 Effect of HAc on 2,4-DCP degradation

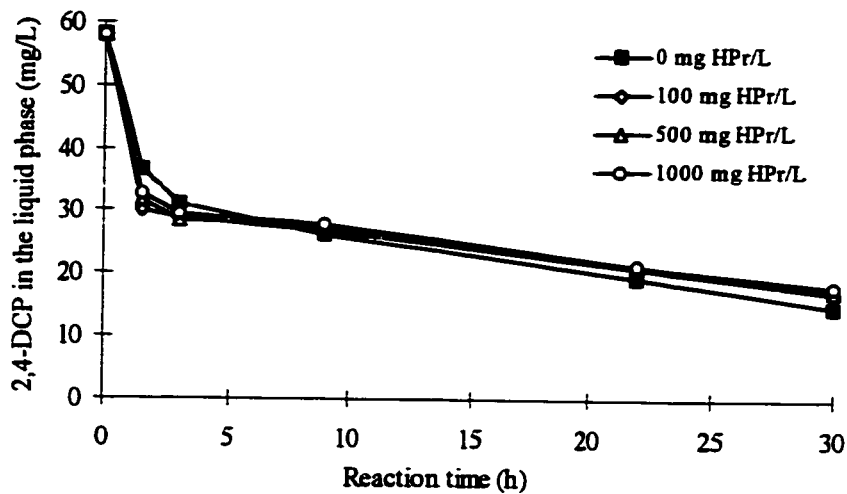


Figure 5-10 Effect of HPr on 2,4-DCP degradation

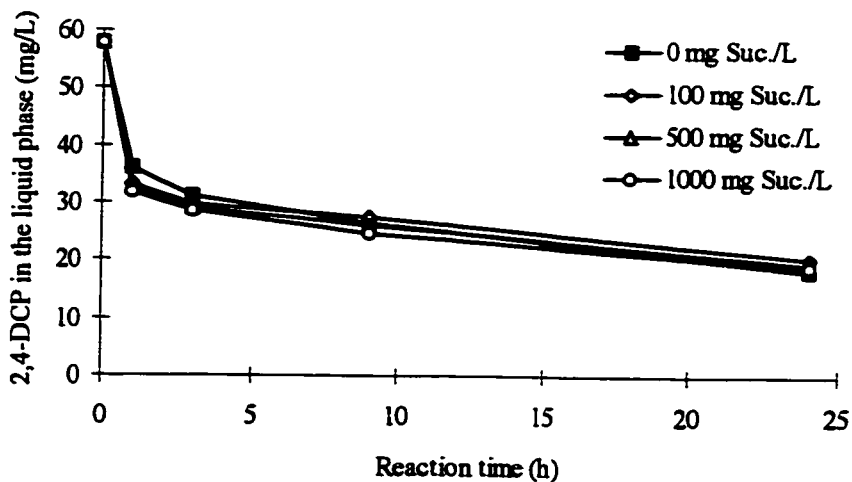


Figure 5-11 Effect of sucrose on 2,4-DCP degradation

Different results were reported regarding the effects of sucrose, HPr and HAc on dechlorination (Table 2-2). Juteau et al. (1995) indicated that HAc was not good in supporting dechlorination. Mohn and Kennedy (1992) observed that sucrose slightly enhanced dechlorination of 2,3,6-TCP but HAc and HPr do not. No stimulating effect of glucose and fructose, which are the hydrolysis products of sucrose, on dechlorination was reported by several investigators (Pak, 1996; Juteau et al., 1995; Perkins et al., 1994). However, Hendriksen et al. (1992) reported that glucose had a strong stimulating effect on PCP dechlorination.

Based on the understanding of reductive dehalogenation of haloaromatic compounds, hydrogen is the source of reducing equivalents required for dechlorination (Schink, 1988). Therefore, 2,4-DCP degradation to 4-MCP can be assumed to proceed as the degradation scheme described below (Armenante et al., 1995),



in which, 2H is a suitable electron donor in the medium rather than elemental hydrogen. If the above dechlorination mechanism is assumed, the addition of any easily degradable organic matter that can act as the source of hydrogen in their degradation would increase the dechlorination rate. However, as indicated above, no stimulation effect was observed for many cosubstrates, including the three cosubstrates used in this study. The reason for this could be that more than enough electron donors were available in this experimental

system, which masked the enhancing effect of sucrose. It was indicated by some researchers (Wrenn and Rittmann, 1995; Mohn and Kennedy, 1992) that even an endogenous electron donor can support dechlorination.

Since no significant effect of cosubstrates on 2,4-DCP degradation rate was observed in these tests, the 2,4-DCP degradation kinetics developed in Section 5.1.2 (Equation 5-3) can be used in modeling the UASB reactors in this study without further modification.

5.2.2 Syntrophic Relation between Dechlorination and Methanogenesis

Considering that hydrogen is the source of reducing equivalents required for dechlorination, it is of interest to know the importance of methanogenesis to 2,4-DCP dechlorination. An experiment for 2,4-DCP degradation was conducted under the condition that methanogenic bacteria were inhibited by an inhibitor, BESA. Since acetophilic methanogenic bacteria can be inhibited at a much lower concentration of BESA (1 mM) than hydrogenophilic methanogenic bacteria (50 mM) (Zinder et al., 1984), only acetophilic methanogenesis was inhibited in this experiment with a BESA concentration in samples of 0.2% (about 1.0 mM). The results from this experiment are presented in Figure 5-12 and 5-13.

The two figures show that, when acetoclastic methanogenesis was inhibited, the

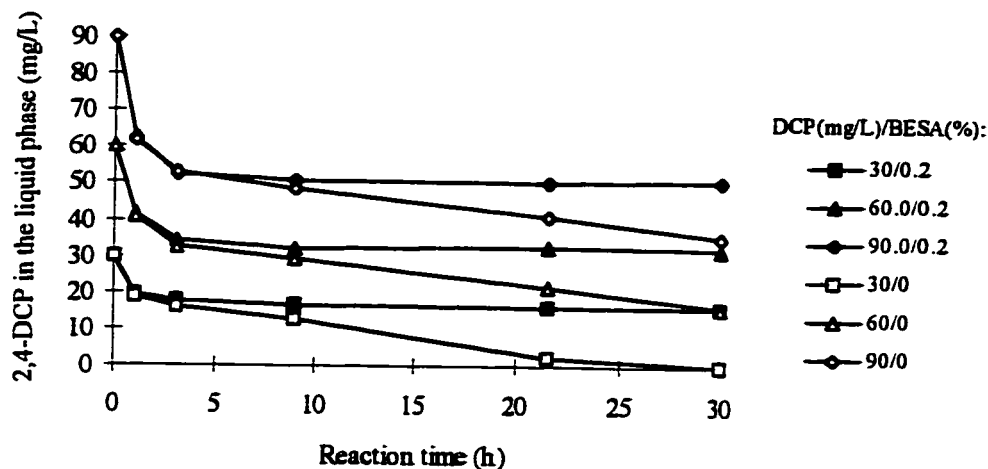


Figure 5-12 2,4-DCP degradation with or without inhibition of methanogenesis

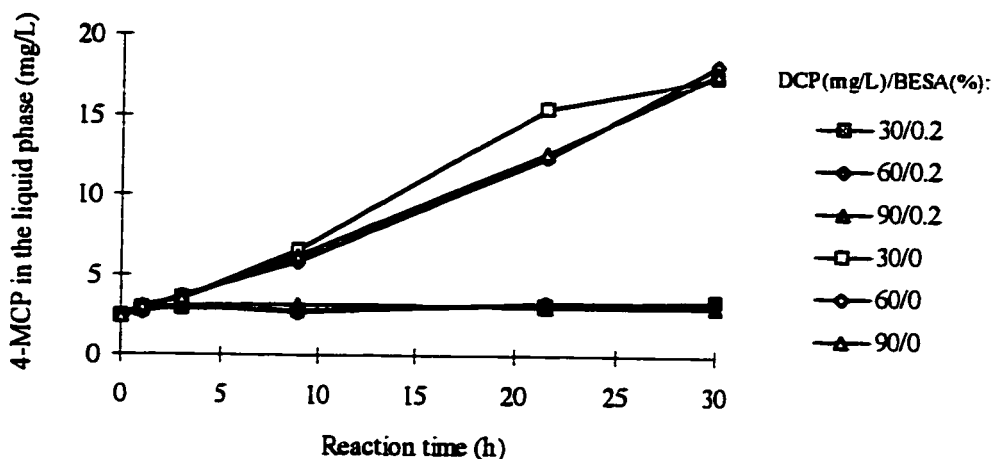


Figure 5-13 4-MCP production with or without inhibition of methanogenesis

2,4-DCP degradation and 4-MCP production were completely stopped. Complete inhibition of dechlorination by BESA was also observed by Hendriksen and Ahring (1992), but they postulated that BESA may also be an inhibitor of the microbial dechlorinator. However, Perkins et al. (1994) indicated that BESA was not an inhibitor of dechlorinators and they observed that with hydrogen as an electron donor, dechlorination

proceeded when methanogenesis was nearly completely inhibited by BESA. Perkins et al. (1994) also reported that with acetate as an electron donor, dechlorination was slowed when BESA inhibited acetoclastic methanogens, suggesting a possible syntrophic relation between acetoclastic methanogens and dechlorinating bacteria. The results obtained in this experiment indicate a close syntrophic relation between dechlorination and methanogenesis since dechlorination stopped when acetoclastic methanogenic bacteria were inhibited. The present experimental evidence is still not sufficient to clarify the mechanism of the syntrophic relation, but these experimental results do indicate the association of methanogenesis from acetate with dechlorination in anaerobic granules.

5.3 Effect of 2,4-DCP on HAc, HPr and Sucrose Degradation

5.3.1 HAc

The experimental results for the degradation of HAc with 2,4-DCP are presented in Figure 5-14. The figure shows a significant influence of 2,4-DCP on degradation of HAc. The slope variation of the degradation process curves with different initial 2,4-DCP/HAc dosage indicated that higher 2,4-DCP dosages caused lower the HAc degradation rates. The HAc degradation rate was also affected by its own concentration. As indicated by the slope of specific process curves, HAc degradation rate slows down when the HAc concentration decreased. Substrate inhibition of HAc and product inhibition of 4-MCP also need to be identified for the degradation system. However, since the inhibition

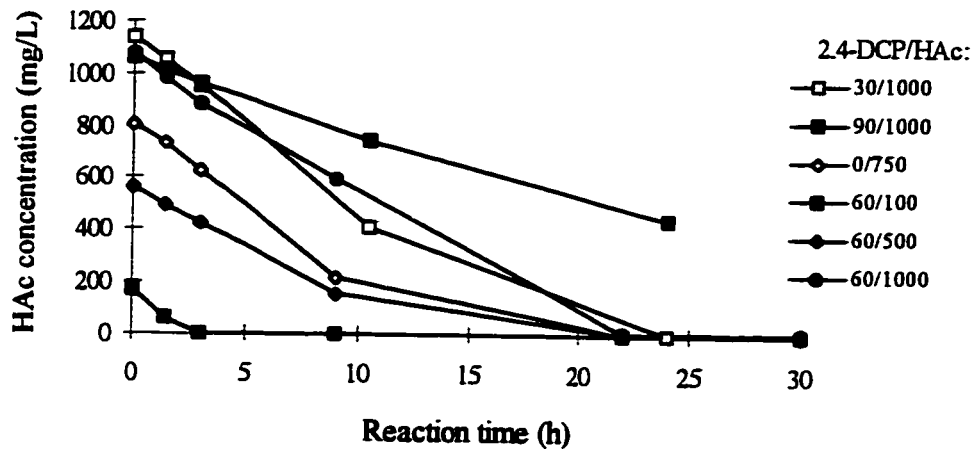


Figure 5-14 Simultaneous degradation of HAc and 2,4-DCP (only HAc data shown)

effects of 2,4-DCP, 4-MCP and HAc on the HAc degradation were highly correlated, direct analysis of the experimental data for each component cannot discriminate the effects. Consequently, model analysis of data was used to explore the degradation kinetics of HAc with 2,4-DCP.

Approaches used in model analysis were: (1) The average HAc degradation rate was determined by using the differentiation equation,

$$\bar{r}_{HAc} = (C_{HAc,1} - C_{HAc,2}) / [(t_2 - t_1)X] \quad (5-6)$$

within each time interval. The relation of \bar{r}_{HAc} determined to HAc and 2,4-DCP concentrations in the liquid phase is shown in Figure 5-15; (2) A few candidate models which covered the possible factors affecting HAc degradation were applied to fit the experimental data in Figure 5-15. The fitted experimental data included HAc, 2,4-DCP, 4-

MCP and \bar{r}_{HAc} . To avoid the effect of diffusion limitation on 2,4-DCP sorption, only the data after 3 h in the experimental run were used in this analysis; and (3) Candidate models

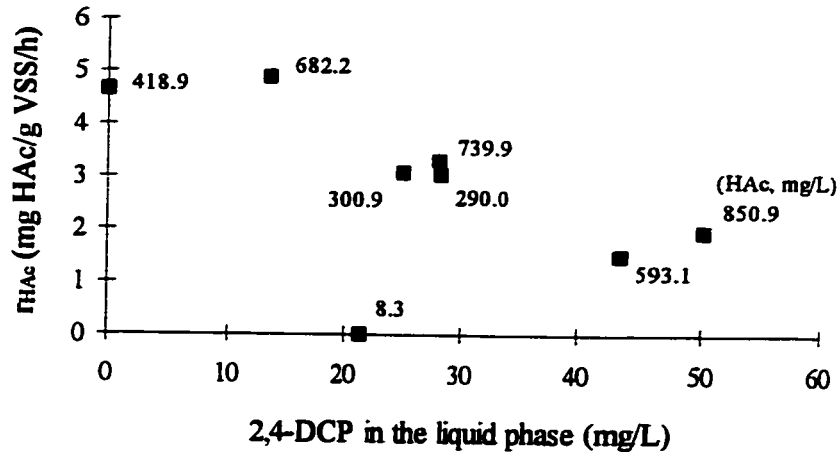


Figure 5-15 Relation of the average HAC degradation rate to 2,4-DCP and HAC concentrations

were discriminated to determine the best fitting model for the HAC degradation process in this simultaneous HAC and 2,4-DCP degradation system. Discrimination functions used were the mean squares lack of fit (MSL), as defined in Equation (5-7),

$$MSL(\hat{f}) = [RSS(\hat{f}) - \hat{\sigma}^2 m] / [n - p - m] \quad (5-7)$$

and the generalized likelihood ratio test (GLRT) for nested models. An α significance level critical region for GLRT was (Borowiak, 1989)

$$n \ln [RSS(f_i) / RSS(f_q)] > \chi^2_{(1-\alpha)} \quad (5-8)$$

where $f_i \subset f_q$

The experimental results (Figure 5-15) showed that inhibition was the major

substrate interaction effect in the HAC degradation process. Therefore, a number of inhibition functions were selected as candidate models. The selected inhibition functions in the data analysis are listed in Table 5-4.

Table 5-4 Candidate models for the kinetics of HAC degradation with 2,4-DCP

Model	Model structure	Note
f_1	$r_{HAC} = \frac{k_{HAC} C_{HAC}}{K_{S,HAC} + C_{HAC} + C_{DCP} / K_{I,DCP}}$	Competitive inhibition by 2,4-DCP
f_2	$r_{HAC} = \frac{k_{HAC} C_{HAC}}{K_{S,HAC} + C_{HAC} + C_{HAC} C_{DCP} / K_{I,DCP}}$	Uncompetitive inhibition by 2,4-DCP
f_3	$r_{HAC} = \frac{k_{HAC} C_{HAC}}{K_{S,HAC} + C_{HAC} + C_{DCP}^2 / K_{I,DCP}}$	Competitive inhibition by 2,4-DCP in C_{DCP}^2
f_4	$r_{HAC} = \frac{k_{HAC} C_{HAC}}{K_{S,HAC} + C_{HAC} + C_{HAC} C_{DCP}^2 / K_{I,DCP}}$	Uncompetitive inhibition by 2,4-DCP in C_{DCP}^2
f_5	$r_{HAC} = \frac{k C_{HAC}}{K_{S,HAC} + C_{HAC} + C_{DCP}^\lambda / K_{I,DCP}}$	Competitive inhibition by 2,4-DCP in C_{DCP}^λ ^a
f_6	$r_{HAC} = \frac{k_{HAC} C_{HAC}}{K_{S,HAC} + C_{HAC} + C_{HAC} C_{DCP}^\lambda / K_{I,DCP}}$	Uncompetitive inhibition by 2,4-DCP in C_{DCP}^λ
f_7	$r_{HAC} = \frac{k_{HAC} C_{HAC}}{K_{S,HAC} + C_{HAC} + C_{HAC}^2 / K_{I,HAC} + C_{DCP}^2 / K_{I,DCP}}$	f_3 + Uncompetitive inhibition of HAC
f_8	$r_{HAC} = \frac{k_{HAC} C_{HAC}}{K_{S,HAC} + C_{HAC} + C_{MCP}^2 / K_{I,MCP} + C_{DCP}^2 / K_{I,DCP}}$	f_3 + Competitive inhibition of MCP
f_9	$r_{HAC} = \frac{k_{HAC} C_{HAC}}{K_{S,HAC} + C_{HAC} + C_{DCP}^2 / (K_{I,DCP} - C_{DCP})}$	Further modification of f_3

^a λ = positive exponent constant (dimensionless)

The selected models in Table 5-4 covered most of the commonly used inhibition functions, such as competitive inhibition (f_1) and uncompetitive inhibition (f_2). Then the

other candidate models were generated by changing the function of inhibition term ($f_3 \sim f_6$) or by considering the substrate inhibition (f_7) and the inhibition from 4-MCP (f_8). An inhibition function similar to the degradation kinetics for 2,4-DCP was also tested (f_9). In the model analysis, some other inhibition functions and their modified forms such as noncompetitive inhibition and mixed inhibition equations were also tested. However, they were not included in Table 5-4 because of their apparent inadequacy in fitting the data.

Model fitting to the experimental data were performed by nonlinear regression using *SAS*. In fitting the candidate models in Table 5-4 to the data, it was found that $K_{S,HAc}$ could not be properly estimated because of the high correlation between k_{HAc} and $K_{S,HAc}$. This correlation was indicated by the correlation matrix in parameter estimation and it can also be observed from Figure 5-14, where the slopes of degradation process curves are almost constant for most initial conditions. Under this high correlation condition, precise estimation of $K_{S,HAc}$ is impossible (Baltes et al., 1994).

As a result, model analysis was conducted by deleting the term $K_{S,HAc}$ in the candidate models, which is similar to accounting for HAc degradation by zero-order kinetics and considering the inhibition term. The fitting results without $K_{S,HAc}$ indicated that the model with the term, $C_{DCP}^2 / K_{I,DCP}$, fitted the experimental data best. The results also showed that the estimated parameter values of $K_{I,HAc}$ and $K_{I,MCP}$, using models f_7 and f_8 , have high values and large standard deviation, suggesting that no substrate

inhibition and inhibition by 4-MCP needs to be considered in the HAC degradation process (Table 5-5). These analysis results are consistent with the reported investigations in the literature. According to Davies-Venn et al. (1992), the maximum specific degradation rate, k_{HAC} , would decrease only about 4%, compared with the control to which no 4-MCP was added, corresponding to the highest 4-MCP concentration of 17.0 mg/L that occurred in this study. Based on a substrate inhibition constant for nonionized HAC of 264 mg DOC/L reported by Kus and Wiesmann (1995), the substrate inhibition caused by the highest initial concentration of HAC 1000 mg/L at pH 7.5 in this experiment, was negligible.

Table 5-5 Fitting results for the models with inhibition by HAC and 4- MCP

Model	R^2	The values of estimated parameters (Value \pm Std)
f_7	0.982	$k_{HAC} = 5.235 \pm 1.492$ (mg/gVSS/h) $K_{I,HAC} = 9346.2 \pm 47756.8$ (mg/L) $K_{I,DCP} = 2.422 \pm 0.902$ (mg/L)
f_8	0.982	$k_{HAC} = 4.950 \pm 0.454$ (mg/gVSS/h) $K_{I,MCP} = 1.804E7 \pm 2.592E14$ (mg/L) $K_{I,DCP} = 2.390 \pm 0.605$ (mg/L)

However, considering that HAC degradation kinetics developed will be used in the modeling of the UASB reactors, deleting the term, $K_{S,HAC}$, could affect a more general use of the HAC degradation kinetics. Additionally, the kinetics without the term, $K_{S,HAC}$, is only an approximation of the Monod type model. To solve this problem, the value of $K_{S,HAC}$ was estimated from the experimental data obtained from the samples without addition of 2,4-DCP (Figure 5-14, DCP/HAC: 0/750). An alternative for obtaining $K_{S,HAC}$

is to select a value from the literature, since HAC degradation has been extensively studied and some reliable values for $K_{S,HAC}$ are available. Kus and Wiesmann (1995) conducted a detailed study on the degradation kinetics of acetate and propionate. They reported a value of 0.128 mg DOC/L for nonionized HAC, which corresponds to a value of 175 mg HAC/L for total HAC at pH of 7.5. This value is close to the value of 154 mg/L reported by Lawrence and MaCarty (1971) and the value of 110 mg/L obtained from the experimental data in this study. Considering that the $K_{S,HAC}$ value from Kus and Wiesmann leads to better fitting results of the experimental data shown in Figure 5-15, and their $K_{S,HAC}$ value is more reliable, since it was derived from a set of experiments which were run in a wide range of pH ($4.68 < \text{pH} < 9.13$), thus the $K_{S,HAC}$ value of 175 mg/L was used for all candidate models (Table 5-4) in model discrimination.

The fitting results of the models with $K_{S,HAC}$ of 175 mg HAC/L are summarized in Table 5-6. Models f_7 and f_8 were not included since no inhibition of HAC and 4-MCP was identified from the experimental data. Model f_9 was excluded because of its poor fitting. Since most models had a high value of the coefficient of variation, R^2 , indicating this coefficient was not sensitive in the model discrimination, hence the mean squares lack of fit, $MSL(\hat{f}_i)$ was used as the discrimination function. The estimator of pure error variance, σ^2 , of r_{HAC} was determined from the replicates in the experimental data and had a value of $0.0138 \text{ (mg/g VSS/h)}^2$.

The fitting results in Table 5-6 shows that model f_6 fitted the data best but

its instability increases because more parameters are used. Since f_4 is a nested model of f_6 with $f_4 \subset f_6$, the necessity of the parameter λ was further tested using GLRT method. Based on Equation (5-8),

$$n \ln[RSS(f_4) / RSS(f_6)] = 16 \times \ln(0.568/0.480) = 2.693.$$

At a significance level $\alpha = 0.05$, $\chi^2_{1-0.05,3-2} = 3.84$, suggesting no significant gain in fit by adding the parameter λ in f_6 .

Table 5-6 Model fitting results for $f_1 \sim f_6$ with $K_{S,HAc}$ of 175 mg/L

Model	Parameter estimated ^a (Value \pm Std)	Convergence	RSS	R ²	$\frac{MSL(\hat{f}_i)}{\sigma^2}$	$F_{0.05}(n_1, n_2)^b$
f_1	$k_{HAc} = 6.969 \pm 1.129$ $K_{I,DCP} = 0.0494 \pm 0.0233$	Yes	4.516	0.944	53.279	4.15
f_2	$k_{HAc} = 7.207 \pm 0.800$ $K_{I,DCP} = 26.520 \pm 8.410$	Yes	2.168	0.973	24.880	4.15
f_3	$k_{HAc} = 6.774 \pm 0.629$ $K_{I,DCP} = 1.722 \pm 0.522$	Yes	1.946	0.976	22.202	4.15
f_4	$k_{HAc} = 6.864 \pm 0.349$ $K_{I,DCP} = 926.91 \pm 159.31$	Yes	0.568	0.993	5.529	4.15
f_5	$k_{HAc} = 6.338$ $K_{I,DCP} = 437.59$ $\lambda = 3.50$	Failed	0.978	0.988	12.594	4.82
f_6	$k_{HAc} = 6.662$ $K_{I,DCP} = 3960.8$ $\lambda = 2.39$	Failed	0.480	0.994	5.371	4.82

^a The dimension of the parameters: k_{HAc} , mgHAc/mgVSS/h; $K_{I,DCP}$, dimensionless for f_1 , mg/L for f_2 and f_3 , (mg/L)² for f_4 and (mg/L) ^{$\lambda-1$} for f_5 and f_6 ; λ , dimensionless.

^b For $f_1 \sim f_4$, $n_1 = 6$ and $n_2 = 8$; For f_5 and f_6 , $n_1 = 5$ and $n_2 = 8$.

Since a better fitting result was obtained from f_3 than f_4 when $K_{S,HAc}$ was not included in the models, it may also be questioned that f_3 could be a better model than f_4 .

when a different $K_{S,HAc}$ value was used. However, model fitting of f_3 to the data indicated that no significant improvement of fit can be obtained by taking $K_{S,HAc}$ as a parameter in the regression analysis. $MSL(f_4) \ll MSL(f_3)$ suggested that f_4 is better than f_3 in fitting to the experimental data. In Table 5-6, the values of $MSL(\hat{f}_i)$ were larger than $F_{0.05}(n_1, n_2)$ for all the models. However, since all the models in Table 5-6 were nonlinear, the lack of fit test was only approximate and f_4 should not be rejected.

To further test the lack of fit of the models in Table 5-6, plots of the residuals between the predicted r_{HAc} and the observed r_{HAc} for the models f_4 , f_3 and f_3 without $K_{S,HAc}$ were constructed (Figure 5-16). Comparing the residual plots for the three models, the plot for f_4 showed an absence of unusual trends and indicates no apparent lack of fit. Summarizing the above model discrimination results, it was concluded that f_4 is the best model for the HAc degradation with 2,4-DCP (Equation 5-9).

$$r_{HAc} = \frac{6.864 C_{HAc}}{175.3 + C_{HAc} + C_{HAc} C_{DCP}^2 / 926.9} \quad (5-9)$$

5.3.2 HPr

Experimental procedures and data analysis methods for the degradation kinetics of HPr were the same as those for HAc. However, the experimental results for HPr indicated that

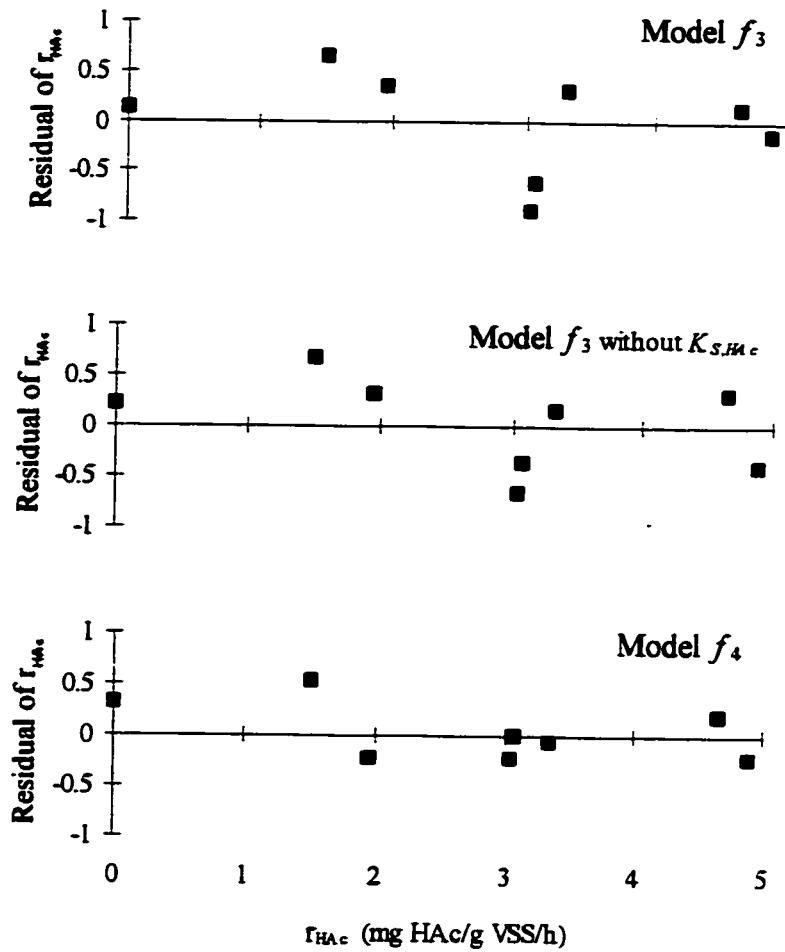


Figure 5-16 Plot of r_{HAc} residual with r_{HAc} for models f_3 , f_3 without $K_{S,HAc}$ and f_4

the degradation process of HPr was more significantly influenced by 2,4-DCP (Figure 5-17), suggesting that acetogenic bacteria responsible for degradation of HPr are more sensitive to 2,4-DCP than methanogenic bacteria. As shown in the figure, the degradation of HPr was very slow or stopped when the initial concentration of 2,4-DCP was above 60 mg/L. Similar to the HAC degradation process, to identify whether the 4-MCP and HPr

inhibited the degradation of HPr or not, the model analysis approach was used in analyzing the data.

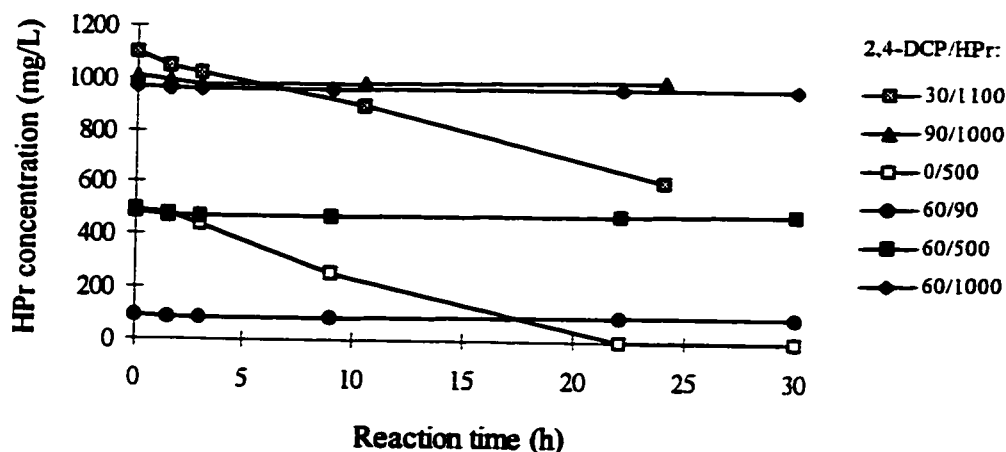


Figure 5-17 Simultaneous degradation of HPr and 2,4-DCP (only HPr data shown)

Using a differentiation method (Equation 5-5) for the HPr data, the relation between the average HPr degradation rate, \bar{r}_{HPr} , and the HPr concentration was obtained (Figure 5-18). In determining proper kinetics for HPr degradation with 2,4-DCP, the

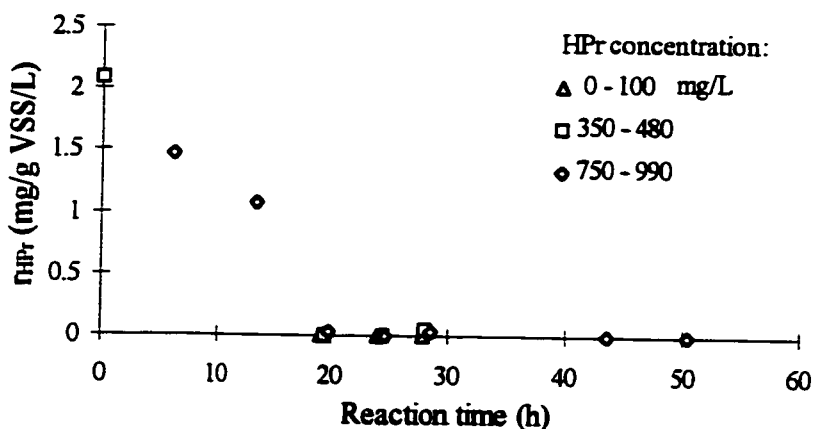


Figure 5-18 Relation of the HPr degradation rate to 2,4-DCP and HPr concentrations

same group of equations shown in Table 5-5 was employed in model discrimination. Figure 5-17 indicated that, similar to HAC degradation process, it was difficult to precisely estimate the parameter K_{S,HP_r} from the experimental data due to the high correlation between k_{HP_r} and K_{S,HP_r} . Consequently, the K_{S,HP_r} was selected from the reported values in the literature and justified with the estimated value from the data shown in the degradation process curve of DCP/HP_r: 0/500 in Figure 5-17.

The value for K_{S,HP_r} reported by Kus and Wiesmann (1995) was 0.33 mg DOC/L for unionized form of HP_r, which is equivalent to a value of 282 mg HP_r/L for total HP_r at pH of 7.5. Their experiment to obtain the kinetic parameter value was conducted in a pH range of 5.16 to 7.24. Comparatively, a lower K_{S,HP_r} value of 39.5 mg/L was reported by Lawrence and MaCarty (1971). The K_{S,HP_r} value estimated from the experimental data in Figure 5-17 (DCP/HP_r: 0/500) was 108.9 mg/L. However, a higher value, 1.80 mg COD/L, for unionized HP_r, corresponding to 494.1 mg HP_r/L at pH of 7.5, was reported by Fukuzaki et al. (1990b). Considering that Kus and Wiesmann's K_{S,HP_r} value was supported by the experimental data from a wide pH range and their value fitted better the experimental data in this study (Figure 5-18), therefore $K_{S,HP_r} = 282$ mg/L was selected and used in the following data analysis.

As for the HAC degradation process, 4-MCP and HP_r have no inhibition effect on the HP_r degradation based on the very large corresponding inhibition constants $K_{I,MCP}$

(5.831×10^9) and $K_{I,HP}$ (5.006×10^8) obtained in parameter estimation. Therefore, the same group of candidate models as those in Table 5-6 were used in the data analysis by nonlinear regression (Table 5-7). In estimating $MSL(\hat{f}_i)$ in Table 5-7, pure error variance of \bar{r}_{HP} , σ_p^2 , calculated from replicates in the experimental data was $0.0183 \text{ (mg/g VSS/h)}^2$.

Table 5-7 Model fitting results for $f_1 \sim f_6$ with $K_{S,HP}$ of 282 mg/L ^a

Model	Parameter estimated ^b (Value \pm Std)	RSS	R^2	$\frac{MSL(\hat{f}_i)}{\sigma^2}$	$F_{0.05}(n_1, n_2)$ ^c
f_1	$k_{HP} = 3.921 \pm 0.562$ $K_{I,DCP} = 0.00281 \pm 0.000956$	1.155	0.851	3.205	2.64
f_2	$k_{HP} = 3.883 \pm 0.625$ $K_{I,DCP} = 1.988 \pm 0.775$	1.429	0.815	4.183	2.64
f_3	$k_{HP} = 3.385 \pm 0.333$ $K_{I,DCP} = 0.0411 \pm 0.00984$	0.423	0.945	0.593	2.64
f_4	$k_{HP} = 2.837 \pm 0.409$ $K_{I,DCP} = 29.246 \pm 8.631$	0.633	0.918	1.344	2.64
f_5	$k_{HP} = 3.728 \pm 0.337$ $K_{I,DCP} = 0.108 \pm 0.110$ $\lambda = 3.382$	0.380	0.951	0.581	2.74
f_6	$k_{HP} = 3.705 \pm 0.408$ $K_{I,DCP} = 105.7 \pm 133.6$ $\lambda = 2.511$	0.558	0.928	1.174	2.74

^a Regressions were converged for all models.

^b The dimension of the parameters: k_{HP} , mg HAC/mg VSS/h; $K_{I,DCP}$, dimensionless for f_1 , mg/L for f_2 and f_3 , $(\text{mg/L})^2$ for f_4 and $(\text{mg/L})^{\lambda-1}$ for f_5 and f_6 ; λ , dimensionless.

^c For $f_1 \sim f_4$, $n_1 = 12$ and $n_2 = 14$; For f_5 and f_6 , $n_1 = 11$ and $n_2 = 14$.

Table 5-7 shows that models f_3 and f_5 have better fitting results than other candidates.

Since $f_3 \subset f_5$, GLRT test (Equation 5-8) was used to identify whether f_5 with the extra

parameter, λ , was superior to f_3 . The result of the test was $n \ln[RSS(f_3) / RSS(f_5)] = 28 \times \ln(0.423/0.0381) = 2.928 < \chi_{1-0.05,3-2}^2 = 3.84$, suggesting that f_3 is more appropriate model for the data than f_5 .

Since model f_5 should not be considered, the lack of fit test based on $MSL(\hat{f}_i)$ in Table 5-7 suggested that f_3 was the best model for the data [Equation (5-10)]

$$r_{HPr} = \frac{3.385C_{HPr}}{2819 + C_{HPr} + C_{DCP}^2 / 0.0411} \quad (5-10)$$

The residual plot for r_{HPr} with model f_3 was tested (Figure 5-19). The plot indicated an unsatisfactory experimental design in the study of HPr degradation kinetics. More data should have been available for r_{HPr} from 0.2 to 2.5 mg/g VSS/h. However, since no significant trend was found in Figure 5-19, adequacy of the model f_3 was not rejected.

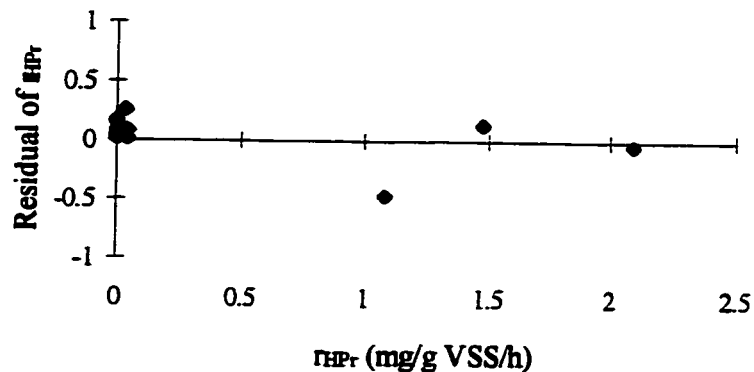


Figure 5-19 Plot of r_{HPr} residual with r_{HPr} for model f_3

5.3.3 Sucrose

Experimental results

The same experimental methods as for HAc and HPr were followed in the investigation of sucrose degradation kinetics with 2,4-DCP. Experimental results for sucrose degradation showed that only HPr and HAc were detected in the SBT tests. These results were also consistent with the observation for the UASB reactor system in this study (see Chapter 6). The results from the SBT tests for sucrose degradation with 2,4-DCP are given in Figures 5-20~5-22 for HAc, HPr and COD concentration variation with time, respectively.

Comparing Figures 5-20 and 5-21, degradation of HPr was more significantly inhibited by 2,4-DCP, which was consistent with the results from the tests using HAc and HPr as single cosubstrate. For HAc degradation, a final drop in the HAc concentration was observed for all initial conditions of DCP/sucrose addition (Figure 5-20).

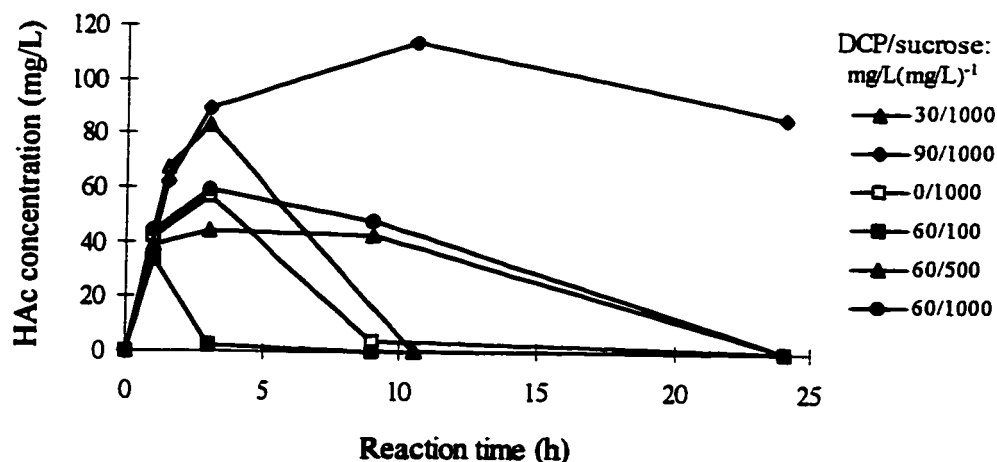


Figure 5-20 Variation of HAc concentration with time during the sucrose degradation with 2,4-DCP

However, the HPr concentration continuously increased when initial addition of 2,4-DCP was above 60 mg/L (Figure 5-21). This observation was also consistent with the results in Figure 5-17. Figure 5-22 shows that only the process curve for initial DCP/sucrose condition of 0/1000 had a continued decrease of COD concentration, indicating a significant inhibiting effect from 2,4-DCP for all other experimental runs.

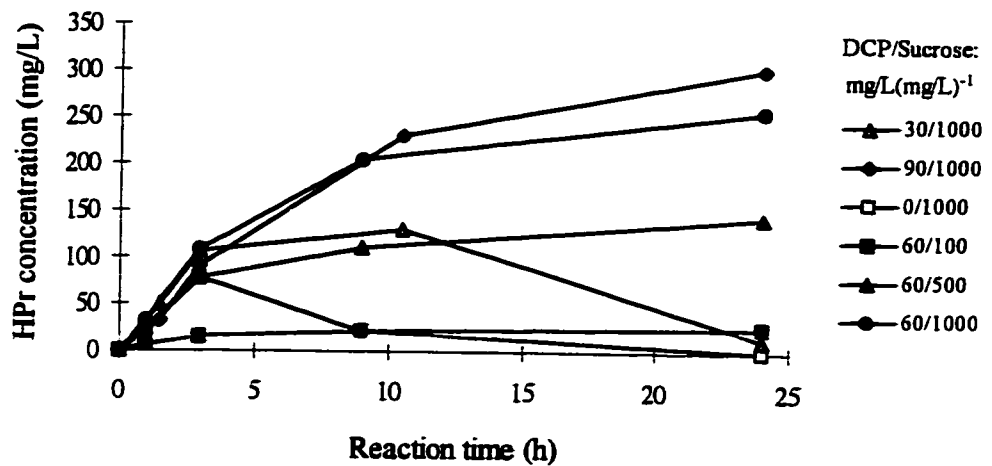


Figure 5-21 Variation of HPr concentration with time during the sucrose degradation with 2,4-DCP

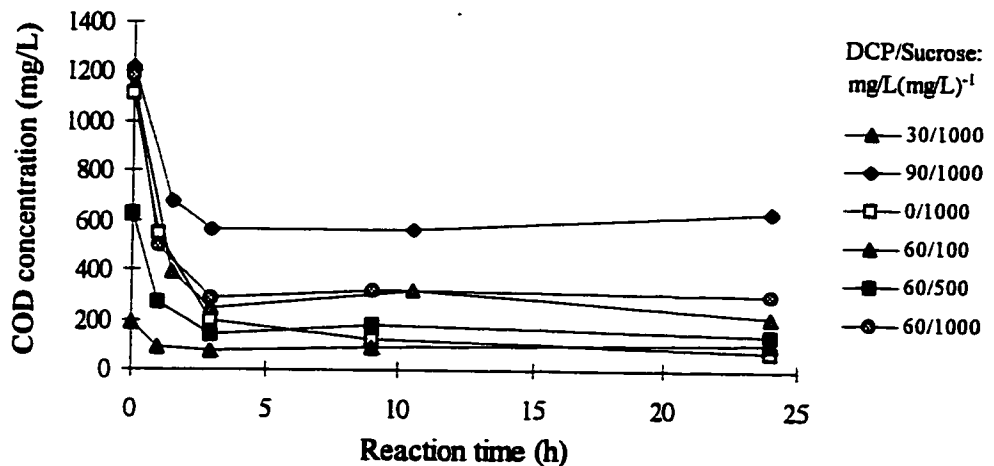


Figure 5-22 Variation of COD concentration with time during the sucrose degradation with 2,4-DCP

Analysis of the sucrose degradation process

From the experimental observations presented in Figure 5-20 ~ 5-22, it was seen that direct evaluation of degradation rate of sucrose to HPr and HAc, as done in the case of HAc and HPr degradation kinetics, was no longer possible, since:

(1) The sucrose degradation involved two further degradable intermediate products, HPr and HAc. The sucrose degradation rate to both HPr and HAc needs to be determined. However, the relative magnitude of the degradation rate of sucrose to HPr or HAc varied, and it was uncontrollable during experiments;

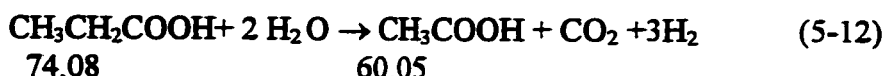
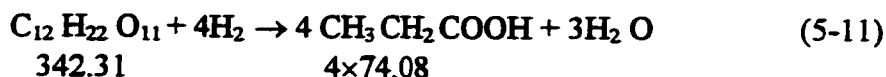
(2) During degradation of sucrose to HPr or HAc, sucrose was first hydrolyzed to glucose and fructose then further degraded to VFAs. Since some other intermediate products other than HPr and HAc were involved in the sucrose degradation process, and the limiting step during the process was not defined, evaluating the sucrose degradation rate to HAc or HPr by sucrose concentration measurement may not be reliable. Consequently, COD was used in the test to describe the sucrose degradation rate to HPr and HAc for convenience (DOC is better than COD for this purpose);

(3) The inhibition scheme in this degradation system was unknown, which may be related to substrate interaction of sucrose, HAc, HPr, 2,4-DCP, 4-MCP and hydrogen.

As a result, an indirect approach was developed in this study to estimate the degradation rate of sucrose, and the procedures involved are shown below. Similar to

Mosey (1983), anaerobic degradation of sucrose can be stoichiometrically expressed by the following equations:

For the degradation of sucrose \rightarrow HPr \rightarrow HAc,



and for the degradation of sucrose \rightarrow HAc,



The bioreactions in 5-11 to 5-13 are mediated by acidogenic and acetogenic bacteria. Then, HAc and hydrogen are further degraded by methanogens to carbon dioxide and methane gas,



Based on mass balance and Equation (5-11) to (5-14), the variation of HAc and HPr concentration in the sucrose degradation system can be described by Equations (5-16) and (5-17) below, respectively.

$$\frac{dC_{\text{HAc}}}{dt} = \frac{240.2}{342.3} \frac{dC_{\text{Suc} \rightarrow \text{HAc}}}{dt} + \frac{60.05}{74.08} \frac{dC_{\text{HPr} \rightarrow \text{HAc}}}{dt} - \frac{dC_{\text{HAc} \rightarrow \text{CH}_4}}{dt} \quad (5-16)$$

and

$$\frac{dC_{HPr}}{dt} = \frac{296.3}{342.3} \frac{dC_{Suc \rightarrow HPr}}{dt} - \frac{dC_{HPr \rightarrow HAC}}{dt} \quad (5-17)$$

In Equations (5-16) and (5-17), the terms, $dC_{Suc \rightarrow HAC} / dt$ and $dC_{Suc \rightarrow HPr} / dt$ are to be determined in the analysis. Assuming the degradation kinetics for HAC and HPr determined by Equations (5-9) and (5-10) are also valid in the sucrose degradation process, then the terms, $dC_{HPr \rightarrow HAC} / dt$ and dC_{HAC} / dt can be calculated. Since the variation of HAC and HPr concentration in the system, expressed in the terms, dC_{HAC} / dt and dC_{HPr} / dt , can be estimated from the experimental data of HAC and HPr (Figures 5-20 and 5-21) using the differentiation method, the degradation rates of sucrose to HPr and HAC, i.e., $dC_{Suc \rightarrow HAC} / dt$ and $dC_{Suc \rightarrow HPr} / dt$, can be finally determined. However, it should be noted that the determined degradation rates of sucrose to HAC and HPr are virtually the lumped degradation rates of sucrose to these two VFAs because, as indicated before, the limiting step of degradation from sucrose to HPr or HAC was not defined.

Besides $dC_{Suc \rightarrow HAC} / dt$ and $dC_{Suc \rightarrow HPr} / dt$, the concentration of sucrose related to the two degradation rates must be known in order to determine the degradation kinetics of sucrose to HPr and HAC. Assuming sucrose, HAC, HPr, 2,4-DCP and 4-MCP were the main components of COD in the reaction medium, a relation of COD to these components can be written:

$$COD_{Suc} = COD_T - COD_{HAC} - COD_{HPr} - COD_{2,4DCP} - COD_{4MCP} \quad (5-18)$$

Approximation of Equation (5-18) was apparent. COD_{suc} not only included sucrose concentration in the reaction medium but it may also include other undetected components such as glucose, fructose and so on. However, lumping glucose into sucrose was a consistent consideration and related to $dC_{Suc \rightarrow HAC} / dt$ and $dC_{Suc \rightarrow HPr} / dt$ for which no limiting step was defined. Compared with HAC and HPr concentration, the contribution of chlorobenzoate, 2-MCP and other possible 2,4-DCP degradation products to total COD was very small. Based on the known inorganic compounds contained in the reaction medium, the effect of inorganic matter on COD measurement was considered to be negligible.

Since the chemical formulas for all components in Equation (5-18) are known, it can be rewritten as Equation (5-19) on the basis of theoretical oxygen demand (THOD) of these components involved in the former equation.

$$1.127C_{Suc} = COD_T - 1.066C_{HAC} - 1.512C_{HPr} - 1.215C_{2,4DCP} - 1.541C_{4MCP} \quad (5-19)$$

Using Equations (5-16), (5-17) and (5-19), the sucrose concentration and the corresponding degradation rates $dC_{Suc \rightarrow HAC} / dt$ and $dC_{Suc \rightarrow HPr} / dt$ were obtained (Table 5-8). The calculated results at which the sucrose concentration equaled zero are not included in the table.

Table 5-8 C_{Suc} and corresponding $dC_{Suc \rightarrow HAc} / dt$ and $dC_{Suc \rightarrow HPr} / dt$

Initial conditions	Reaction time (h)	C_{Suc} (mg/L)	$dC_{Suc \rightarrow HAc} / dt$ (mg/L/h)	$dC_{Suc \rightarrow HPr} / dt$ (mg/L/h)	$\frac{dC_{Suc \rightarrow HAc} / dt}{dC_{Suc \rightarrow HPr} / dt}$
0/1000	0.5	700.45	5.01	1.92	2.61
	2	214.02	2.39	2.82	0.85
30/1000	0.75	588.41	5.91	2.64	2.24
	2.25	84.30	3.80	3.01	1.26
	6.75	30.96	0.75	0.36	2.10
60/100	0.5	48.08	3.99	0.57	6.95
60/500	0.5	310.02	5.16	1.96	2.62
	2	35.53	2.38	2.10	1.13
60/1000	0.5	651.36	4.73	2.58	1.83
	2	166.86	2.15	2.97	0.72
90/1000	0.75	706.95	4.84	1.66	2.92
	2.25	331.69	3.24	3.17	1.02
	6.75	130.06	2.15	1.47	1.46
	17.25	22.62	1.90	0.44	4.29

Hydrogen inhibition on the degradation of sucrose

Dramatic variation of $dC_{Suc \rightarrow HAc} / dt$ and $dC_{Suc \rightarrow HPr} / dt$ can be seen from Table 5-8. First a check was made to see if it was caused by the inhibiting effect of 2,4-DCP. The results indicated that no significant inhibition of 2,4-DCP on the sucrose degradation process was observed (Figure 5-23). A similar result was also observed for 4-MCP.

However, a graphic presentation showed a strong association between reaction time and $dC_{Suc \rightarrow HAc} / dt$, $dC_{Suc \rightarrow HPr} / dt$ or the ratio of $dC_{Suc \rightarrow HAc} / dt$ to $dC_{Suc \rightarrow HPr} / dt$ (Figure 5-24). Since HPr and HAc concentrations in the system were quite low, product inhibition cannot be expected to have such an effect. As observed in Figure 5-24,

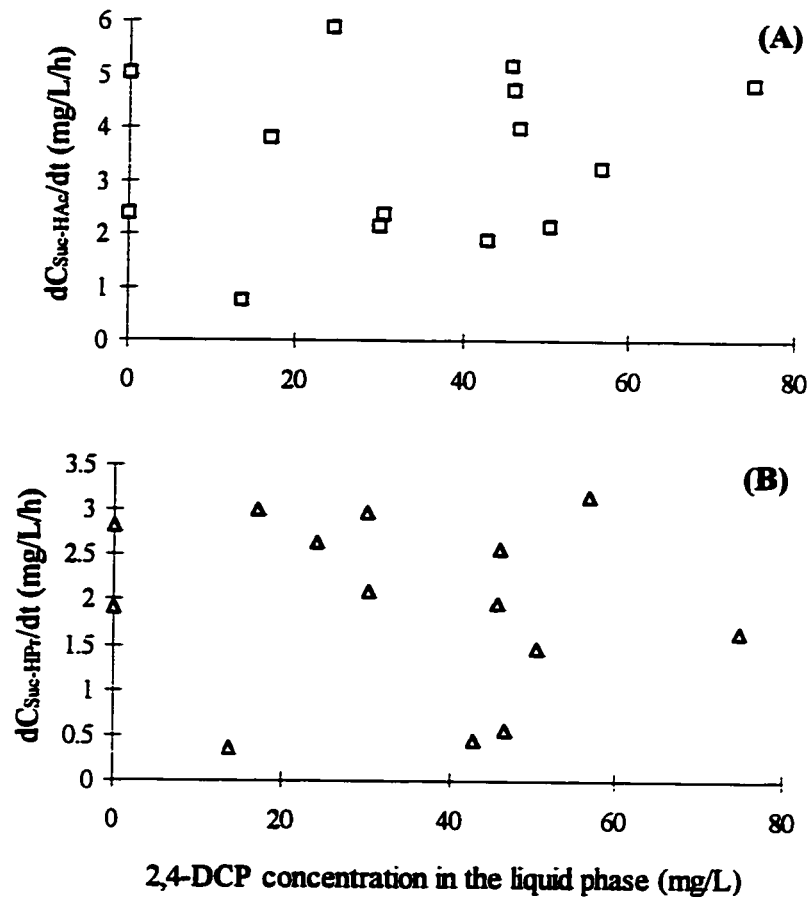


Figure 5-23 Effect of 2,4-DCP on the sucrose degradation to HAc (A) and HPr (B)

$dC_{\text{Suc} \rightarrow \text{HAc}} / dt$ drops significantly with time, and $dC_{\text{Suc} \rightarrow \text{HPr}} / dt$ undergoes an initial increase then it decreases gradually with time. These two curves have similar profiles to the results reported by Mosey (1983) for hydrogen inhibition on the degradation of glucose to HAc and HPr, suggesting that hydrogen inhibition may occur in the batch degradation system. From a viewpoint of thermodynamics, HPr can only be degraded within a narrow P_{H_2} range of $3 \times 10^{-6} \sim 1 \times 10^{-4}$ bar (McCarty, 1981). In this experiment for sucrose degradation, hydrogen inhibition could happen after a pulse input of sucrose into

the serum bottle, in which the hydrogen production rate could be much faster than its consumption by methanogenesis since sucrose is easily degradable.

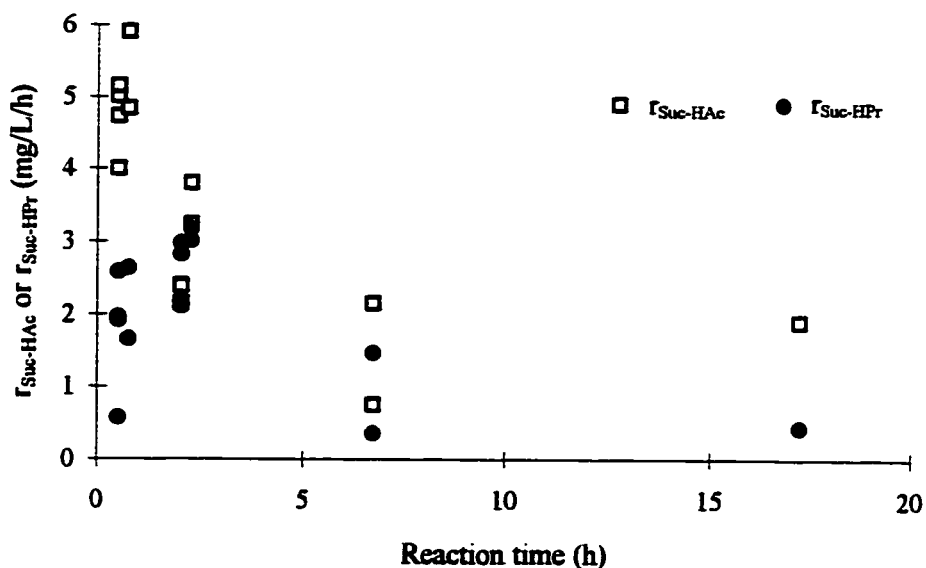


Figure 5-24 Possible hydrogen inhibition to sucrose degradation to HAc and HPr

Degradation kinetics of sucrose to HAc and HPr

Only hydrogen inhibition occurred in the sucrose degradation system, hence no other inhibition needs to be considered. However, hydrogen concentration was not measured during this experiment, thus quantitative consideration of hydrogen inhibition in the degradation kinetics was not possible. On the other hand, the sucrose degradation kinetics would be used in a dynamic model for the UASB reactors, in which no pulse input of sucrose was involved. Therefore, hydrogen inhibition was not considered in the degradation kinetics according to the objective of this study.

To minimize the effect of hydrogen inhibition on the determination of sucrose degradation kinetics, only the data at times 0.5 and 0.75 h (Table 5-8) were used for the data analysis. It was considered that with such a data selection, the effect of hydrogen inhibition can be minimized or restricted to a relatively constant range. Consequently, the structure of sucrose degradation kinetics would not be significantly affected. Once the sucrose degradation kinetics were developed and used in the dynamic modeling of the UASB system, the kinetic parameter values could be further adjusted in the UASB system modeling.

Since no inhibition was found in the degradation of sucrose to HAc and HPr, the commonly used Monod equation was employed and the parameter values in the sucrose degradation kinetics were estimated by nonlinear regression. Assuming that the same group of bacteria were responsible for the degradation of sucrose, no matter what kind of product, HPr or HAc, was produced, the same $K_{S,Suc}$ value was used in the regression analysis. The model structure and parameter estimation results for sucrose degradation kinetics are summarized in Table 5-9. Because of the general use of the Monod equation in such a situation, no other model and model discrimination need to be considered.

Table 5-9 Degradation kinetics of sucrose to HAc and HPr

Kinetics	Parameters	R^2
$R_{Suc \rightarrow HAc} = \frac{k_{Suc \rightarrow HAc} C_{Suc}}{K_{S,Suc} + C_{Suc}}$	$k_{Suc \rightarrow HAc} = 5.259 \pm 0.259$ $K_{S,Suc} = 14.742 \pm 8.825$	0.994
$R_{Suc \rightarrow HPr} = \frac{k_{Suc \rightarrow HPr} C_{Suc}}{K_{S,Suc} + C_{Suc}}$	$k_{Suc \rightarrow HPr} = 2.048 \pm 0.264$ $K_{S,Suc} = 14.742 \pm 8.825$	0.925

5. 3. 4 Degradation Kinetics of HAc and HPr with Nonionized Substrates

In determining the degradation kinetics of HPr and HAc in Sections 5.3.1 and 5.3.2, total HAc, HPr and 2,4-DCP were used in the data analysis for simplicity and clarity. However, organisms can not obtain enough energy for the transportation of ionized forms of these substrates in anaerobic treatment systems, and only the nonionized form of substrate is degradable (Kus and Wismann, 1995, Grady and Lim, 1980, Andrews and Graef, 1971). Therefore, the degradation kinetics of HPr and HAc should be further modified. Since the experiments for HPr and HAc kinetics investigation were conducted at a controlled pH value of 7.5, it will become clear that such a modification of the degradation kinetics is simple, and parameter reestimation is not necessary.

According to the model structure of HAc degradation kinetics shown in Equation (5-9), and considering only the nonionized form of HAc was degradable and the nonionized form of 2,4-DCP had an inhibiting effect on the degradation process, the degradation kinetics can be rewritten as

$$r_{HAc} = \frac{k_{HAc^o} C_{HAc^o}}{K_{S,HAc^o} + C_{HAc^o} + C_{HAc^o} C_{DCP^o}^2 / K_{I,DCP^o/HAc^o}} \quad (5-20)$$

Note that the subscripts, HAc^o and DCP^o , are used on the right side of Equation (5-20) to express nonionized HAc and 2,4-DCP. The nonionized HAc or 2,4-DCP can be described as a function of total HAc or 2,4-DCP, respectively, as follows.

$$C_{HA_c^o} = \frac{C_{HA_c}}{1 + 10^{pH - pK_{a,HA_c}}} = \alpha_{HA_c} C_{HA_c} \quad (5-21)$$

and

$$C_{DCP^o} = \frac{C_{DCP}}{1 + 10^{pH - pK_{a,DCP}}} = \alpha_{DCP} C_{DCP} \quad (5-22)$$

where $\alpha_{HA_c} = 1 / (1 + 10^{pH - pK_{a,HA_c}}) = 0.001825$ at pH of 7.5, K_{a,HA_c} has a value of 1.73×10^{-5} at 35°C (CRC, 1993); $\alpha_{DCP} = 1 / (1 + 10^{pH - pK_{a,DCP}}) = 0.711$ at pH 7.5 based on the value of $pK_{a,DCP}$, 7.89 (Kennedy et al., 1992). Substituting Equations (5-21) and (5-22) into Equation (5-20) and rearranging it results in Equation (5-23).

$$r_{HA_c} = \frac{k_{HA_c^o} C_{HA_c}}{(K_{S,HA_c^o} / \alpha_{HA_c}) + C_{HA_c} + C_{HA_c} C_{DCP}^2 / (K_{I,DCP^o/HA_c^o} / \alpha_{DCP}^2)} \quad (5-23)$$

Comparing Equation (5-23) with Equation (5-9) gives

$$k_{HA_c^o} = k_{HA_c} \quad (5-24a)$$

$$K_{S,HA_c^o} = \alpha_{HA_c} K_{S,HA_c} \quad (5-24b)$$

$$K_{I,DCP^o/HA_c^o} = \alpha_{DCP}^2 K_{I,DCP/HA_c} \quad (5-24c)$$

In this way, Equation (5-24) provides the relationships between the parameters for Equation (5-20) and the parameters for Equation (5-9). Also, Equation (5-24) is helpful to explain the reason why the value of k was relatively stable, but K_s values varied dramatically as reported in the literature (Pavlostathis and Giraldo-Gomez, 1992).

Similarly, according to Equation (5-10), the degradation kinetics of HPr with nonionized substrates can be obtained [Equation (5-25)],

$$r_{HPr} = \frac{k_{HPr^o} C_{HPr^o}}{K_{S,HPr^o} + C_{HPr^o} + C_{DCP^o}^2 / K_{I,DCP^o/HPr^o}} \quad (5-25)$$

where

$$C_{HPr^o} = \frac{C_{HPr}}{1 + 10^{pH - pK_{a,HPr}}} = \alpha_{HPr} C_{HPr} \quad (5-26)$$

and $\alpha_{HPr} = 1 / (1 + 10^{pH - pK_{a,HPr}})$. Based on $K_{a,HPr} = 1.31 \times 10^{-5}$ at 35°C (CRC, 1993), the value of α_{HPr} at pH 7.5 is equal to 0.002408. Substituting Equations (5-26) and (5-22) into (5-25), Equation (5-27) is obtained:

$$r_{HPr} = \frac{k_{HPr^o} C_{HPr}}{(K_{S,HPr^o} / \alpha_{HPr}) + C_{HPr} + C_{DCP}^2 / (K_{I,DCP^o/HPr^o} \alpha_{HPr} / \alpha_{DCP}^2)} \quad (5-27)$$

Comparing Equation (5-27) with Equation (5-10) gives

$$k_{HPr^o} = k_{HPr} \quad (5-28a)$$

$$K_{S,HPr^o} = \alpha_{HPr} K_{S,HPr} \quad (5-28b)$$

$$K_{I,DCP^o/HPr^o} = (\alpha_{DCP}^2 / \alpha_{HPr}) K_{I,DCP/HPr} \quad (5-28c)$$

From Equation (5-24) and (5-28), it can be realized that, for both total or nonionized forms of substrates, the specific degradation rate constant k always has the same value;

for K_s and K_I , the parameter values for the nonionized form of substrate are constant, but the parameter values for total concentration of the substrates varies with pH. In applying the degradation kinetics of HPr and HAc to the UASB system, Equations (5-23) and (5-27) are preferred, since the effect of pH on reactor operation and the degradation rates of these substrates can be described.

To obtain the parameter values for nonionized form substrates, Equations (5-21), (5-22) and (5-26) were used to transform the experimental data for HAc, HPr and 2,4-DCP concentrations into nonionized form, then the parameter values were reestimated by nonlinear regression. Also, Equations (5-24) and (5-28) could be used to calculate the parameter values for nonionized form of substrates from the known parameter values estimated in Sections 5.3.1 and 5.3.2. As expected, both methods give almost identical results (Table 5-10).

Table 5-10 Parameter estimation results for degradation kinetics of HAc and HPr with nonionized form of substrates

Kinetic equation	Parameters ^a	Estimated by regression	Calculated based on Equations (5-23) and (5-27)
Kinetics for HAc (Eq. 5-19)	k_{HAc}^o	6.868±0.349	6.864±0.349
	$K_{I,DCP^o/HAc}^o$	468.29±80.46	468.57±80.53
	$K_{S,HAc}^o$	0.32	0.32
Kinetics for HPr (Eq. 5-24)	k_{HPr}^o	3.822±0.332	3.835±0.333
	$K_{I,DCP^o/HPr}^o$	8.605±2.059	8.628±2.066
	$K_{S,HPr}^o$	0.679	0.679

^a $K_{S,HAc}^o$ and $K_{S,HPr}^o$ were calculated from the reported values by Kus and Wiesmann (1995).

5. 3. 5 Discussion

In this study, relatively simple schemes of substrate interaction during the simultaneous degradation of HAc, HPr or sucrose and 2,4-DCP were observed. The major feature of substrate interaction was the inhibiting effect of 2,4-DCP on degradation of cosubstrates and its own degradation. Since reaction media in these experiments seem to have enough electron donor and even endogenous carbon sources can well support dechlorination (Wrenn and Rittmann, 1995; Mohn and Kennedy, 1992), the effect of electron donor on the dechlorination was negligible. Additionally, the effect of electron acceptor on the degradation of 2,4-DCP was not studied in this investigation, considering that a stable and specific electron acceptor source could be maintained in the UASB reactors. The simplicity of substrate interaction found in the investigation was mainly contributed by the simple degradation pathway of 2,4-DCP, where 4-MCP was the major product of 2,4-DCP dechlorination and the inhibition of 4-MCP on the degradation of cosubstrates was not significant. One can imagine that the substrate interaction scheme could become very complicated when a highly chlorinated phenol, such as PCP, is involved in the degradation system.

The degradation kinetics of HAc, HPr and sucrose with 2,4-DCP degradation by anaerobic granules was developed. The results indicated that the degradation kinetics of HAc with 2,4-DCP follows an uncompetitive inhibition function, which is similar to the

observation reported by Kim et al. (1994) on methanogenesis influenced by monochlorinated aromatics. However, the degradation of HPr followed the Haldane type inhibition function with 2,4-DCP as the inhibitor and no inhibiting effect from chlorophenols was observed on the acidogenesis in this study. Because of the difference in operating modes and experimental conditions between the SBT test and the UASB reactors, the parameter values estimated in this chapter will be further adjusted in modeling the UASB reactor system.

Data analysis results in this chapter suggest that the model analysis method is a useful tool to deal with the substrate interaction problem since the interactions in the degradation of multiple substrates are often indistinguishable or time consuming by experimental investigation. For example, without model analysis, the degradation kinetics of sucrose to HAc and HPr may not be easily available from experiments; it was only by model analysis that the inhibiting properties of 4-MCP could be identified without the need to pursue further experiments. Considering that the experimental investigation of the degradation process of toxic organic compounds are often complicated and expensive in cost and equipment demand, model analysis should be fully utilized to minimize the experimental work.

EXPERIMENTAL INVESTIGATION IN THE UASB REACTORS

The results from the experimental investigation on simultaneous degradation of primary substrates (sucrose and HAc) and 2,4-DCP in continuous UASB reactors are presented in this chapter. The data obtained in this investigation will be used to validate and verify a dynamic UASB reactor model to be developed in the next chapter. Setup of the UASB reactor system was described in Chapter 3.

6.1 Experimental Design

Experiments were designed to test performance of UASB reactors at different operating conditions under dynamic situations. The experimental approach used in the investigation was: (1) four UASB reactors were operated for 6 months using the same feed (Appendix A) plus 2,4-DCP (controlled at 10 mg/L) to cultivate and acclimate biomass; (2) when the reactors were stabilized, transient changes in the concentration of 2,4-DCP and COD were applied to each reactor over a short period of time (4 ~72 h); and (3) after the transient change period, the reactors were returned to their original feeding condition. Routine operating conditions for the UASB reactors were summarized in Table 3-6. During this

investigation, a specific reactor received a transient change in feed 1 ~ 3 times. About one month of routine operational time was maintained between two successive transient changes in the feed to stabilize operation of the reactors.

Execution of the proposed experimental design is summarized in Table 6-1. For reactor R2, only one transient change was applied because algae growth was observed in the reactor after experimental run RUN II.2 (all reactors were covered with cloth during the whole experimental period to minimize algae growth). During routine operation, some white bacterial flocs were observed in reactor R4 for a short period of time (about two weeks). A longer acclimation time was used for this reactor to eliminate the bacterial flocs. Consequently, a total of 9 transient feed condition changes were applied to the UASB systems. The profiles of feeding conditions (HAc, COD and 2,4-DCP) during the 9 transient change periods are presented in Figures 6-1(a) to 6-1(i). Besides substrate concentrations, feed flowrates were also changed in some runs. Table 6-2 shows the variations of the feed flowrate, HRT, OLR for 2,4-DCP and COD for each experimental run. More detailed information on these feeding conditions are given in Appendix D.

Table 6-1 Experiments with transient feed condition change for the UASB reactors

Reactor	Code number of the experimental runs ^a		
R1	RUN I.1	RUN II.1	RUN III.1
R2	-	RUN II.2	-
R3	RUN I.3	RUN II.3	RUN III.3
R4	-	RUN II.4	RUN III.4

^a The experiments with code number RUN I, II, III were conducted sequentially with about one month of routine operation between them. Numbers, 1, 2, 3 or 4 denote the UASB reactor.

Table 6-2 Feeding conditions during transient change periods for the 9 experimental runs

Code number of runs	Run time interval (h)	Feeding flowrate, Q (L/h)	HRT (h)	OLR for 2,4-DCP (mg DCP/L/d)	OLR for COD (g COD/L/d)
RUN I.1	0 - 3.0	0.13	42.3	4.2	3.5
	3.0 - 24.0	0.16	34.4	32.7	3.8
	24.0 - 60.0	0.13	42.3	4.4	3.6
RUN I.3	0.0 - 12.0	0.28	19.6	10.0	8.0
	12.0 - 24.0	0.30	18.3	71.7	7.8
	24.0 - 50.0	0.30	18.3	12.1	8.2
RUN II.1	0.0 - 13.0	0.14	39.3	4.7	3.5
	13.0 - 17.5	0.11	50.0	41.5	2.4
	17.5 - 21.0	0.61	9.0	258.1	10.3
	21.0 - 50.0	0.15	36.7	4.3	3.9
RUN II.2	0.0 - 15.0	0.20	27.5	6.3	4.8
	15.0 - 19.0	0.46	12.0	200.7	10.1
	19.0 - 24.5	0.49	11.2	237.3	4.9
	24.5 - 50.0	0.22	25.0	6.9	5.5
RUN II.3	0.0 - 14.0	0.30	18.3	9.8	7.7
	14.0 - 26.0	0.29	19.0	66.8	3.8
	26.0 - 38.0	0.29	19.0	74.3	6.1
	38.0 - 70.0	0.30	18.3	9.8	7.7
RUN II.4	0.0 - 13.0	0.22	25.0	6.8	6.5
	13.0 - 21.0	0.20	27.5	44.5	5.2
	21.0 - 25.0	0.23	23.9	6.8	6.8
	25.0 - 29.0	0.36	15.3	77.8	4.6
	29.0 - 50.0	0.23	23.9	6.8	6.8
RUN III.1	0.0 - 18.0	0.15	36.7	4.0	4.3
	18.0 - 71.0	0.11	50.0	55.5	2.7
	71.0 - 120.0	0.15	36.7	4.6	4.2
RUN III.3	0.0 - 13.0	0.31	17.7	8.1	8.6
	13.0 - 42.0	0.30	18.3	104.7	7.2
	42.0 - 120.0	0.32	17.2	8.4	8.4
RUN III.4	0.0 - 16.0	0.22	25.0	6.1	6.5
	16.0 - 41.0	0.20	27.5	117.6	5.5
	41.0 - 100.0	0.22	25.0	6.1	6.4

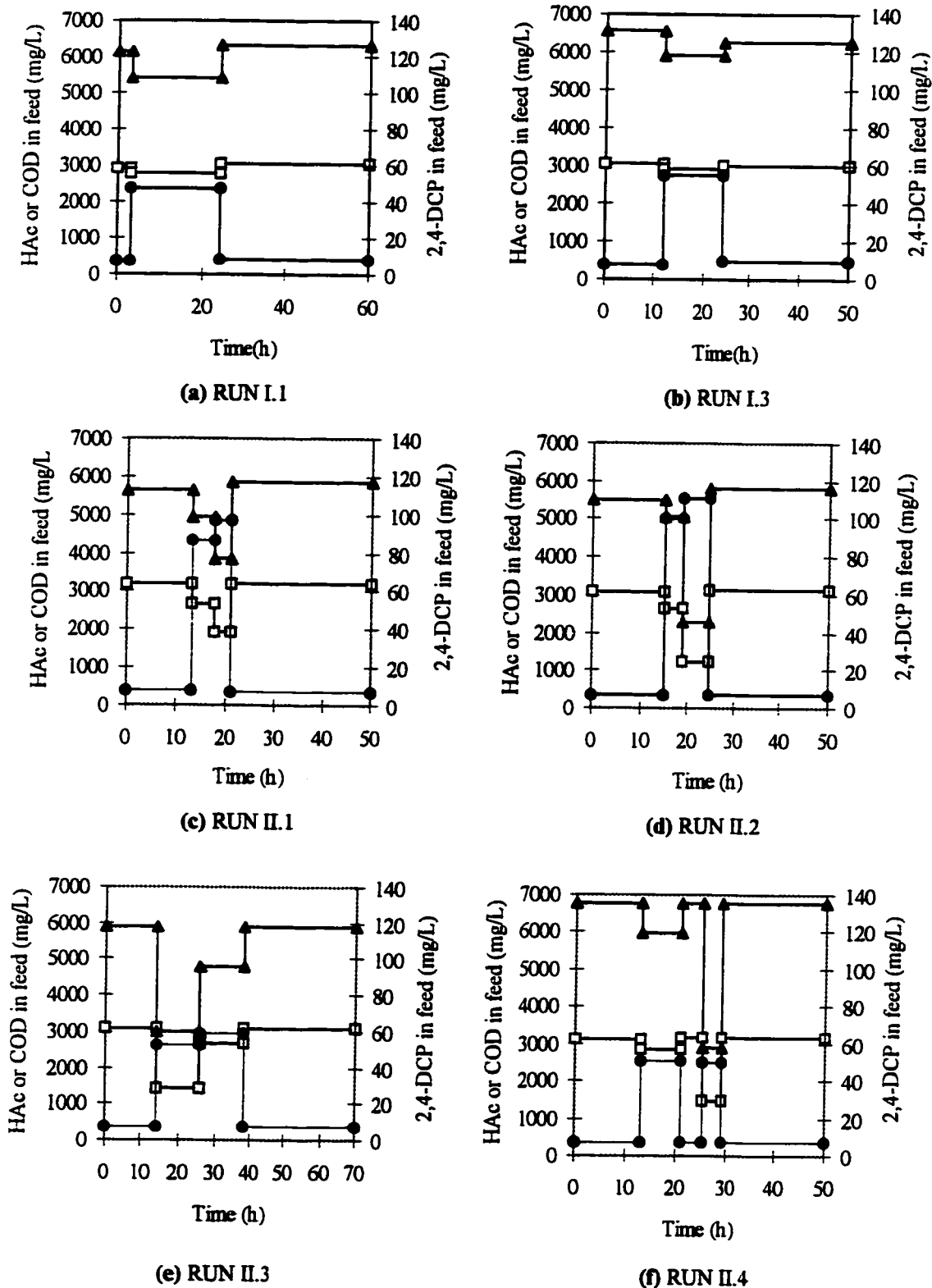
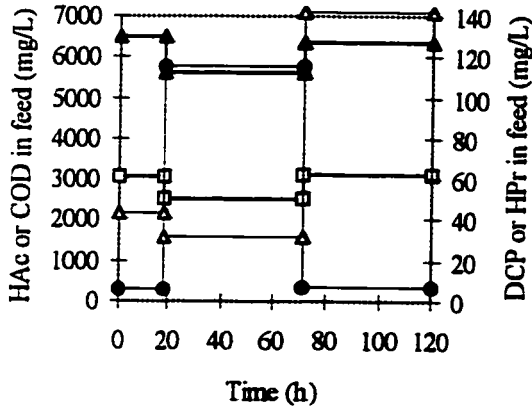
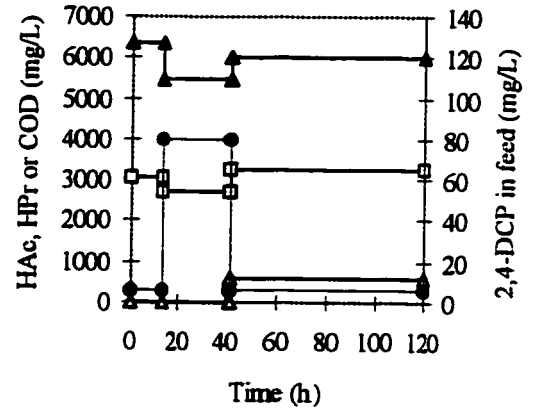


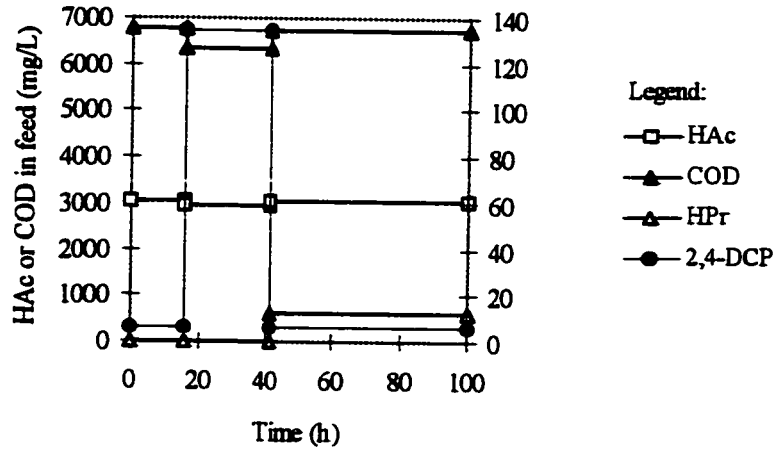
Figure 6-1 Variation of the substrate concentrations in feed during the transient change periods for UASB reactors (*see next page for (g)~(i) and legend*)



(g) RUN III.1



(h) RUN III.3



(i) RUN III.4

Figure 6-1 (continued) Variation of the substrate concentrations in feed during the transient change periods for UASB reactors

6.2 Performance of UASB Reactors

The 2,4-DCP concentration in the effluent of all UASB reactors during routine operation was less than detection limit of the HPLC. Removal efficiencies of primary substrates, expressed as COD, for the reactors are listed in Table 6-3.

Table 6-3 The soluble COD removal efficiencies for the UASB reactors

Experimental run	COD removal efficiency for each reactor (%) ^a			
	R1	R2	R3	R4
RUN I	98	97	88	97
RUN II	96	94	87	94
RUN III	98	NM ^b	75	77

^a The COD measurements for the values presented were made before each experimental run was conducted.

^b Not measured.

Data in the above table show that the COD removal efficiencies for reactors R3 and R4 decreased significantly after RUN II was conducted. It was observed that after RUN II was finished, the COD removal efficiencies stepped down gradually and stabilized to a new level although the 2,4-DCP concentration in the reactors became undetectable within 3 days. This observation may be explained with inactivation of biomass caused by the high 2,4-DCP input during the transient feed condition change in RUN II. For batch degradation tests (Chapter 5), it was observed that about 13% of the 2,4-DCP was either degraded by another pathway than to 4-MCP or the 4-MCP was further degraded. However, further degradation of 4-MCP or the alternative degradation pathway were found to be less significant in the continuous UASB reactors. A mass balance of 2,4-DCP dechlorination in four reactors during routine operation showed that the 4-MCP produced could account for 93.1% of 2,4-DCP added. The reason for the difference in 2,4-DCP degradation between batch tests and continuous flow reactors was not clarified further in this study. Difference in operational mode, experimental procedures, the chemical

composition of the dilution water for the batch tests (Appendix B) and the feed for routine operation of the reactors (Appendix A) could be factors influencing 2,4-DCP degradation.

System responses measured during the transient change periods for the reactors are the concentrations of HAc, HPr, 2,4-DCP, 4-MCP and COD in the effluent (Appendix E). Other data such as effluent pH (Appendix D), biogas production rates and composition were also collected. Corresponding to the transient feed condition changes (Figure 6-1), the system responses for the effluent concentrations of 2,4-DCP, 4-MCP, HAc, HPr and COD are presented in Figures 6-2a ~ 6-2i for each experimental run. The legend for the figure is shown in Figure 6-2a. As shown in these figures, the system responses have quite diverse concentration variation profiles and change dramatically from reactor to reactor.

The effect of sorption on system performance is highlighted in Figures 6-1 and 6-2. From the figures, the 2,4-DCP concentration in the effluent was significantly decreased and stabilized due to 2,4-DCP sorption and degradation by anaerobic sludge in reactors. Comparatively, effluent concentrations of the primary substrates were more sensitive to changes in the feeding conditions. Modeling analysis must be pursued to understand the diversity of the system responses from the multiple substrate degradation process.

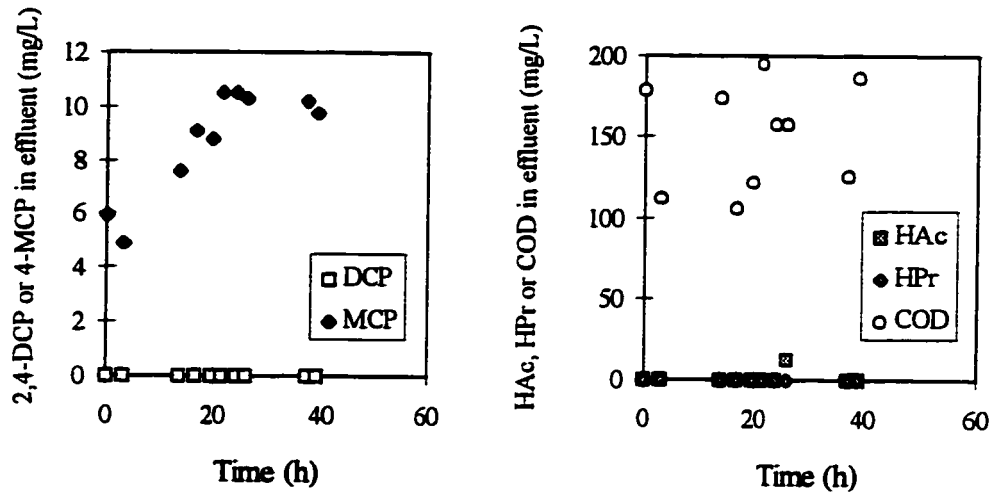


Figure 6-2a System responses for RUN I.1

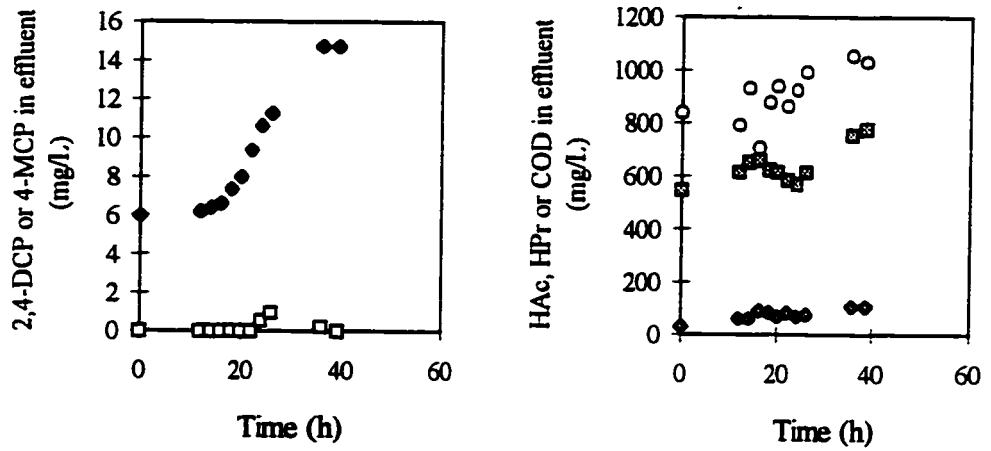


Figure 6-2b System responses for RUN I.3

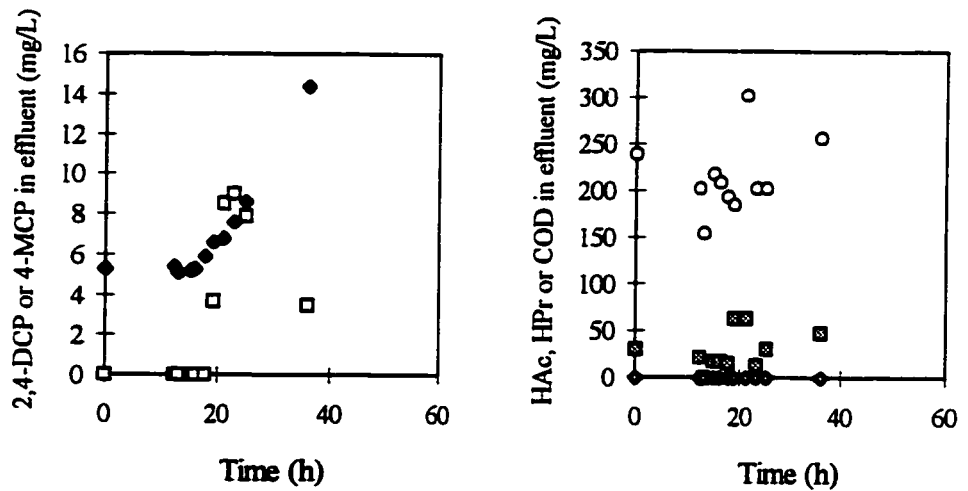


Figure 6-2c System responses for RUN II.1

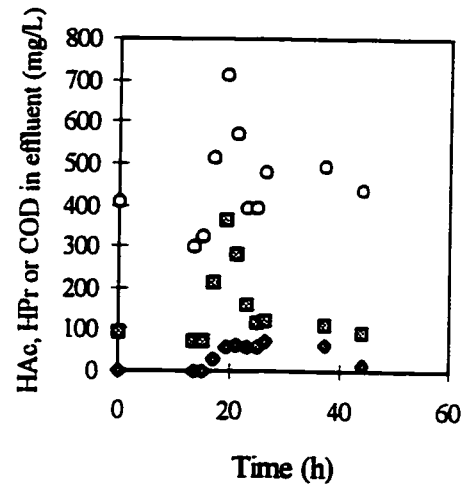
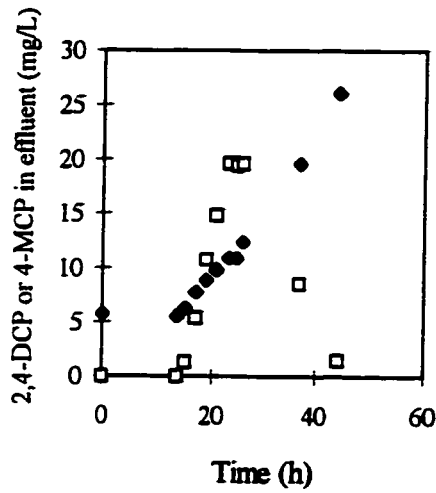


Figure 6-2d System responses for RUN II.2

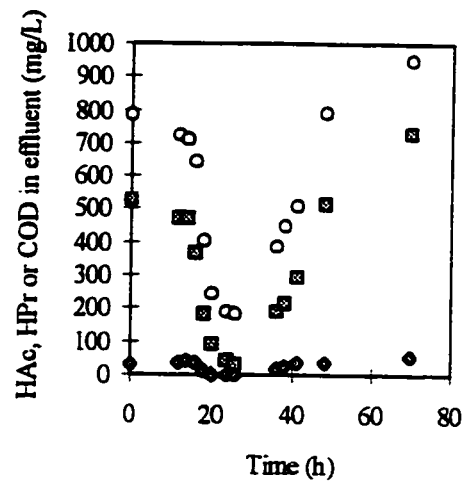
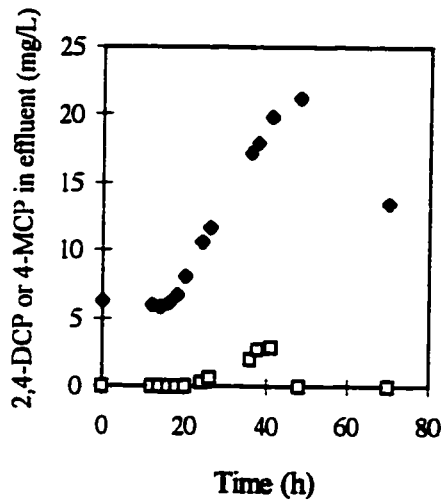


Figure 6-2e System responses for RUN II.3

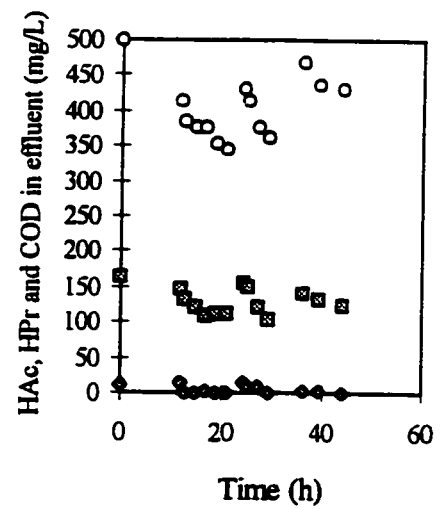
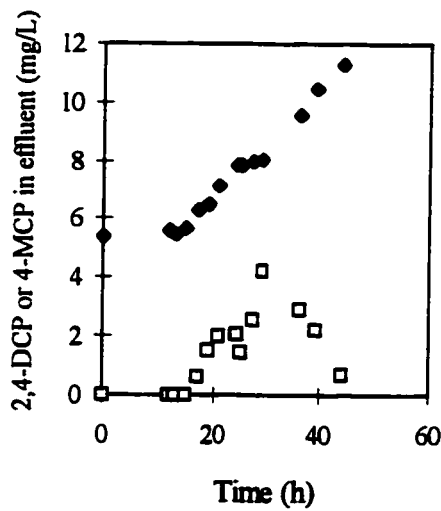


Figure 6-2f System responses for RUN II.4

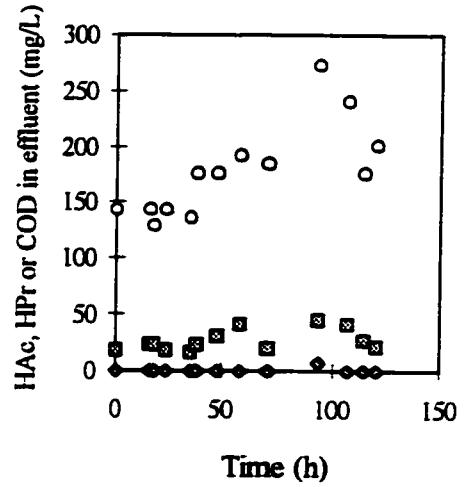
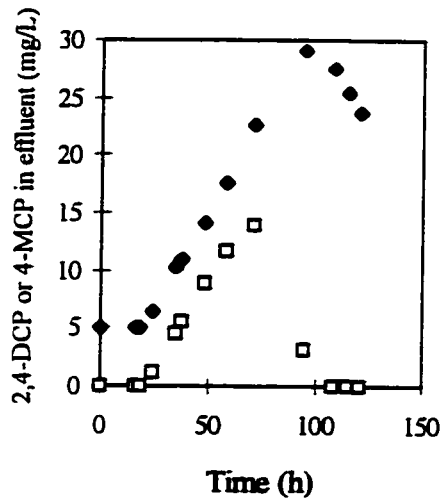


Figure 6-2g System responses for RUN III.1

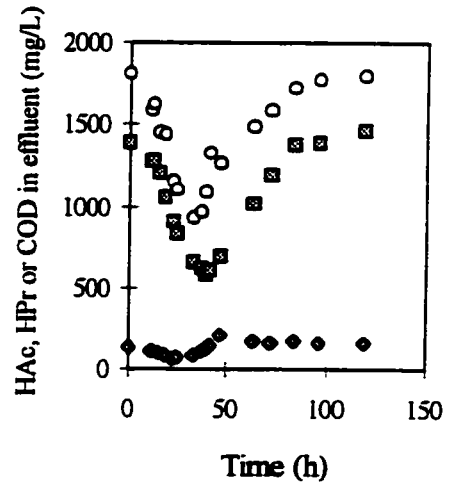
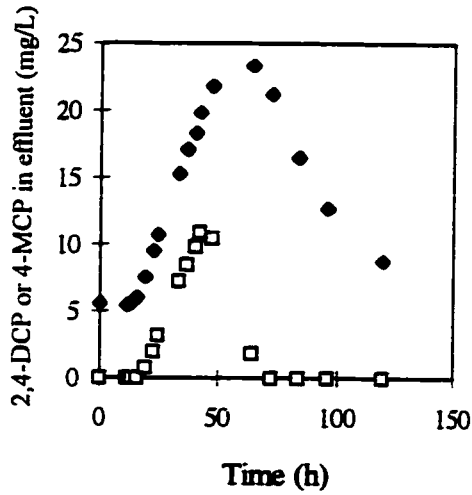


Figure 6-2h System responses for RUN III.3

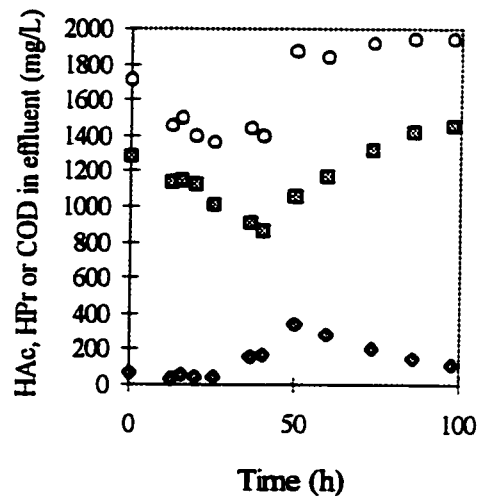
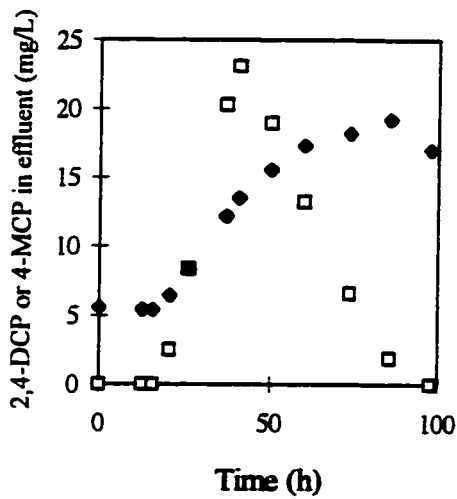


Figure 6-2i System responses for RUN III.4

DYNAMIC MODELING OF THE UASB REACTORS

Considering sorption and substrate interaction in degradation as two critical subprocesses for multiple substrate degradation in UASB reactors, a dynamic model for the system was developed based on information presented in Chapter 4 and 5. The dynamic model was validated and verified using the system responses during the transient UASB reactor operation (Chapter 6).

7.1 Model Development

7.1.1 Substrate Interaction Schemes in the UASB Reactors

It was proven in batch degradation tests that inhibition of HPr and HAc degradation by 2,4-DCP is the major feature for simultaneous degradation of 2,4-DCP, sucrose, HAc and HPr. Considering that the biomass used in the batch degradation tests was harvested from the UASB reactors, it is reasonable to assume that the same substrate interaction schemes exist in the UASB reactors. Figure 7-1 gives the schematic representation of the substrate interaction schemes of biodegradation in the UASB reactors.

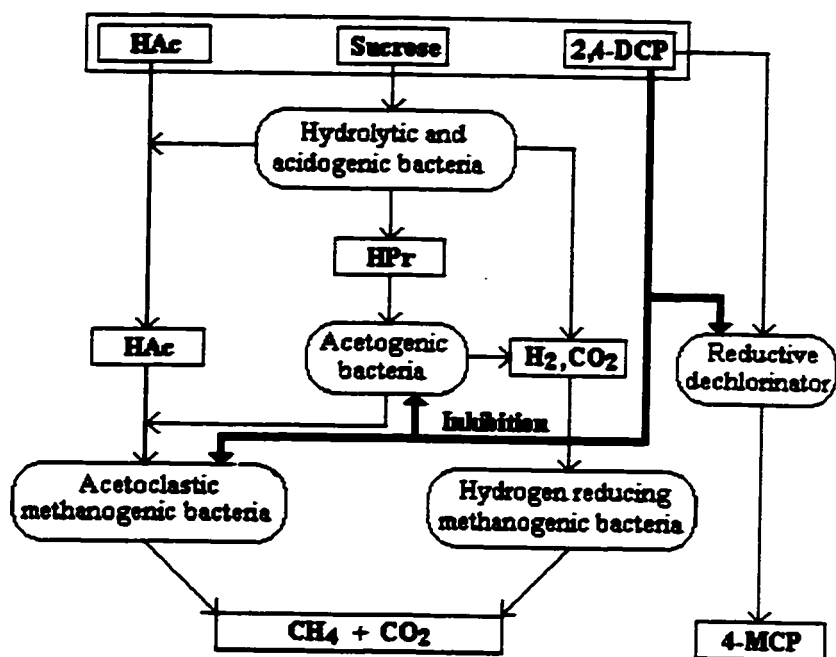


Figure 7-1 Schematic representation of the substrate interactions in the degradation processes in the UASB reactors for which the feed was sucrose/HAc based wastewater with 2,4-DCP.

It should be noted that the schematic representation was constructed based on the results obtained from batch degradation tests and the feeding conditions for the UASB reactors. For example, inhibition of acidogenesis by 2,4-DCP was not considered since the batch tests indicated no 2,4-DCP inhibition of sucrose degradation to HAc or HPr. Inhibition of hydrogen reducing bacteria by 2,4-DCP was also not included in this scheme because hydrogen inhibition was not considered in modeling the UASB reactors. The effect of electron donor on the dechlorination of 2,4-DCP was not described in Figure 7-1 since the effect was found to be negligible (Section 5.2). Based on observations from the operation of the UASB reactors, further degradation of 4-MCP was not considered. Adequacy of this scheme will be tested in model validation and verification.

7.1.2 Dynamic Model

Model assumptions

In developing the dynamic model for the UASB reactors, the following assumptions are made based on the results in preceding chapters.

(1) *Sorption of 2,4-DCP and 4-MCP to anaerobic granules in reactors follows linear sorption equation and the intereffect of multiple sorption of 2,4-DCP and 4-MCP in the reactors is negligible.* This assumption was supported by the investigation results in Chapter 3. However, sorption constants obtained in serum bottle tests may not be the same as those for sorption in the UASB reactors since a small portion of the chlorophenols may be sorbed to system components (Section 3.3). Additionally, this assumption is equivalent to assuming that conditions of local equilibrium, isotherm singularity and isotherm linearity exist in their sorption processes since nonideal sorption could happen while anyone of the three conditions is violated (Brusseau and Rao, 1989). The local equilibrium means that sorption process is fast relative to other processes that may affect solute concentrations in reactors so that local sorption equilibrium can be always achieved.

(2) *Substrate interaction schemes of the simultaneous degradation of sucrose, HAc and 2,4-DCP in the UASB reactors follow the schematic diagram described in Figure 7-1.*

The rationale of the assumption has been discussed. Based on this assumption, no

substrate and product inhibition of easily degradable substrates and the 4-MCP inhibition need to be considered in model development.

(3) *Biomass production within the transient change period of feed for the UASB reactors is not significant.* The reported values for yields in anaerobic digestion for glucose and HAc are 0.15 kg VSS/kg COD and 0.03 kg VSS/kg COD, respectively (Henze and Harremoës, 1983; Lawrence and McCarty, 1969). According to the COD removal efficiency of the UASB reactors, the estimated mean SRT is 26~65 d (Appendix F), varying from reactor R1 operated at the lowest SOLR to R3 operated at the highest SOLR. Since the transient change of feed for the UASB reactors was controlled in a short period of time (4~72 h), the variation of biomass concentration in the reactors within this period should not be significant.

(4) *The mixed liquor in the UASB reactors is under CM conditions.* Considering that mixing conditions have a strong influence to the sorption and degradation of the 2,4-DCP (Figure 4-24), this assumption was checked by tracer test (Figure 3-4). It was shown that all four reactors displayed CM conditions, with exception of reactor R1 which had a dead volume of 15%.

(5) *The 2,4-DCP and 4-MCP in the effluent of the UASB reactors mainly exist in the liquid phase, and the portion of both chemicals sorbed on suspended solids in the effluent are negligible.* The VSS concentrations measured for the UASB reactors varied in the

range of 116~457 mg/L. With an effluent VSS concentration of 400 mg/L, and the sorption coefficients of 0.045 and 0.018 L/g VSS for 2,4-DCP and 4-MCP (Table 3-2), the 2,4-DCP and 4-MCP discharged with VSS are only 1.8% and 0.7% of the amount discharged in the liquid phase for the two chemicals, respectively.

Model development

Based on the above assumptions, a dynamic model for the UASB reactors was developed describing the following responses: 2,4-DCP, 4-MCP, HAc, HPr and COD.

(1) 2,4-DCP

By means of a mass balance the 2,4-DCP in the system is,

$$V \left(\frac{dC_{DCP}}{dt} + X \frac{dq_{DCP}}{dt} \right) = Q(C_{0,DCP} - C_{DCP}) - r_{DCP \rightarrow MCP} XV \quad (7-1)$$

Using linear sorption equation, $q = K_{d,DCP} C_{DCP}$ [Assumption (1)], the above equation becomes:

$$(1 + K_{d,DCP} X) \frac{dC_{DCP}}{dt} = \frac{Q}{V} (C_{0,DCP} - C_{DCP}) - r_{DCP \rightarrow MCP} X \quad (7-2)$$

Kinetics of 2,4-DCP degradation, $r_{DCP \rightarrow MCP}$, was determined in Chapter 5 (Equation 5-3) although the parameter values in Equation (5-3) may need to be adjusted in modeling the UASB reactors.

(2) 4-MCP

Using a similar mass balance relation as for 2,4-DCP, the mass balance equation for 4-

MCP can be written as:

$$(1 + K_{d,MCP} X) \frac{dC_{MCP}}{dt} = \frac{Q}{V} (C_{0,MCP} - C_{MCP}) + 0.788 r_{DCP \rightarrow MCP} X \quad (7-3)$$

where, the last term on the right side of the equation accounts for the production of 4-MCP. The numerical value, 0.788, in the term is the ratio of the molecular weight of 4-MCP to 2,4-DCP ($M_{2,4-DCP} / M_{4-MCP} = 128.5/163.0$) since the 2,4-DCP degradation rate is used to describe production of 4-MCP based on their stoichiometric relation.

(3) HAc

Several degradation processes in the system can affect the mass balance of HAc, such as HAc production from degradation of sucrose and HPr, and degradation of HAc to methane gas (Figure 7-1). However, sorption of HAc to sludge is considered negligible. Therefore the mass balance relation for HAc in reactors is:

$$V \frac{dC_{HAc}}{dt} = Q(C_{0,HAc} - C_{HAc}) + (0.702 r_{SUC \rightarrow HAc} + 0.811 r_{HPr \rightarrow HAc} - r_{HAc-Meth.}) XV \quad (7-4)$$

where the numerical values of 0.702 and 0.811 are the mass ratios of HAc produced to sucrose and HPr consumed in anaerobic biodegradation, respectively. Stoichiometric relations of sucrose and HPr degradation to HAc have been shown in Equations (5-12) ($240.2/342.3 = 0.702$) and (5-11) ($60.05/74.08 = 0.811$), respectively.

(4) HPr

In the mass balance of HPr in reactors, HPr is produced from the degradation of sucrose and consumed by its degradation to HAc,

$$V \frac{dC_{HPr}}{dt} = Q(C_{0,HPr} - C_{HPr}) + (0.866r_{SUC \rightarrow HPr} - r_{HPr \rightarrow HAc})XV \quad (7-5)$$

In the equation, the numerical value, 0.866, is determined from Equation (5-11).

(5) COD

From Equations (7-4) and (7-5), it can be seen that the concentration of sucrose is a critical variable in calculating the degradation rate of $r_{SUC \rightarrow HPr}$ and $r_{SUC \rightarrow HAc}$. A mass balance relation for sucrose can be described as follows:

$$V \frac{dC_{Suc}}{dt} = Q(C_{0,Suc} - C_{Suc}) - (r_{Suc \rightarrow HPr} + r_{Suc \rightarrow HAc})XV \quad (7-6)$$

Based on Equation (7-6), the sucrose concentration in the reactor during transient change periods can be determined since the sucrose concentration in the feed was known during the experiment (Appendix A). Consequently, the COD concentration can be calculated using the following equation, which is similar to Equation (5-18).

$$C_{COD} = 1.127C_{Suc} + 1.066C_{HAc} + 1.512C_{HPr} + 1.215C_{DCP} + 1.541C_{MCP} + C_{NCOD} \quad (7-7)$$

In this way, although sucrose concentration in the system was not measured during the experiment for the reasons stated in Section 5.3.3, the fifth system response, COD, can be defined.

However, an extra term [compared to Equation (5-18)], C_{NCOD} , has been added in Equation (7-6) to account for nondegradable COD in the effluent. The existence of nondegradable COD, as a part of soluble microbial products (SMP), in the effluent of biological reactors has been reported for both aerobic (Namkung and Rittmann, 1986; Rittmann et al., 1987) and anaerobic (Noguera et al., 1994) treatment systems. Noguera et al. (1994) observed that SMP did not accumulate significantly during methanogenesis from acetate but SMP comprised the majority of the effluent COD in glucose-fed anaerobic chemostats with retention times longer than 20 days. With a retention time of 10~40 d, SMP accounted for 20~100% of the soluble COD in the effluent. The majority of SMP was the products associated with biomass which was hard to degrade (first-order degradation constant of 0.000219 L/mg-d, compared with the steady-state rate of glucose utilization, 505 mg/L-d, in their investigation).

In this study, no investigation on SMP formation and degradation in the UASB reactors was conducted. In modeling the UASB reactors, nondegradable COD was estimated by overall COD degradation efficiency. By examining all measurements for effluent COD (the routine operation and the transient change period) of four reactors in the study, it was found that the lowest effluent COD was approximately 100 mg COD/L.

In the investigation by Noguera et al.(1994), 360 mg/L SMP was detected for an influent glucose concentration of 20,400 mg COD/L and retention time 10 d. This corresponds to a SMP concentration of 53 mg/L for an influent glucose concentration of 3000 mg COD/L. For the UASB reactors operated in this study, the feeding concentration of sucrose was controlled at about 3000 mg COD/L. The higher nondegradable COD concentration (100 mg/L vs. 53 mg/L) observed in this study was probably due to the high sludge concentration in this study. As indicated by Noguera et al. (1994), the production of biomass associated products (BAP, one major type of SMP) was related to the biomass concentration in reactors. In their investigation, a biomass concentration of about 3 g VSS/L was maintained in an anaerobic chemostat, which is lower than the granule concentration of 17~26 g VSS/L in the UASB reactors in this study.

Once the nondegradable COD, C_{NCOD} , in Equation 7-7 has been defined, the concentration of COD in the dynamic model can be determined. Since COD was one of the responses that were measured in the experimental investigation of the UASB reactors, the model prediction of COD can be validated and verified. One should not be confused to see that one more response (sucrose) can be predicted in the dynamic model than the observed responses, since C_{Suc} is dependent on C_{COD} , or *vice versa* (see Equation 7-7).

(6) VSS

Since the information on the yields for each group of bacteria (acidogenic, acetogenic, methanogenic organisms and dechlorinator) are not available for this multiple substrate

degradation system, the mass balance for total biomass in the system was considered based on COD degradation, instead of considering each kind of substrates.

$$V \frac{dX}{dt} = Y_{COD} Q(C_{0,COD} - C_{COD}) - Q(X_0 - X_e) - k_d XV \quad (7-8)$$

where, Y_{COD} is overall yield based on COD (g VSS/g COD), and k_d is endogenous decay constant (d^{-1}). Based on assumption (3), $V(dX/dt) = 0$ during the transient change period, therefore, the VSS concentration in the reactors could be considered constant.

For clarity, Table 7-1 summarizes the dynamic model developed for the UASB reactor with the model-related kinetic equations developed in Chapter 5. Since the biomass concentration could be considered to be constant, Equation (7-8) is not included in Table 7-1. The values of the parameters in the model are summarized in Table 7-2. Except for the pK_a values for 2,4-DCP, HAc and HPr, all other parameter values were estimated from batch sorption and degradation tests (see Chapter 4 and 5).

7.2 Model Validation

From Table 7-1, it can be seen that the dynamic model developed for the UASB reactors is a multiresponse model described by systems of nonlinear ordinary differential equations (ODE's). In the model 14 parameters need to be estimated. Although the values of these parameters have been obtained from batch tests, their values needed to be adjusted when applied to the continuous UASB reactors because of the difference of operating mode and

Table 7-1 Summary of the equations in the dynamic model for the UASB reactors

Model Description:

$$(1 + K_{d,DCP} X) \frac{dC_{DCP}}{dt} = \frac{Q}{V} (C_{0,DCP} - C_{DCP}) - r_{DCP \rightarrow MCP} X$$

$$(1 + K_{d,MCP} X) \frac{dC_{MCP}}{dt} = \frac{Q}{V} (C_{0,MCP} - C_{MCP}) + 0.788 r_{DCP \rightarrow MCP} X$$

$$V \frac{dC_{HAc}}{dt} = Q(C_{0,HAc} - C_{HAc}) + (0.702 r_{SUC \rightarrow HAc} + 0.811 r_{HPr \rightarrow HAc} - r_{HAc \rightarrow Meth.}) XV$$

$$V \frac{dC_{HPr}}{dt} = Q(C_{0,HPr} - C_{HPr}) + (0.866 r_{SUC \rightarrow HAc} - r_{HPr \rightarrow HAc.}) XV$$

$$V \frac{dC_{Suc}}{dt} = Q(C_{0,Suc} - C_{Suc}) - (r_{Suc \rightarrow HPr} + r_{Suc \rightarrow HAc}) XV$$

$$C_{COD} = 1.127 C_{Suc} + 1.066 C_{HAc} + 1.512 C_{HPr} + 1.215 C_{DCP} + 1.541 C_{MCP} + C_{NCOD}$$

Kinetics in the Model:

$$r_{DCP \rightarrow MCP} = \frac{k_{DCP^0} C_{DCP}}{K_{s,DCP^0} / \alpha_{DCP} + C_{DCP} + C_{DCP}^2 / (K_{i,DCP^0} / \alpha_{DCP} - C_{DCP})}$$

$$\text{where, } \alpha_{DCP} = 1 / (1 + 10^{pH - pK_{a,DCP}})$$

$$r_{Suc \rightarrow HAc} = \frac{k_{Suc \rightarrow HAc} C_{Suc}}{K_{S,Suc} + C_{Suc}}$$

$$r_{Suc \rightarrow HPr} = \frac{k_{Suc \rightarrow HPr} C_{Suc}}{K_{S,Suc} + C_{Suc}}$$

$$r_{HAc \rightarrow Meth} = \frac{k_{HAc \rightarrow Meth} C_{HAc}}{(K_{S,HAc^0} / \alpha_{HAc}) + C_{HAc} + C_{HAc} C_{DCP}^2 / (K_{i,DCP^0/HAc^0} / \alpha_{DCP}^2)}$$

$$\text{where, } \alpha_{HAc} = 1 / (1 + 10^{pH - pK_{a,HAc}})$$

$$r_{HPr \rightarrow HAc} = \frac{k_{HPr \rightarrow HAc} C_{HPr}}{(K_{S,HPr^0} / \alpha_{HPr}) + C_{HPr} + C_{DCP}^2 / (K_{i,DCP^0/HPr^0} \alpha_{HPr} / \alpha_{DCP}^2)}$$

$$\text{where, } \alpha_{HPr} = 1 / (1 + 10^{pH - pK_{a,HPr}})$$

Table 7-2 Parameter values in the dynamic model estimated from batch tests

<u>For Sorption Equation:</u>		
$K_{d,DCP} = 0.045 \text{ L/g VSS}$	$K_{d,MCP} = 0.018 \text{ L/g VSS}$	
<u>For Degradation Kinetics:</u>		
$k_{DCP^0} = 0.14 \text{ mg/g VSS-h}$	$k_{HPr \rightarrow HAC} = 3.82 \text{ mg/g VSS-h}$	
$K_{S,DCP^0} = 2.07 \text{ mg/L}$	$K_{S,HPr^0} = 0.68 \text{ mg/L}$	
$K_{I,DCP^0} = 65.1 \text{ mg/L}$	$K_{I,DCP^0/HPr^0} = 8.61 \text{ mg/L}$	
$k_{Suc \rightarrow HAC} = 5.26 \text{ mg/g VSS-h}$	$k_{HAc \rightarrow Meth} = 6.87 \text{ mg/g VSS-h}$	
$k_{Suc \rightarrow HPr} = 2.05 \text{ mg/g VSS-h}$	$K_{S,HAc^0} = 0.32 \text{ mg/L}$	
$K_{S,Suc} = 14.74 \text{ mg/L}$	$K_{I,DCP^0/HAc^0} = 468.3 \text{ (mg/L)}^2$	
<u>The values of pK_a (35°C):</u>		
$pK_{a,DCP} = 7.89$	$pK_{a,HPr} = 4.88$	$pK_{a,HAc} = 4.76$

conditions between batch and continuous systems. The parameter values estimated from the batch tests were used as the starting values in model validation.

7.2.1 Parameter Estimation Criterion

Parameter estimation criterion for the multiresponse case under several assumptions can be derived using a likelihood or Bayesian argument (Bates and Watts, 1988). Bates and Watts (1988) showed that the maximum likelihood estimates of parameters, θ , can be obtained by minimizing the determinant of $Z^T Z$, where, θ is the parameter matrix and Z is the residual matrix which is defined as

$$Z(\theta) = Y - H(\theta) \quad (7-9)$$

in which \mathbf{Y} is the $N \times M$ observed response matrix with the (n, m) th element and $\mathbf{H}(\theta)$ is the $N \times M$ predicted response matrix with the same size of element. In this study, $\theta^T = (K_{d,DCP}, K_{d,MCP}, k_{DCP^0}, \dots, K_{I,DCP^0/HAC^0})$ which has 14 elements (Table 7-2); N is the number of observations taken for each response in an experimental run ($n = 1, 2, \dots, N$), and M is the number of responses measured in the experiment ($m = 1, 2, \dots, M$ and $M = 5$ in this study).

Under the situation where the variance and covariance for different responses are unknown, appropriate criterion for the multiresponse was derived using a Bayesian argument. The marginal posterior density function for θ is of the form

$$p(\theta|\mathbf{Y}) \propto \det(\mathbf{Z}^T\mathbf{Z}) \quad (7-10)$$

Thus, same as the likelihood approach, the posterior density is maximized when the determinant of $\mathbf{Z}^T\mathbf{Z}$ is minimized (Bates and Watts, 1988).

Different from the criterion stated above, the LS estimation criterion for multiresponse is to minimize the trace of $\mathbf{Z}^T\mathbf{Z}$ (sum of the entries along its principle diagonal), $\text{tr}(\mathbf{Z}^T\mathbf{Z})$. However, since some assumptions required by LS estimation criterion are not realistic, such as that the variances of different responses are equal, the LS estimation criterion are often not appropriate. Hence, minimizing the determinant of $\mathbf{Z}^T\mathbf{Z}$ was used as the criterion of parameter estimation in this study.

7.2.2 Parameter Estimation and Model Adequacy

A general algorithm for the multiresponse estimation in a system described by ODEs was discussed by McLean (Bates and Watts, 1985). For the parameter estimation problem in this study, an additional difficulty arises due to the discontinuity in carrying out model computation. The discontinuity describes the transient change of feeding conditions in the experiments for the UASB reactors (Figure 6-1). Because of the complexity of this estimation problem and since no statistical estimation package was available, the parameters in the dynamic model were estimated by fitting the dynamic model to the data using the principle of minimizing $\det(\mathbf{Z}^T\mathbf{Z})$.

A FORTRAN program was written to solve the dynamic model and to estimate the parameters (Appendix G). In the program, the model was solved numerically with certain set of values of θ , using the Runge-Kutta method. Then $\det(\mathbf{Z}^T\mathbf{Z})$ with respect to θ was calculated to evaluate the model fitting results. The parameter values shown in Table 7-3 were used as the starting points in the estimation. The parameter estimated, $\hat{\theta}$, was defined while the $\det(\mathbf{Z}^T\mathbf{Z})$ was minimized.

The system responses from experimental run, RUN III.4 (Table 6-1, Figure 6-2), were arbitrarily selected for parameter estimation. The other 8 sets of experimental data were used in verification of the dynamic model. The parameters estimated and the model fitting results are presented in Table 7-3 and Figure 7-2, respectively.

Table 7-3 Parameters estimated by fitting the model to data from RUN III.4

<u>For Sorption Kinetics:</u>	
$K_{d,DCP} = 0.15 \text{ L/g VSS}$	$K_{d,MCP} = 0.056 \text{ L/g VSS}$
<u>For Degradation Kinetics:</u>	
$k_{DCP^0} = 0.11 \text{ mg/g VSS-h}$	$k_{HPr \rightarrow HAC} = 3.5 \text{ mg/g VSS-h}$
$K_{S,DCP^0} = 2.07 \text{ mg/L}$	$K_{S,HPr^0} = 0.68 \text{ mg/L}$
$K_{I,DCP^0} = 65.1 \text{ mg/L}$	$K_{I,DCP^0/HPr^0} = 62.0 \text{ mg/L}$
$k_{Suc \rightarrow HAC} = 6.2 \text{ mg/g VSS-h}$	$k_{HAC \rightarrow Meth} = 9.7 \text{ mg/g VSS-h}$
$k_{Suc \rightarrow HPr} = 1.2 \text{ mg/g VSS-h}$	$K_{S,HAc^0} = 0.32 \text{ mg/L}$
$K_{S,Suc} = 14.74 \text{ mg/L}$	$K_{I,DCP^0/HAc^0} = 1686 \text{ (mg/L)}^2$

Comparing the parameter values in Table 7-3 with Table 7-2, it can be seen that the values of the inhibition constants, $K_{I,DCP^0/HPr^0}$ and $K_{I,DCP^0/HAc^0}$, were adjusted to fit the observed system responses. This suggested that inhibition of methanogenesis and acetogenesis in the UASB reactors by 2,4-DCP was less significant than in serum bottles. The sorption coefficients for both 2,4-DCP and 4-MCP were increased. The reason for the increase may be partially due to the sorption of these two chemicals to system components. This consideration is supported by observation during the continuous sorption tests with step input (Chapter 4). Besides the four parameters mentioned above, the specific degradation constants for 2,4-DCP (k_{DCP^0}), HAC ($k_{HAC \rightarrow Meth}$), HPr ($k_{HPr \rightarrow HAC}$), sucrose to HPr ($k_{Suc \rightarrow HPr}$) and sucrose to HAC ($k_{Suc \rightarrow HAC}$) were found to be sensitive to model fitting results. Necessary adjustment of these parameter values could be due to

many reasons, such as the different operating conditions between the UASB reactors and the batch degradation tests, the difference of biomass characteristics between the sludge in reactor (R4) and the sludge used in batch degradation tests (from R3, except specified). However, the saturation constants for 2,4-DCP, HAc, HPr and sucrose were found not to be sensitive to model fitting results. Consequently, their values were not adjusted.

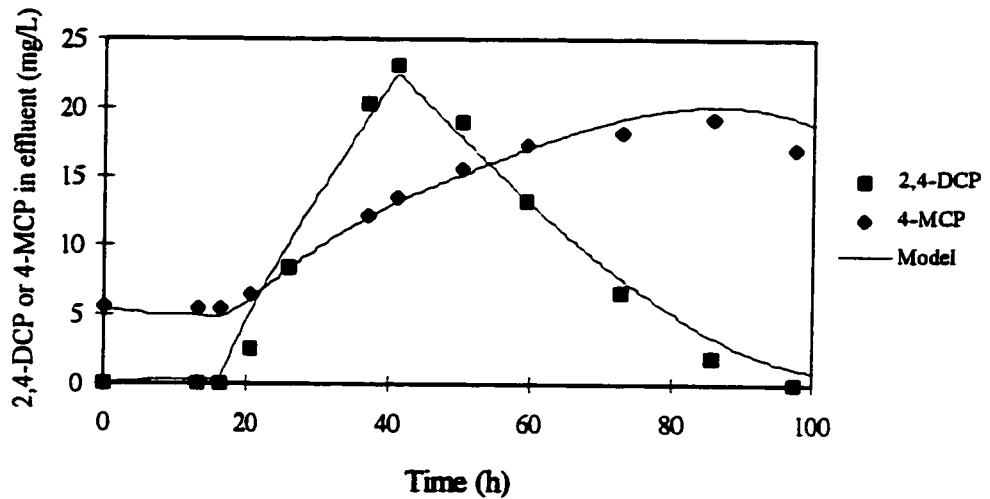


Figure 7-2a Model fitting results for 2,4-DCP and 4-MCP (RUN III.4)

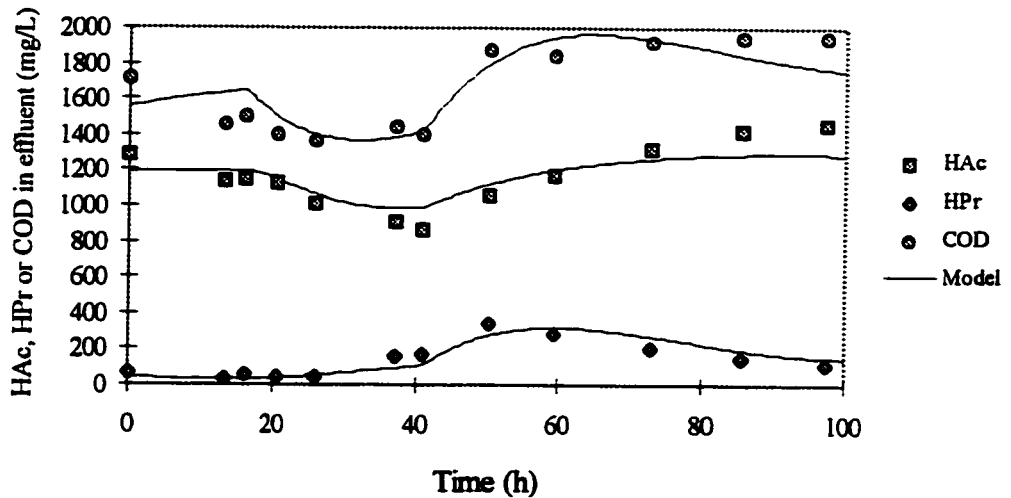


Figure 7-2b Model fitting results for HAc, HPr and COD (RUN III.4)

Figure 7-2a shows an excellent fit between the model and data, indicating linear sorption kinetics were adequate in describing the sorption process in the UASB reactors. In Figure 7-2b, the model for HPr and HAc fit the data quite well, except the model predicted a faster biomass activity recovery from inhibition for HAc degradation after the 2,4-DCP concentration in the system decreased (at time 80-100 h in Figure 7-2b). Similar results were also seen in predicting the COD concentration. The deviation of prediction from the observation suggests that the process of inhibition of biomass is different from the process of the biomass recovery from inhibition. However, the determination of the degradation kinetics was made only from the experiments considering inhibition (Chapter 5). Since this problem has not been addressed and no information on the kinetic difference between the inhibition of biomass and the biomass recovery from inhibition is available in the literature, the problem was not investigated further in this study. Except for this shortcoming, overall fitting results of the dynamic model to all five dependent variables in the system were reasonably good. Since no other lack of fit in the model fitting results was identified, model adequacy was accepted.

7.3 Model Verification

The dynamic model was verified by using the other 8 sets of experimental UASB reactor data (Figure 6-2). Preliminary model fitting results indicated that, if the specific degradation rate constants in the model (k_{DCP^0} , $k_{HAc \rightarrow Math}$, $k_{HPr \rightarrow HAc}$, $k_{Suc \rightarrow HPr}$, $k_{Suc \rightarrow HAc}$)

were not adjusted, the model could not simultaneously describe the 8 sets of experimental data well. In the model development, it has been implicitly assumed that biomass characteristics are kinetically identical for all UASB reactors. This assumption has been utilized extensively in modeling biological treatment systems and worked well for systems treating nontoxic organic matters (Siegrist et al., 1993; Sam-soon et al., 1991). However, since few investigations on anaerobic degradation of toxic organic compounds have been reported, this assumption has not been fully justified in the situation under which the simultaneous degradation of primary substrates and toxic organics are involved. Compared with traditional modeling of the degradation of nontoxic organic matter, the inactivation of biomass related to degradation of toxic organic compounds has been considered in the study of cometabolism kinetics (Criddle, 1993). Recently, Ely et al. (1995) developed a cometabolic kinetics for describing the degradation of trichloroethylene (TCE) by ammonia-oxidizing bacteria with ammonia as growth substrate. In their model, variation of the maximum degradation rate constants for TCE and ammonia degradation were described by incorporating enzyme inhibition, inactivation and recovery in the model.

As a result, the adjustment of parameters values was undertaken in the model fitting. According to the sensitivity of the parameters to model fitting results, only five maximum specific degradation rate constants were adjusted. The parameter values defined for the model fitting to the 8 sets of data are summarized in Table 7-4. The original parameter values from the model validation are also listed for comparison.

The model prediction results for the 8 sets of experimental data are presented in Figure 7-3 to Figure 7-10, respectively. Although the observed responses for the five dependent variables in the 8 sets of experimental data have very diverse profiles, the dynamic model has followed their trends quite well. Overall fitting of the model with adjusted parameters to the data for 2,4-DCP, 4-MCP, HAc, HPr and COD was satisfactory (Appendix H). Adequacy of the dynamic model and necessary of parameter adjustment are supported by the model simulation results.

Table 7-4 The parameter values used in the model verification

Data source	Parameter values (mg/gVSS-h)				
	k_{DCP^0}	$k_{HAc \rightarrow Meth}$	$k_{HPr \rightarrow HAc}$	$k_{Suc \rightarrow HAc}$	$k_{Suc-HPr}$
<i>Validation:</i>					
RUN III.4	0.11	9.5	3.5	6.2	1.2
<i>Verification:</i>					
RUN II.4	0.13	18.6	9.8	6.2	1.2
RUN III.3	0.19	11.0	4.0	6.8	2.6
RUN II.3	0.19	13.0	4.8	6.8	2.6
RUN I.3	0.19	12.8	4.0	6.8	2.6
RUN II.2	0.19	13.8	4.6	5.8	1.8
RUN III.1	0.09	20.5	9.2	7.5	0.1
RUN II.1	0.10	20.5	9.2	7.5	0.1
RUN I.1	0.11	28.5	9.2	7.5	0.1

The good prediction of 2,4-DCP and 4-MCP concentrations in effluents by the model indicates appropriateness of linear sorption equation and 2,4-DCP degradation kinetics. The some unsatisfactory fitting results for 2,4-DCP concentrations in Figure 7-5a, 7-6a and 7-10a were not surprising. The reason for this was probably due to the very low concentration of 2,4-DCP in the effluent since the sensitivity of HPLC in measuring the chemical is about 0.5~1.0 mg/L. Additionally, loss of a portion of the 2,4-DCP during sample preparation may also have a more significant effect on results at low

concentrations. The deviation of the model prediction from the 2,4-DCP data in Figure 7-7a may be caused by nonideal mixing conditions in this reactor during operation. Detailed analysis shows that if a 10% dead volume was considered in the reactor, fitting results would be significantly improved. However, since no dead volume was observed in the tracer test for the reactor, the dead volume was not considered in the model prediction, although it may have happened at the time the experiment was run. Lack of fit in model prediction can be seen in some experimental runs for HAc (Figure 7-3b and 7-4b), HPr (Figure 7-3b and 7-5b) and COD data (Figure 7-3b, 7-4b and 7-9b) although the model follows the data variation fairly well. The estimated value used for C_{NCOD} (100 mg/L) in model building could be a reason for the lack of fit. The value, 100 mgCOD/L, was used for all experimental runs but it could be different from reactor to reactor due to the different SOLR operating conditions. The shortcoming of the model in describing the recovery of biomass from inhibition would also have an effect (Figure 7-4b). Considering the factors mentioned above, it is believed that the dynamic model described the simultaneous degradation process successfully.

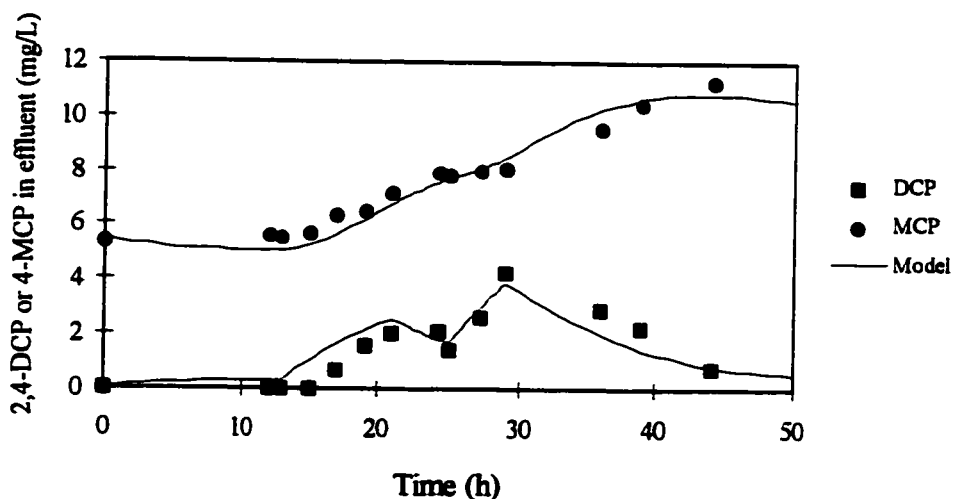


Figure 7-3a Model fitting results for RUN II.4. (A) 2,4-DCP and 4-MCP

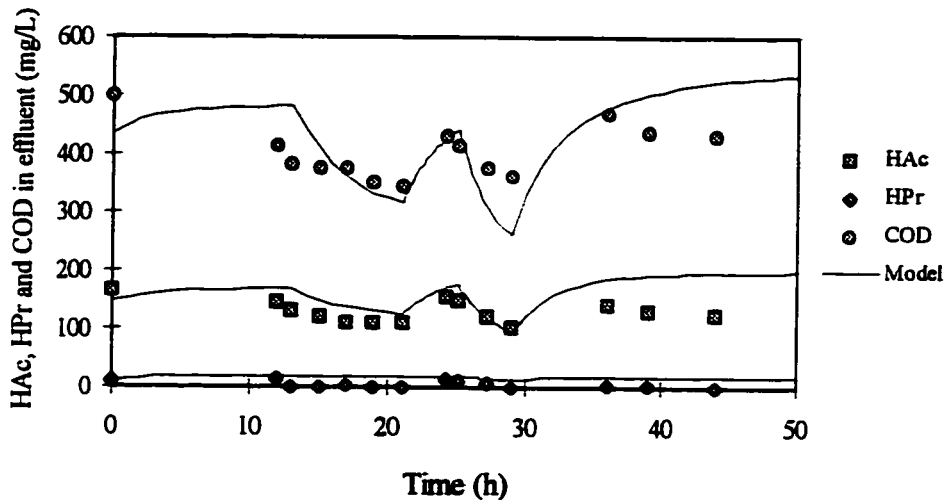


Figure 7-3b Model fitting results for RUN II.4. (B) HAC, HPr and COD

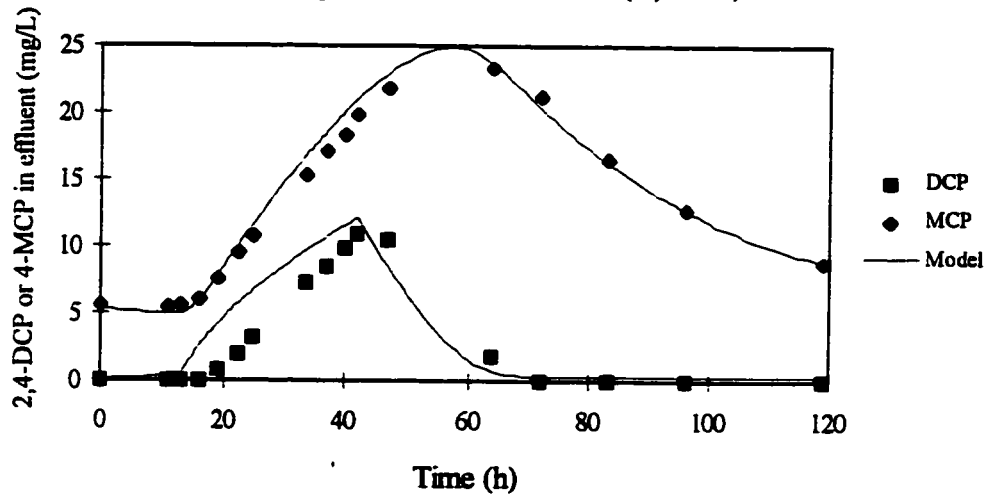


Figure 7-4a Model fitting results for RUN III.3. (A) 2,4-DCP and 4-MCP

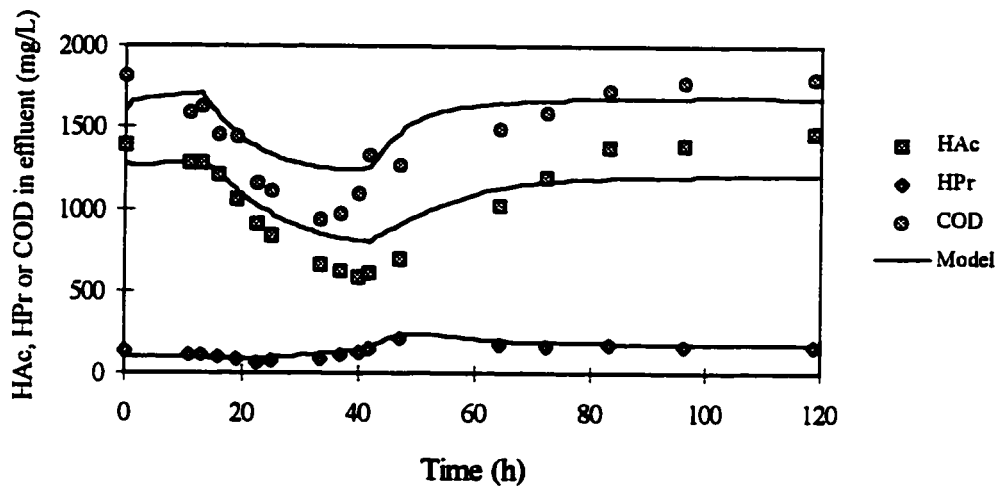


Figure 7-4b Model fitting results for RUN III.3. (B) HAC, HPr and COD

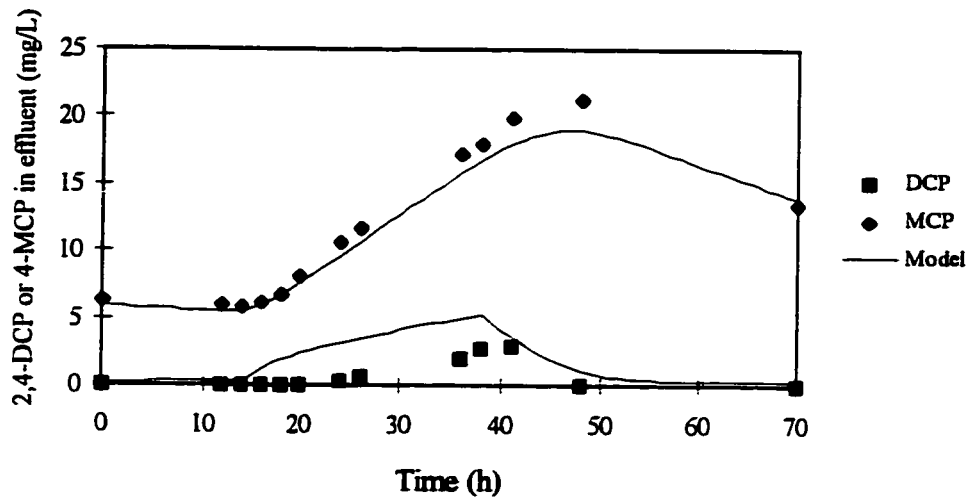


Figure 7-5a Model fitting results for RUN II.3. (A) 2,4-DCP and 4-MCP

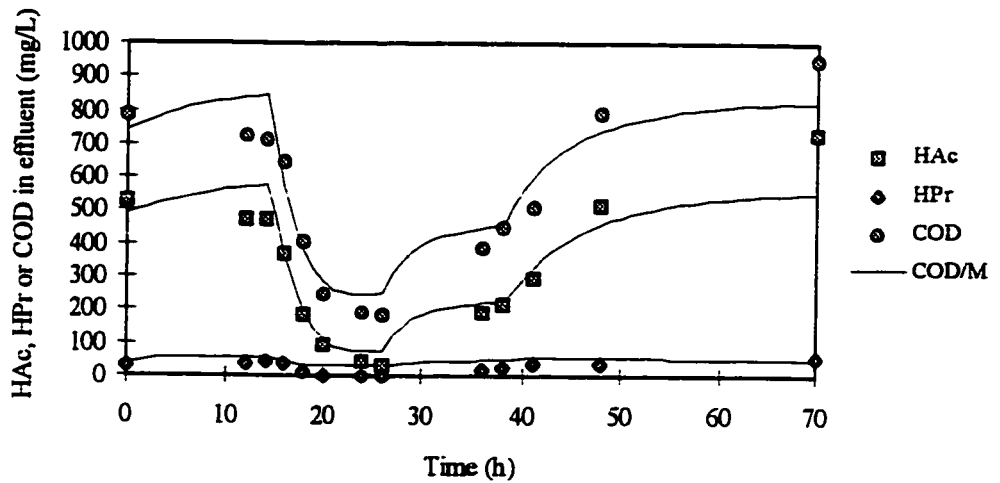


Figure 7-5b Model fitting results for RUN II.3. (B) HAc, HPr and COD

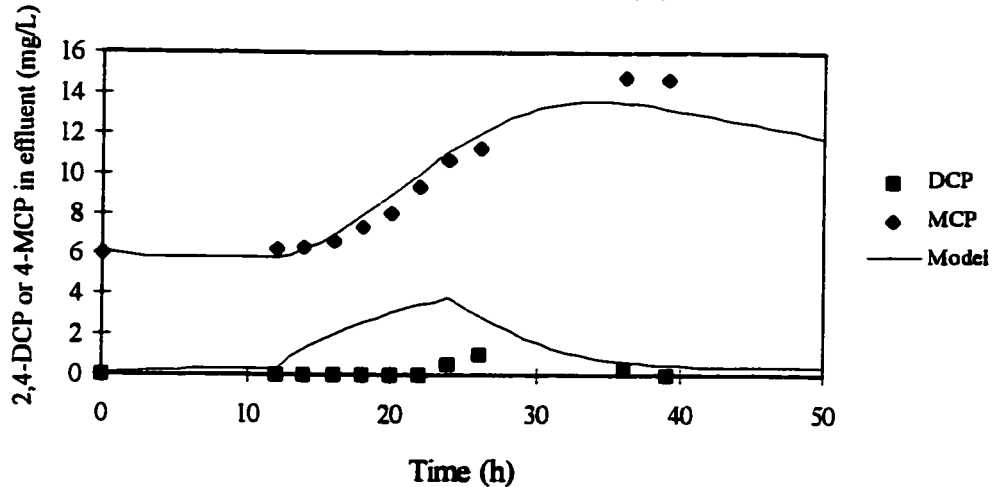


Figure 7-6a Model fitting results for RUN I.3. (A) 2,4-DCP and 4-MCP

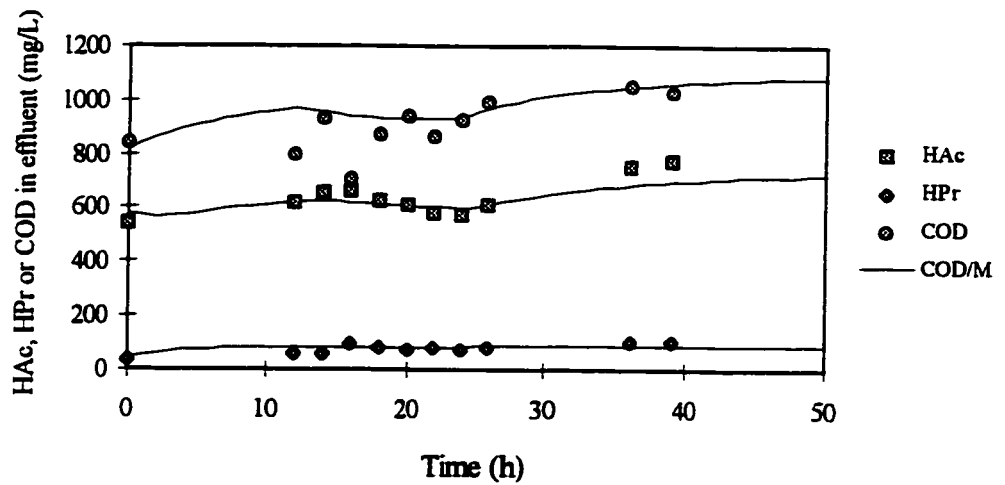


Figure 7-6b Model fitting results for RUN I.3. (B) HAC, HPr and COD

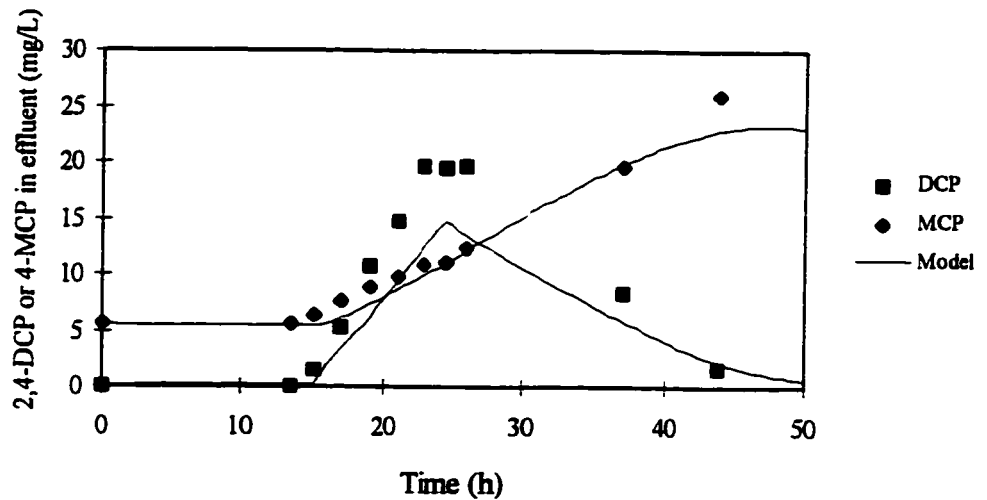


Figure 7-7a Model fitting results for RUN II.2. (A) 2,4-DCP and 4-MCP

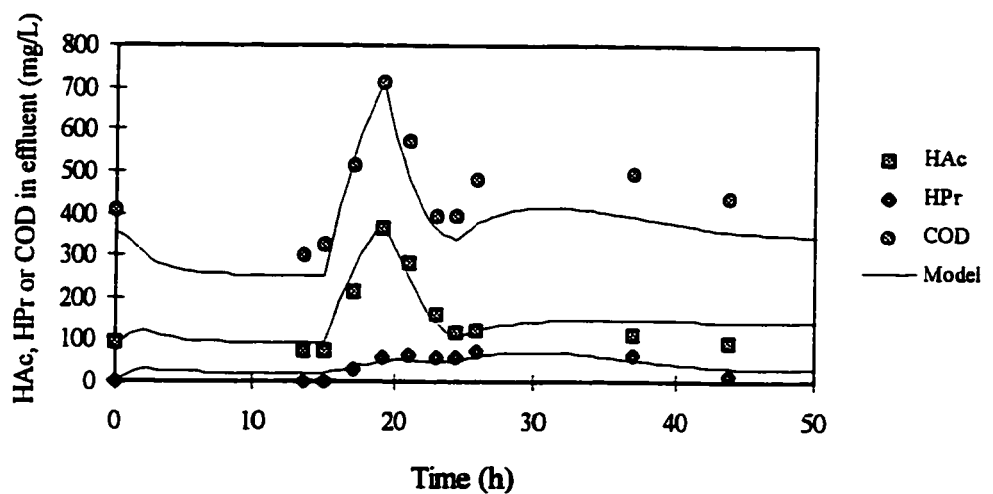


Figure 7-7b Model fitting results for RUN II.2. (B) HAC, HPr and COD

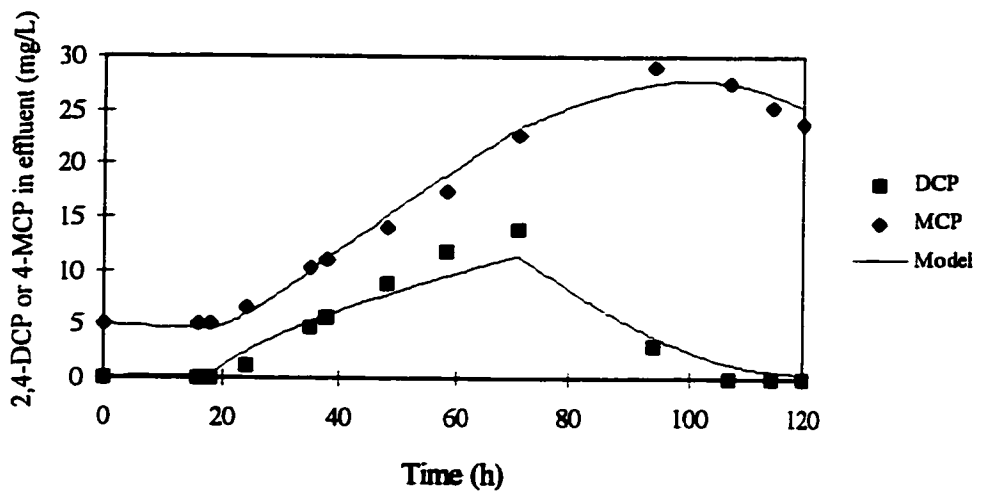


Figure 7-8a Model fitting results for RUN III.1. (A) 2,4-DCP and 4-MCP

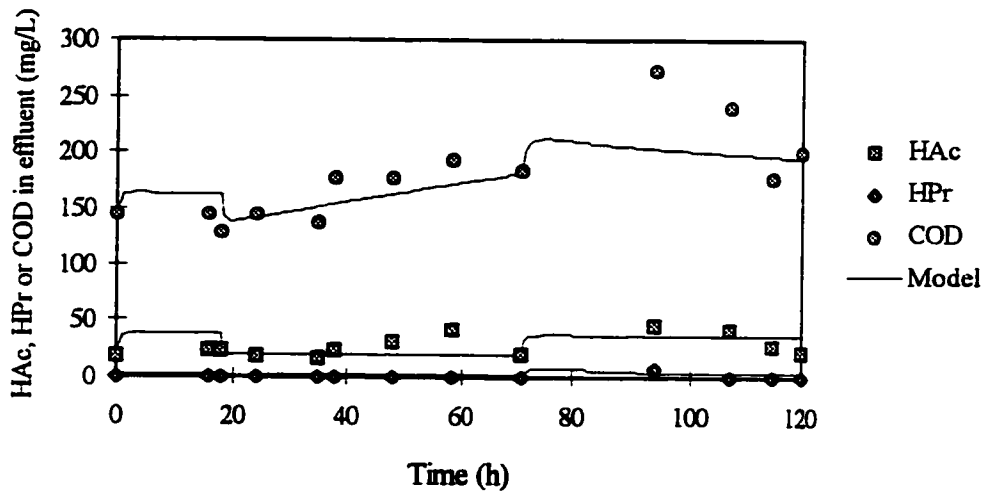


Figure 7-8b Model fitting results for RUN III.1. (B) HAc, HPr and COD

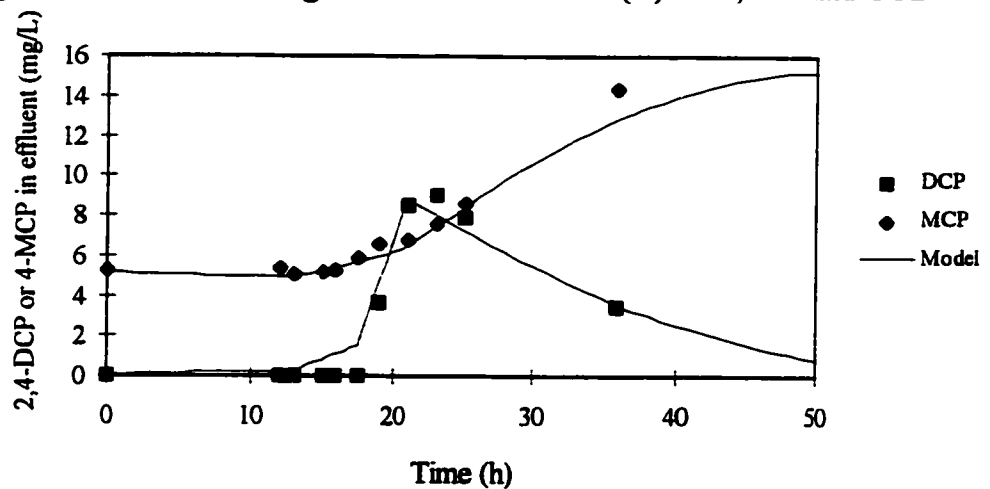


Figure 7-9a Model fitting results for RUN II.1. (A) 2,4-DCP and 4-MCP

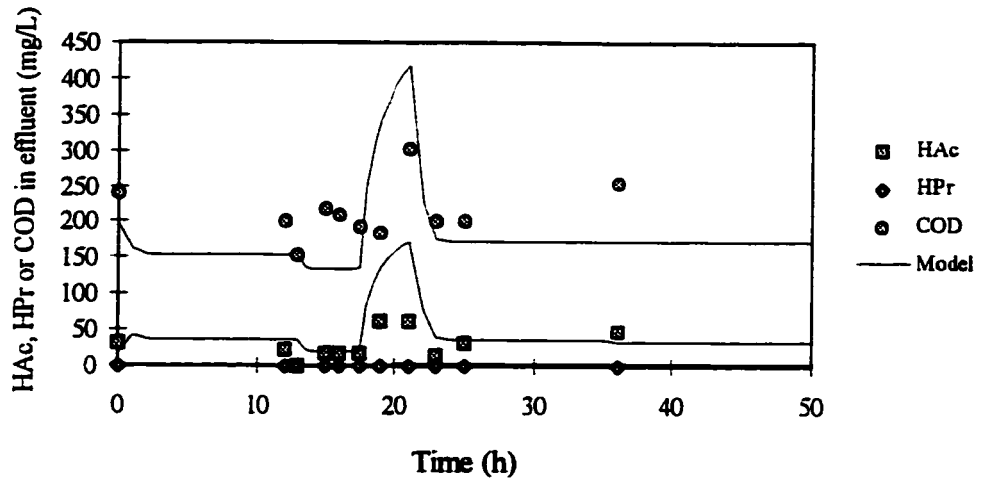


Figure 7-9b Model fitting results for RUN II.1. (B) HAC, HPr and COD

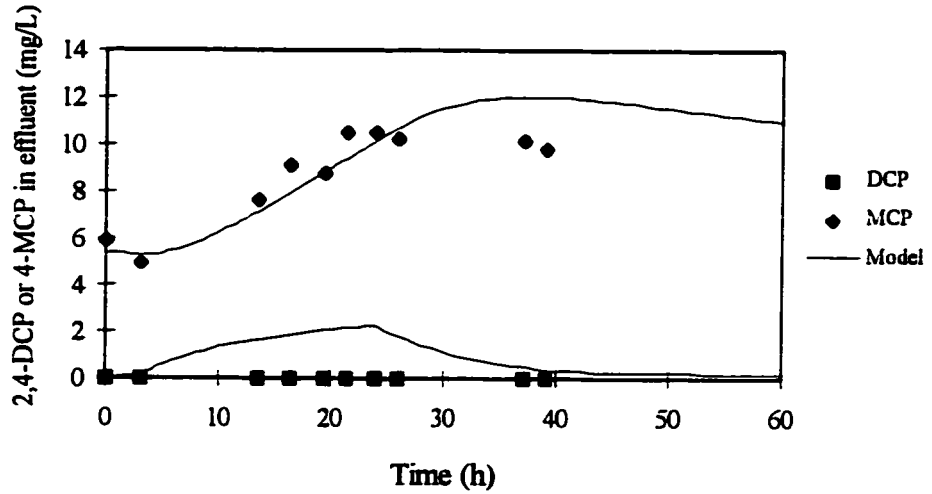


Figure 7-10a Model fitting results for RUN I.1. (A) 2,4-DCP and 4-MCP

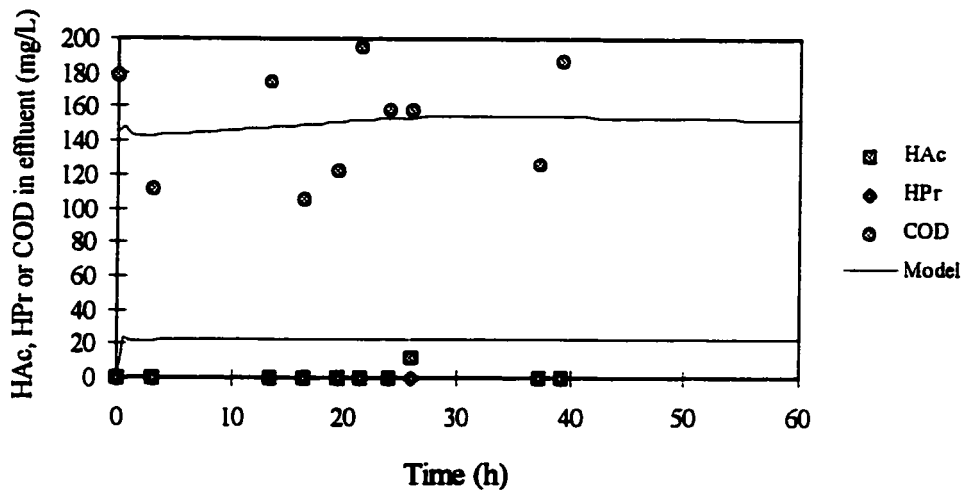


Figure 7-10b Model fitting results for RUN I.1. (B) HAC, HPr and COD

From the parameter values listed in Table 7-4, it was seen that variation of the parameter values for different runs was not random but was more comparable for the same reactor, suggesting that SOLR was a factor affecting parameter values. Figure 7-11 and 7-12 show the relation of SOLR to the specific degradation rate constants, k_{DCP^0} and $k_{HAC \rightarrow Meth}$, respectively. The values of k_{DCP^0} increase as SOLR increases but the opposite trend was found for the HAC degradation constant: as the SOLR increases, the values of $k_{HAC \rightarrow Meth}$ decrease. The same trend as for $k_{HAC \rightarrow Meth}$ was also found for the degradation rate constants of HPr (see Table 7-4, not graphically presented).

Statistical analysis on the data also indicated a high correlation between SOLR and the parameter value of k_{DCP^0} or $k_{HAC \rightarrow Meth}$. The correlation coefficients, ρ , calculated were 0.81 for SOLR and k_{DCP^0} , and -0.79 for SOLR and $k_{HAC \rightarrow Meth}$, respectively. Linear relations between SOLR and k_{DCP^0} and between SOLR and $k_{HAC \rightarrow Meth}$ were obtained by linear regression. The relations are presented in Figure 7-11 and 7-12, respectively. It should be noted that the true relations between SOLR and k_{DCP^0} or $k_{HAC \rightarrow Meth}$ are not necessarily linear. More data are required to obtain the relation more precisely.

7.4 Discussion

The observed variation of k_{DCP^0} vs. SOLR (Figure 7-11) is not surprising. During the acclimation of anaerobic biomass to 2,4-DCP in UASB reactors, the same feed was used

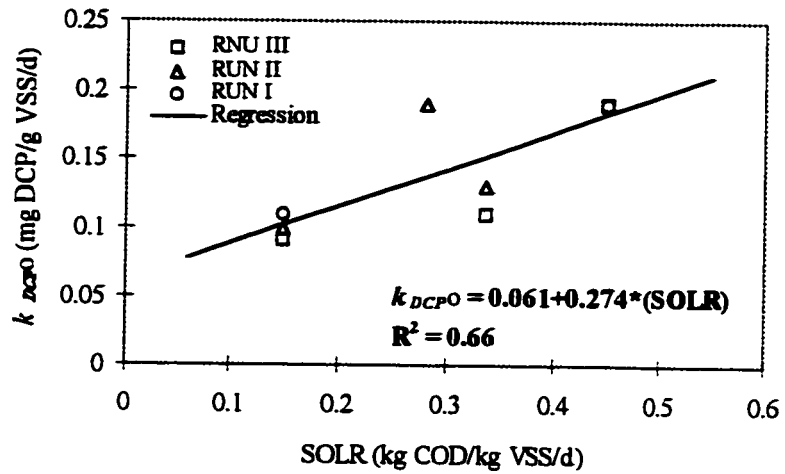


Figure 7-11 Effect of SOLR on the values of k_{DCP0}

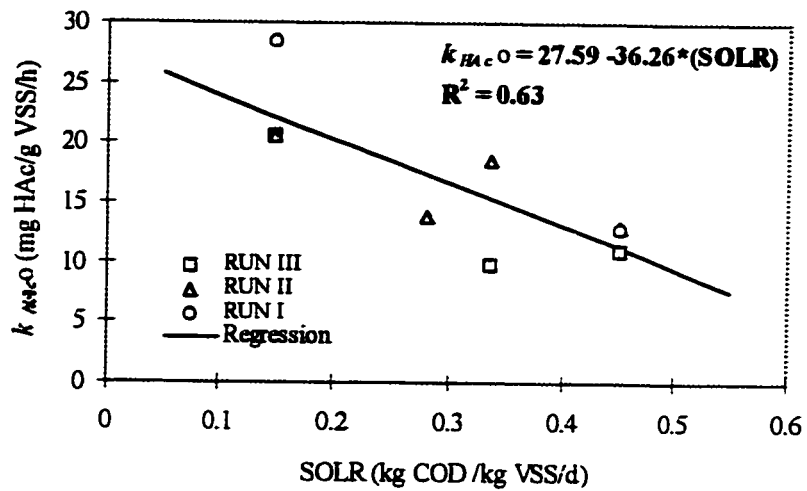


Figure 7-12 Effect of SOLR on the values of $k_{HAc \rightarrow Meth}$

for all four reactors. Therefore, the reactor with the highest SOLR also had the highest 2,4-DCP loading rate (R3). As a result, the highest concentration of 2,4-DCP dechlorinators would be developed in reactor R3, which may lead to the higher specific

2,4-DCP degradation rate that was observed.

Figure 7-12 can not be interpreted simply. During routine operation, the SOLR (COD basis) for all reactors was not too high (0.15~0.45 kgCOD/kgVSS-d), consequently no substrate and product inhibition was observed. Treatment efficiency of 2,4-DCP was 100% and the concentration of 2,4-DCP in the reactor was not detectable in the effluent during routine operation. Therefore, inhibition of primary substrate by 2,4-DCP should not be significant. The concentration of 4-MCP in the effluent was only about 7 mg/L. Compared with the concentration of 4-MCP for significant inhibition on methanogenesis (50 mg/L) reported by Kim et al. (1994), the inhibitory effect of 4-MCP in the UASB reactors was also negligible. During the transient feeding period, feed with high concentration of 2,4-DCP was applied to the reactors. It is reasonable to consider that the relationship shown in Figure 7-12 may be due to acute inhibition and biomass inactivation caused by the high 2,4-DCP input in a short time period. However, this does not fully explain the results in Figure 7-12.

Another explanation of Figure 7-12 is that, under the selection pressure caused by 2,4-DCP, the mixed culture in the UASB reactors has been ecologically changed at different SOLR. The ecological change concept would explain why the biomass under the highest 2,4-DCP loading had the lowest HAc degradation rate when no inhibitory amount of 2,4-DCP had been applied. The implication of this could be important in determining the strategy of anaerobic treatment of wastewaters with toxic organics. The explanation

suggests that, since the ecological change will lead to a lower degradation rate of primary substrates, the separation of toxic organic compounds from the wastewater to be treated should be considered first in determining a process diagram for treating the wastewater. If direct biological treatment of the wastewater (treating toxic organics and primary substrates simultaneously in one reactor) was considered, system performance in treatment the primary substrates may deteriorate when a new ecological balance in the biomass develops, no matter how well the sludge is acclimated to the toxic organics.

To provide further evidence for the possible ecological change, kinetic parameter values obtained in this study with those from the literature were compared (Table 7-5). It was surprising to find that the values of the parameters in this study were low, compared with those reported in the literature. The parameter values were also lower than the values reported by Fernandes et al. (1993). In their study, anaerobic reactors treated the same

Table 7-5 Comparison of the parameter values for the acetoclastic methanogenesis

No.	Process Type (Mixed culture, 35°C)	$k_{HAc \rightarrow Meth}$ (gHAc/gVSS-d)	Ref.
1	Continuous	8.2 ^a	Lawrence and McCarty, 1969
2	Batch	2.4 -4.8	van den Berg, 1977
3	Continuous	4.0 ^c	Kus and Wiesmann, 1995
4	Sequencing batch	2.4	Fernandes et al. , 1993
5	Continuous	10.5 ^b	Sam-Soon et al, 1991
6	Continuous	0.23 - 0.68	This study

^a Mean values of five sets of data.

^b Mean values of seven sets of data from reported investigations.

^c Calculated using the yield constant, 0.03 kgVSS/kgHAc.

wastewater as in this study, but without addition of 2,4-DCP. Since it would be unlikely that a short time of transient 2,4-DCP input could cause such a significant drop in the values of $k_{HAc \rightarrow Meth}$, compared to the values reported under situations without 2,4-DCP, this comparison supports the assumption of ecological change in the mixed culture.

In summary, it seems that biomass inactivation and ecological change may both be factors for the relation shown in Figure 7-12. However, since no microbiological analysis of anaerobic bacterial populations from different reactors was made in this study, more direct evidence is needed to further confirm this finding. The relationships shown in Figures 7-11 and 7-12 also suggest that, since the treatment efficiencies of primary substrates and toxic organic compounds change inversely as a function of SOLR, an optimum SOLR for a specific treatment system may be selected to meet designated treatment objectives.

CONCLUSIONS, CONTRIBUTIONS AND RECOMMENDATIONS

8.1 Conclusions and Contributions

1. A dynamic model for the simultaneous degradation of easily degradable cosubstrates (sucrose and HAc) and 2,4-DCP in UASB reactors was developed and verified. The model predicts five system responses: the effluent concentrations of 2,4-DCP, 4-MCP, HAc, HPr and COD of the reactors reasonably well, under the condition of that the maximum specific degradation rate constants, k , for 2,4-DCP, 4-MCP, HAc, HPr and COD were adjusted. Sorption and substrate interaction in degradation are two critical factors dominating the multiple substrate degradation process.

2. Concerning sorption of chlorophenols to anaerobic granules, it was concluded:
 - Difference in the sorption of 2,4-DCP to live and chemically inactivated anaerobic granules is not significant, suggesting that sorption can be considered mainly as a physical-chemical process.

 - pH was the most important factor affecting sorption of chlorophenols to

anaerobic granules, which can be described by the relationship between pH, pKa, and the sorption constants of phenolate ion and molecular 2,4-DCP (Equation 4-8).

- Intereffects of multiple sorption of chlorophenols to anaerobic sludge are chemical dependent. No significant intereffect was observed for co-sorption of 2,4-DCP and 4-MCP but a strong intereffect was observed for co-sorption of 2,4-DCP and PCP.

- For chlorophenols which follow linear sorption isotherm and sorption-desorption isotherm singularity, the dynamic sorption process in anaerobic reactors can be described by a model incorporating linear sorption equation. Nonequilibrium sorption in anaerobic reactors caused by diffusion limitations is negligible.

3. Concerning substrate interaction and the degradation kinetics of 2,4-DCP and co-substrates:

- Inhibition of methanogenesis and acetogenesis in the presence of 2,4-DCP is the major characteristic of substrate interaction during simultaneous degradation of readily degradable substrates (sucrose and HAc) and 2,4-DCP. The effect of electron donors (sucrose, HPr and HAc) on 2,4-DCP degradation is minimal.

- 2,4-DCP degradation can be described by a modified Haldane type inhibition function. The 2,4-DCP concentration in the liquid phase determined its toxic effect

and degradation rate.

- The degradation kinetics of HAc in presence of 2,4-DCP follow a uncompetitive inhibition function while HPr degradation is described by the Haldane type inhibition function. Degradation of sucrose to HAc or HPr follows the Monod equation.

4. Concerning the overall performance and the modeling of UASB reactors:

- With increasing UASB reactor SOLR for primary substrates and 2,4-DCP, the degradation rates of HAc and HPr decrease but the degradation rate of 2,4-DCP increases.

- Maximum degradation rate constants for 2,4-DCP in the dynamic model were comparable with values reported in the literature, but the degradation rate constants for HAc were about 10 times smaller than reported values in the absence of 2,4-DCP.

8.2 Recommendations for Future Studies

1. The opposite variation trends in the degradation rate of primary substrates and 2,4-DCP as a function of SOLR in the UASB reactors was explained by biomass inactivation and biomass ecological change in this study. The biomass inactivation and recovery from inhibition is one of the essential problems in understanding the multiple

substrates degradation process as well as modeling the system. The anaerobic toxicity assay (ATA) was designed to test the inhibition effect of toxic organics, but it can not measure the recovery and inactivation of biomass from inhibition. A new experimental approach needs to be developed to investigate this problem.

2. Further study on the ecological change of biomass under 'selection pressure' caused by SOLR of toxic organic compounds is recommended. Confirmation of this interpretation may lead to a new strategy in treating industrial wastewater that contains toxic organic compounds.
3. Model analysis was found to be a useful approach in relieving financial and labor demand in this type of experimental investigation. More studies for mathematical modeling of the multiple substrate degradation process should be conducted.
4. Investigations are required to further understand the mechanistic and kinetics aspects of effect of electron donor on anaerobic degradation of chlorophenols.

REFERENCES

- Ahring, B.K., Sandberg, M. and Angelidaki, I. (1995) Volatile fatty acids as indicators of process imbalance in anaerobic digestors. *Appl. Microbiol. Biotechnol.*, **43**, 559-565.
- Ahring, B.K. and Westermann, P. (1987) Kinetics of butyric, acetate and hydrogen metabolism in a thermophilic, anaerobic, butyric-degrading triculture. *Appl. Environ. Microbiol.*, **53**, 434-439.
- Alexander, M. (1981) Biodegradation of chemicals of environmental concern. *Science*, **211**, 132-150.
- Alvarez-Cohen, L. and McCarty, P.L. (1991) A cometabolic biotransformation model for halogenated aliphatic compounds exhibiting product toxicity. *Environ. Sci. Technol.*, **25**, 1381-1387.
- Alvarez-Cohen, L., McCarty, P.L. and Roberts, P.V. (1993) Sorption of trichloroethylene onto a zeolite accompanied by methanotrophic biotransformation. *Environ. Sci. Technol.*, **27**, 2141-2148.
- Amy, G.L., Bryant, C.W., Alleman, B.C. and Barkley, W.A. (1988) Biosorption of organic halide in a kraft mill generated lagoon. *J. Wat. Pollut. Control Fed.*, **60**, 1445-1453.
- Andreadakis, D.A. (1993) Physical and chemical properties of activated sludge floc. *Wat. Res.*, **27**, 1707-1714.
- Andrews, J.F. and Graef, S.P. (1971) Dynamic modeling and simulation of the anaerobic digestion process. *Advances in Chemistry Series 105*, American Chemical Society, 126-162.
- Archer, D.B., Hilton, M.G., Adams, P. and Wieko, H. (1986) Hydrogen as a process control index in a pilot scale anaerobic digester. *Biotechnol. Lett.*, **8**, 197-202.
- Armenante, P.M., Kafkewitz, D., Jou C.J. and Lewandowski, G. (1993) Effect of pH on the anaerobic dechlorination of chlorophenols in a defined medium. *Appl. Microbiol. & Biotech.*, **39**, 772-777.
- Armenante, P.M., Shu, H.Y., Huang, C.R., Kung, C.M. and Kafkewitz, D. (1995) Kinetics of the sequential dechlorination of 2,4,6-trichlorophenol by an anaerobic microbial population. *Biotechnol. Lett.*, **17**, 663-668.

- Baltes, M., Schneider, R., Sturm, C. and Reuss, M. (1994) Optimal experimental design for parameter estimation in unstructured growth models. *Biotechnol. Prog.*, **10**, 480-488.
- Bates, D.M. and Watts, D.G. (1985) Multiresponses estimation with special application to systems of linear differential equation (with discussion by D.D. McLean). *Technometrics*, **27**, 329-360.
- Bates, D.M. and Watts, D.G. (1988) *Nonlinear regression analysis and its application*. John Wiley & Sons, 134-154.
- Battery, N.S. and Wilson, V. (1989) Survey of the anaerobic biodegradation potential of organic chemicals in digesting sludge. *Appl. Environ. Microbiol.*, **55**, 433-439.
- Bell, J., Melcer, H., Monteith, H., Osinga, I. and Steel, P. (1993) Stripping of volatile organic compounds at full-scale municipal wastewater treatment plants. *Wat. Environ. Res.*, **65**, 708-716.
- Bell, J.P. and Tsezos, M. (1987) Removal of hazardous organic pollutants by biomass adsorption. *J. Wat. Pollut. Control. Fed.*, **59**, 191-198.
- Borowiak D.S. (1989) *Model Discrimination for Nonlinear Regression Models*. Marcel Dekker, Inc. New York and Basel, 55-136.
- Boyd, S.A. (1982) Adsorption of substituted phenols by soil. *Soil Sci.*, **134**, 337-343.
- Boyd, S.A. and Shelton, D.R. (1984) Anerobic biodegradation of chlorophenols in fresh and acclimated sludge. *Appl. Environ. Microbiol.*, **47**, 272-277.
- Brenner, H. (1962) The diffusion model of longitudinal mixing in beds of finite length. Numerical values. *Chem. Eng. Sci.*, **17**, 229-243.
- Brusseau, M.L. and Rao, P.S.C. (1989) Sorption nonideality during organic contaminant transport in porous media. *Crit. Review in Environ. Control*, **19**, 33-99.
- Brusseau, M.L. and Rao, P.C.S. (1991) Influence of sorbate structure on nonequilibrium sorption of organic compounds. *Environ. Sci. Technol.*, **25**, 1501-1506.
- Chang, H. and Alvarez-Cohen, L (1995) Model for the cometabolic biodegradation of chlorinated organics. *Environ. Sci. Technol.*, **29**, 2357-2367.
- Chang, M.K., Voice, T.C. and Criddle, C.S. (1993) Kinetics of competitive inhibition and cometabolism in the degradation of benzene, toluene, and *p*-xylene by two *pseudomonas* isolates. *Biotech. Bioeng.*, **41**, 1057-1065.

- Christiansen, N., Hendriksen, H.V., Jarvinen, K.T. and Ahring, B.K. (1995) Degradation of chlorinated aromatic compounds in UASB reactors. *Water Sci. Technol.*, **31**, 249-259.
- CRC (1992) *Handbook of Chemistry and Physics*. David, R.L. (Editor-in-chief), 73rd edition, 8-41.
- Criddle, C. S. (1993) The kinetics of cometabolism. *Biotech. Bioeng.*, **41**, 1048-1056.
- Davies-Venn, C., Young, J.C. and Tabak, H.H. (1992) Impact of chlorophenols and chloroanilines on the kinetics of acetoclastic methanogenesis. *Environ. Sci. Technol.*, **26**, 1627-1635.
- Dhawan, S., Fan, L.T., Erickson, L.E. and Tuitemwong, P. (1991) Modeling, analysis, and simulation of bioremediation of soil aggregates. *Environ. Prog.*, **10**, 251-258.
- Distefano, T.D., Gossett, J.M. and Zinder, S.H. (1992) Hydrogen as an electron donor for dechlorination of tetrachloroethene by an anaerobic mixed culture. *Appl. Environ. Microbiol.*, **58**, 3622-3629.
- Dobbs, R.A., Wang, L. and Govind, R. (1989) Sorption of toxic organic compounds on wastewater solids: correlation with fundamental properties. *Environ. Sci. Technol.*, **23**, 1092-1097.
- Dobbs, R. A., Shan, Y., Wang, L. and Govind, R. (1995) Sorption on wastewater solids: elimination of biological activity. *Wat. Environ. Res.*, **67**, 327-329.
- Dolfing, J. and Tiedje, J.M. (1987) Growth yield increase linked to reductive dechlorination in a defined 3-chlorobenzotes degrading methanogenic coculture. *Arch. Microbiol.*, **149**, 102-105.
- Dolfing, J. (1988) Acetogenesis. *Biology of Anaerobic Microorganisms* (Edited by Zehnder, A.J.B.) John Wiley & Sons, Inc., 417-468.
- Draper, N.R. and Smith, H. (1966) *Applied regression analysis*. John Wiley & Sons, Inc., 26-32.
- Duff, S.J.B., Kennedy, K.J. and Brady, A.J. (1995) Treatment of dilute phenol/PCP wastewaters using the upflow anaerobic sludge blanket (UASB) reactor. *Wat. Res.*, **29**, 645-651.
- Echkenfelder, W.W. and Grau, P. (1992) *Water Quality Management Library Vol.1- Activated Sludge Process, Design and Control Theory and Practice*. Technomic Lancaster, PA, 170-172.

- Ely, R. L. Hyman, M. R. Arp, D. J. Guenter, R. B. and Williamson, K. J. (1995) A cometabolic kinetics model incorporating enzyme inhibition, inactivation, and recovery: II. Trichloroethylene degradation experiments. *Biotech. & Bioeng.* **46**, 232-245.
- Fahmy, M., Kut, O.M. and Heinzle, E. (1994) Anaerobic-aerobic fluidized bed biotreatment of sulphite pulp bleaching effluents-I. Global parameters. *Wat. Res.*, **28**, 1987-1996.
- Fernandes, L., Kennedy, K.J. and Ning, Z.(1993) Dynamic modeling of substrate degradation in sequencing batch anaerobic reactor SBAR. *Wat. Res.* **27**, 1619-1628.
- Fukuzaki, S., Nishio, N. and Nagai, S. (1990a) Kinetics of the methanogenic fermentation of acetate. *Appl. Environ. Microbiol.*, **56**, 3158-3163.
- Fukuzaki, S., Nishio, N., Shobayashi, M. and Nagai, S. (1990b) Inhibition of fermentation of propionate to methane by hydrogen, acetate and propionate. *Appl. Environ. Microbiol.*, **56**, 719-723.
- Fukuzaki, S., Nishio, N. and Nagai, S. (1995) High rate performance and characterization of granular methanogenic sludges in upflow anaerobic sludge blanket reactors fed with various defined substrates. *J. Ferment. and Bioeng.*, **79**, 354-359.
- Gordon, A.S. and Millero, F.J. (1985) Adsorption mediated decrease in the biodegradation rate of organic compounds. *Microb. Ecol.*, **11**, 289-298.
- Grady, C.P.L. Jr (1991) Biodegradation of toxic organics: status and potential. *J. Environ. Eng., ASCE.* **116**, 805-828.
- Grady, C.P.L. Jr and Lim, H.C. (1980) *Biological Wastewater Treatment, Theory and Applications.* Marcel Dekker, Inc., NY, 336-340.
- Grotenhuis, J.T.C., Smit, M., Van Lameren, A.A.M., Stams, A.J.M. and Zehnder, A.J.B. (1991) Localization and quantification of extracellular polymer in methanogenic granular sludge. *Appl. Microb. Biotech.*, **36**, 115-119.
- Gu, Y. and Korus, R.A. (1995) Kinetics of pentachlorophenol degradation by a Flavobacteria species. *Appl. Microbiol. Biotechnol.*, **43**, 374-378.
- Hägglom, M. M. Rivera, M.D. and Young, L.Y. (1993a) Influence of alternative electron acceptors on the anaerobic degradability of chlorinated phenols and benzoic acids. *Appl. Environ. Microbiol.*, **59**, 1162-1167.
- Hägglom, M. M., Rivera, M.D. and Young, L.Y. (1993b) Effects of auxiliary carbon sources and electron acceptors on methanogenic degradation of chlorinated phenols. *Environ. Toxicol. Chem.*, **12**, 1395-1403.

- Hägglom, M.M. and Young, L.Y. (1990) Chlorophenol degradation coupled to sulfate. *Appl. Environ. Microbiol.*, **56**, 3255-3260.
- Hägglom, M.H. and Young, L.Y. (1995) Anaerobic degradation of halogenated phenols by sulfate-reducing consortia. *Appl. Environ. Microbiol.*, **61**, 1546-1550.
- Han, K. and Levenspiel, O. (1988) Extended Monod kinetics for substrate, product and cell inhibition. *Biotech. Bioeng.*, **32**, 430-437.
- Hendriksen, H.V. and Ahring, B.K. (1992). Metabolism and kinetics of pentachlorophenol transformation in anaerobic granular sludge. *Appl. Microb. Biotech.*, **37**, 662-666.
- Hendriksen, H.V. and Ahring, B. K. (1996) Integrated removal of nitrate and carbon in an upflow anaerobic sludge blanket (UASB) reactor: operating performance. *Wat. Res.* **30**, 1451-1458.
- Hendriksen, H.V., Larsen, S. and Ahring, B.K. (1992) Influence of a supplemental carbon source on anaerobic dechlorination of pentachlorophenol in granular sludge, *Appl. Environ. Microbiol.*, **58**, 365-370.
- Henze, M. and Harremoës, P. (1983) Anaerobic treatment of wastewater in fixed film reactors - a literature review. *Wat. Sci. Tech.*, **15**, 1-101.
- Hess, T.F., Schmidt, S.K. Silverstein, J. and Howe, B. (1990) Supplemental substrate enhancement of 2,4-dinitrophenol mineralization by a bacterial consortium. *Appl. Environ. Microbiol.*, **56**, 1551-1558.
- Heyes, R.H. and Hall, R.J. (1983) Kinetics of two subgroups of propionate-using in anaerobic digestion. *Appl. Environ. Microbiol.*, **46**, 710-715.
- Hu, Z.C., Korus, R.A., Levinson, W.E. and Crawford, R.L. (1994) Adsorption and biodegradation of pentachlorophenol by polyurethane-immobilized *Flavobacterium*. *Environ. Sci. Technol.*, **28**, 491-496.
- Jacobsen, B.J., Nyholm, N., Pedersen, B.M., Poulsen, O. and Ostfeldt, P. (1993) Removal of organic micropollutants in laboratory activated sludge reactors under various operating conditions: sorption. *Wat. Res.*, **27**, 1505-1510.
- Jafvert, C.T. (1990) Sorption of organic acid compounds to sediments: initial model development. *Environ. Toxicol. Chem.*, **9**, 1259-1268.
- Jain, S., Lala, A.K., Bhatia, S.K. and Kudchadker, A.P. (1992) Modeling of hydrolysis controlled anaerobic digestion. *J. Chem. Tech. Biotechnol.*, **53**, 337-344.

- Juteau, P., Beaudet, R., McSween, G., Lepine, F. and Bisaillon, J.G. (1995) Study of the reductive dechlorination of pentachlorophenol by a methanogenic consortium. *Canad. J. of Microbiol.*, **41**, 862-868.
- Karickhoff, S.W. (1981) Semi-empirical estimation of sorption of hydrophobic pollutants on natural sediments and soils. *Chemosphere*, **10**, 833-846.
- Kennes, C., Wu, W.M., Bhatnagar, L. and Zeikus, J.G. (1996) Anaerobic dechlorination and mineralization of pentachlorophenol and 2,4,6-trichlorophenol by methanogenic pentachlorophenol-degrading granules. *Appl. Microb. & Biotech.*, **44**, 801-806.
- Kennedy, K.J. (1985) Startup and steady state kinetics of anaerobic downflow stationary fixed film reactors. Ph.D. thesis, University of Ottawa.
- Kennedy, K.J., Lu, J. and Mohn, W.W. (1992) Biosorption of chlorophenols to anaerobic sludge. *Wat. Res.*, **26**, 1085-1092.
- Kennedy, K.J., and Pham, T.P. (1995) Effect of anaerobic sludge source and condition on sorption of halogenated aromatics. *Wat. Res.*, **29**, 2360-2366.
- Kim, I.S., Young, J.C. and Tabak, H.H. (1994) Kinetics of acetogenesis and methanogenesis in anaerobic reactions under toxic conditions. *Water Environ. Res.*, **66**, 119-132.
- Klecka, G.M. and Maier, W.J. (1985) Kinetics of microbial growth on pentachlorophenol. *Appl. Environ. Microbiol.*, **49**, 46-53.
- Klecka, G.M. and Maier, W.J. (1988) Kinetics of microbial growth on mixtures of pentachlorophenol and chlorinated aromatic compounds. *Biotech. Bioeng.*, **31**, 328-335.
- Klein, C.M. (1996) The effect of inhibitors on the biosorption of 2,4-dichlorophenol and 2,3,6-trichlorophenol by anaerobic granules. B.A.Sc. thesis, University of Ottawa.
- Kohring, G.W., Rogers, J.E. and Wiegel, J. (1989) Anaerobic biodegradation of 2,4-dichlorophenol in freshwater lake sediments at different temperature. *Appl. Environ. Microbiol.*, **55**, 348-353.
- Kookana, R.S., Schuller, R.D. and Aylmore, L.A.G. (1993) Simulation of simazine transport through soil columns using time-dependent sorption data measured under flow conditions. *J. Contam. Hydrol.*, **14**, 93-115.
- Kuhn, G.T., Townsend, G.T. and Suflita, J.M. (1990) Effect of sulfate and organic carbon supplements on reductive dehalogenation of chloroanilines in anaerobic aquifer slurries. *Appl. Environ. Microb.*, **56**, 2630-2637.

- Kus, F. and Wiesmann, U. (1995) Degradation kinetics of acetate and propionate by immobilized anaerobic mixed cultures. *Wat. Res.*, **29**, 1437-1443.
- Lapat-Polasko, L.T., McCarty, P.L. and Alexander, J.B.Z. (1984). Secondary substrate utilization of methylene chloride by an isolated strain of *Pseudomonas* sp. *Appl. Environ. Microbiol.*, **47**, 825-830.
- Lawrence, A.W. and McCarty, P.L. (1969) Kinetics of methane fermentation in anaerobic treatment. *J. Wat. Pollut. Control Fed.*, **41**, R1-R17.
- Lee, L.S., Rao, P.S.C. and Brusseau, M.L. (1991) Nonequilibrium sorption and transport of neutral and ionized chlorophenols. *Environ. Sci. Technol.*, **25**, 722-729.
- Lettinga, G. (1995) Anaerobic digestion and wastewater treatment systems. *Antonie van Leeuwenhoek*, **67**, 3-28.
- Lin, C.Y., Sato, K., Noike, T. and Matsumoto, J. (1986) Methanogenic digestion using mixed substrate of acetate, propionic and butyric acids. *Wat. Res.*, **20**, 385-394.
- Lindqvist, R. and Endfield, C.G. (1992) Biosorption of dichlorodiphenyltrichloroethane and hexachlorobenzene in groundwater and its implications for facilitated transport. *Appl. Environ. Microbiol.*, **58**, 2211-2218.
- Liu, D. and Pacepavicius, G. (1990) A systematic study of the aerobic and anaerobic biodegradation of 18 chlorophenols and 3 cresols. *Toxicity Assessment: A Intel. J.*, **5**, 367-387.
- Lu, C.J. and Chen, S.J. (1992) The effects of the secondary carbon source on the biodegradation of chlorinated phenols in biofilm reactors. *Wat. Sci. Tech.*, **26**, 2113-2116.
- Machado, R.J. and Grady, C.P.L. Jr (1989) Dual substrate removal by an axenic bacterial culture. *Biotech. Bioeng.*, **33**, 327-337.
- MacLeod, F.A., Guiot, S.R. and Costerton J.W. (1990) Layered structure of bacterial aggregates produced in upflow anaerobic sludge bed filter reactors. *Appl. Environ. Microbiol.*, **56**, 1598-1607.
- Madsen, T. and Aamand, J. (1992) Anaerobic transformation and toxicity of trichlorophenols in a stable enrichment culture. *Appl. Environ. Microbiol.* **58**, 557-561.
- Marshman, N.A. and Marshall, K.C. (1981) Bacterial growth on proteins in the presence of clay minerals. *Soil Biol. Biochem.*, **13**, 127-136.
- Mawson, A.J., Earle, R.L. and Larsen, V.F. (1991) Degradation of acetic and propionic acids in the methane fermentation. *Wat. Res.*, **25**, 1549-1554.

- McGinley, P.M., Katz, L.E. and Weber, W.J., Jr. (1993) A distributed reactivity model for sorption by soils and sediments. 2. Multicomponent system and competitive effects. *Environ. Sci. Technol.*, **27**, 1524-1531.
- McCarty, P.L. (1981) One hundred years of anaerobic treatment, *Anaerobic digestion*, Elsevier, Amsterdam, 3-22.
- Mikesell, M. and Boyd, S.A. (1986) Complete reductive dechlorination and mineralization of pentachlorophenol by anaerobic microorganisms. *Appl. Environ. Microbiol.*, **52**, 861-865.
- Mohn, W.M. and Kennedy, K.J. (1992) Limited degradation of chlorophenols by anaerobic sludge granules. *Appl. Environ. Microbiol.*, **58**, 2131-2136.
- Monteith H.D. and Stephenson J.P. (1981) Mixing efficiencies in full-scale anaerobic digestors by tracer methods. *J. Wat. Pollut. Control Fed.*, **53**, 78-84.
- Morvai, L., Mihaltz, P. and Hollo, J. (1992) Comparison of the kinetics of acetate biomethanation by raw and granular sludges. *Appl. Microbiol. Biotechnol.*, **36**, 561-567.
- Mosey, F.E. (1983) Mathematical modeling of the anaerobic digestion process: regulatory mechanism for the formation of short chain volatile fatty acids from glucose. *Wat. Sci. Technol.*, **15**, 209-232.
- Mosey, F.E. and Fernandes, X.A. (1989) Patterns of hydrogen in biogas from the anaerobic digestion of milk-sugars. *Wat. Sci. Technol.*, **21**, 186-196.
- Murray, W.D. and Richardson, M. (1993) Development of biological and process technologies for the reduction and degradation of pulp mill wastes that pose a threat to human health. *Crit. Rev. in Environ. Sci. & Technol.*, **23**, 157-194.
- Namkung, E. and Rittmann, B.E. (1986) Soluble microbial products (SMP) formation kinetics by biofilms. *Wat. Res.*, **20**, 795-806.
- Nicholson, D.K., Woods, S., Istok, J.D. and Peek, D. C. (1992) Reductive dechlorination of chlorophenols by a pentachlorophenol-acclimated methanogenic consortium. *Appl. Environ. Microbiol.*, **58**, 2280-2286.
- Noguera, D.R., Araki, N. and Rittmann, B.E. (1994) Soluble microbial products (SMP) in anaerobic chemostats. *Biotech. Bioeng.*, **44**, 1040-1047.
- O'Brien, G.J. and Teather, E.W. (1995) A dynamic model for predicting effluent concentration of organic priority pollutants from an industrial wastewater treatment plant. *Wat. Environ. Res.*, **67**, 935-942.

- Ogram, A.V., Jessup, R.E., Ou, L.T. and Rao, P.S.C. (1985) Effects of sorption on biological degradation rates of (2,4-dichlorophenoxy) acetic acid in soils. *Appl. Environ. Microbiol.*, **49**, 582-587.
- Owen, W.F., Stuckey, D.C., Healy, J.B., Yong, L.Y. and McCarty, P.L. (1979) Bioassay for monitoring biochemical methane potential and anaerobic toxicity. *Wat. Res.*, **13**, 485-492.
- Pak, D. (1996) Enhanced dechlorination of 2,4,6-trichlorophenol by anaerobic microbial populations in the presence of ethanol. *Biotechnol. Letters*, **18**, 981-984.
- Parker, W.J., Monteith, H.D. and Melcer, H. (1994) Estimation of anaerobic biodegradation rates for toxic organic compounds in municipal sludge digestion. *Wat. Res.*, **28**, 1779-1789.
- Patankar, S.V. (1980) *Numerical Heat Transfer and Fluid Flow*. Hemisphere Publishing Corporation, Washington, 25-96.
- Pauss, A. and Guiot, S. R. (1993) Hydrogen monitoring in anaerobic sludge bed reactors at various hydraulic regimes and loading rates. *Wat. Environ. Res.*, **65**, 276-280.
- Pavlostathis, S.G. and Giraldo-Gomez, E. (1991) Kinetics of anaerobic treatment: a critical review. *Critical Review in Environmental Control*, **21**, 411-490.
- Perkins, P.S., Komisar, S.J., Puhakka, J. A. and Ferguson, J.A. (1994) Effects of electron donors and inhibitors on reductive dechlorination of 2,4,6-trichlorophenol. *Wat. Res.*, **28**, 2101-2107.
- Petrasek, A.C., Kugelman, I.J., Austern, B.M., Pressley, T.A., Winslow, L.A. and Wise, R.H. (1983) Fate of toxic organic compounds in wastewater treatment plants. *J. Wat. Pollut. Control Fed.*, **55**, 1286-1296.
- Rittmann, B.E., Bae, W., Namkung, E. and Lu, C.J. (1987) A critical evaluation of microbial product formation in biological processes. *Wat. Sci. Tech.*, **19**, 517-528.
- Rittmann, B.E. and McCarty, P.L. (1980) Utilization of dichloromethane by suspended and fixed-film bacteria. *Appl. Environ. Microbiol.*, **39**, 1225-1226.
- Saéz, P.B. and Rittmann, B.E. (1993) Biodegradation kinetics of a mixture containing a primary substrate (phenol) and an inhibitory co-metabolite (4-chlorophenol). *Biodegradation*, **4**, 3-21.

- Sam-soon, P., Wentzel, M.C., Dold, P.L., Loewenthal, R.E. and Marais, G. (1991) Mathematical modeling of upflow anaerobic sludge bed (UASB) systems treating carbohydrate waste waters. *Water SA*, **17**, 91-106.
- Schink, B. (1988) Principles and limits of anaerobic degradation: environmental and technological aspects. in *Biology of Anaerobic Microorganisms*, edited by Zehnder, A.J.B., John Wiley & Sons, Inc., NY, 771-845.
- Schmidt, J.E. and Ahring, B.K. (1995) Interspecies electron transfer during propionate and butyrate degradation in mesophilic, granular sludge. *Appl. Environ. Microbiol.*, **68**, 2765-2767.
- Schmidt, S.K., Scow, K.M. and Alexander, M. (1987) Kinetics of p-nitrophenol mineralization by a *pseudomonas* sp.: effects of second substrates. *Appl. Environ. Microbiol.*, **53**, 2617-2623.
- Schmidt, S.K. Simkins, S. and Alexander, M. (1985) Models for the kinetics of biodegradation of organic compounds not supporting growth. *Appl. Environ. Microbiol.*, **50**, 323-331.
- Schwarzenbach, R.P., Gschwend, P.M. and Imboden, D.M. (1993) *Environmental Organic Chemistry*, John Wiley & Sons, Inc., NY, 124-341.
- Scow, K.M. and Hutson, J. (1992) Effect of diffusion and sorption on the kinetics of biodegradation: theoretical consideration. *Soil Sci. Soc. Am. J.*, **56**, 119-127.
- Selvakumar, A. and Hsieh, H-N. (1988) Correlation of compound properties with biosorption of organic compounds. *J. Environ. Sci. and Health, Part A: Environ. Sci. and Eng.*, **A23**, 543-557.
- Shelton, D.R. and Tiedje, J.M. (1984) Isolation and partial characterization of bacteria in anaerobic consortium that mineralizes 3-chlorobenzoic acid. *Appl. Environ. Microbiol.*, **48**, 840-848.
- Siegrist, H., Renggli, D. and Gujer, W. (1993) Mathematical modeling of anaerobic mesophilic sewage sludge treatment. *Wat. Sci. Tech.*, **27**, 25-36.
- Silva, S.J. (1981) EPA moving to control industrial toxic pollutants with new NPDES permits. *Civil Engineering-ASCE*, Sept., 76-78.
- Skeen, R.S., Gao, J., and Hooker, B.S. (1995) Kinetics of chlorinated ethylene dehalogenation under methanogenic conditions. *Biotechnol. Bioeng.*, **48**, 659-666.

- Spurlock, F.C., Huang, K. and van Genuchten, M.T. (1995) Isotherm nonlinearity and nonequilibrium sorption effects on transport of fenuron and monuron in soil columns. *Environ. Sci. Technol.*, **29**, 1000-1007.
- Stapleton, M.G., Sparks, D.L. and Dentel, S.K. (1994) Sorption of pentachlorophenol to HDTMA-caly as a function of ionic strength and pH. *Environ. Sci. Technol.*, **28**, 2330-2335.
- Streat, M., Patrick J. W. and Camporro Perez, M. J. (1995) Sorption of phenol and para-chlorophenol from water using conventional and novel activated carbons. *Wat. Res.* **29**, 467-472.
- Strong, G.E. and Cord-Ruwisch, R. (1995) An in situ dissolved-hydrogen probe for monitoring anaerobic digestors under overload conditions. *Biotech. Bioeng.*, **45**, 63-68.
- Sugiura, K.S., Sato, S. and Goto, M. (1975) Adsorption-diffusion mechanism of BHC-residues. A consideration based on bacteria as models. *Chemosphere*, **4**, 189-194.
- Susarla, S., Bhaskar, G.V. and Bhamidimarri, S.R.M. (1993) Adsorption-desorption characteristics of some phenoxyacetic acids and chlorophenols in a volcanic soil: I. equilibrium and kinetics. *Environ. Technol.*, **14**, 159-166.
- Togna, M.T., Kafkewitz, D. and Armenante, P.M. (1995) Rapid dehalogenation of 2,4,6-trichlorophenol at alkaline pH by an anaerobic enrichment culture. *Lett. Appl. Microbiol.*, **20**, 113-116.
- Tsezos, M. and Bell, J. P. (1988) Significance of biosorption for the hazardous organics removal efficiency of a biological reactor. *Wat. Res.*, **22**, 391-394.
- Tsezos, M. and Bell, J.P. (1989) Comparison of the biosorption and desorption of hazardous organic pollutants by live and dead biomass. *Wat. Res.*, **23**, 561-568.
- Utkin, I., Dalton, D.D. and Wiegel, J. (1995) Specificity of reductive dehalogenation of substituted ortho-chlorophenols by *Desulfitobacterium dehalogenans* JW/TU-DC1. *Appl. Environ. Microb.*, **61**, 346-351.
- Valocchi, A. (1985) Validity of the local equilibrium for modeling sorbing solute transport through homogeneous soils. *Water Resour. Res.*, **21**, 808-820.
- van den Berg, L. (1977) Effect of temperature on growth and activity of a methanogenic culture utilizing acetate. *Can. J. Microbiol.*, **23**, 898-902.
- Vavilin, V.A., Vasiliev, V.B., Ponomarev, A.V. and Rytow, S.V. (1994) Simulation model 'METHANE' as a tool for effective biogas production during anaerobic conversion of complex organic matter. *Bioresource Technology*, **48**, 1-8.

- Wang, L., Govind, R. and Dobbs, R.A. (1993) Sorption of toxic organic compounds on wastewater solids: mechanism and modeling. *Environ. Sci. Technol.*, **27**, 152-158.
- Wang, X. and Grady C.P.L., Jr. (1993) The effects of biosorption on the biodegradation of di-n-butyl phthalate. *66th Annual Conference & Exposition, Anaheim, CA, U.S.*
- Wang, X. and Grady, C.P.L., Jr. (1994) Comparison of biosorption isotherm for di-N-butyl phthalate by live and dead bacteria. *Wat. Res.*, **28**, 1247-1251.
- Weber, W.J., Jr., McGinley, P.M. and Katz, L.E. (1992) A distributed reactivity model for sorption by soil and sediments 1. conceptual basis and equilibrium assessments. *Environ. Sci. Technol.*, **26**, 1955-1962.
- Wedemeyer, G. (1966) Uptake of 2,4-dichlorophenoxyacetic acid by *Pseudomonas Fluorescens*. *Appl. Microb.*, **14**, 486-491.
- Woods, S.L. (1985) Fate of chlorinated, hydroxylated and methoxylated benzenes in anaerobic wastewater treatment. Ph.D. thesis, University of Washington.
- Wrenn, B.A. and Rittmann, B.E. (1995) A model for the effects of primary substrates on the kinetics of reductive dehalogenation. *Biodegrad.*, **6**, 295-308.
- Wu, Wei-min, Bhatnagar, L. and Zeikus, J.G. (1993) Performance of anaerobic granules for degradation of pentachlorophenol. *Appl. Environ. Microb.*, **59**, 389-397.
- Yan, G. and Allen, D.G. (1994) Biosorption of high molecular weight organochlorines in pulp mill effluent. *Wat. Res.*, **28**, 1933-1941.
- Yang, S.T. and Okos, M.R. (1987) Kinetic study and mathematical modeling of methanogenesis of acetate using pure cultures of methagens. *Biotechnol. Bioeng.*, **30**, 661-667.
- Young, J.C. and Tabak, H.H. (1993) Multilevel protocol for assessing the fate and effect of toxic organic chemicals in anaerobic treatment processes. *Wat. Environ. Res.*, **65**, 34-45.
- Zhang, X. and Wiegel, J. (1990) Sequential anaerobic degradation of 2,4-dichlorophenol in freshwater sediments. *Appl. Environ. Microbiol.*, **56**, 1119-1127.
- Zinder, S.H., Anguish, T. and Cardwell, S.C. (1984) Selective inhibition by 2-bromoethanesulfonate of methanogenesis from acetate in a thermophilic anaerobic digester. *Appl. Environ. Microbiol.*, **47**, 1343-1345.

APPENDIX

Appendix A Composition of Feed for UASB Reactors

Substances ^a	Concentration in feed for Phase I (g/L) ^b	Concentration in feed for Phase II (g/L) ^b
Sucrose	5.00	3.00
Acetic acid	5.00	3.00
NH ₄ HCO ₃	2.00	1.20
NaHCO ₃	5.00	3.00
KHCO ₃	6.25	3.75
(NH ₄) ₂ SO ₄	0.50	0.30
K ₂ HPO ₄	0.20	0.12
KH ₂ PO ₄	0.26	0.16
Yeast abstract	0.10	0.06
2,4-DCP	-	0.01
COD ^c	10.97	6.58

^a Modified from the feed composition reported by Kennedy (1985). The feed was prepared with tap water.

^b Phase I: unacclimated sludge cultivation; Phase II: routine operation with 2,4-DCP.

^c Calculated based on stoichiometry of full oxidation to CO₂ and H₂O without considering the oxidation of yeast abstract and 2,4-DCP.

Appendix B Composition of Dilution Solution for Batch Degradation Tests

Substances ^a	Concentration (mg/L)
KHCO ₃	3000
FeCl ₂ ·4H ₂ O	1500
NH ₄ Cl	500
MgCl ₂	100
CaCl ₂	100
CoCl ₂ ·6H ₂ O	10
(NH ₄) ₆ MO ₇ O ₂₄ ·4H ₂ O	2.0
H ₃ BO ₃	0.3
ZnSO ₄ ·7H ₂ O	0.1
AlK(SO ₄) ₂ ·12H ₂ O	0.1
MnCl ₂ ·4H ₂ O	0.03
NiSO ₄ ·6H ₂ O	0.03

^a Modified from the reported mineral media (Owen et al., 1979; Wu et al., 1993). The solution was prepared with distilled water. Before use, the solution pH was adjusted to designated pH using 0.1 M H₂SO₄ (Unadjusted solution, pH = 8.1).

Appendix C Relation Between C_{sw} and C_e for Sorption of 2,4-DCP to Anaerobic Granules.

For a sorption system with a total effective volume of V_T and sludge concentration of X , the following relation exists for a total amount of 2,4-DCP, $M = V_T C_T$ added to the system:

$$V_T C_T = V_w C_e + V_{sw} C_{sw} \quad (1)$$

where, V_T , V_w and V_{sw} are the volume of the mixed liquor, the liquid phase and the granules (including both intra-granule pores and solid phase); and C_T , C_e and C_{sw} are the sorbate concentrations at equilibrium in those three domains, respectively. It should be noted that the concentrations of C_T and C_{sw} cannot be measured since they are defined as the average concentrations in the mixed liquor and in the interior of sludge, respectively. Only the concentration of sorbate in the liquid phase, C_e , can be determined by measurement.

The second term on the right of Equation (1) can be determined in sorption tests by the extraction approach (Kennedy et al., 1992) and it is generally defined as adsorbed sorbate in the sorption test:

$$V_{sw} C_{sw} = X V_T q_e \quad (2)$$

in which X is the biomass concentration in the solution and q_e is the sorbate adsorbed to biomass, respectively. Substituting linear sorption equation, $q_e = K_d C_e$ into Equation (2), we have,

$$\frac{C_{sw}}{C_e} = \frac{XV_T}{V_{sw}} K_d \quad (3)$$

in which, K_d is the sorption coefficient. However, since V_{sw} is usually not known, Equation (3) cannot be easily used.

Assuming density of the liquid phase of the sorption system is not affected by low concentrations of toxic organic compounds in solution, Equation (4) based on mass balance can be used.

$$V_{sw}\rho_{sw} = V_s\rho_s + (V_{sw} - V_s)\rho \quad (4)$$

or

$$V_{sw} = V_s \frac{\rho_s - \rho}{\rho_{sw} - \rho} \quad (5)$$

where, ρ_s , ρ_{sw} and ρ are the densities of solid, wet sludge and water in the sorption system, respectively. Since, $V_s = XV_T / \rho_s$, Equation (5) becomes

$$\frac{XV_T}{V_{sw}} = \frac{\rho_{sw} - \rho}{1 - \rho / \rho_s} \quad (6)$$

Combining Equation (3) and (6), the following equation is obtained,

$$\frac{C_{sw}}{C_e} = K_d \frac{\rho_{sw} - \rho}{1 - \rho / \rho_s} \quad (7)$$

To further simplify Equation (7), the following relation can be obtained from Equation (5):

$$\frac{\rho_{sw} V_{sw}}{\rho_{sw} V_s} = \frac{\rho_s - \rho}{\rho_{sw} - \rho}$$

or,

$$\frac{\rho_{sw} V_{sw}}{\rho_{sw} V_s \rho_s} = \frac{1 - \rho / \rho_s}{\rho_{sw} - \rho} \quad (8)$$

Rearranging the left hand side of Equation (8),

$$\frac{\rho_{sw} V_{sw}}{\rho_{sw} V_s \rho_s} = \frac{1}{\rho_{sw}} \frac{1}{\frac{V_s \rho_s}{\rho_{sw} V_{sw}}} = \frac{1}{\rho_{sw}} \frac{1}{1 - P_w} \quad (9)$$

where, P_w is the moisture content of the sludge and it can be determined by measurement.

Substituting Equation (9) into Equation (7), the relation between C_{sw} and C_e for the sorption of 2,4-DCP to anaerobic granules is obtained:

$$\frac{C_{sw}}{C_e} = K_d \rho_{sw} (1 - P_w) \quad (10)$$

Appendix D Feeding Conditions During Transient Change Periods for the 9 Experimental Runs.^a

Code Number of runs	Run time interval (h)	Feeding flowrate, Q (L/h)	Sludge conc., X_v (gVSS/L)	Influent pH/effluent pH ^b	2,4-DCP concentration (mgDCP/L)	HAc concentration (mgHAc/L)	HPr concentration (mgHPr/L)	COD concentration (mgCOD/L)
RUN I.1 ^c	0 - 3.0	0.13	26.2	NM/7.24	7.48	2908	0	6128
	3.0 - 24.0	0.16	26.2	NM/7.24	46.87	2777	0	5397
	24.0 - 60.0	0.13	26.2	NM/7.24	7.75	3050	0	6330
RUN I.3	0.0 - 12.0	0.28	19.3	NM/7.18	8.22	3060	0	6565
	12.0 - 24.0	0.30	19.3	NM/7.18	54.78	2921	0	5929
	24.0 - 50.0	0.30	19.3	NM/7.18	9.25	3017	0	6282
	0.0 - 13.0	0.14	26.2	6.46/7.29	7.64	3183	0	5652
RUN II.1	13.0 - 17.5	0.11	26.2	6.95/7.20	86.45	2665	0	4955
	17.5 - 21.0	0.61	26.2	6.83/7.24	96.96	1919	0	3871
	21.0 - 50.0	0.15	26.2	6.56/7.23	6.63	3186	68	5884
	0.0 - 15.0	0.20	20.3	6.54/7.14	7.17	3066	0	5491
RUN II.2	15.0 - 19.0	0.46	20.3	6.95/7.14	100.0	2653	0	5043
	19.0 - 24.5	0.49	20.3	7.24/7.14	111.0	1216	0	2283
	24.5 - 50.0	0.22	20.3	6.07/7.15	7.14	3147	0	5790
	0.0 - 14.0	0.30	19.3	6.42/7.19	7.49	3069	0	5914
RUN II.3	14.0 - 26.0	0.29	19.3	6.56/7.18	52.78	1420	0	2995
	26.0 - 38.0	0.29	19.3	7.28/7.15	58.74	2683	43	4800
	38.0 - 70.0	0.30	19.3	NM/7.15	7.49	3069	0	5914

Table cont.

RUN II.4	0.0 - 13.0	0.22	16.9	6.59/7.25	7.04	3139	0	6758
	13.0 - 21.0	0.20	16.9	7.15/7.30	50.97	2846	0	5990
	21.0 - 25.0	0.23	16.9	NM/7.30	6.82	3179	0	6760
	25.0 - 29.0	0.36	16.9	6.80/7.25	49.54	1479	0	2918
	29.0 - 50.0	0.23	16.9	NM/7.30	6.82	3179	0	6760
RUN III.1	0.0 - 18.0	0.15	26.2	6.30/7.20	6.12	3044	43	6507
	18.0 - 71.0	0.11	26.2	6.85/7.20	115.6	2524	31	5623
	71.0 - 120.0	0.15	26.2	6.11/7.20	7.00	3084	142	6346
RUN III.3	0.0 - 13.0	0.31	19.3	6.54/7.21	6.00	3056	0	6366
	13.0 - 42.0	0.30	19.3	6.77/7.21	80.0	2696	0	5471
	42.0 - 120.0	0.32	19.3	6.35/7.20	6.00	3258	567	6022
RUN III.4	0.0 - 16.0	0.22	16.9	6.31/7.06	6.36	3028	15	6788
	16.0 - 41.0	0.20	16.9	6.78/7.10	134.8	2929	0	6306
	41.0 - 100.0	0.22	16.9	6.21/7.07	6.34	3030	617	6708

^a The feeding conditions were used in modeling the UASB reactors as boundary conditions. The effective volumes for reactors R1, R2, R3 and R4 are 4.68, 5.50, 5.50 and 5.50 L, respectively.

^b The effluent pH values are included in this table for their use as boundary conditions in the modeling. NM: not measured.

^c See Table 6-1 for the code number.

Appendix E System Responses for UASB Reactors in the 9 Experimental Runs.

RUN L1

Time (h)	2,4-DCP (mg/L)	4-MCP (mg/L)	HAc (mg/L)	HPr (mg/L)	COD (mg/L)
0.0	0	5.95	0	0	178
3.0	0	4.92	0	0	112
13.5	0	7.64	0	0	175
16.5	0	9.12	0	0	106
19.5	0	8.79	0	0	122
21.5	0	10.54	0	0	195
24.0	0	10.50	0	0	158
26.0	0	10.28	12	0	158
37.0	0	10.18	0	0	126
39.0	0	9.80	0	0	187

RUN L3

Time (h)	2,4-DCP (mg/L)	4-MCP (mg/L)	HAc (mg/L)	HPr (mg/L)	COD (mg/L)
0	0	6.01	547	34	840
12	0	6.25	615	61	794
14	0	6.39	655	60	928
16	0	6.67	664	96	709
18	0	7.39	626	82	875
20	0	8.01	615	73	939
22	0	9.36	584	81	865
24	0.50	10.67	571	71	925
26	0.97	11.27	612	80	992
36	0.26	14.77	753	106	1052
39	0	14.71	774	105	1031

RUN IL1

Time (h)	2,4-DCP (mg/L)	4-MCP (mg/L)	HAc (mg/L)	HPr (mg/L)	COD (mg/L)
0	0	5.25	29.75	0	240
12	0	5.32	22.23	0	201
13	0	5.05	0	0	155
15	0	5.13	16.34	0	217
16	0	5.22	17.88	0	209
17.5	0	5.89	16.04	0	194
19	3.62	6.55	62.80	0	186
21	8.50	6.77	62.27	0	302
23	9.03	7.57	13.80	0	201
25	7.94	8.63	30.32	0	201
36	3.49	14.38	47.57	0	255

RUN IL2

Time (h)	2,4-DCP (mg/L)	4-MCP (mg/L)	HAc (mg/L)	HPr (mg/L)	COD (mg/L)
0	0	5.67	91	0	407
13.5	0	5.57	72	0	303
15	1.36	6.36	73	0	325
17	5.28	7.72	215	31	512
19	10.69	8.91	366	57	713
21	14.79	9.85	282	61	572
23	19.65	10.90	161	58	392
24.5	19.50	11.01	116	60	392
26	19.58	12.42	120	75	482
37	8.43	19.67	113	62	497
44	1.56	26.03	93	17	437

RUN II.3

Time (h)	2,4-DCP (mg/L)	4-MCP (mg/L)	HAc (mg/L)	HPr (mg/L)	COD (mg/L)
0	0	6.25	530	33	783
12	0	5.95	470	36	722
14	0	5.84	471	43	714
16	0	6.17	366	35	645
18	0	6.71	181	11	407
20	0	8.04	94	0	246
24	0.26	10.65	40	0	192
26	0.62	11.71	32	0	184
36	2.01	17.15	191	20	384
38	2.70	18.00	214	26	445
41	2.87	19.94	295	34	507
48	0	21.21	512	35	791
70	0	13.50	732	56	952

RUN II.4

Time (h)	2,4-DCP (mg/L)	4-MCP (mg/L)	HAc (mg/L)	HPr (mg/L)	COD (mg/L)
0	0	5.40	164	11	499
12	0	5.60	146	13	415
13	0	5.48	133	0	384
15	0	5.67	122	1	376
17	0.66	6.32	110	4	376
19	1.54	6.52	111	0	353
21	2.01	7.15	112	1	346
24.25	2.10	7.87	156	15	430
25	1.43	7.84	149	10	415
27.18	2.59	8.01	120	8	376
29	4.24	8.06	104	0	361
36	2.92	9.55	141	4	468
39	2.25	10.47	132	2	438
44	0.71	11.29	124	0	430

RUN III.1

Time (h)	2,4-DCP (mg/L)	4-MCP (mg/L)	HAc (mg/L)	HPr (mg/L)	COD (mg/L)
0	0	5.06	18	0	145
16	0	5.02	24	0	145
18	0	5.00	24	0	129
24	1.18	6.54	18	0	145
35	4.62	10.35	17	0	137
38	5.56	11.07	23	0	177
48	8.87	14.15	30	0	177
58.5	11.72	17.53	41	0	193
71	13.93	22.64	20	0	185
94	3.07	29.13	45	6	273
107	0	27.55	42	0	241
114.5	0	25.38	26	0	177
120	0	23.75	21	0	201

RUN III.3

Time (h)	2,4-DCP (mg/L)	4-MCP (mg/L)	HAc (mg/L)	HPr (mg/L)	COD (mg/L)
0	0	5.58	1388	135	1815
11	0	5.44	1280	114	1591
13	0	5.54	1283	114	1626
16	0	6.13	1205	102	1454
19	0.71	7.51	1061	84	1437
22.5	2.04	9.53	907	67	1161
25	3.24	10.83	834	73	1110
33.5	7.31	15.24	660	82	938
37	8.46	17.09	622	113	972
40	9.84	18.39	585	120	1092
42	10.91	19.89	612	148	1333
47	10.50	21.88	694	211	1264
64	1.78	23.32	1018	176	1488
72	0	21.17	1192	167	1591
83	0	16.59	1383	169	1729
96	0	12.68	1391	159	1781
119	0	8.79	1466	157	1798

RUN III.4

Time (h)	2,4-DCP (mg/L)	4-MCP (mg/L)	HAc (mg/L)	HPr (mg/L)	COD (mg/L)
0	0	5.63	1285	69	1717
13	0	5.42	1132	34	1456
16	0	5.50	1148	61	1496
20.5	2.54	6.53	1121	51	1396
26	8.38	8.37	1010	45	1356
37	20.33	12.22	906	156	1436
41	23.12	13.51	868	171	1396
50	18.96	15.56	1055	345	1878
59.5	13.30	17.41	1166	279	1838
73	6.55	18.19	1314	207	1918
85.5	1.97	19.31	1416	142	1938
97.5	0	17.03	1451	114	1938

Appendix F Estimation of the mean SRT for the UASB reactors

Since the effluent SS varied significantly during operation of the UASB reactors, the mean SRT was estimated based on yield coefficients reported.

The yield coefficients reported by Henze and Harremoës (1983):

$$Y_{suc} = 0.15 \text{ g VSS/g COD removed (acid producing bacteria)}$$

$$Y_{HAc} = 0.03 \text{ g VSS/g COD removed (methanogenic bacteria)}$$

$$Y_C = 0.18 \text{ g VSS/g COD (combined yield for acid producing and methanogenic bacteria)}$$

UASB reactor	R1	R2	R3	R4
Influent COD (g/L) ^a	6.0	6.0	6.0	6.0
Effluent Vol. (L/d) ^a	3.6	5.2	7.8	5.2
COD removal (%) ^c	98	89	83	89
COD removed (g/d)	21.2	27.8	38.8	27.8
Sucrose removed (g COD/d) ^b	10.6	13.9	19.4	13.9
HAc removed (g COD/d) ^b	10.6	13.9	19.4	13.9
Sludge produced (g/d) ^c	2.23	2.92	4.07	2.92
Total sludge in reactor (g) ^a	144.2	111.4	106.4	92.8
SRT estimated (d) ^d	65	38	26	32

^a The measured values

^b From the composition of the feed for UASB reactors (Appendix A), COD contributed by sucrose and HAc are approximately equal.

^c Example based on R1: $10.6 \times 0.18 + 10.6 \times 0.03 = 2.3$ (g/d)

^d Example based on R1: $SRT = 144.24 / 2.23 = 65$ (d)

^e See Table 6-3

Appendix G FORTRAN Program for Solving the Dynamic Model (Table 7-2) and Evaluating the Determinant of $Z^T Z$.

```

C-----
C   MODEL SIMULATION OF THE UASB REACTORS' PERFORMANCE
C-----
C The program is written for solving the dynamic model for the UASB
C reactors treating SUCROSE/HAc based wastewater with 2,4-chlorophenol
C (2,4-DCP) and evaluating the model fitting results by the product of
C transpose of the residual matrix and the residual matrix (ZTZ). The
C model has a form of coupled ordinary differential equations which is
C solved using Runge-Kutta fourth order method (subroutine RUNGKU).
C
C M: Number of differential equations;
C T0 and TF: Initial and final time of each simulation run;
C NH: Number of trajectories in output for each simulation run;
C NHS: Total number of trajectories in output for all simulation run;
C WT: Trajectories of dependent variables output in simulation run;
C IT: Time in output for dependent variables;
C WTE: Array for transferring the values of dependent variables between
C simulation runs;
C NHS,SIT,SWT: Same as NH, IT, WT respectively, for ZTZ evaluation;
C NFG: Flag to control the number of simulation runs (max. 5)
C
C INPUT DATA FILES
C DATA44: The observed system responses;
C IPAR44: The model parameters;
C INIR44: Initial conditions;
C INPUR44A, INPUR44B and INPUR44C: Boundary conditions in each runs.
C OUTPUT FILES
C OUTF44A: The model simulation results;
C ZTZ44: The evaluated ZTZ determinant.
C-----
C
C INTEGER M,NH,NFG,NHS
C INTEGER NSTP
C REAL WT(0:250,6),IT(0:250),WTE(6)
C REAL SIT(250),SWT(250,6)
C REAL T0,TF
C REAL PDCPO,PSDCPO,PIDCPO,PDDCP,PDMCP,PSUCHAC,PSUCHPR,PSSUC,
C +   PHPRHAC,PSHPR,PIDCPHPR,PHAC,PSHAC,PIDCPHAC,
C +   QIN,XV,PH,DCP00,HAC00,HPR00,SUC00,COD00,V,
C +   CDCP0,CMCP0,CHAC0,CHPR0,CSUC0,CCOD0
C
C COMMON/BLOCK1/IT,WT,M
C COMMON/BLOCK2/PDCPO,PSDCPO,PIDCPO,PDDCP,PDMCP,PSUCHAC,PSUCHPR,
C +   PSSUC,PHPRHAC,PSHPR,PIDCPHPR,PHAC,PSHAC,PIDCPHAC
C COMMON/BLOCK3/QIN,XV,PH,DCP00,HAC00,HPR00,SUC00,COD00,V
C COMMON/BLOCK4/CDCP0,CMCP0,CHAC0,CHPR0,CSUC0,CCOD0
C COMMON/BLOCK5/NSTP

```



```
COMMON/BLOCK6/SIT,SWT
EXTERNAL RUNGKU,OUTPUT,PARASSR
```

C

```
M=5
NFG=3
NHS=0
NSTP=0
```

C

```
OPEN (UNIT=5,FILE='IPAR44.DAT', STATUS='UNKNOWN')
READ (5,*)PDCPO,PSDCPO,PIDCPO,PDDCP,PDMCP,PSUCHAC,PSUCHPR,PSSUC,
+   PPHRHAC,PSHPR,PIDCPHPR,PHAC,PSHAC,PIDCPHAC
CLOSE(5,STATUS='KEEP')
```

C

```
OPEN (UNIT=5,FILE='INIR44.DAT', STATUS='UNKNOWN')
READ(5,*)CDCPO,CMCP0,CHAC0,CHPR0,CCOD0
CLOSE(5,STATUS='KEEP')
CSUC0=(CCOD0-100.0-(1.066*CHAC0+1.512*CHPR0+1.215*CDCPO+
+   1.541*CMCP0))/1.127
```

C

```
IF (CSUC0.LT.0.0) THEN
CSUC0=0.0
ENDIF
```

C

```
OPEN (UNIT=5,FILE='INPUR44A.DAT', STATUS='UNKNOWN')
READ (5,*) QIN,XV,PH,DCP00,HAC00,HPR00,COD00,V,T0,TF,NH
CLOSE(5,STATUS='KEEP')
SUC00=(COD00-HAC00*1.066-HPR00*1.512-DCP00*1.215)/1.127
NHS=NHS+NH
```

C

```
OPEN (UNIT=6,FILE='OUTR44A', STATUS='UNKNOWN')
```

C

```
I=1
WRITE (6,1) I
WRITE (6,9)
CALL RUNGKU(NH,T0,TF,M,IT,WT)
CALL OUTPUT(NH,IT,WT,WTE)
IF (NFG.EQ.1) THEN
    GOTO 66
ENDIF
```

C

```
DO 55 I=2,NFG
```

```
IF (I.EQ.2) THEN
    OPEN (UNIT=5,FILE='INPUR44B.DAT',STATUS='UNKNOWN')
ELSE
    IF (I.EQ.3) THEN
        OPEN (UNIT=5,FILE='INPUR44C.DAT',STATUS='UNKNOWN')
    ELSE
        IF (I.EQ.4) THEN
            OPEN (UNIT=5,FILE='INPUTF5D.DAT',STATUS='UNKNOWN')
        ELSE
            IF (I.EQ.5) THEN
                OPEN (UNIT=5,FILE='INPUTF5E.DAT', STATUS=
+                   'UNKNOWN')
```

```

        ENDIF
        ENDIF
        ENDIF
        ENDIF
C
    READ (5,*) QIN,XV,PH,DCP00,HAC00,HPR00,COD00,V,T0,TF,NH
    CLOSE(5,STATUS='KEEP')
    SUC00=(COD00-HAC00*1.066-HPR00*1.512-DCP00*1.215)/1.127
    NHS=NHS+NH
C
    CDCP0=WTE(1)
    CMCP0=WTE(2)
    CHAC0=WTE(3)
    CHPR0=WTE(4)
    CSUC0=WTE(5)
    CCOD0=WTE(6)
C
    WRITE (6,1) I
    WRITE (6,9)
    CALL RUNGKU(NH,T0,TF,M,IT,WT)
    CALL OUTPUT(NH,IT,WT,WTE)
C
55 CONTINUE
66 CLOSE(6,STATUS='KEEP')
C
    CALL ZTZ(NHS)
C
1  FORMAT(/1H ,17X,36HRESULTS OF THE UASBs SIMULATION RUN /1H ,
+ 14X,10H(STAGE NO.,11,32H/FOURTH ORDER RUNGE-KUTTA METHOD))
9  FORMAT(/3H ,
+=====)
C
    STOP
    END
C
-----
C
SUBROUTINE RUNGKU(NH,T0,TF,M,IT,WT)
C
    INTEGER M,NH,I,L,J,K
    INTEGER INTC,NEV,NWTP,NK
    INTEGER NSTP
    REAL DT,PDT,T,T0,TF
    REAL IT(0:250),WT(0:250,6)
    REAL C(0:4),DY(4,5),Y(5),FF(5),YAA(5)
    REAL CDCP0,CMCP0,CHAC0,CHPR0,CSUC0,CCOD0
    REAL SIT(250),SWT(250,6)
    COMMON/BLOCK4/CDCP0,CMCP0,CHAC0,CHPR0,CSUC0,CCOD0
    COMMON/BLOCK5/NSTP
    COMMON/BLOCK6/SIT,SWT
C
    INTRINSIC IDINT
    EXTERNAL FUNW
C
    WT(0,1)=CDCP0

```

```

WT(0,2)=CMCP0
WT(0,3)=CHAC0
WT(0,4)=CHPRO
WT(0,5)=CSUC0
WT(0,6)=CCOD0
IT(0)=T0
DO 10 J=1,M
    Y(J)=WT(0,J)
10 CONTINUE
C
C(1)=0
C(2)=0.5
C(3)=0.5
C(4)=1.0
DO 11 L=1,M
    DY(0,L)=0
11 CONTINUE
C
T=T0
DT=0.001
PDT=(TF-T0)/NH
INTC=1+IDINT(PDT/DT)
NEV=0
NWTP=0
NK=1+IDINT((TF-T0)/DT)
C
DO 30 I=1,NK
    DO 40 K=1,4
        TK=T+DT*C(K)
        DO 50 L=1,M
            YAA(L)=Y(L)+C(K)*DY(K-1,L)
50        CONTINUE
            CALL FUNW(YAA,FF)
            DO 60 L=1,M
                DY(K,L)=DT*FF(L)
60        CONTINUE
40        CONTINUE
C
DO 70 L=1,M
    Y(L)=Y(L)+(DY(1,L)+2.0*DY(2,L)+2.0*DY(3,L)+DY(4,L))/6.0
70 CONTINUE
C
NEV=NEV+1
IF (NEV.EQ.INTC) THEN
    NWTP=NWTP+1
    NSTP=NSTP+1
    DO 80 L=1,M
        WT(NWTP,L)=Y(L)
        SWT(NSTP,L)=Y(L)
80    CONTINUE
    WT(NWTP,M+1)=1.127*Y(5)+1.066*Y(3)+1.512*Y(4)+
+    1.215*Y(1)+1.541*Y(2)+100.0
    SWT(NSTP,L)=WT(NWTP,M+1)
    NEV=0

```

```

      IT(NWTP)=T0+I*DT
      SIT(NSTP)=T0+I*DT
    ENDIF
C
      T=T0+I*DT
30  CONTINUE
      RETURN
      END
C-----
      SUBROUTINE FUNW(PAA,FF)
C
      REAL FF(5),PAA(5)
      REAL PDCPO,PSDCPO,PIDCPO,PDDCP,PDMCP,PSUCHAC,PSUCHPR,PSSUC,
+       PHPRHAC,PSHPR,PIDCPHPR,PHAC,PSHAC,PIDCPHAC
      REAL QIN,XV,PH,DCP00,HAC00,SUC00,HPR00,COD00,V
      REAL ALPHA1,ALPHA2,ALPHA3
      COMMON/BLOCK2/PDCPO,PSDCPO,PIDCPO,PDDCP,PDMCP,PSUCHAC,PSUCHPR,
+       PSSUC,PHPRHAC,PSHPR,PIDCPHPR,PHAC,PSHAC,PIDCPHAC
      COMMON/BLOCK3/QIN,XV,PH,DCP00,HAC00,HPR00,SUC00,COD00,V
C
      ALPHA1=1/(1+10**(PH-4.762))
      ALPHA2=1/(1+10**(PH-4.883))
      ALPHA3=1/(1+10**(PH-7.89))
C
      FF(1)=(1/(1+PDDCP*XV))*((QIN/V)*(DCP00-PAA(1))-(PDCPO*(PAA(1)*
+       ALPHA3)/(PSDCPO+PAA(1)*ALPHA3+(PAA(1)*ALPHA3)**2
+       /(PIDCPO-PAA(1)*ALPHA3)))*XV)
      FF(2)=(1/(1+PDMCP*XV))*((QIN/V)*(0.0-PAA(2))+0.788*(PDCPO*(PAA(1)*
+       ALPHA3)/(PSDCPO+PAA(1)*ALPHA3+(PAA(1)*ALPHA3)**2
+       /(PIDCPO-PAA(1)*ALPHA3)))*XV)
      FF(3)=(QIN/V)*(HAC00-PAA(3))+0.702*(PSUCHAC*PAA(5)/
+       (PSSUC+PAA(5)))+0.811*(PHPRHAC*(PAA(4)*ALPHA2)/(PSHPR+
+       (PAA(4)*ALPHA2)+(PAA(1)*ALPHA3)**2/PIDCPHPR))-(PHAC*(PAA(3)
+       *ALPHA1)/(PSHAC+(PAA(3)*ALPHA1)+(PAA(3)*ALPHA1)*
+       (PAA(1)*ALPHA3)**2/PIDCPHAC))*XV)
      FF(4)=(QIN/V)*(HPR00-PAA(4))+0.866*(PSUCHPR*PAA(5)/(PSSUC+PAA(5)
+       ))-(PHPRHAC*(PAA(4)*ALPHA2)/(PSHPR+(PAA(4)*ALPHA2)+
+       (PAA(1)*ALPHA3)**2/PIDCPHPR))*XV)
      FF(5)=(QIN/V)*(SUC00-PAA(5))-(PSUCHPR*PAA(5)/(PSSUC+PAA(5))+
+       PSUCHAC*PAA(5)/(PSSUC+PAA(5)))*XV
C
      RETURN
      END
C-----
      SUBROUTINE OUTPUT(NH,IT,WT,WET)
C
      INTEGER I,NH
      REAL IT(0:250),WT(0:250,6),WET(6)
C
      WRITE(6,4)
      DO 10 I=0,NH
        WRITE(6,6) I+1,IT(I),WT(I,1),WT(I,2),WT(I,3),WT(I,4),
+       WT(I,6)
        IF (I.EQ.NH) THEN

```

```

                DO 12 L=1,6
                   WET(L)=WT(L,L)
12              CONTINUE
                ENDIF
10             CONTINUE
C
                WRITE(6,8)
C
4              FORMAT(/1H ,3X,3HNo.,3X,8HTime(hr),3X,5HC.DCP,4X,5HC.MCP,6X,
+                 5HC.HAc,6X,5HC.HPr,6X,5HC.COD/)
6              FORMAT(1H ,3X,I3,1X,F9.3,2X,F7.2,2X,F7.2,4X,F7.2,4X,F7.2)
8              FORMAT(/3H ,=====
+=====)
C
                RETURN
                END
C-----
                SUBROUTINE ZTZ(NHS)
C
                INTEGER I,J,K,NEXP,NHS,NSTP
                REAL TEXP(30),WTEXP(30,6),SIT(250),SWT(250,6),SSR(5),TRZ
                INTRINSIC ABS
                INTEGER L,N,M
                REAL ZT,ZO,ZZ,XM,XM1,X
                DIMENSION ZT(100,100),ZO(100,100),ZZ(100,100)
                COMMON/BLOCK5/NSTP
                COMMON/BLOCK6/SIT,SWT
C
                OPEN (UNIT=5,FILE='DATA44.DAT', STATUS='UNKNOWN')
                READ (5,*) NEXP
                DC 10 I=1,NEXP
                   READ (5,*) TEXP(I),WTEXP(I,1),WTEXP(I,2),WTEXP(I,3),
+                   WTEXP(I,4),WTEXP(I,6)
10             CONTINUE
                   CLOSE(5,STATUS='KEEP')
C
                DO 20 I=1,5
                   SSR(I)=0.0
20             CONTINUE
                   DO 25 I=1,NEXP
                      DO 40 J=1,NHS
                         IF (ABS((SIT(J)-TEXP(I))).LT.0.00001) THEN
                            DO 50 K=1,4
                               ZO(I,K)=SWT(J,K)-WTEXP(I,K)
                               SSR(K)=SSR(K)+(ZO(I,K))**2
50                             CONTINUE
                               ZO(I,5)=SWT(J,6)-WTEXP(I,6)
                               SSR(5)=SSR(5)+ZO(I,5)**2
                               GOTO 25
                            ENDIF
80                          CONTINUE
25             CONTINUE
C
                N=NEXP

```

```

M=5
C
DO 200 I=1,M
  DO 200 J=1,N
    ZT(I,J)=ZO(J,I)
200 CONTINUE
C
DO 100 I=1,M
  DO 100 J=1,M
    ZZ(I,J)=0
  DO 100 L=1,N
    ZZ(I,J)=ZZ(I,J)+ZT(I,L)*ZO(L,J)
100 CONTINUE
C
L=1
K=2
XM1=1.
70 XM=ZZ(L,L)
DO 95 J=L,M
  ZZ(L,J)=ZZ(L,J)/XM
95 CONTINUE
DO 140 I=K,M
  X=ZZ(I,L)
DO 140 J=L,M
  ZZ(I,J)=ZZ(I,J)-ZZ(L,J)*X
140 CONTINUE
C
L=L+1
K=K+1
XM1=XM1*XM
IF (L.NE.M) THEN
  GO TO 70
ENDIF
XM1=XM1*ZZ(M,M)
C
TRZ=0.0
DO 150 I=1,5
  TRZ=TRZ+SSR(I)
150 CONTINUE
OPEN (UNIT=8,FILE='ZTZ44', STATUS='UNKNOWN')
WRITE(8,1)
WRITE(8,2)
WRITE(8,11)
WRITE(8,12)
DO 30 K=1, N
  WRITE(8,13) TEXP(K), ZO(K,1),ZO(K,2),ZO(K,3),ZO(K,4).
+      ZO(K,5)
30 CONTINUE
C
WRITE(8,14)
WRITE(8,15) XM1
WRITE(8,16) TRZ
WRITE(8,18)
CLOSE(8,STATUS='KEEP')

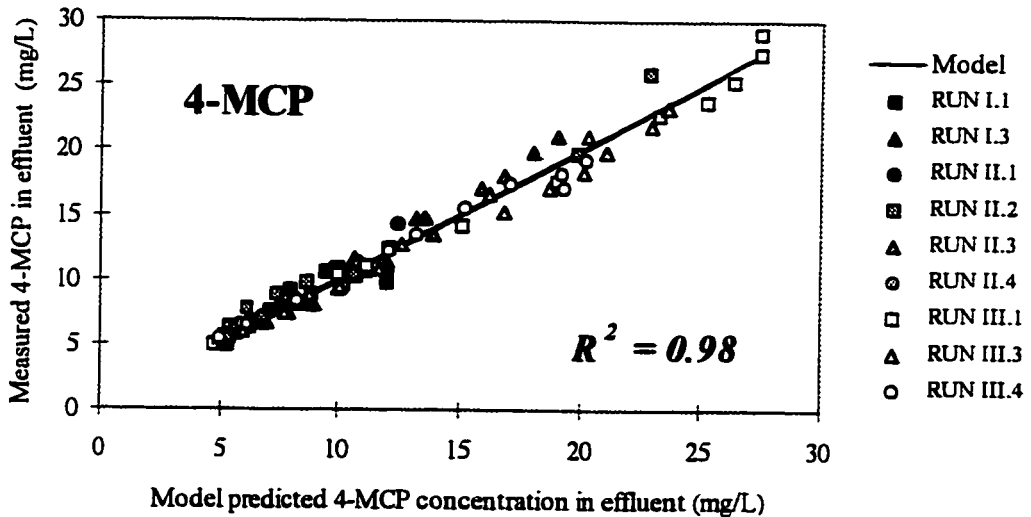
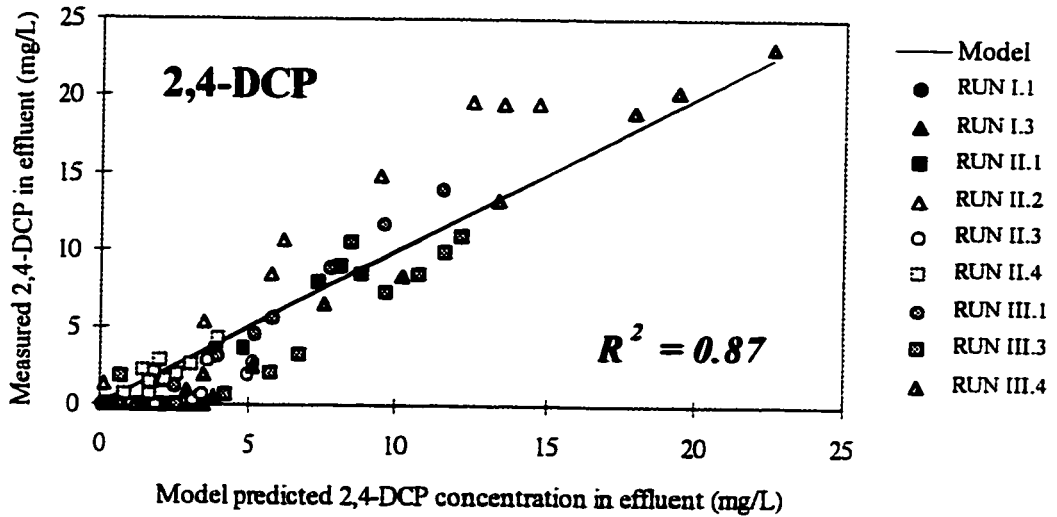
```

```

C
1  FORMAT(/24X,26HSUMMARY ON FITTING RESULTS)
2  FORMAT(22X,30H=====)
11 FORMAT(///13X,46HRESIDUALS FOR EACH RESPONSES AT DIFFERENT TIME)
12 FORMAT(/1H ,3X,8HTime(hr),2X,5HC.DCP,6X,5HC.MCP,8X,
+    5HC.HAc,8X,5HC.HPr,8X,5HC.COD/)
13 FORMAT(1H ,2X,F5.1,2X,F9.4,2X,F9.4,4X,F9.4,4X,F9.4)
14 FORMAT(/3H ,'-----'
+-----')
15 FORMAT(///3H ,'Determinant of ZTZ matrix:', E30.6)
16 FORMAT(/3H ,'Trace of ZTZ matrix:', E38.6)
18 FORMAT(/3H ,'=====
+=====')
C
RETURN
END
C-----

```

Appendix H Fitting Results of the Dynamic Model to the Data for the System Responses (2,4-DCP, 4-MCP, HAc, HPr and COD)of the UASB Reactors with Adjusted Parameters.



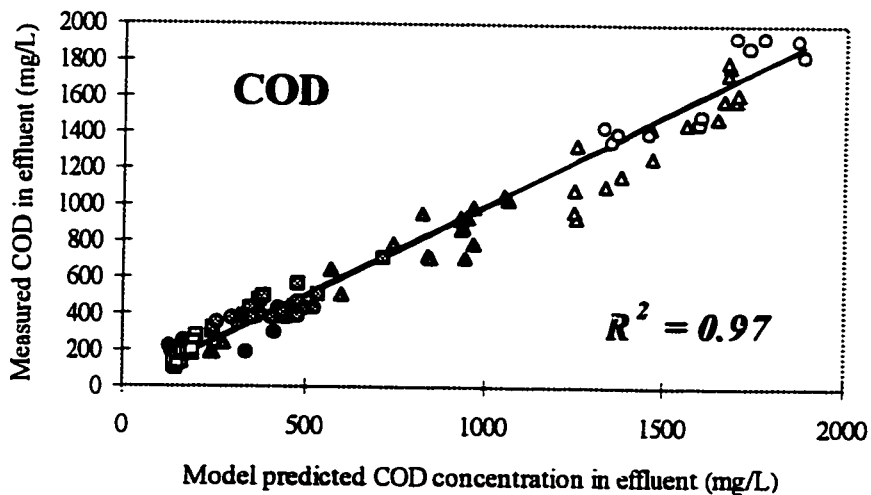
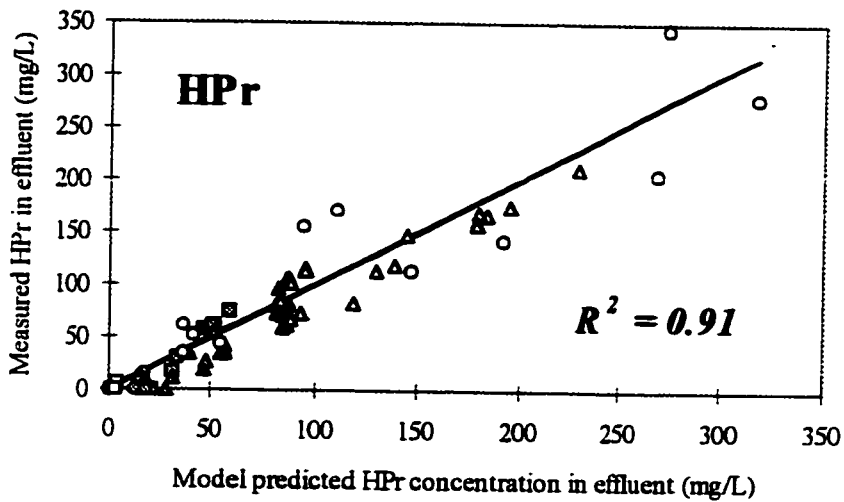
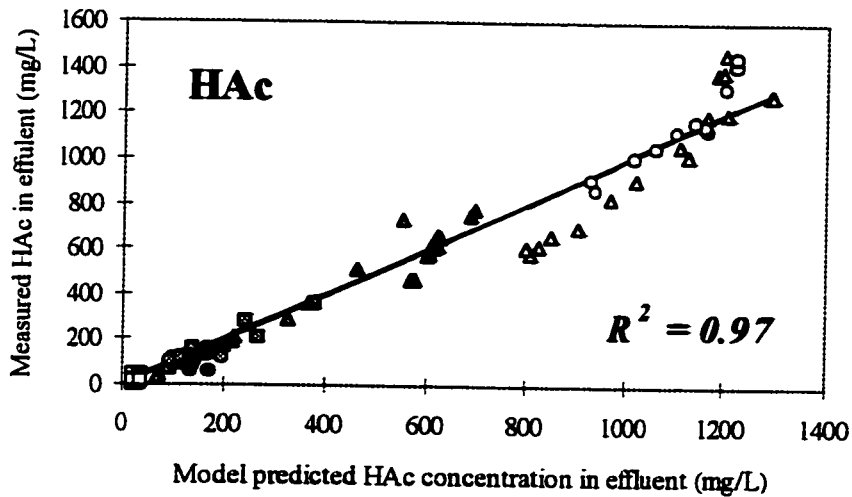
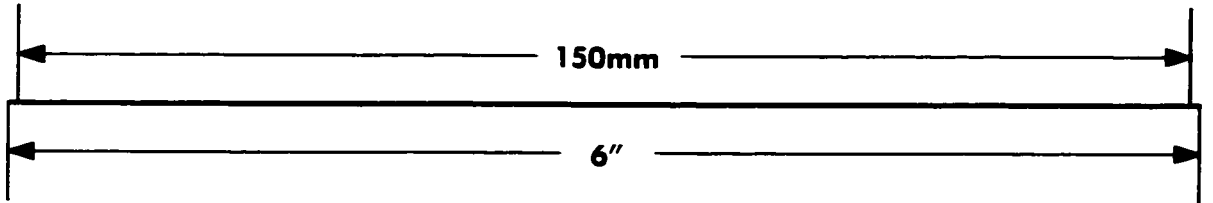
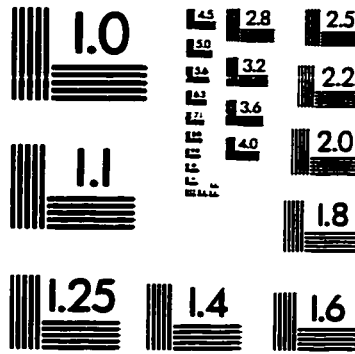
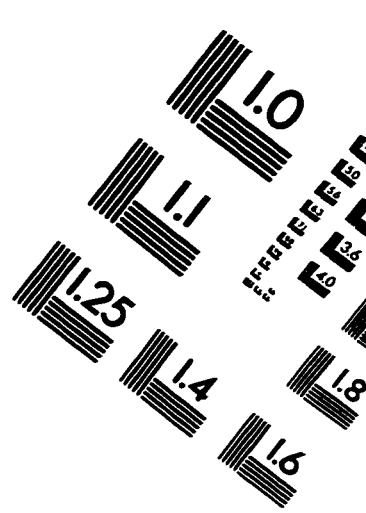
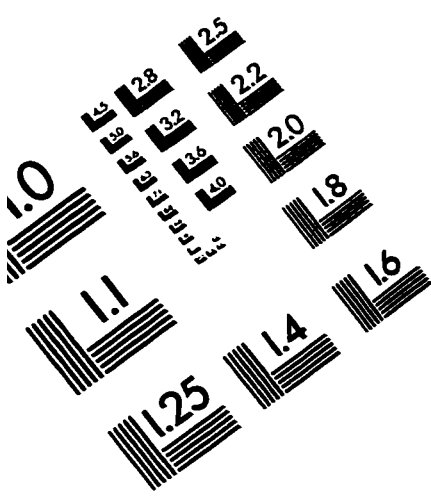


IMAGE EVALUATION TEST TARGET (QA-3)



APPLIED IMAGE, Inc
1653 East Main Street
Rochester, NY 14609 USA
Phone: 716/482-0300
Fax: 716/288-5989

© 1993, Applied Image, Inc., All Rights Reserved

